MAX-PLANCK-GESELLSCHAFT

IPSC-BASED MODELLING OF NIJMEGEN BREAKAGE SYNDROME

Dissertation
to obtain the academic degree
"doctor rerum naturalium"
(Dr. rer. nat.)

submitted to the
Department of Biology, Chemistry and Pharmacy
Free University Berlin

by
Barbara Mlody
from Salzkotten

February, 2015

Barbara Mlody: **IPSC-based Modelling of Nijmegen Breakage Syndrome**, Dissertation to obtain the academic degree *"doctor rerum naturalium"* (Dr. rer. nat.), © February 2015

The dissertation "IPSC-based Modelling of Nijmegen Breakage Syndrome" was prepared under the direction of Prof. James Adjaye in the period from March 2011 till February 2015 at the Max-Planck Institute of Molecular Genetics Berlin.

1st Reviewer:	Prof. Dr. James Adjaye Max Planck Institute for Molecular Genetics, Berlin Heinrich Heine Universität, Düsseldorf
2nd Reviewer:	Prof. Dr. Christian Freund Free University Berlin

Date of defence: 24.06.2016

To accomplish great things, we must not only act, but also dream;
not only plan, but also believe.

— Anatole France

Dedicated to my family and my friends, who let me become the person that I am today.

Our greatest weakness lies in giving up.
The most certain way to succeed is always to try just one more time.

— Thomas A. Edison

ACKNOWLEDGMENT

I would like to thank Prof. James Adjaye for giving me the opportunity to work in his group for my thesis and for his excellent supervision and encouragement throughout my studies. I am very grateful to Prof. Christian Freund who kindly agreed to review my thesis as a representative of the Free University Berlin. I also want to show my appreciation to Prof. Karl Sperling, who not only provided me with the "lucky" cells, but also encouraged me to work on this great topic. Further, I want to thank the Max-Planck Society and the Max-Planck Institute for Molecular Genetics for providing me a wonderful work place and surrounding me with great people. Especially, I would like to thank Dr. Ying Wang for her fruitful discussions and invaluable help with the reprogramming experiments, which was a one-shot, one-hit success due to her expert knowledge. In addition, I like to thank Dr. Alessandro Prigione who taught me ES cell culture and Dr. Katharina Drews for her tips and tricks with microarray analyses and excel shortcuts. Thank you, Peggy Matz, for your support and help with all the daily things and worries one can have; you are truely a "Goldstück". Thank you to all my other former lab colleges: Dr. Justyna Jozefczuk, Matthias Megges, Dr. Heiko Fuchs, Dr. Raed Abu Dawud, Dr. Smita Sudheer and Dr. Björn Lichtner for being funny as well as brilliant colleagues. The layout of this work was based on the LaTeX style "classicthesis" which was originally developed by André Miede. I also want to thank my better half, Matthias Berg, who gave me the strength to endure the adventure of publishing a "book" single-handedly.

Finally, I want to thank my wise mother for supporting me in every possible way and my father, who was always so proud of the future "doctor" in the family, but unfortunately did not live to see it come true.

ABSTRACT

Nijmegen Breakage Syndrome (NBS) is a rare autosomal recessive genetic disorder, first described 1981 in Nijmegen, Holland. The characteristics of NBS include genomic instability (resulting in early onset of malignancies), premature aging, microcephaly and other growth retardations, immune deficiency, and impaired puberty and fertility in females. The consequence of these manifestations is a severe decrease in average life span, caused by cancer or infection of the respiratory and urinary tract.

In more than 90 % of NBS patients a 5 base pair deletion (657del5) within the NBN gene is the cause of the syndrome, which occurs with an estimated prevalence of 1 in 100.000 worldwide. However, in some regions like Eastern Europe the prevalence is much higher (1:177). The deletion in the NBN gene introduces alternative initiation of translation of the p95-NIBRIN protein and results in the loss of the FHA and one BRCT domain. In contrast to this viable form, studies in mice have shown that complete knockouts and other mutations result in embryonic lethality. The truncated form p70-NIBRIN however, is still capable of executing the core functions of NIBRIN like MRN complex forming, which is an essential component of DNA repair. The MRN complex binds to DNA double strand breaks (DSBs) and is involved in repair and signaling for homologous recombination (HR), non-homologous end joining (NHEJ) and microhomology-mediated end joining (MMEJ). In addition, NBN is involved in telomere maintenance and therefore plays a role in the aging process.

In 2006 Yamanaka and Takahashi found, that somatic cells can be reprogrammed into induced pluripotent cells (iPSCs), which enabled new possibilities for *in vitro* studies and future clinical applications. It was also found that, both human embryonic stem cells (hESCs) and iPSCs rely on glycolysis rather than oxidative phosphorylation as their main source of energy. Reactive oxygen species (ROS) are constantly generated as by-products of mitochondrial respiration, but can also induce DNA damage. Therefore, ROS are probably detrimental for NBS cells under physiological conditions. Thus, it was hypothesized that antioxidants or induction of pluripotency in NBS fibroblasts might suppress and maybe bypass ROS-mediated genome instability.

The aim of this thesis was to provide a cellular model system for NBS, to overcome several problems associated with NBS research: A) small number of patients, B) cell cultures limited to fibroblasts and lymphocytes, C) premature senescence in cell culture as a consequence of high levels of ROS, D) finding new molecular mechanisms of NBS, E) providing new, therapeutically relevant concepts.

The NBS model was established by reprogramming fibroblasts from NBS patients into iPSCs, using retroviral transduction of OCT4, SOX2, KLF4 and C-MYC. Further, by employing somatic cells and iPSCs of NBS, global transcriptome analysis was performed, to identify new phenotypes and changes in the signaling network of NBS cells compared to normal cells. In addition, the influence of oxidative stress, radiomimetics and antioxidants was tested on the genomic integrity of NBS cells before and after reprogramming.

As a result of cellular reprogramming, iPSCs derived from fibroblasts of NBS patients bypassed senescence and expressed pluripotency associated proteins (Alkaline phosphatase, OCT4, NANOG, TRA1-81, TRA1-60, SSEA4). Pluripotency was further confirmed both *in vitro* (EB assays) and *in vivo* (teratoma formation in mice). Comparative transcriptome and associated pathway analyses revealed that, (a) NBS fibroblasts compared to normal fibroblasts seem to have a high impact on cell cycle regulation, apoptosis, TP53 signaling and the Fanconi Anemia pathway. (b) The comparison between NBS-iPSCs and normal hESCs presented regulated genes and pathways associated with DNA replication, glycolysis, pyrimidine, fructose and mannose metabolism as well as DNA repair related pathways. Notably, all of these pathways are known to be associated with ROS homeostasis. Comparative tests based on sensitivity towards oxidative stress and DNA damaging agents such as hydrogen peroxide and bleomycin, revealed that NBS-iPSCs and NBS-fibroblasts compared to normal fibroblasts were highly sensitive to DSB inducer bleomycin, but similar sensitive towards oxidative stress induced by exogenous hydrogen peroxide. Interestingly, DNA damage from hydrogen peroxide was efficiently relieved by addition of EDHB, an inducer of the hypoxia (HIF) pathway.

The results indicate, that NBS-iPSCs can serve as an excellent model to study NBS *in vitro*. Because only one specific functional domain is affected, which is also a common motif within DNA repair signaling, it is also a good model to study DNA repair and cell cycle checkpoint regulation. This could also aid in elucidating the mechanisms underlying the disease and can also provide a screening system for treatments which can increase life span and life quality for those patients and patients with similar diseases like Fanconi Aneamia, LIG4 syndrome, Bloom syndrome, NBS-like disorder, ataxia-telangectasia-like disorder, NHEJ1 syndrome and Seckel syndrome, which all derive from mutated genes in repair pathways.

ZUSAMMENFASSUNG

Nijmegen Breakage Syndrom (NBS) ist eine seltene, autosomal-rezessive genetisch bedingte Erkrankung, die erstmalig 1981 in Nijmegen, Niederlande beschrieben wurde. Zu den typischen Eigenschaften von NBS gehören genomische Instabilität (was zu frühzeitigen Malignomen führt), vorzeitiges Altern, Mikrozephalie und anderen Wachstumsverzögerungen, Immunschwäche sowie Beeinträchtigung von Pubertät und Fruchtbarkeit bei Frauen. Die Konsequenz von NBS ist ein deutlicher Rückgang der durchschnittlichen Lebensdauer, die hauptsächlich durch Krebs und Infektionen verursacht wird.

In mehr als 90 % der NBS Patienten ist eine 5 Basenpaardeletion (657del5) im NBN-Gen der Ursprung des Syndroms, welches mit einer geschätzten Prävalenz von 1 in 100.000 weltweit auftritt. In einigen Regionen wie Osteuropa ist die Prävalenz jedoch viel höher (1:177). Die Deletion in dem NBN Gen führt zu einer alternativen Translation des p95-Nibrin Proteins und resultiert in dem Verlust der FHA und einer BRCT Domäne. Im Gegensatz zu dieser lebensfähiger Variante, haben Studien gezeigt, dass Mäuse mit kompletten Knockouts und anderen Mutationen schon im embryonalen Stadium sterben. Die trunkierte Form p70-Nibrin ist jedoch noch in der Lage die Hauptfunktionen von Nibrin auszuführen. Dazu gehört die Bildung des MRN Komplex, der eine wesentliche Komponente in der DNA-Reparatur ist. Der MRN-Komplex bindet an DNA-Doppelstrang- brüche (DSB) und ist an Prozessen wie homologe Rekombination (HR), nichthomologes End Joining (NHEJ) und mikro-homologie-vermitteltes End Joining (MMEJ) beteiligt. Zusätzlich ist NBN in der Telomererhaltung beteiligt und spielt daher eine Rolle bei Alterungs- prozessen.

Seit Yamanaka und Takahashi herausgefunden haben, dass Körperzellen in induzierte pluripotente Zellen (iPS-Zellen) umprogrammiert werden können, gibt es neue Möglichkeiten für *in-vitro*-Studien und zukünftige klinische Anwendungen. Es wurde auch festgestellt, dass hESCs und iPS-Zellen die Glykolyse als Hauptenergiequelle bevorzugen und nicht oxidative Phosphorylierung. Bei der mitochondrialen Atmung werden reaktive Sauerstoffspezies (ROS) ständig als Nebenprodukte erzeugt, sie können jedoch auch DNA-Schäden induzieren. Daher kann ROS wahrscheinlich auch schädlich für NBS Zellen unter physiologischen Bedingungen sein. Deshalb wurde die Hypothese aufgestellt, dass Antioxidantien oder Induktion von Pluripotenz in NBS Fibroblasten die durch ROS verursachte Genominstabilität umgehen könnte.

Das Ziel dieser Arbeit war es, eine zelluläres Modellsystem für NBS zu erstellen, um einige bekannte Probleme in der NBS Forschung zu überwinden: A) kleine Anzahl von Patienten, B) Zellkultur is limi-

tiert auf Fibroblasten und Lymphozyten, C) vorzeitige Seneszenz in der Zellkultur als Folge genomischer Instabilität, D) neue molekulare Mechanismen von NBS identifizieren, E) neue, therapeutisch relevante Konzepte entwickeln.

Das NBS Modell wurde durch Reprogrammierung von Fibroblasten von NBS-Patienten in iPS-Zellen unter Verwendung retroviraler Transduktion von OCT4, SOX2, KLF4 und C-MYC etabliert. Mit den somatischen und iPS-Zellen von NBS wurden globale Transkriptom-Analysen durchgeführt, um neue Phänotypen und Veränderungen in molekularen Signalwegen der NBS-Zellen im Vergleich zu normalen Zellen identifizieren. Darüber hinaus wurde der Einfluß von oxidativem Stress, Mutagenen und Antioxidantien auf die genomische Integrität der NBS-Zellen vor und nach der Reprogrammierung getestet.

Zu den Hauptergebnissen gehörte die erfolgreiche Reprogramierung der Fibroblasten von NBS Patienten in iPS-Zellen und die damit verbundene Umgehung von Seneszenz. Die Zellen exprimierten Pluripotenz assoziierte Proteine (Alkaline Phosphatase, OCT4, NANOG, TRA1-81, TRA1-60, SSEA4). Der Nachweis von Pluripotenz wurde *in vitro* durch EB-Assays und *in vivo* durch Teratom-Bildung bei Mäusen weiter gefestigt. Vergleichende Transkriptom- und Signalweg-Analysen zeigten, dass (a) NBS-Fibroblasten im Vergleich zu normalen Fibroblasten einen großen Einfluss auf die Regulation von Zellzyklus, Apoptose, TP53 und Fanconi-Anämie haben. (b) Der Vergleich von NBS-iPSCs und normalen hESCs zeigte veränderte Genregulation und Signalwege in DNA-Replikation, Glykolyse, Pyrimidin, Fructose und Mannose Stoffwechsel sowie in DNA-Reparatur. Bemerkenswert ist, das alle diese Wege bekannt sind, mit ROS-Homöostase verbunden zu sein. Die Empfindlichkeit gegenüber oxidativem Stress und Mutagenen (Wasserstoffperoxid, Bleomycin) war in NBS-iPSCs und NBS-Fibroblasten im Vergleich zu normalen Fibroblasten höher bei dem Mutagen Bleomycin, dagegen aber ähnlich bei exogener Zugabe von Wasserstoffperoxid. Interessanterweise wurden durch Wasserstoffperoxid erzeugte DNA-Schäden effizient durch Zugabe von EDHB, einem Aktivierer des Hypoxie-Signalwegs (HIF-pathway) reduziert.

Die Ergebnisse zeigen, dass die NBS-iPS-Zellen als hervorragendes Modell für *in vitro* Studien dienen können. Es wäre auch ein gutes Modell, um die DNA-Reparatur und Zellzyklus-Checkpoint-Regulierung zu studieren, besonders weil nur eine spezielle funktionelle Domäne beeinträchtigt ist. Dies könnte bei der Aufklärung der Mechanismen, die der Krankheit zugrunde liegen, unterstützen und könnte durch Drug-Screening auch die Behandlungsmöglichkeiten erweitern, was Lebenserwartung und Lebensqualität für die Patienten und Patienten mit ähnlichen Krankheiten verbessert.

CONTENTS

LIST OF FIGURES

LIST OF TABLES

SEMANTICS

Å	Ångström
°C	degree Celsius
%	Percentage
g	gram(s) / gravity
mg	milligram(s)
µg	microgram(s)
ng	nanogram(s)
h/hr/hrs	hour(s)
min	minute(s)
kDa	kilo Daltons
M	mol per liter
mM	millimol per liter
µM	micromol per liter
ml	milliliter(s)
mm	millimeter(s)
µm	micrometer(s)
nm	nanometer(s)
mA	milliampere(s)
V	Volt(s)

ABBREVIATIONS

8-oxoG	8-oxoguanine
BCA	bicinchoninic acid
BER	Base excision repair
BSA	Bovine serum albumin
CDK	cyclin-dependent kinase
CM	Conditioned medium
d.p.c.	days post-coitum
DAPI	4′,6-diamidino-2-phenylindole
ddH2O	Bi-distilled water

DDR	DNA damage response
dH2O	Distilled water
dHJ	double Holliday junction
DMEM	Dulbecco's Modified Eagle Medium
DNMT	DNA methyl transferase
dNTPs	Deoxynucleotide Triphosphates
DSBs	Double-strand-breaks
DSF	Disulfiram
E. coli	Escherichia coli
EB	Embryoid body
ECM	Extracellular matrix
EDHB	Ethyl 3,4-dihydroxybenzoate
ELISA	Enzyme Linked Immunosorbent Assay
EMT	epithelial-to-mesenchymal transition
ER	Endoplasmatic reticulum
ESC	Embryonic stem cells
FA	Fanconi anemia
FACS	Fluorescence assisted cell sorting
FSC	Forward Scatter
GA	Gallic acid
gDNA	Genomic DNA
GOI	Gene of interest
HDACs	histone deacetylases
hESC	Human embryonic stem cells
HFF1	Human foreskin fibroblasts 1
hPSC	Human pluripotent stem cells
HR	Homologous recombination
HRR	Homologous recombination repair
ICLs	interstrand cross-links
ICM	inner cell mass
iPSC	Induced pluripotent stem cells
IR	ionizing radiation
KO-DMEM	Knockout- Dulbecco's Modified Eagle Medium
LCLs	lymphoblastoid cell lines
MCS	Multiple cloning site
MEFs	Murine embryonic fibroblasts
MET	mesenchymal-to-epithelial transition
MGMT	methyl guanine methyl transferase

NBN	NBS gene; Nibrin gene
NBS	Nijmegen Breakage Syndrome
NER	Nucleotide excision repair
NHEJ	Non-homologous end-joining
NSG	NOD scid gamma (mice)
O/S/K/M	OCT4, SOX2, KLF4, C-MYC
ORF	open reading frame
PA	Phoenix amphotropic 293
pH	potentia Hydrogenii
Poly I:C	Poly-iosinic-polycytidylic acid
PTMs	post translational modifications
SDS PAGE	sodium dodecyl sulphate polyacryamide gel electrophoresis
SOD	superoxide dismutase
SSA	Single strand annealing
SSBs	Single-strand-breaks
SSC	Side Scatter
ssDNA	single stranded DNA
ssRNA	Single stranded ribonucleic acid
STAP	stimulus-triggered acquisition of pluripotency
TFBS	transcription factor binding site
TU	transducing units
UM	Unconditioned medium
UV	ultraviolett
w/o	without

Part I

INTRODUCTION

1 INTRODUCTION

1.1 NIJMEGEN BREAKAGE SYNDROME

1.1.1 *Overview*

Nijmegen Breakage Syndrome (NBS) is a rare autosomal recessive congenital disease which is caused by a mutation in the NBS gene, NIBRIN (NBN). The disease was discovered in 1981 by Weemaes *et al.* at the University of Nijmegen in the Netherlands and was hence named accordingly. The characteristics of the disease which affects DNA repair and signaling, include genomic instability (resulting in early onset of malignancies), premature aging, microcephaly and other growth retardations, immune deficiency, impaired fertility and puberty in females. Microcephaly is usually the most striking symptom and is used as a diagnostic tool to initiate further tests to verify the disease in newborn infants or young children (Figure 1 on page 3). There are several diseases with similar characteristics of which NBS must be clinically defined, called Fanconi Aneamia, LIG4 syndrome, Bloom syndrome, NBS-like disorder, ataxia-telangiectasia-like disorder, NHEJ1 syndrome and Seckel syndrome, which all derive from mutated genes in DNA repair pathways.

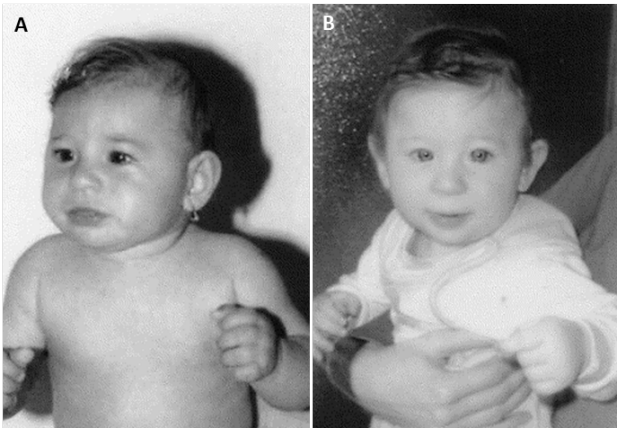

Figure 1: **Facial phenotype in NBS**
(A) Girl at the age of 7 months with head circumference at the time was 35.5 cm (well under the third percentile). Note the typical facial characteristics of NBS: prominent midface, oblique eyelids, retromandibula, large ears. (B) Boy at the age of 7 months with head circumference at that time was 36 cm. Note small receding chin, large ears, prominent midface, and oblique eyelids. Source: Modified after (Seeman *et al.*, 2004).

The major consequence of NBS is the decrease in average life span. 40 % of patients develop cancer before the age of 20 years, which is together with infection, the most likely cause of death. The oldest known survivors died at the ages of 53, 33 and 31 years (International Nijmegen Breakage Syndrome Study Group, 2000).

Mutations in the NBS gene (NBN, NIBRIN) are estimated to affect 1 in 100.000 worldwide, but show much higher frequencies in Poland, Czech Republic, Ukraine (1:177) (Varon *et al.*, 2000) and Germany (1:866) (Carlomagno *et al.*, 1999). The most frequent mutation (> 90 % of all cases) causing NBS, is a 5 base pair deletion (657del5) in the NBN gene (Chr. 8, band q21), causing a truncation of the wild type protein (p95-NIBRIN) into two distinct fragments (p26-NIBRIN, p70-NIBRIN, Figure 3 on page 5). Until today, there were ten other unique mutations found to affect the NBN gene (Figure 2 on page 4), but with much lower frequencies (Cerosaletti *et al.* (1998); Varon *et al.* (2006, 1998); Seemanová *et al.* (2006); Resnick *et al.* (2002); Maraschio *et al.* (2001)). All those mutations occour in the same region (exon 6 to 10) and lead to protein truncation, but no cases are known with total loss of NBN. In fact, it was shown in mice, that knockout mutations are lethal (Demuth *et al.*, 2004), but expression of the truncated version (p70-NIBRIN) is enough for survival. Even more, expression levels of the p70 variant correlated with frequency of cancer (Krüger *et al.*, 2007). An expression study of NBS in mouse embroys was performed to focus on the role of NBN in embryonic development (Wilda *et al.*, 2000), and a humanized mouse model was generated, which highlighted the important role of NBN in T-cell and oocyte development (Difilippantonio *et al.*, 2005).

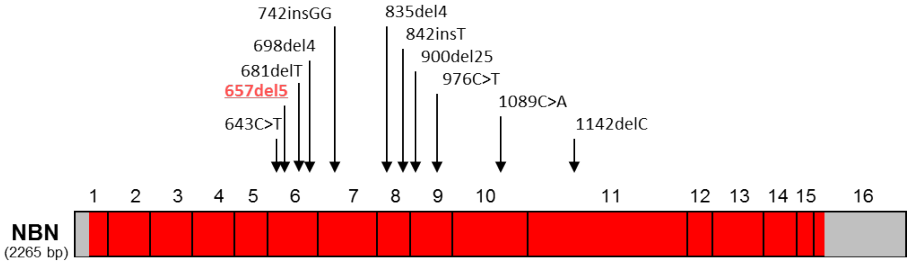

Figure 2: **NBN gene structure**
The exon structure of the gene is shown with the sites of mutations in NBS patients. The coding sequence is shown in red, untranslated regions (UTR) in grey. Legend: ">" base pair exchange; "del" deletion; "ins" insertion.

1.1.2 *NBN Gene and Protein Structure*

The NBN gene (NBS1, NBN, NIBRIN) consists of 16 exons and spans a DNA region of more than 50 kilobases on chromosome 8 and was initially cloned by (Varon *et al.*, 1998). NBN was found expressed ubiq-

uitously in all tissues and with high expression in testis (Matsuura *et al.*, 1998). The translated product consists of 754 amino acids and folds into one FHA, two BRCT domains and C-terminal part which consists of a nuclear localization signal and binding sites for MRE11 and ATM to form the MRN complex in the nucleus. It also has various sites which can be phosphorylated or ubiquitinated in response to DNA damage as depicted in Figure 3 on page 5. There are also sites that are acetylated by PCAF and p300 (inhibiting NBN phosphorylation) which is counteracted by SIRT1 (Yuan *et al.*, 2007). Further post-translational modification can be viewed at www.phosphosite.org. The 657del5 mutation causes translation into two distinct fragments by premature termination at codon 219 (p26) and alternative initiation from two cryptic ATG start codons within the NBS1-ORF that are brought into frame by the 5-bp deletion in NBN 657del5 mRNA (p70) (Maser *et al.*, 2001a). Recent studies on NBN identified binding partners that require the FHA and BRCT domains, which indicates the distinct functions of NBN, especially in NBS (see Table 2 on page 6). A very recent publication reported various new potential binding partners by immunoprecipitation, separation and subsequent MS/MS protein identification, specific to the full-length NBN and the fragments p26 and p70 (Cilli *et al.*, 2014).

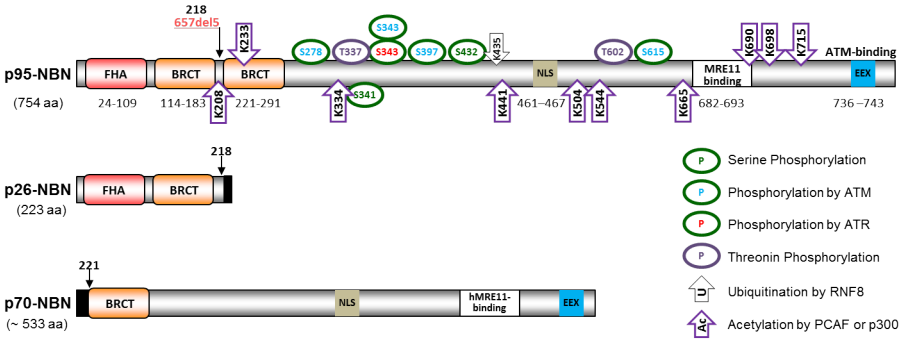

Figure 3: **Post-translational modifications of NIBRIN**
The location of the FHA and BRCT domains within the protein sequence of NBN is indicated by the range of amino acids (aa). The binding sites for MRE11 and ATM are located at the C-terminal end of NBN. Various sites for post-tranlational modifications are indicated by circles or arrows depending on the nature of the modification and the signs are labeled with number and one letter code for the modificated amino acid. The location of the 657del5 mutation starts after amino acid 218. The amino acid sequence of the truncated product p26 of the 657del5 mutation is identical with the wild type until aa 218, the p70 product has the identical sequence ranging from aa 221 to 754 (unidentical sequence = black filling). NLS: nuclear localization signal; EEX: EEXXXDDL motif for ATM-binding.

Table 2: **NBN interaction partners**

Gene	Binding Domain	Function	Reference
BRCA1	via RAD50	DNA repair signaling	(Zhong *et al.* 1999; Wang *et al.* 2000)
RAD50	via MRE11	DSB repair, MRN complex	(Desai-Mehta *et al.* 2001; Carney *et al.* 1998)
PARP1	FHA-BRCT (only p26)	p26 inhibitor of PARP1; DNA repair signaling	(Cilli *et al.*, 2014)
Lif1/LIG4	FHA-BRCT	NHEJ	(Williams *et al.*, 2009)
MDC1	FHA-BRCT	DSB repair signaling	(Williams *et al.*, 2009)
CtIP (=RBBP8)	FHA-BRCT	HR repair	(Yuan & Chen 2009; Williams *et al.* 2009)
γ-H2AX	FHA-BRCT	DNA DSB detection	(Kobayashi *et al.*, 2002)
TRF2 WRN	FHA-BRCT	Telomere maintanance	(Kobayashi *et al.* 2010; Zhu *et al.* 2000; Simonato *et al.* 1989)
DNMT1	FHA-BRCT	Regulation of heterochromatin status	(Hayashi *et al.*, 2013)
ATR/TRIP	FHA-BRCT	DNA damage response	(Olson *et al.*, 2007)
E2F1	FHA-BRCT	cell cycle progression	(Ren *et al.*, 2002)
TCOF1 Treacle	FHA-BRCT	Ribosomal RNA transcription in response to DNA damage	(Larsen *et al.*, 2014)
SP100	FHA-BRCT	Telomere maintanance	(Naka *et al.* 2002; Cilli *et al.* 2014)
53BP1	FHA-BRCT	DNA damage response	(Cilli *et al.*, 2014)
HSP90	FHA-BRCT	chaperone	(Cilli *et al.*, 2014)
MRE11	C-terminal	DSB repair, MRN complex	(Desai-Mehta *et al.*, 2001)
ATM	C-terminal	DNA damage response	(Falck *et al.*, 2005)
SIRT1	C-terminal	Deacetylation of NBN; DNA damage response	(Yuan *et al.*, 2007)
KPNA2	C-terminal	nuclear localization of NBN	(Tseng *et al.*, 2005)
mTOR Rictor SIN1	BRCT2 (221-402)	Akt activation, cell proliferation	(Wang *et al.*, 2013)
SMC1	BRCA1 dependent	part of cohesin complex	(Antoccia *et al.*, 2008)
ATF2		DNA damage response	(Bhoumik *et al.*, 2005)
HJURP		HR repair	(Kato *et al.*, 2007)
INTS3		sensor of ssDNA	(Huang *et al.*, 2009b)

1.1.3 *MRN Complex*

There is no function known of NBN as a monomere. Instead, all its functions take place in combination with MRE11 and RAD50, which is therefore called the MRN complex and is composed of two copies of each of the three proteins (see Figure 4 on page 8). Together they bind to DNA double strand breaks (DSBs) and are involved in repair and signaling for homologous recombination (HR), non-homologous end joining (NHEJ) and microhomology-mediated end joining (MMEJ). MRN is also present at replication forks and telomeres and plays key roles in preventing DSBs (Costes & Lambert, 2012; Ammazzalorso *et al.*, 2010).

"The MRN complex can be considered a flexible scaffold that acts as a combined sensor, signaling and effector complex via dynamic states that control biological outcomes to DSBs. MRN imparts three key functions critical for its diverse roles: 1) DNA binding and processing, 2) DNA tethering to bridge DNA over short and long distances, and 3) activation of DSB response and checkpoint signaling pathways. MRN structural architecture, separated into distinct "head", "coil", "hook" and flexibly attached adapter regions, underlies these roles. [...] These MRN assemblies and states are further impacted by post-translational modifications (PTMs), providing additional layers of complexity and regulation. Thus, MRN states in terms of shape, conformation, and interactions are information controlling its functions and biological outcomes."(Williams *et al.*, 2010)

MRE11 connects NBN and RAD50 and can directly bind to DNA, either bridging the two ends of DSBs or binding to single-ended breaks from replication forks. It has also DNA nuclease activity which restores blocked DNA ends for HR (Williams *et al.*, 2008).

RAD50 forms a long (~500 Å) extended anti-parallel coiled-coil which can bind to each other at the tip (in complex with Zn^{2+}) whithin one MRN complex or to a second MRN complex. This allows bridging of DNA up to 1,000 Å away on the sister cromatid (to enable HR) Lammens *et al.* (2011); Hopfner *et al.* (2002). RAD50 has regulatory ATPase and adenylate kinase activities, which are important for switching between inter- and intramolecular linking of the Zn-hooks (Hopfner *et al.*, 2000) and is affecting MRE11 nuclease activities in an NBN-dependent manner in eukaryotes (Paull & Gellert, 1999).

NBN is essential for localization of MRN to the nucleus, and works in tandem with RAD50 to regulate MRE11 nuclease activities. NBN also acts as a multimodal adapter, linking MRN to host of proteins that are phosphorylated as part of the DNA damage response (see Table 2 on page 6). The most crucial protein for the damage signaling cascade is the kinase ATM, which is recruited to MRN via NBN and the interaction with ATM is critical for MRN-dependent activation of ATM following DSBs (Lee & Paull, 2005).

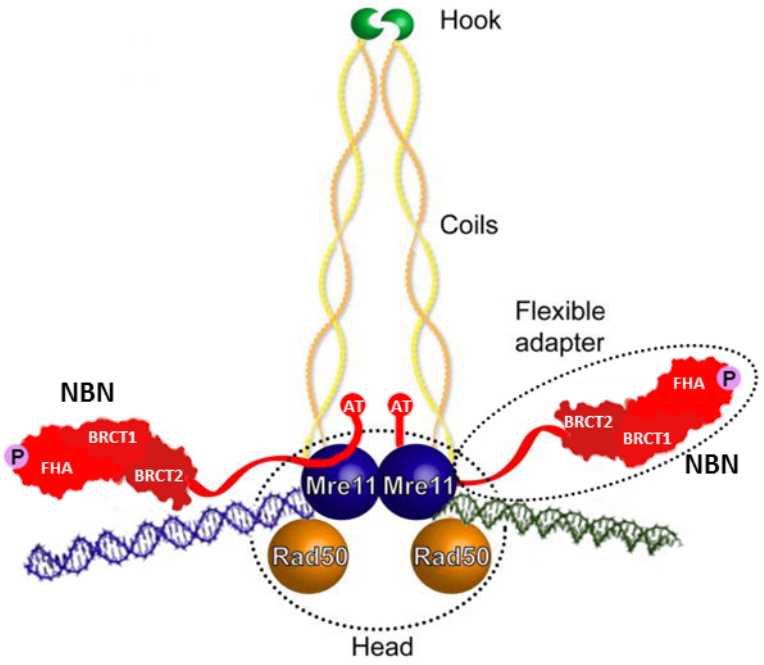

Figure 4: **MRN complex**
Model of MRN complex bound at a bridging DNA DSB. The flexible NBN C terminus links other DNA damage signaling proteins (e.g. ATM) to an MRE11-RAD50 hetero-tetrameric core complex. The complex can bind to a second complex on the sister chromatid via Zn-hooks (green) of RAD50. AT: ATM binding site; p: phosphorylation. Source: Modified after (Williams *et al.*, 2010) and (Williams *et al.*, 2009).

1.1.4 *NBN Signaling*

Even though NBN has no enzymatic function itself, it is a target for a variety of PTMs and plays an important role as adaptor protein, that helps to recruit different sets of proteins depending on the (damage) situation and modulates the enzymatic actions of its partner MRE11. An overview of the distinct functions of NBN in complex with MRE11 and RAD50 is given in Figure 5 on page 9.

In its function as a DNA damage sensor, NBN is one of the very early proteins that accumulate at the side of DNA breaks, which can occur via DNA binding by MRE11, but NBN was also reported to bind phosphorylated histone H2AX (γ-H2AX) via the FHA-BRCT domain directly, or via MDC1 Kobayashi *et al.* (2002); Chapman & Jackson (2008). Once bound to the damage site, NBN recruits ATM Lim *et al.* (2000); Lee *et al.* (2003), which is the key kinase to amplify and transduce the damage signal by phorphorylating various targets, including NBN, H2AX and TP53 (Khalil *et al.*, 2012) (for further targets see Figure 6 on page 10). ATM, which inactive form is a homodimer, becomes activated by autophosphorylation and transition into two active monomers (Bakkenist & Kastan, 2003). Depending on the kind

and severity of the damage and the cell cycle phase, the signaling can take several paths, resulting in checkpoint activation (and simultaneous repair), senescence or apoptosis (Czornak *et al.*, 2008). Also, the choice of HRR, NHEJ or MMEJ is dependent on the cell cycle phase and the character of break (SSB, DSB, clean end, dirty end) Andres *et al.* (2014); Shrivastav *et al.* (2007); Chapman *et al.* (2012). The MRN complex is involved in guarding the genomic integrity during S-phase by patrolling replication forks and detecting SSBs at stalled replication forks Bruhn *et al.* (2014); Lee & Dunphy (2013); Pichierri & Franchitto (2004). SSBs also induce cell cycle checkpoints but are primarily mediated by ATR instead of ATM (Figure 7 on page 10) (Ashwell & Zabludoff, 2008).

There are also non-pathological DNA breaks that occur in a controlled manner during V(D)J recombination and immunoglobulin class switching, which are influenced by NBN Deriano *et al.* (2009); Helmink *et al.* (2009); Dinkelmann *et al.* (2009).

As the telomeres at the end of chromosomes are structurally similar to a DSB, NBN plays a role in telomere maintenance which also involves TRF2, PML and parts of the NHEJ proteins and the MRN complex (Zhang *et al.*, 2006).

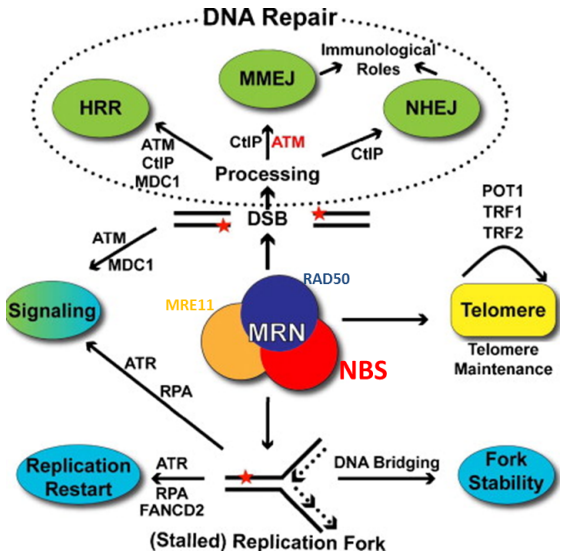

Figure 5: **NBN signaling overview**
The MRN complex acts as a sensor, signaler and effector to protect DNA ends and process DSBs. MRN senses DSBs and, in collaboration with CtIP, processes DNA ends before channeling into one of 3 distinct DNA repair pathways. MRN's MMEJ and NHEJ functions are also important for immunological roles during V(D)J and class-switch recombination. MRN is also associated with the replication fork and functions to stabilize forks through its DNA bridging activity and is involved in replication restart pathways. Red stars indicate DNA damage. Source: Modified after (Williams *et al.*, 2010)

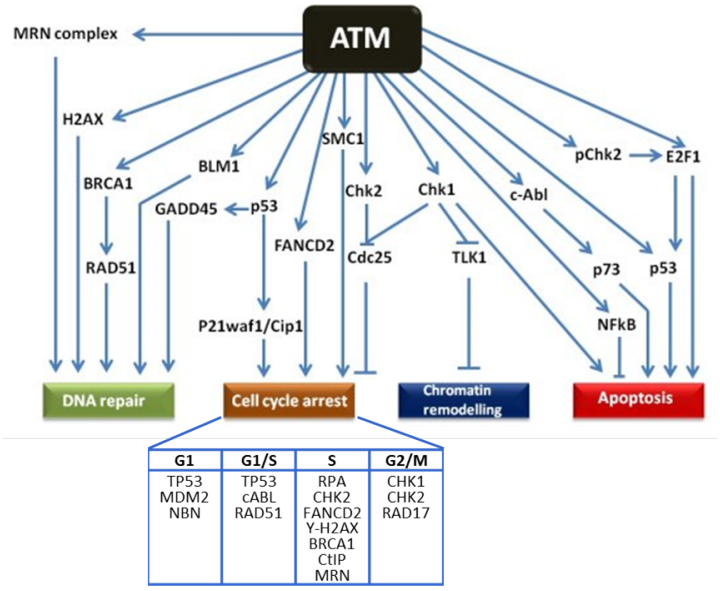

Figure 6: **ATM targets**
ATM is present at the core of DNA damage pathway, activated upon DSBs and functions via multiple routes. While great deal of cross-talk exists between individual pathways, its major downstream substrates for DNA repair are MRN complex, BRCA1, RAD51and, TP53, for cell cycle arrest are SMC1, CIP/KIP family of proteins via P53 and checkpoint kinases, for chromatic remodelling are CHK1 and for apoptosis are c-ABL, TP53, CHK2, E2F1, P73 and NFkB. Source: Modified after (Khalil *et al.*, 2012).

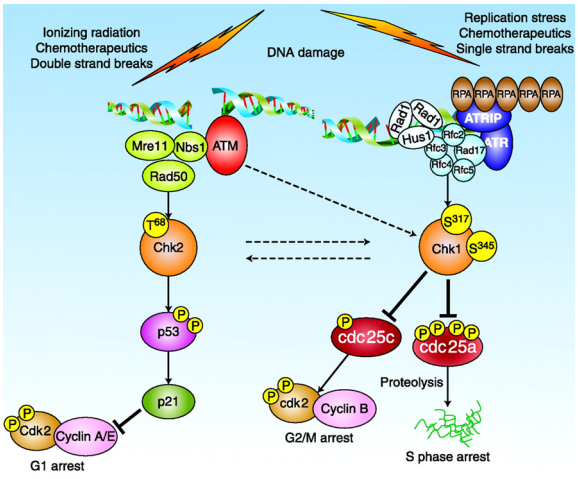

Figure 7: **Checkpoint activation by ATM and ATR**
CHK1 and CHK2 kinases are serine/threonine kinases that are activated by the ATM and ATR kinases in response to DNA damage. The G1 checkpoint is modulated primarily by the ATM-CHK2-P53 pathway, as expression of ATR, CHK1, and CDC25A is limited until the cell passes this restriction point. In S phase, the same cascade can result in an intra-S arrest in response to stalled replication forks. The G2-M checkpoint prevents entry into mitosis with unrepaired DNA lesions. Source: Modified after (Ashwell & Zabludoff, 2008).

1.2 CELL CYCLE

1.2.1 *Overview*

"Mammalian cell proliferation is controlled by a large number of proteins that modulate the mitotic cell cycle [...] [Figure 8 on page 12]. Progression through the cell cycle requires the activation of holoenzymes composed of a catalytic cyclin-dependent protein kinase (CDK) and the regulatory subunit cyclin. Specific CDKs are sequentially activated during different phases of the cell cycle by the oscillating synthesis and degradation of their cyclin partners. The activity of CDK/cyclins is also regulated by phosphorylation/dephosphorylation cycles and by their interaction with CDK inhibitory proteins (CKIs) of the Cip/Kip (CDK interacting protein/kinase inhibitory protein: $p21^{Cip1}$, $p27^{Kip1}$, $p57^{Kip2}$) and Ink4 (inhibitor of CDK4: $p16^{Ink4a}$, $p15^{Ink4b}$, $p18^{Ink4c}$, $p19^{Ink4d}$) families. (Vidal & Koff, 2000) All Cip/Kip proteins bind to and inhibit a wide spectrum of CDK/cyclin complexes, while the Ink4 proteins specifically inhibit cyclin D-associated CDKs. Mitogenic and anti-mitogenic stimuli affect the rates of CKI synthesis and degradation, as well as their redistribution among different CDK/cyclin heterodimers. In addition, other proteins, such as the transcriptional regulator p53, modulate the expression and function of CKIs to ensure that cells do not progress to the next phase of the cell cycle before appropriate conditions have been reached. CDK/cyclin activity modulates E2F/DP- and retinoblastoma protein (Rb)-dependent transcription of target genes involved in cell cycle control and DNA biosynthesis [...]. In non-proliferating cells, lack of CDK/cyclin activity leads to the accumulation of hypophosphorylated Rb, which binds to and inactivates the dimeric transcription factor E2F/DP. In proliferating cells, CDK/cyclin activation causes the accumulation of hyperphosphorylated Rb during late G1-phase, thus causing the release of E2F/DP and the transactivation of various target genes necessary for cell cycle progression." (Fuster *et al.*, 2010)

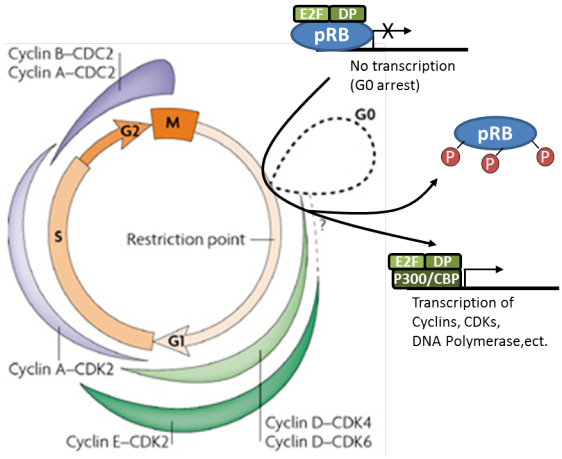

Figure 8: **Progression through the mammalian cell cycle**
The phases of a cell cycle are shown. Restriction point: the point after which cells are no longer responsive to extracellular signals and have committed to completion of the cell cycle. Quiescence or the Go phase is shown as an out-of-cycle state that cells might enter at a point in G1 before the restriction point (dotted loop). The phases of the cell cycle at which different cyclin-dependent kinase (CDK) complexes are active are also indicated. Source: Modified after (Coller, 2007).

1.2.2 *Cell Cycle Checkpoints*

The DNA can be affected by a variety of damage caused by intra- and extracellular sources (e.g. stalled replication forks, ionizing radiation, mutagens, ROS) resulting in base dimerization, oxidation, deamination, breaks of single and double strands and other damage (Andres *et al.*, 2014). While the cell can tolerate a certain amount of damage (cf. translesion-synthesis (Saugar *et al.*, 2014)) and maintain their function, accumulation of mutations or genomic aberrations may disrupt cellular functions and lead to senescence or apoptosis. In addition, proliferating cells, stem cells and germ cells have to maintain their genomic integrity, to prevent damage transmission to their daughter cells and to avoid tumorigenesis and disabilities in offspring. To deal with DNA damage, the cell (here focused on the mammalian cell) acquired a complex network of repair mechanisms, as described in more detail in the next chapter (Section 1.3). The most toxic and time consuming kind of damage to repair are chromosomal breaks. In order to repair them properly and prevent DNA damage to be passed on to the sister chromatids, the cell can initiate several delays during the cell cycle also called checkpoints. The checkpoints can also be initiated by other damage, oxidative stress or oncogenic activity (Campisi & di Fagagna, 2007). During all phases, checkpoints can be initiated by inhibition of cyclin/CDK complexes to prevent transition to the next phase. This is achieved with CDK inhibitory proteins (CKIs) of the Cip/Kip and INK4 families, which are activated by TP53 or mitogenic regulators (Figure 9 on page 13). NBN is part of the DNA dam-

age sensor and signal transducer proteins which result in activation of ATM, ATR and subsequent phosphorylation of many effector proteins responsible for DNA repair and checkpoint induction. Two of their targets, CHK1 and CHK2 (checkpoint kinase 1/2) play a major role in inducing checkpoints, by phophorylating and thereby destabilizing members of the CDC25 family. Without CDC25, CDK2 and CDC2 cannot be activated, which results in S-phase delay or G2/M arrest.

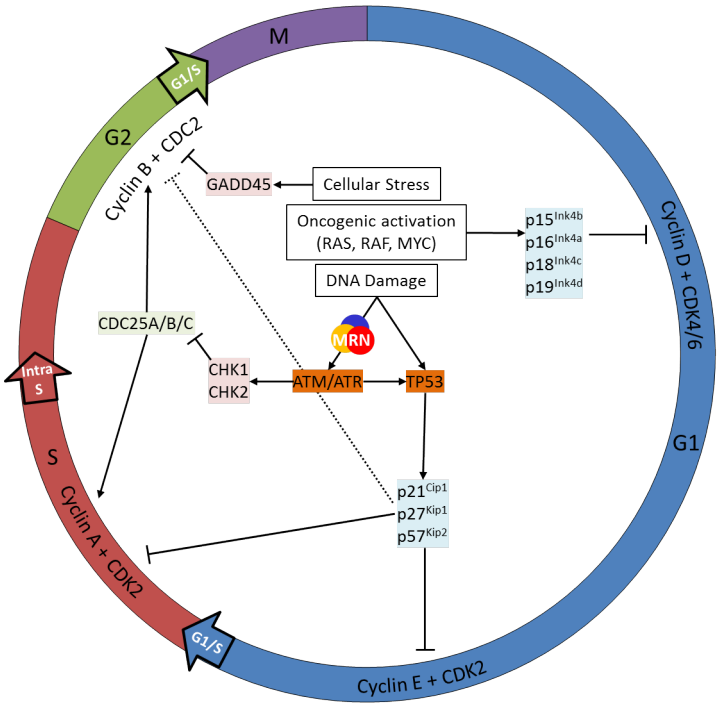

Figure 9: **Cell cycle checkpoints**
The progression of the cell cycle can be interrupted at specific checkpoints (G1/S, intra S, G2/M) which are induced by stress, oncongenes or DNA damage to increase time for repair or initiate apoptosis or senescense. The major mediators of signaling DNA damage to the effector proteins are ATM/ATR and TP53. The activity of CDK/Cyclins is regulated by their interaction with CDK inhibitory proteins (CKIs) of the Cip/Kip (CDK interacting protein/kinase inhibitory protein: $p21^{Cip1}$, $p27^{Kip1}$, $p57^{Kip2}$) and INK4 (inhibitor of CDK4: $p16^{Ink4a}$, $p15^{Ink4b}$, $p18^{Ink4c}$, $p19^{Ink4d}$) families. Some CDKs are usually activated by de-phosphorylation mediated by CDC25A/B/C. But CHK1 and CHK2 mediated phophorylation increases turnover speed of CDC25 family which in turn results in S-phase delay or G2/M arrest.

1.3 DNA REPAIR

1.3.1 *Overview*

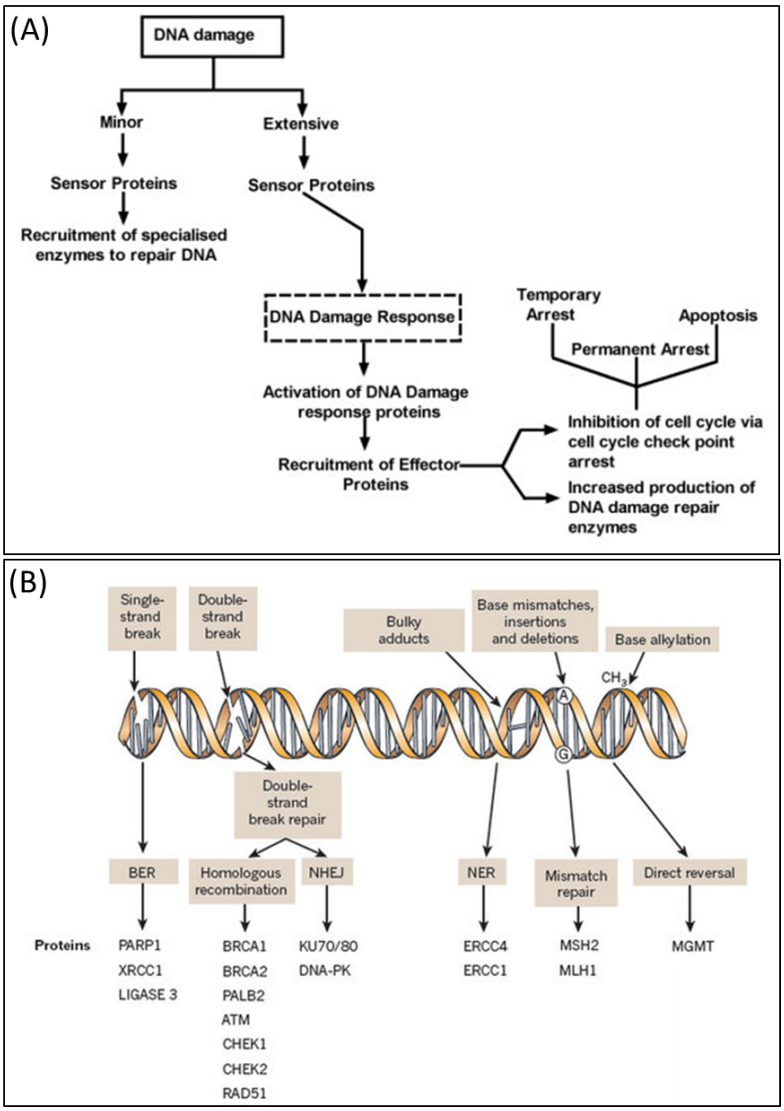

Figure 10: **DNA damage response**
(A) Depending upon the scale of DNA damage, one of the several cell fates are activated. (B) The choice of repair mechanism is largely defined by the type of lesion. Key proteins involved in each DDR mechanism, the tumour types usually characterized by DDR defects are shown. BER: base excision repair; NER: nucleotide excision repair; NHEJ: non-homologous end-joining. Source: Modified after (Khalil *et al.*, 2012) and (Lord & Ashworth, 2012).

DNA damage can have many forms and origins. One or few point mutations (depending on the location) might be tolerated, but a single DSB can be lethal for the cell (Blöcher, 1982). Statistically, DSB can occur as frequent as 50x per cell cycle (Vilenchik & Knudson, 2003). Therefore cells must have an efficient system to counter this damage.

In fact, the DNA Damage Response (DDR) is very fast, because most repair proteins are ubiquitously expressed and the response is executed by activation and deactivation of those proteins by PTMs (see Figure 6 on page 10, Figure 7 on page 10). The half-life of DSB repair can occur in little as 8 min for simple DSBs, but increases to more than one hour depending on the complexity of the break (Reynolds *et al.*, 2012).

Depending upon the complexity and scale of DNA damage, as well as status of the cell, different paths can be enacted to antagonize the problem. If the DNA damage is minor, sensor proteins are activated which recruit specialized DNA repair enzymes to the damaged site and DNA is repaired. However, if the DNA damage is extensive, the DDR pathways are activated. Specialized transducer proteins amplify the damage signal and activate effector proteins. The effector proteins cause cell cycle arrest and increase the production of DNA damage repair enzymes. The arrest at the cell cycle checkpoints may result in temporary halting of the cell cycle, a permanent arrest or induction of apoptotis (Figure 10 on page 14, A) (Khalil *et al.*, 2012).

Each form of DNA damage has its own form of repair mechanism (see Figure 10 on page 14, B). For damage concerning the single strand there are repair strategies like nucleotide excision repair (NER), which repairs bulky, helix distorting damage like thymine dimers (Schärer, 2013), Base excision repair (BER), which repairs damage to a single nitrogenous base (Dianov & Hübscher, 2013) and mismatch repair, which corrects errors that are not handled by proofreading and cleaves the newly synthesized DNA strand close to the region of damage (Brierley & Martin, 2013). In addition, methylation events of guanine bases can be directly reversed by the protein methyl guanine methyl transferase (MGMT). This is an expensive process because each MGMT molecule can be used only once (Kaina *et al.*, 2001). For repair of DSBs there are three major mechanisms: nonhomologous end joining (NHEJ), microhomology-mediated end joining (MMEJ, also alt-NHEJ), and homologous recombination (HR). In contrast to nucleotide-based repair, the pathway choice DSB repair is not only dependent on the chemical nature of the break, but also on the cell cycle phase as for HR, the repair pathway requires the template of the sister chromatid which is only available during G2 and late S phase (Shrivastav *et al.*, 2007). Here, I want to focus on the mechanisms of DSB repair, because NBN is primarily involved there.

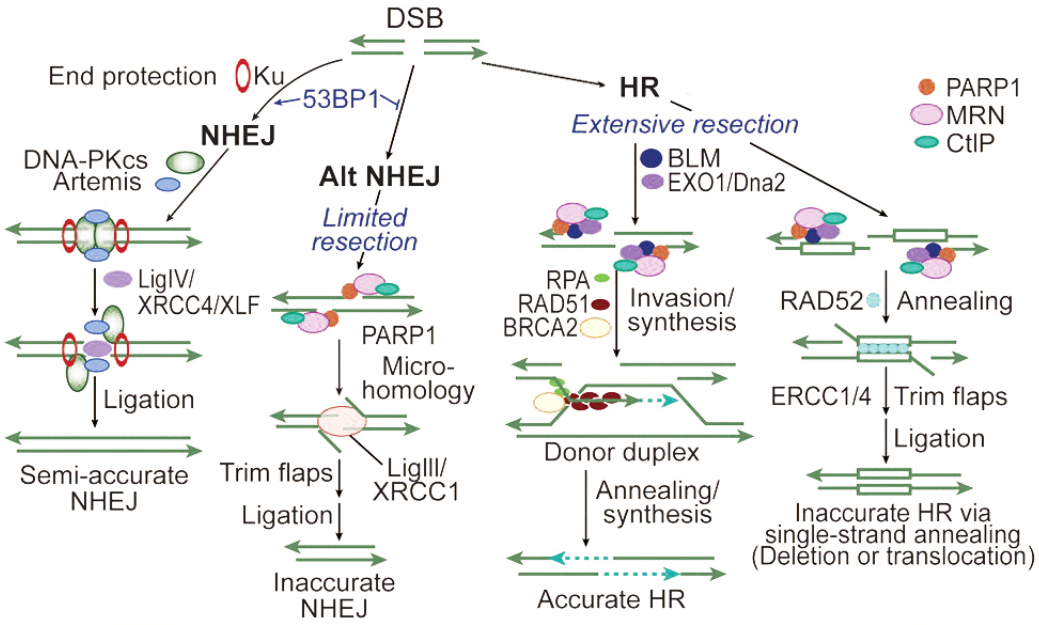

Figure 11: **DSB repair pathways**
"DSBs are repaired by 2 NHEJ and 2 HR subpathways. Classic NHEJ initiates with broken ends bound by Ku, which protects ends, leading to accurate or semi-accurate repair. Mutations in classic NHEJ factors shunt DSBs toward alternative NHEJ, which involves limited resection by MRN/CtIP and annealing via microhomology, yielding inaccurate repair. 53BP1 also serves to increase NHEJ accuracy by blocking MRN/CtIP resection. PARP1 promotes more extensive end-resection by EXO1 and BLM to reveal ssDNA and promote HR. RPA binds to ssDNA, BRCA2 mediates replacement of RPA with RAD51, the RAD51 nucleoprotein filament invades a homologous donor sequence (typically the sister chromatid in S/G2 phase), and repair synthesis extends the invading 3′ end, which then anneals with resected end to provide accurate repair. If long homologous repeats flank the DSB (white boxes), extensive resection can reveal complementary ssDNA that is annealed in a reaction promoted by RAD52, leading to deletion of one repeat and DNA between repeats, or translocations if DSBs occur on different chromosomes." Source: Modified after (Shaheen *et al.*, 2011).

1.3.2 *Homologous Recombination Repair (HRR)*

"[...] HRR requires intact homologous DNA sequences to remove DSBs and to faithfully restore the DNA sequence in their vicinity (San Filippo *et al.*, 2008). One form of HRR [...] [left branch of HR in Figure 11 on page 16] utilizes the sister chromatid as a donor for homologous sequence and is therefore active only in S and G2 phases of the cell-cycle Onn *et al.* (2008); San Filippo *et al.* (2008). In principle, HRR could also be carried out in diploid cells during the G1 phase of the cell-cycle using the homologous chromosome as template. However, the distinct compartmentalization of the nuclear domains of homologous chromosomes make required interactions unfavorable; in fact, it is thought that HRR is actively suppressed in G1 cells in an effort to

prevent loss of heterozygosity (LOH) Pâques & Haber (1999); Aylon & Kupiec (2004).

DNA end-resection is a necessary requirement for the initiation of HRR, as a long single-stranded 3´-DNA overhang has to be formed in order to start homology search (West, 2003). Activities implicated in diverse aspects of end-resection include the MRE11-RAD50-NBS1 (MRN complex), the CtIP, as well as Exonuclease 1 (EXO1), DNA2, and the Bloom's syndrome helicase (BLM) [...]. In order to execute their function during HRR initiation, the MRN complex is quickly recruited to DSB, where it cooperates with CtIP to promote end-resection Sartori *et al.* (2007); Kousholt *et al.* (2012); Leslie (2013). [...]

The combined action of DNA end-resection enzymes results in the formation of single-stranded DNA, decorated by the replication protein A (RPA). [...] In the subsequent steps of HRR, RPA is replaced by RAD51 recombinase [...]. The replacement of RPA by RAD51 requires the activity of mediator proteins, such as Breast cancer susceptibility gene 2 (BRCA2) and a group of five RAD51 paralogs (RAD51B, RAD51C, RAD51D, XRCC2, and XRCC3), which share 20–30% sequence similarity with the RAD51 recombinase (West, 2003). [...]

In the subsequent steps of HRR, the RAD51 nucleoprotein filament invades the intact double-stranded DNA molecule to search for homologous sequences and form a structure termed displacement loop (D-loop). When homology is found (synapsis) DNA synthesis will start elongating the 3´-end of the invading strand [...]. For elongation to commence, RAD51 in the synaptic complex has to be removed from the very 3´ tip of the invading strand to reveal the 3´-OH group for priming; this reaction is facilitated by RAD54 and its interacting partner RAD54B (Li & Heyer, 2009). HRR can take several different routes from this point. Frequently, elongation of the invading 3´-end can continue over a limited distance, followed by displacement of the newly synthesized stretch and re-ligation with the original DNA end resulting in the repair of the DSB (synthesis-dependent strand annealing; SDSA) [...]. This is the most frequent event during DSB repair in cells of higher eukaryotes and is equivalent to gene conversion. Alternatively, second end-capture can occur, leading to the formation of a double Holliday junction (dHJ) [...]. Depending on the resolution of the dHJ by specialized resolving enzymes, GEN1 and possibly MUS81/EME1, this branch of HRR will result in either crossover or non-crossover (gene conversion) outcomes Constantinou *et al.* (2002); Wu & Hickson (2003); Ip *et al.* (2008) [...].

First reported in yeast and later in higher eukaryotes, recombination events between areas of homology present in the same DNA molecule could be observed. This process is known as [single strand annealing] SSA (Ivanov *et al.*, 1996) [right branch of HR in Figure 11 on page 16]. When this pathway is used to repair a DSB it leads to loss of the DNA segment between the regions of homology and there-

fore it is considered as mutagenic. [But] the role of SSA in the repair of randomly induced DSBs, such as those generated by IR, remains uncharacterized and is likely to be small." (Mladenov *et al.*, 2013)

1.3.3 *NHEJ*

Non-homologous end-joining (NHEJ, or D-NHEJ) "catalyzes a simple rejoining reaction between two DNA ends irrespective of their origin (Lieber, 2010) and does not require homology at the ends or elsewhere; these facts render NHEJ operational throughout the cell-cycle. Indeed, D-NHEJ is active in all phases of the cell-cycle, where it removes DSBs from the genome with similar efficiency, but possesses only limited functionality for single-ended DSBs that arise during replication Metzger & Iliakis (1991); Rothkamm *et al.* (2003); Helleday *et al.* (2007).

The key steps of the classical form of NHEJ are summarized in [Figure 11 on page 16]. The high affinity of KU heterodimer for free DNA ends (1–10 × 10–9 M, depending on the DNA end-structures), makes it the ultimate initiation factor of this repair pathway (Arosio *et al.*, 2002). [...] The binding of KU to DSBs blocks nucleolytic processing of DNA ends, which is required for the initiation of other DSB repair pathways [...]. [...] the essential role of KU during NHEJ is to recruit the catalytic subunit of the DNA-PKcs, which dominates and drives the repair of DSBs in cells of higher eukaryotes. [...]

The binding and dimerization of DNA-PKcs immobilizes the two DNA ends and thus facilitates the rejoining reaction (Meek *et al.*, 2004). The interactions of DNA-PKcs with KU, as well as the binding of DNA-PKcs to the DNA result in almost 10-fold increase in DNA-PKcs kinase activity. Accumulating evidence shows that a variety of proteins specifically involved in D-NHEJ, or generally in the DNA damage response (DDR), are phosphorylation targets of DNA-PKcs. [...] Depending on the nature of DNA lesions, DNA-PKcs can be phosphorylated at multiple residues, which is a prerequisite for its dissociation from the damaged sites and the recruitment of other repair factors [Figure 11 on page 16]. [...]

The final step during D-NHEJ is mediated by a highly specialized ligation complex consisting of DNA Ligase 4 (LIG4) and the X-ray cross complementing 4 (XRCC4) protein (LIG4/XRCC4) [...]. Assisted by the auxiliary factor XLF (Cernunnos, [NHEJ1]), LIG4/XRCC4 mediates ligation that results in fast and efficient restoration of DNA integrity, albeit often at the cost of sequence information loss." (Mladenov *et al.*, 2013)

1.3.4 *MMR / alt-NHEJ / B-NHEJ*

There are several terms for repair pathways in addition to HR and NHEJ, which overlap in the participating proteins, but vary in the regulation mechanism and micro-homology requirements. The pathways are termed micro-homology mediated end-joining (MMR, (McVey & Lee, 2008)), alternative NHEJ (alt-NHEJ, (Hefferin & Tomkinson, 2005)), or backup NHEJ (B-NHEJ, (Mladenov *et al.*, 2013)). Here, I refer only to B-NHEJ, which will cover the basic mechanism.

"This alternative form of DSB repair efficiently substituted for D-NHEJ, but appeared to have backup functions, coming to the fore mainly after failure of D-NHEJ; therefore the term B-NHEJ was proposed for this repair pathway Iliakis (2009); Mladenov & Iliakis (2011). [...] Subsequent work documented the function of such alternative pathways of NHEJ in several processes involving the formation of DSBs, such as V(D)J recombination and class switch recombination (Corneo *et al.*, 2007), and were also implicated in cancer formation (Simsek *et al.*, 2011). [...]

A major protein implicated in B-NHEJ is poly (ADP-ribose) polymerase 1 (PARP-1), which plays a main role in the repair of SSBs [...] and which may effectively compete with KU heterodimer for DNA end-binding (Wang *et al.*, 2006). [...] It has also been reported that B-NHEJ benefits from microhomology at the break sites, which may be best found if the DNA ends become resected. Indeed, MRE11 and C-terminal binding protein 1 interacting protein (CtIP), both involved in DNA end-resection during HRR [...], were found to facilitate B-NHEJ Zha *et al.* (2009); Lee-Theilen *et al.* (2011). [...] A ligation activity finalizing B-NHEJ is DNA Ligase 3 (LIG3), a versatile ligase, which in complex with XRCC1 also participates in the repair of SSBs and DNA base damages Wang *et al.* (2005); Della-Maria *et al.* (2011). Assisted by its unique structural properties, LIG3 ensures the ligation of both DNA strands during DSB repair (Ellenberger & Tomkinson, 2008). [...] Backup NHEJ is much slower than D-NHEJ and is highly error-prone causing translocations and other genomic rearrangements with high probability. Moreover, a high number of B-NHEJ associated genetic rearrangements have been observed in chromosomal translocations associated with both spontaneous and therapy-related cancers (Greaves & Wiemels, 2003)." (Mladenov *et al.*, 2013)

NBN specifically, might play an important role in the pathway choice between HRR and NHEJ as suggested by a recent review by (Panier & Boulton, 2013) on HRR and 53BP1. Wether 53BP1 is bound to the chromatin or not seems to determine the possibility for extensive resection which is required for HRR. The interaction of NBN with CtIP, which is mediated via FHA-BRCT domains of NBN, enables phosphorylation of CtIP and BRCA1 by CDKs (thereby linked

to the cell cycle) which inhibits 53BP1 in an yet unknown manner (see Figure 12 on page 20).

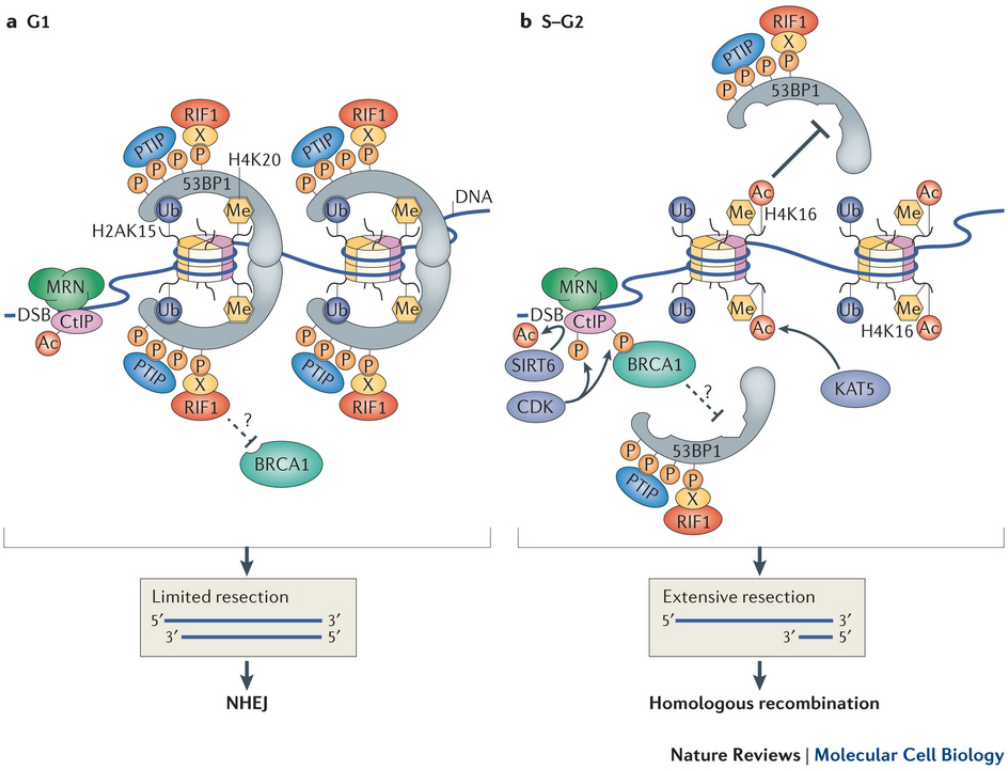

Figure 12: **Connection between NBN, 35BP1 and DSB pathway choice** p53-binding protein (53BP1), ubiquitylated Lys15 of histone 2 (H2AK15ub), dimethylated H4K20 (H4K20me2), RAP1-interacting factor 1 (RIF1), PAX transactivation activation domain-interacting protein (PTIP), ataxia-telangiectasia mutated (ATM), breast cancer 1 (BRCA1), MRE11–RAD50–NBS1 (MRN), cyclin-dependent kinase (CDK), Lys acetyltransferase 5 (KAT5), acetylation of H4K16 (H4K16ac), deacetylase sirtuin 6 (SIRT6), CtBP interacting protein (CtIP). Source: Modified after (Panier & Boulton, 2013).

1.4 REACTIVE OXYGEN SPECIES (ROS)

Reactive oxygen species (ROS) is a description for a variety of molecules and free radicals derived from molecular oxygen, including superoxide anions ($O_2^{-}\bullet$), hydroxyl radicals (OH•) and hydrogen peroxide (H_2O_2). Some of these species, such as superoxide or hydroxyl radicals, are extremely unstable, whereas others like hydrogen peroxide are freely diffusible and relatively long-lived (Finkel & Holbrook, 2000).

ROS can be generated from external sources like radiation (UV light, gamma- and X-rays), byproducts of alcohol metabolism (Bondy, 1992), ozone (O_3), cytokines, growth factors, chemotherapeutic agents, hyperthermia, smoking and other toxins (Ozbek, 2012).

The majority of intracellular ROS production is generated as a result of normal metabolism in mitochondria. The production of mitochondrial superoxide radicals ($O_2^{-}\bullet$) occurs primarily at complex I (NADH dehydrogenase) and at complex III (ubiquinone-cytochrome c reductase) while under normal metabolic conditions, complex III is the main site of ROS production (Turrens, 2003). The superoxide anion is the precursor of most ROS and a mediator of oxidative chain reactions but can be neutralized by dismutation (either spontaneously or through a reaction catalysed by superoxide dismutases), that produces hydrogen peroxide, which in turn may be fully reduced to water. H_2O_2 can also become partially reduced to a hydroxyl radical (OH•) which is one of the strongest oxidants in nature (Liochev & Fridovich, 1999). Reactive free radicals such as OH• are especially dangerous, because they can also start a chain reaction of lipid peroxidation (Halliwell, 2005).

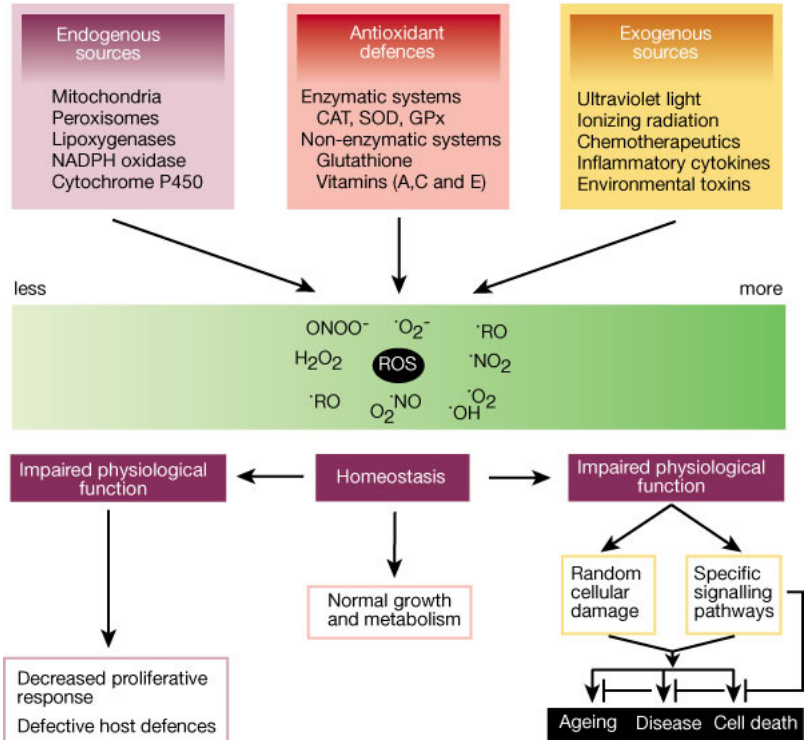

Figure 13: **Reactive oxygen species (ROS) in the cellular system** ROS homeostasis is affected by contributers to oxidative stress from intracellular and extracellular sources and the antioxidant defence system. Disturbance of ROS homeostasis can result in cellular damage until arrest, disease, tumorigenesis and apoptosis, or misregulation of ROS-dependent pathways. Source: Modified after (Finkel & Holbrook, 2000).

To maintain a physiological balance, ROS production is counteracted by a complex antioxidant defence system that includes enzymatic scavengers like superoxide dismutases (SOD), catalase, glutathione peroxidase and thioredoxins. The family of superoxide dismutases converts superoxide to hydrogen peroxide, whereas catalase and glu-

tathione peroxidase convert hydrogen peroxide to water (Halliwell, 2005). Thioredoxins function by a basic catalytic mechanism, in which an active-site cysteine (the peroxidatic cysteine) is oxidized to a sulfenic acid by the peroxide substrate (Wood *et al.*, 2003).

Cells use or produce also non-enzymatic, low molecular mass antioxidants like ascorbate, pyruvate, flavonoids, carotenoids and perhaps most importantly, glutathione, which is present in millimolar concentrations within cells (Barhoumi *et al.*, 1993).

ROS can also be regulated by changes in metabolism, because its primary intracellular source is through respiration by the mitochondria. Under hypoxic conditions, the cells can switch from respiration (via tricarboxylic acid cycle) to anearobic glycolysis (mitochondria-independent) as the primary energy source (Kim *et al.*, 2006). Hypoxia-inducible factor 1 (HIF-1) is a transcription factor that regulates the oxygen homeostasis and is constantly destabilized by hydroxylation under normoxia. HIF-1 activity is induced in response to continuous hypoxia, intermittent hypoxia, growth factor stimulation, and Ca^{2+} signaling (Semenza, 2009). Hypoxia paradoxically leads to increased ROS at first (Guzy & Schumacker, 2006), but activation of the HIF pathway helps to decrease ROS levels (Kim *et al.*, 2006).

The balance between ROS production and antioxidant defences determines the degree of oxidative stress (Finkel & Holbrook, 2000). While a certain ROS level contributes to important physiological functions like signaling pathways and pathogen defence Ray *et al.* (2012); Rivera *et al.* (2013); Dickinson & Chang (2011), consequences of oxidative stress include modifications to cellular proteins, lipids and DNA. On the other hand, low levels of ROS are known to cause aneuploidy (Li & Marbán, 2010) and disrupt signaling pathways (Martin & Barrett, 2002). When the stress is severe, survival is dependent on the ability of the cell to adapt, or to resist the stress, and to repair (see Section 1.3) or replace the damaged molecules. Alternatively, cells may respond to the insult by undergoing apoptosis or senescence. The most widely studied oxidative stress-induced modification to DNA are guanines, which are oxidized to 8-hydroxyguanine. Oxidative damage to the DNA can also cause SSBs (as a result from base or sugar damage) and DSBs by blocking replication forks from progressing (Cox *et al.*, 2000) and other mechanisms (Woodbine *et al.*, 2011). ROS damage to proteins often creates carbonyl derivatives (Stadtman, 1992) and is removed by protein degradation in proteasomes and lysosomes, or repair by methionine sulfoxide reductases, the thioredoxin/thioredoxin reductase system and protein disulfide isomerases (Höhn *et al.*, 2013).

Several studies have shown, that ageing cells and organisms accumulate increased levels of oxidant-damaged nuclear DNA and mitochondrial DNA, the latter is generally considered to be even more sensitive to oxidative damage because of its proximity to the main

source of oxidant generation, or because of a limited DNA repair system (Finkel & Holbrook, 2000). Additionally, mitochondrial DNA does not contain histones, and therefore is less protected against oxidative stress than the nuclear DNA. This results in a 10- to 20- fold increase in the content of 8-hydroxyguanine, the product of guanine oxidation (Richter *et al.*, 1988).

In relation to stem cells, it has been shown that physiological levels of ROS are required to maintain genomic stability (Li & Marbán, 2010). In vitro cell culture is usually carried out at atmosphearic oxygen levels (21 %). In physiological oxygen levels (5 %), karyotypic abnormalities in primary human cardiac stem cells were suppressed, but addition of high-dose antioxidants to the medium unexpectedly increased aneuploidy. Antioxidants given at increasing concentration, decreased intracellular ROS monotonically, but DNA damage showed a biphasic response in stem cells, with a narrow concentration range for low DNA damage. High-dose antioxidants decreased cellular levels of the ATM (ataxia-telangiectasia mutated) and other DNA repair enzymes, providing a potential mechanistic basis for those effects (Li & Marbán, 2010).

1.5 HUMAN PLURIPOTENT STEM CELLS

1.5.1 *Human Embryonic Stem Cells (hESCs)*

Upon fertilization of the human oocyte the resulting totipotent zygote travels from the oviduct to the uterus, where it implants itself 7 days post-fertilization. During this pre-implantation development (see Figure 14 on page 24), the oocyte undergoes several symmetric and asymmetric mitotic cell divisions until formation of the morula, a compact sphere of 16 blastomeres. During the following compaction, these roundish daughter cells become bound tightly together with the formation of desmosomes and gap junctions. Five days post-fertilization the cells polarize and segregate into a thin outer layer of epithelium, the trophoblast, and the inner cell mass (ICM) to form the blastocyst, with a fluid filled cavity, that results from the active transport of sodium ions from trophoblast cells and osmosis of water. The surrounding trophectoderm cells, which express trophoblast markers such as BMP4, will later on give rise to the embryonic part of the placenta and other supporting tissues, whereas the embryo will arise from the OCT4, SOX2 and NANOG expressing, pluripotent ICM, or embryoblast (Adjaye *et al.*, 2005). A more detailed review on human pre-implantation embryogenesis can be found in the article of (Cockburn *et al.*, 2010).

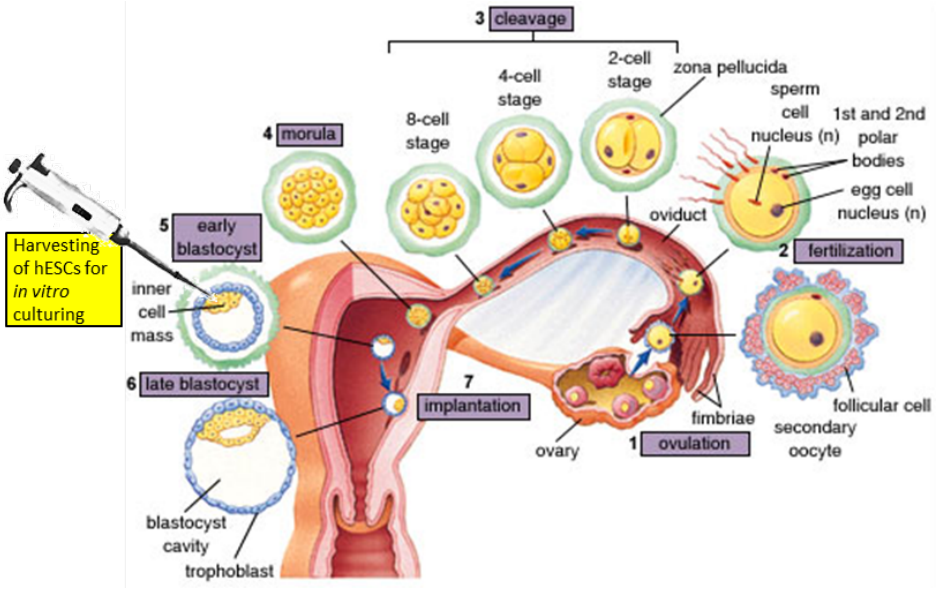

Figure 14: **Human embryonic pre-implantation development**
The stages of development during the first week and stage for extraction of hESCs from the inner cell mass (ICM) of the blastocyst. Source: Modified after http://ehumanbiofield.wikispaces.com. The original picture is licenced under a Creative Commons License.

(Thomson *et al.*, 1998) derived the first pluripotent human embryonic stem cells (hESCs) from the inner cell mass of surplus blastocyst stage embryos generated by in vitro fertilization. These cells maintain the potential to form derivatives of all three embryonic germ layers throughout prolonged undifferentiated proliferation in vitro, as characterized by staining for the cell surface markers SSEA-3, SSEA-4, TRA-1-60, TRA-1-81 and alkaline phosphatase (AP) as well as the formation of teratomas after injection of hESCs into immune-deficient mice in vivo (Thomson *et al.*, 1998). hESCs grow as flat, sharp-edged colonies, have a high nucleus to cytoplasmic ratio and express high levels of telomerase activity, enabling them to escape senescence and to self-renew indefinitely (Thomson *et al.*, 1998).

In vitro cultivation of embryonic stem cells enabled studies on the regulatory networks responsible for pluripotency and self-renewal. OCT4, SOX2 and NANOG were identified as the core transcriptional regulatory circuitry of hESCs by (Boyer *et al.*, 2005). According to their findings, these three proteins cooperate to establish auto-regulatory and feed-forward loops, thereby activating or repressing genes encoding components of distinct signaling pathways and developmental processes, chromatin regulators and regulatory miRNAs to shape hESC identity. Furthermore, various extracellular stimuli contribute to the maintenance of the undifferentiated hESC phenotype. One of the external signals that promotes this circuit, is the basic fibroblast growth factor (bFGF, or FGF2) which functions as a key component of

hESC culture medium Thomson *et al.* (1998); Amit *et al.* (2000); Greber *et al.* (2007).

1.5.2 *Induced Pluripotent Stem Cells (iPSCs)*

In the years preceding 2006, Takahashi and Yamanaka screened a library of 24 genes with essential roles in the maintenance of ESC identity, for their potential to induce pluripotency in somatic cells, leading to the groundbreaking achievement in stem cell biology and earning them acknowledgement through the Nobel Prize in 2012: They found that ectopic expression of a combination of four transcription factor genes, namely Pou5f1 (encoding Oct4), Sox2, Klf4 and c-Myc, was sufficient to reprogram mouse somatic cells back to an ESC-like developmental stage (Takahashi & Yamanaka, 2006) and confirmed their findings in human somatic cells in the following year (Takahashi *et al.*, 2007).

In the subsequent years, many studies were performed on these grounds and also identified critical steps in the mechanistics of reprogramming. One of the essential steps is the chromatin remodeling and the activation of the (before) methylated promoters of the core transcription factors OCT4, SOX2, NANOG for their self-substained feed-back loop (Do & Schöler, 2009). Another critical step in the process of cellular reprogramming is the suppression of epithelial-to-mesenchymal transition (EMT) and promotion of the reverse process, the mesenchymal-to-epithelial transition (MET), as shown for mouse cells of mesenchyme origin Li *et al.* (2010); Samavarchi-Tehrani *et al.* (2010); Liao *et al.* (2011).

In response to viral infection which is used to deliver the reprogramming factors, levels of reactive oxygen species (ROS) increased significantly, leading to DNA damage and ultimately to the activation of TP53 (Mah *et al.*, 2011). As part of the DNA damage response, TP53 is responsible for arresting the cell cycle, inducing apoptosis and senescence, which is counterproductive to the reprogramming process Mah *et al.* (2011); Marión *et al.* (2009). Hence, overcoming the TP53-mediated cell cycle arrest is a crucial step in acquiring the pluripotent state as was also shown in knock-down experiments by Marión *et al.* (2009); Kawamura *et al.* (2009).

In addition to several signaling mechanisms, also metabolic properties were found to influence cellular reprogramming. Findings from Prigione *et al.* (2011); Armstrong *et al.* (2010); Suhr *et al.* (2010) suggest, that the derivation of iPSCs is associated with a reconfiguration of mitochondria and bioenergetic metabolism. Oxidative phosphorylation is decreased in iPSCs, which is realized by increased glycolysis and lower mitochondrial activity, which also results in lower production of ROS Prigione *et al.* (2010, 2014). As these metabolic changes occur before the establishment of the human ESC-like properties they

are likely to be essential for the process of cellular reprogramming (Folmes *et al.*, 2011).

Since the first reprogramming reports, which employed retro virus to deliver the reprogramming factors, many alternative methods have sprouted to replace virus-based methods because of their transformation potential. The ultimative goal is a xeno-free process, which is only dependent on small molecules, to make iPSCs saver for clinical applications. A detailed review on the current methods on reprogramming can be found in my article Tavernier *et al.* (2013) and is also discussed in 4.1.2.2.

1.5.3 *Pluripotent Stem Cells in Regenerative Medicine and Disease Modeling*

Even today there many diseases which are treated by relieving the symptoms, but cannot be cured, because the origin is based on a loss of tissue (e.g. type-I diabetes) or mutations (e.g. leukemia). Modern medicine has already successfully established therapies which target diseases at the source, by replacing diseased tissues with transplantation of healthy cells like autologous and allogenic bone marrow transplantation for leukemia patients. But the access to specialized human cell types, which can be obtained from biopsies and have to go to the stress of expansion and implantation, is limited. Also, some cells types are nearly impossible to obtain from living donors, like neuronal cells or tissues. All this types of therapies which replace or regenerate human cells, tissue or organs to restore or establish normal function are summarized by the term regenerative medicine (Mason & Dunnill, 2008).

One solution for the limited availability of specialized cells are several kinds of so called adult stem cells, which reside in their particular tissue or organ of origin to contribute to homeostasis and repair. They are thought to be applicable in the treatment of various disorders as reviewed by (Mimeault *et al.*, 2007). Their differentiation potential, however, is generally restricted to certain lineages and some have reported decreased differentiation potential and limited proliferation capacities of adult stem cells maintained in vitro Banfi *et al.* (2000); Glimm *et al.* (2000); Baxter *et al.* (2004); Wagner *et al.* (2008). Therefore, the limitations in availability of most specialist somatic cells and the restriction in adult stem cell cultivation, drives a great interest in pluripotent stem cells (hESCs and iPSCs) which have the ability to replicate indefinitely and to develop into derivates of all three primary germ layers, which means any cell type of the embryo, fetus and adult. The first clinical trials involving hESC-derived, specialized cell types have already started since 2010 (Alper, 2009), but with mixed results concerning their efficiency and safety Lee *et al.* (2013); Schwartz *et al.* (2012). Healthy, diseased and genetically modified hESCs can

also be used for drug discovery, pre-clinical drug testing and toxicity tests, as well as the opportunity to model diseases in a dish Thomson *et al.* (1998); Maury *et al.* (2011).

But there are enormous ethical and practical concerns associated with hESC handling. First, to derive hESC lines destruction of human pre-implantation embryos is necessary and second, immune rejections can occur if non-autologous hESCs are transplanted.

After the discovery of reprogramming human somatic cells back to full pluripotency by (Takahashi *et al.*, 2007), there was a solution to address both problems. Because human iPSCs are nearly identical to hESCs, they are considered as equally potent for studies of differentiation processes, drug discovery, pre-clinical drug testing, toxicity studies and repair and replacement of impaired tissues. The fact that iPSCs could potentially be derived from ethically safe biopsies is one of the main advantages of human iPSCs over hESCs. At the same time, derivation of iPSCs from virtually any individual is feasible and therefore also solving immune rejection concerns. Meanwhile, a number of human iPSC lines have been generated from patients suffering from a variety of diseases. Table 3 on page 28 shows selected disease models of iPSCs, which have been shown to possess some disease phenotype in vitro (Sterneckert *et al.*, 2014). An updated overview of the worldwide established human iPSC lines (and hESCs) with a focus on genetic disorders, can be viewed at the International Stem Cell Registry.

However, before human iPSCs play a role in clinical studies and treatments, it will be essential to obtain a more detailed understanding and control of the molecular processes involved in cellular reprogramming. We also have to establish efficient reprogramming techniques, which do not interfere with the genetical integrity of the cells in order to make it save in clinical applications.

Table 3: **Subset of published human iPSC disease models.** Modified after (Sterneckert *et al.*, 2014).

Disease	Mutant locus
A1AT deficiency	A1AT
Amyotrophic lateral sclerosis and frontotemporal dementia	Sporadic
	C9orf72
	PGRN
	SOD1
	TARDBP
Alzheimer's disease	Sporadic
	APP
	PS1 or PS2
	Trisomy 21
Beta-thalassemia and sickle cell disease	HBB
Chronic granulomatous disease	NADPH oxidase
Catecholaminergic polymorphic ventricular tachycardia	CASQ2
	RYR2
hCMV infection	Wild type
Familial hypercholesterolemia	LDLR
Fragile X syndrome	FMR1
Glycogen storage disease	G6PC
Hepatitis C virus infection	Wild type
Huntington's disease	HTT
Long QT syndrome	KCNH2
	KCNQ1
	SCN5A
Marfan syndrome	FBN1
Myeloproliferative disorder	JAK2 (somatic)
Pancreatic ductal adenocarcinoma	Multiple (somatic)
Parkinson's disease	Sporadic
	LRRK2
	PARKIN
	PINK1
	SNCA
Pompe disease	GAA
Pulmonary alveolar proteinosis	CSF2R
Rett syndrome	MECP2
Schizophrenia	Familial cases, but unknown gene(s)
Spinal muscular atrophy	SMN1
Timothy syndrome	CACNA1C
Wilson's disease	ATP7B

1.6 AIM OF THIS WORK

NBS is a rare disease, but is extensively studied: over 800 publications can be found since the first description (Weemaes *et al.*, 1981) alone on NBS and many more on related diseases and genes. NBS can serve as an excellent model to study DNA repair and cell cycle checkpoint regulation, because only one specific functional domain is affected, which is also a common motive within the whole repair machinery Lloyd *et al.* (2009); Mohammad & Yaffe (2009). But up to today, there is a limitation on possibilities to study the molecular mechanisms of the disease. Only a small number of living patients exist and the somatic cell cultures derived from NBS patients are limited to fibroblasts and lymphocytes and exhibit premature senescence Davis *et al.* (2014). Several NBS mouse models were created and revealed interesting insights into the background of NBS, but have limited significance for human physiology.

Because of the hereditary nature of the disease, it cannot be cured. But a good human cellular model system could aid in elucidating the mechanisms underlying the disease and provide a screening system for treatments which can increase life span and life quality for those patients and patients with similar diseases. For example, one treatment is already in practice: bone marrow transplantation to treat lymphoid malignancies Albert *et al.* (2010), which are common in NBS patients. Genetically corrected patient-derived hematopoietic stem cells or iPSCs could also provide autologous transplants for those patients in the future.

In order to not only generate an unlimited cell source, but also enable access to cell types of a wide variety of tissues of the human body, fibroblasts cells from patients with NBS were transduced with the four transcription factors OCT4, SOX2, KLF4 an C-MYC in order to reprogram them to iPSCs with full pluripotency and unlimited self-renewal. But NBS cells exhibit premature senescence and also higher susceptibility to cellular stress which can result in TP53 stabilization, one of the roadblocks in cellular reprogramming. Thus, the outcome of the process itself can also address the question, if the special nature of NBS cells pose a hindrance to reprogramming. Once reprogrammed, the NBS-iPSCs can be tested for known or unknown features of the disease and for drug testing. Here, I compared sensitivity of NBS and normal cells towards oxidative stress, antioxidants and DNA damaging agents and performed global transcriptional analysis of NBS fibroblasts and NBS-iPSCs to identify NBS related transcriptional changes in networks and pathways.

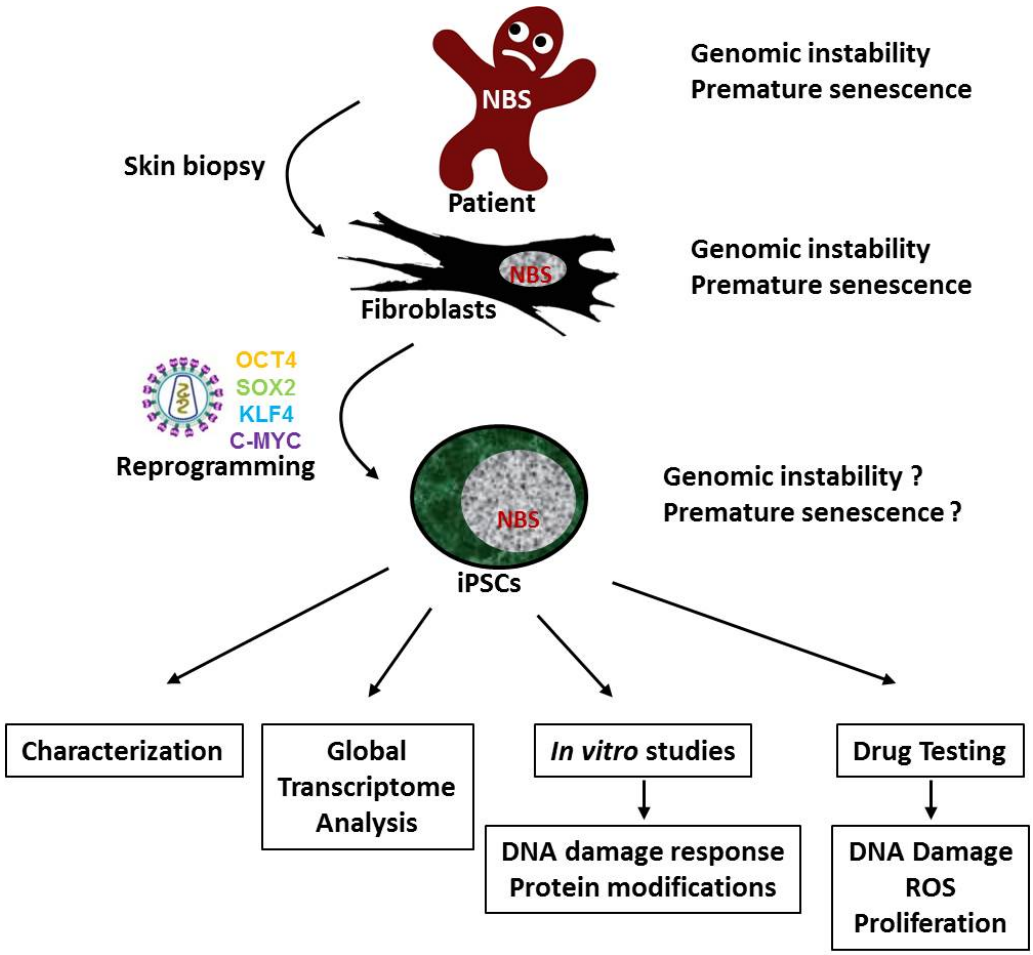

Figure 15: **Workflow**
Skin-derived fibroblasts from patients with Nijmegen Breakage Syndrome (NBS) were reprogrammed to induced pluripotent stem cells (iPSCs) by retroviral transduction with the transcription factors OCT4, SOX2, KLF4 and C-MYC. NBS-iPSCs were characterized by comparison to human embryonic stem cells (hESCs) in various assays and characteristics of the disease were studied by global transcriptome analysis (Illumina Microarray) and quantifying ROS and DNA damage after induction of stress or treatment with antioxidants.

Part II

MATERIALS AND METHODS

2

MATERIALS & METHODS

2.1 *in vitro* CELL CULTURE

All cells used were cultured at 37°C, 5 % CO_2 and either 21 % (standard) or 5 % oxygen in an incubator under humidified atmosphere. All treatments and maintenance procedures were carried out in a sterile environment using a clean bench type HeraSafe.

2.1.1 *Maintenance of Somatic Cell Lines*

Somatic cells were usually cultured in DMEM medium containing 10 % FBS and 1x penicillin/streptomycin until reaching 90 % confluency and then were split 1:4. For passaging, the cells were briefly washed with PBS and incubated with 0.05 % trypsin for 1 minute. After that, trypsin solution was removed and the cells were further incubated at 37°C for 5 minutes until the cells became detached from the flask or well. The activity of trypsin was stopped by adding prewarmed DMEM medium including 10 % FBS and 1x penicillin/streptomycin. Afterwards the the cells were collected by centrifuging (300 g; 5 min) and washed once with sterile PBS before passaging onto new plates.

Table 4: **Listing of somatic cell lines in culture**

Cell line	Medium	Special	Origin
NBS-1 to -7 (also see Table 7 on page 53)	DMEM, EMEM	5 % oxygen	Prof. Karl Sperling, Charité, Berlin
HFF1	DMEM	21 % oxygen (or 5 % when indicated)	ATCC; SCRC-1041
HEK293	DMEM		ATCC; CRL-1573
Phoenix amphotropic 293	DMEM		ATCC; SD-3443
BJ		not cultured; but RNA was used in Microarray analyses	ATCC; CRL-2522

2.1.2 *Maintenance of Pluripotent Stem Cells*

The limiting factor in culturing hESCs or iPSCs is to maintain their undifferentiated state during long-term culture in vitro. When hESCs were first established (Thomson *et al.*, 1998), their growth on a layer of mouse embryonic fibroblasts (MEFs), also called "feeder cells", or "feeders", were found to support the undifferentiated state. In this project, hESCs and iPSCs were usually expanded on a layer of mitotically-inactivated MEFs. The conditions for passaging human pluripotent stem cells (hPSC) were a combination of methods adapted from several published protocols Thomson *et al.* (1998); Xu *et al.* (2001); Du & Zhang (2010) and applied to the culture of the human ESC-lines H1 and H9 (WiCell Research Institute, Madison, WI, USA) and iPSCs generated from NBS and HFF1 cells. In combination with MEFs, hPSCs were usually cultivated in plates coated with with 0,2 % gelatine and fed with hESC medium (see Section A.3) and 4 ng/ml FGF-2, which was replaced every second day.

2.1.2.1 *Without feeders*

Prior to performing experiments to assess hPSC characteristic, hPSCs were switched to feeder-free conditions. To achieve this without disturbing the balance of pluripotency-supporting effects between MEFs and hPSCS, the cells were gradually adapted to the new conditions, by reducing the number of MEFs between passaging and increasing the volume of conditioned medium (or mTeSR^{TM}1, or Essential 8^{TM} medium) in the course of at least two passagings. Finally the cells were cultivated in Matrigel$^{®}$-coated plates and 100 % CM (or mTeSR^{TM}1, or Essential 8^{TM}) which was replaced every two days.

2.1.3 *Freezing and Thawing of Cells*

For freezing, the cells were harvested by trypsinization or mechanical isolation, according to their respective passaging method. After centrifugation, the cell pellet was resuspended in freezing media and the cells were aliquoted into cryovials. Slow freezing was acomplished by putting the vials into a special freezing container (Nalgene) and gradual cooling to -80°C overnight in a freezer. The next day, vials were transferred to liquid nitrogen for long-term storage.

For regeneration of frozen cells, the cryovials were removed from the liquid nitrogen and quickly defrosted using a 37°C water bath. Afterwards, 70 % ethanol was used to sterilize the outside of the cryo vials and they were shortly allowed to air dry before opening. The content of the vial was transferred into 10 ml pre-warmed media (choice of medium respective to cell line) in a 15 ml tube. The suspension was spun down at 300 g for 5 minutes at room temperature. The

supernatant was removed and the cell pellet was resuspended in the respective amount of media needed for the culturing plate.

2.1.4 *Isolation, Culturing and Inactivation of MEFs*

The preparation of MEFs was performed according to previous reports of our lab (Jozefczuk *et al.* 2012; Jozefczuk 2009). In brief: Pregnant female mice (CF-1, Harlan, USA) were sacrificed at 13 or 14 d.p.c. (days post-coitum) by cervical dislocation. Uterine horns were dissected out, briefly rinsed in 70 % ethanol and placed into a tube containing PBS without Ca^{2+} and Mg^{2+}. Afterwards each embryo was mechanically separated from its placenta and embryonic sac. Next, head and red organs were dissected, the remaining carcas was washed in PBS and was placed in a clean petri dish. Using a sterile razor blade, the tissue was finely minced until it become pipettable. Then, 1 ml of 0.05 % trypsin/EDTA and DNase I (100 units per ml of trypsin) was added per embryo. Afterwards the tissue was transferred into 50 ml tubes and incubated for 15 minutes at 37°C. After each 5 minutes of incubation, cells were further dissociated by pipetting up and down. Then, trypsin was inactivated by adding the same volume of freshly prepared medium consisting of DMEM with 10 % FBS and 1 % glutamine. Remaining pieces of tissue were allowed to settle down to the bottom of the tube and were discarded. After low-speed centrifugation, the cell pellet was resuspended in pre-warmed medium. Approximately 3-4 embryos were plated in each 150 cm^2 flask (coated with 0.2 % gelatine for 2 hours). The fibroblasts (P0, passage 0) were the only cells with the ability to attach onto gelatine-coated flasks. The next day, cells were 80-90 % confluent and at this stage a major part of P0 cells were frozen for future use. The remaining 150 cm^2 flask of P0 was expanded till P3 or P4, then inactivated and used as feeders for culturing hESCs or to produce conditioned medium (CM).

For inactivation of MEFs, mitomycin C was diluted in PBS (1 mg/ml) and filter-sterilized. MEFs were washed with PBS without Ca^{2+} and Mg^{2+}. Then, 20 ml of medium (DMEM with 10 % FBS and 1 % glutamine), containing 10 µg/ml of mitomycin C was placed on MEFs. After 2h incubation at 37°C, mitomycin C containing media was removed and cells were washed twice with PBS, trypsinized, centrifuged and resuspended in prewarmed media. Afterwards the cells were counted and plated at a density of $5.6*10^4$ cells/cm^2 in 150 cm^2 flasks to be used for CM production for the next 6 days.

2.1.5 *Preparation of CM*

One day after plating inactivated MEFs at a density 56.000 cells/cm^2, the medium was replaced with (0.5 ml/cm^2) hESC medium (UM, unconditioned medium) supplemented with 4 ng/ml of FGF-2. CM was

collected from feeder flasks after 24 hours incubation and fresh hESC medium containing 4 ng/ml of FGF-2 was added to the feeders. This procedure was repeated for the next 6 days. Each day, collected CM was placed at -20°C. After 6 days the media was combined and filtered. Then 50 ml aliquots were made and stored at -80°C. CM was supplemented with additional 4 ng/ml of FGF-2 before adding to cells grown on Matrigel®. The quality of CM was assessed by perfoming an Activin A ELISA (R&D Systems) according to the manufacturers instructions.

2.2 WESTERN BLOTTING

2.2.1 *Protein Preparation and Measurement*

Cells grown in a monolayer were kept on ice and rinsed with ice-cold PBS. RIPA lysis buffer supplemented with protease and phosphatase inhibitor cocktail, was added to the cells and incubated on ice for 30 minutes. Usually 200 µl (6-well format) or 100 µl (12- well format) of lysis buffer was used respectively. Cells were detached from the culture plate by using a cell scraper. Cells were collected in a 1.5 ml centrifuge tube, then lysed using a 1 ml syringe and an injection needle (22 gauge). Afterwards samples were centrifuged at 10.000 g for 30 minutes at 4°C. The supernatant was collected and stored at -80°C.

Protein samples were quantified using the bicinchoninic acid (BCA) assay. Standard protein solutions (BSA in concentrations of: 0.125 mg/ml, 0.25 mg/ml, 0.5 mg/ml, 0.75 mg/ml, 1.5 mg/ml, 2 mg/ml) were used to prepare a standard curve. 100 µl freshly made BCA solution was mixed with 5 µl of each standard or sample in 96-well plates. Then samples were incubated for 30 minutes at 37°C and afterwards measured at 562 nm wavelength using the Omega FLUOstar microplate reader.

2.2.2 *Gel Preparation, Protein Loading and Separation*

Protein gels were prepared in Mini PROTEAN ® 3 System protein chambers. The resolving gel (10 %) was prepared by mixing 8.2 ml of dH_2O, 5.0 ml of 1.5 M Tris-Cl pH 8.8 (resolving gel buffer), 200 µl of 10 % SDS, 4.6 ml of 40 % acrylamid, 100 µl APS and 10 µl TEMED. The surface of the gel was covered with isopropanol or distilled water to get an even surface. After polymerization the isopropanol (or water) was discarded and a 5 % stacking gel was poured. Stacking gel consists of: 5.7 ml of dH_2O, 2.5 ml of 0.5 M Tris-Cl pH 6.8 (stacking gel buffer), 100 µl of 10 % SDS, 1.7 ml of 40 % acrylamid, 100 µl APS and 20 µl TEMED. If not mentioned otherwise, 10 µg of protein was mixed with 5x loading buffer (to a 1x final concentration) and water (to adjust equal volume). The samples and 6 µl of prestained protein

marker were heated to 95°C for 5 minutes and afterwards cooled on ice for 1 minute before loading. The gel was run in 1x running buffer at 100 V until the bromphenol-blue front reached the end of the stacking gel. Gels were then released from their glass chamber and further processed during tranfer of proteins to a nitrocellulose membrane.

2.2.3 *Transfer to Nitrocellulose Membrane and Ponceau® Staining*

12 filter papers and Hybond™ ECL™ nitrocellulose membrane were cut to the shape of the gel. 4 filter papers were incubated for 10 minutes in semi-dry blotting buffer 1 and 2 filter papers plus the nitrocellulose membrane in semi-dry blotting buffer 2. The gel and 6 filter papers were incubated in semi-dry blotting buffer 3. Then, a sandwich was formed in the order of the previously listed filters, membrane and gel on top of the anode plate of the semi-dry blotter. Afterwards, air bubbles between the layers were removed by rolling a pipette carefully across the sandwich. The cathode plate was placed on top and the transfer completed at 20–25 V after 60 minutes. Success and equal transfer was tested by staining the proteins on the nitrocellulose membrane with the reversible Ponceau® staining solution.

2.2.4 *Blocking, Washing and Antibody Incubation*

The membrane was rinsed with dH_2O and then blocked with 5 % milk powder or 5 % BSA in PBS-T (blocking solution) by shaking for 1 hour at RT. BSA blocking solution was used for phospho-specific antibodies, in all other cases blocking was perfomed with milk. After blocking, the membrane was incubated by shaking at 4°C over night with primary antibody dissolved in PBS-T with 5 % milk powder or 5 % BSA. Afterwards the membrane was washed 3 times for 10 minutes in PBS-T on the shaking machine, exchanging buffer between each step. Then, the secondary antibody dissolved in milk or BSA blocking solution was applied by shaking for 1 hour at RT. Afterwards the membrane was washed 3 times for 10 minutes in PBS-T. Primary and secondary antibodies used are listed in Section A.4.

2.2.5 *Film Developement*

One volume of detection reagent 1 and 1/40 volume of detection reagent 2 of ECL Plus Western Blotting Detection Reagents were mixed and kept in the dark for 5 minutes. The membrane was then covered with the detection solution and incubated for 1 minute in the dark. After moving to a dark room, it was placed in a Hypercassette™ and chemiluminescence was detected using BioMAX XAR film and the Curix 60 film developing machine.

2.3 POLYMERASE CHAIN REACTION (PCR)

In a typical PCR reaction, a total sample volume of 25 µl was used, consisting of 20.55 µl DNAse-free water, 0.1 µl of each primer (forward and reverse), 0.25 µl 25 mM dNTPs, 2.5 µl 10x PCR buffer, 0.5 µl Taq-Polymerase and 50 ng DNA. The mix was cycled 35 times with 94°C for 1 min, 55°C for 1 min, and 72°C for 1 min. The annealing temparature step was always adapted to the respective primer melting temperature. The sequences of primers are listed in Section A.9.

2.3.1 *DNA Isolation*

Cells were harvested by trypsinization and centrifugation (500 g, 5 min). The supernatant was removed and genomic DNA (gDNA) was isolated using the QIAamp DNA Mini Kit (Qiagen) according to manufacturer's instructions. gDNA was eluted from the membrane by 100 µl DNase/RNase free distilled water.

The quantity and purity of gDNA was analysed with a spectrophotometer type NanoDrop® ND-1.000. 1.5 µl of the respective sample was applied to the device and measured at a wavelength of 260 nm to determine the concentration. For quality control the ratio of sample absorbance at 260 nm and 280 nm was determined, which should be higher than 1.8 for DNA.

2.3.2 *Gel Electrophoresis*

To separate PCR products by size, they were mixed with 5x DNA loading buffer (to a final concentration of 1x) and then loaded on 1 % agarose gels (if not specified otherwise) containing 0.5 µg/ml ethidium bromide. The gel was placed in a chamber containing boric acid buffer and was electrophorized for approx. 40 minutes at 70 V. Afterwards the gel was viewed under UV light for analysis. A digital picture was taken for documentation.

2.3.3 *Applications*

2.3.3.1 *Fingerprinting*

As described in (Park *et al.*, 2008), a PCR was used to amplify across discrete genomic intervals containing highly variable numbers of tandem repeats (VNTR) in order to verify the genetic relatedness of iPSC-lines relative to their parent fibroblasts. A total of 50 ng of genomic DNA was used per reaction, cycled 35 times through 94°C for 1 min, 55°C for 1 min, and 72°C for 1 min, and run on 10 % acryamid gel in TBE buffer for 2 hours at 100 V.

2.3.3.2 *657del5 PCR*

The 657del5 mutation in exon 6 of the NBN gene was identified by a PCR with primers flanking the deletion and resulting in either a 60 bp (wt) or 55 bp (657del5) amplicon. The PCR products were resolved by size in a 3 % agarose gel electrophoresis.

2.3.3.3 *Sanger Sequencing*

The 657del5 mutation in exon 6 of the NBN gene was identified by amplification of exon 6 by flanking primers (Section A.9) and subsequent sanger sequencing by employing the same primers. After PCR, the products were purified by QIAamp DNA Mini Kit (Qiagen) according to manufacturer's instructions. The sequencing reaction was performed by in-house service (Dr. Bernd Timmermann) of the Max-Plack Institute. Afterwards the raw data (sequence) was analyzed using "Chromas light 2.01" (McCarthy, 1996).

2.4 REAL-TIME PCR

Real-time PCR was carried out on the Applied Biosystems 7900 instrument, in 96-well or 364-well optical reaction plates. The following program was applied: stage 1: 50°C for 2 min; stage 2: 95°C for 10 min; stage 3: 95°C for 15 s and 60°C for 1 min, for 40 cycles and a final cycle ending with stage 4: 95°C for 15 s, 60°C for 15 s and 95°C for 15 s. Additional dissociation curves of the products were created. The final reaction volume of 10 µl consisted of 5 µl of SYBR® Green PCR Master Mix, 2.5 µM of each primer (3 µl), and 2 µl of cDNA (1:5 dilution). Each gene was analyzed in triplicates. Relative mRNA levels were calculated using the comparative $2^{-\Delta\Delta C_T}$ method (Livak & Schmittgen, 2001). mRNA levels of β-ACTIN or GAPDH genes were used as controls for normalization. Primers are listed in Section A.9.

2.4.1 *RNA Isolation*

The medium was removed and per well of a 6-well plate, 350 µl buffer RLT (provided by kit manufacturer) containing 1 % β-Mercaptoethanol was added. Total RNA was isolated using the RNeasy® Mini Kit (Qiagen) according to manufacturer's instructions. DNase I treatment was performed on column. RNA was eluted by 40 µl DNase/RNase free destilled water.

The quantity and quality of RNA was analysed with a spectrophotometer type NanoDrop® ND-1.000. 1.5 µl of the respective sample was applied to the device and measured at a wavelength of 260 nm to determine concentration. For quality control the ratio of 260 nm and 280 nm was measured which should be higher than 2.0 for RNA.

The quantification of mRNA fragmentation was assessed by resolving mRNA on a agarose gel. 2 µl of purified RNA were mixed with 6 µl distilled water and 2 µl of 5x DNA loading buffer and then loaded on 1 % agarose gels containing 0.5 µg/ml ethidium bromide. The gel was electrophorized for approx. 40 minutes at 70 V. Afterwards the gel was viewed under UV light for analysis. A digital picture was taken for documentation.

2.4.2 *cDNA Generation*

Reverse transcription was carried out as follows: 500 ng of mRNA, 0.5 µg oligo(dT) and 1 µg random primers were incubated for 3 min at 70°C and cooled on ice. Then, a master mix was added, consisting of following components: 5.0 µl of 5x reaction buffer, 0.5 µl of (25 mM) dNTPs, 0.1 µl of MMLV reverse transcriptase and 9.4 µl of dH_2O. After 1 hour of incubation at 37°C and 1 hour at 42°C the reaction was stopped by heating to 65°C for 10 min. Afterwards the cDNA was diluted 1:5 with distilled water.

2.5 FLUORESCENCE ASSISTED CELL SORTING (FACS)

The FACSCalibur and the program "CellQuestPro", which is directing the machine, were used as described by the manufacturers instructions (FACSCalibur, 1996). Programs used for data analysis, were "CellQuestPro", "Cyflogic", "Weasel 3.0" and "Flowing software 2.5.1"

2.5.1 *ROS Measurement*

Fibroblast cells were seeded onto 12-well plates with a density of $5*10^4$ cells per well one day prior to treatment. hESCs and iPSCs were seeded on matrigel in 6-well plates and fed with CM, one week prior to the treatment. To prepare cells for ROS-measurement they were washed once with PBS and then incubated in 15 µM DCF-DA for 20 minutes at 37°C. Afterwards, the solution was removed and the cells were briefly rinsed with PBS. Cells were treated with different concentrations of antioxidants (as indicated) and/or 20 µM H_2O_2 for 30 min. During this incubation, ROS can oxidize the non-fluorescent DCF-DA and further removal of acetate groups by cellular esterases will turn it into the fluorescent DCF. When hESCs and iPSCS were analyzed, pluripotent cell populations were verified by co-staining with immunofluorescent detection of TRA1-60. The primary antibody was co-incubated together with DCF-DA, the secondary antibody was co-incubated with antioxidants and peroxide treatment. To analyze single cells by FACS, they were trypsinized by colourless 0.05 % trypsin solution for 5 minutes. Trypsinization was stopped by adding 10 % FBS in PBS. Cells were then centrifuged by 500 g for 5 minutes and

resuspended in 300 µl PBS. The fluorescence was measured by FACS using the FITC channel. The program "CellQuestPro" was used for acquiring the data and free software like "Cyflogic" was used to analyze the data.

2.5.2 *Quantification of DSBs by Detection of gamma-H2AX*

Fibroblast cells were seeded onto 6-well plates with a density of $4*10^5$ cells per well one day prior to treatment. hESCs and iPSCs were seeded on matrigel in 6-well plates and fed with CM, one week prior to the treatment. Cells were either treated with antioxidants (as indicated) 5 min prior to the addition of 1 mM H_2O_2 or with H_2O_2 alone at a total incubation time of 4h at 37°C in a cell culture incubator under 21 % or 5 % oxygen, as indicated. Other cells were treated with antioxidants (as indicated) 5 min prior to the addition of 30 µg/ml bleomycin for 3h, and released for 1h by switching to bleomycin-free medium.

Afterwards, the cells were briefly rinsed with PBS and trypsinized to generate single cells. The cells were centrifuged at 500 g for 5 min and the cell pellet was resuspended in 100 µl PBS. Under constant shaking (to prevent clumping) 300 µl of 100 % ice-cold ethanol was added dropwise to fix the cells and incubated at -20°C for at least 30 min or until further use. Afterwards the solution was mixed with 1 ml PBS and centrifuged at 2200 g for 5 min. The pellet was resuspend in 50 ml PBS-T with 5 % FBS and incubated 30 min at RT for blocking. FITC-labled gamma-H2AX antibody (1:500) was added and incubated over night at 4°C. The next day, 300 µl PBS were added and the cells were measured by FACS using the FITC channel. In some cases the cells were co-stained with TRA1-60 antibody (to verify pluripotent cell populations) or DNA was stained (to analyze cell cycle phases) with propidium iodide (see next section).

2.5.3 *Cell Cycle Analysis*

To compare cell cycle phases, the cells were arrested in G_0/G_1 phase by maintaining 100 % confluence for 5 days (growing in 6-well plates). Afterwards, the cells were split 1:4 and harvested after different timepoints (as indicated). The cells were trypsinized and fixed with ethanol as describe before (see above). After removal of the fixing solution, the cell pellet was resuspended in 50 µl PBS-T with 5 % FBS, 10 µg/ml propidium iodide and 10 µg/ml RNase A and incubated for 1h in the dark. Afterwards 300 µl of PBS was added and the solution was direcly subjected to FACS measurement. There, the cells were seperated into two groups of "alive" and "dead" cells, by comparison of cell size (FSC) and granularity (SSC). The "alive" population was isolated and cell aggregates were removed by comarison of absolute DNA

content (FL-2-A) and type of the signal (FL-2-W). The "alive" and "single cell" populations were analyzed in a histogram, showing linear propidium iodide staining (which correlates with DNA amount) and cell counts (on y-axis). Because cells double their DNA during S-phase, the two peaks can be assigned to G_1-phase (single set of chromosomes) and G_2-phase (double set of chromosomes) and cells inbetween to S-phase.

2.6 PROLIFERATION ASSAY

This assay can reflect the number of viable cells present by employing cellular oxidoreductases to reduce the MTT reagent 3-(4,5-dimethylthiazol-2-yl)-2,5-diphenyltetrazolium bromide to its insoluble form formezan. Formezan has a purple color and can be measured in a colorimetric assay. Cells were seeded in a 24-well plate at different cell concentrations ranging from $2*10^3$ to $1*10^4$ per well. They were grown for 4 days, before MTT solution (1.6 mM in medium) was added for 3.5 hours at 37°C. The supernatant was collected and the absorbance was measured at 540 nm in a microplate reader.

2.7 MOLECULAR CLONING

2.7.1 *Plasmid Amplification*

The plasmids containing NBN (NM_002485) Human cDNA, the EF1α promoter induced transactivator (pEF1a-TET3G) and the doxycyclin-induced target (pTRE3G-BI-ZsGreen1, see Section A.10) were amplified by transformation into heat-shock competent *E. coli* and subsequent isolation with the "NucleoBond® Xtra Maxi EF" Kit (Macherey-Nagel) according to the manufacturers instructions.

2.7.2 *Digest and Cutting*

To verify successful amplification, the plasmids were digested 3 hours at 37°C, with different sets of restriction enzymes to generate fragments specific to each plasmid. The fragments were then resolved on a 1 % agarose gel.

To release NBN sequence (2265 bp) from the vector and generate an open site (site-specific sticky ends) into the destination vector pTRE3G-BI-ZsGreen1, both were digested with a combination of BamHI and EcoRV restriction enzymes and resolved on a 1 % agarose gel. Both parts were cut from the gel with a clean scalpel and the DNA was purified with the QiaQuick purification Kit (Qiagen).

Table 5: **Restriction digest to confirm sequence**

Plasmid (size)	Restriction enzymes	Resulting fragments
NBN cDNA clone (5700 bp)	BamHI / EcoRV	5.5 kb
		2265 bp
	EcoRI / EcoRV	5.5 kb
		1700 bp
		570 bp
pEF1a-TET3G (7892 bp)	EcoRI / HindIII	6.6 kb
		1232 bp
pTRE3G-BI-ZsGreen1 (3555 bp)	BamHI / XhoI / XbaI	2353 bp
		792 bp
		410 bp

2.7.3 *Ligation*

To prevent self-ligation, the linearized pTRE3G-BI-ZsGreen1 vector was de-phosphorylated by incubation with calf intestinal phosphatase (CIP) for 1 h at 37°C. Afterwards, the enzyme was deactivated by additional incubation for 15 min at 65°C. The de-phophorylated vector was ligated (T4 DNA Ligase) to the linearized NBN fragment at a ratio of 1:3 (vector:insert) at RT for 10 min. The ligation reaction was stopped by heating to 65°C for 15 min. To confirm a successful ligation product (NBN in pTRE3G-BI-ZsGreen1), 10 % of the mixture were resolved on a 1 % agarose-gel and the bands compared to the un-ligated DNA fragments. 2 µl of ligation product was mixed with 100 µl heat-shock competent DH5α *E. Coli* (Invitrogen) on ice, before heat-shock was performed at 42°C for 40 seconds. The cells were then incubated for 1 hour at 37°C in 500 µl of SOC medium, before plating on LB agar-plates with ampicillin (100 µg/ml). The plates were incubated over night at 37°C and several colonies were picked and amplified in 5 ml LB medium (+ ampicillin) by additional incubation at 37°C over night. The plasmids were isolated using the "Invisorb® Spin Plasmid Mini Two" Kit (Invitek) by following the manufacturers instructions. The clones were tested by digesting with restriction enzymes (BamHI, EcoRV and EcoRI) leading to fragments of 3.5 kb, 1.7 kb and 0.57 kb which were visualized on a 1 % agarose gel. One positive clone of pTRE3G-BI-ZsGreen1-NBN was selected for further amplification using the "NucleoBond® Xtra Maxi EF" Kit.

2.7.4 *Transgene Testing*

To test doxycyclin-dependent induction and NBN expression of the cloned product (pTRE3G-BI-ZsGreen1-NBN), the plasmid was transfected into HEK 293 cells, to observe induced GFP expression microscopically and to detect NBN by western blot. Transfection was performed (in a 6-well plate) using Xfect transfection reagent and following the Xfect protocol (PT5003-2 at www.clontech.com/manuals). $2*10^5$ cells/well were seeded the day before. 1 µg of pEF1a-TET3G and 4 µg of pTRE3G-BI-ZsGreen1-NBN were used for transfecting each well. Two wells of the 6-well plate were transfected with the vectors and without doxycycline and two wells were transfected with the vectors and 1 µg/ml doxycycline.

After 48 h, GFP expression was detected by fluorescence microscopy. The cell pellets from each well were harvested and induced expression levels to uninduced expression levels were compared using western blot (see Section 2.2) with anti-myc-tag (mouse, monoclonal, 9B11, Cell Signalling, 1:1000, o.n., 4°C) to detect myc-tagged NBN.

2.8 MICROARRAY

2.8.1 *Sample Hybridization*

All array hybridization steps were performed by Claudia Vogelgesang of the Automation Group (MPI Molecular Genetics). This included biotin-labelling of cRNA by using 500 ng quality-checked total RNA (per sample) as input. Chip hybridizations, washing, Cy3-streptavidin staining, and scanning were performed on an Illumina BeadStation 500 platform (Illumina) using reagents and protocols supplied by the manufacturer. cRNA samples were hybridised in duplicates on Illumina human-8 BeadChips (NBS-1, NBS-3, NBS-5, NBS-7, HFF1, BJ) or Illumina human-12 BeadChips (NBS-8, NBS-8 iPSCs, H1, H9 (single), HFF1-iPSCs, BJ-iPSCs). All basic expression data analysis was carried out using the manufacturer's software GenomeStudio (Illumina). Raw data was background-subtracted and normalised using the "rank invariant" algorithm. Normalized data was then filtered for significant expression (detection pValue) on the basis of negative control beads. Selection for differentially expressed genes was performed on the basis of arbitrary thresholds (1.5-fold changes) and statistical significance according to an Illumina custom model (Kuhn *et al.*, 2004).

2.8.2 *Data Analysis*

In order to test for global gene expression similarities within the hybridized samples, a cluster analysis was performed with the software

GenomeStudio (www.illumina.com). In addition, dot plot graphs depicting the correlation of the gene expression of every possible pair were generated with GenomeStudio and correlation coefficients (R^2) were obtained.

Gene lists of the normalized data, with Illumina Gene IDs, gene symbols, the average signals measured by the Illumina BeadStation 500 platform as well as detection p-values, differential p-values and additional information, were transferred from GenomeStudio to an Microsoft Office Excel table, where all further analyses were based upon. All genes with a detection p-value below 0.01 were considered as expressed. All genes with a differential p-value below 0.05 were considered as differentially expressed.

Groups of significantly expressed or regulated genes were uploaded to an online tool for generation of Venn diagrams called VENNY (Oliveros, 2007). Venn diagrams were generated depicting the number of overlapping genes between different group sets.

Different sets of gene lists were entered into the DAVID functional annotation tool (Dennis Jr *et al.*, 2003; Da Wei Huang & Lempicki, 2008) using the official gene symbol or ILLUMINA-IDs as input, to perform gene-annotation enrichment analysis, functional annotation clustering, KEGG pathway mapping (http://www.genome.jp/kegg/), transcription factor binding site prediction and more.

Heatmaps were created using the MultiExperiment Viewer software (MeV v4.4.1, http://www.tm4.org/mev/) (Saeed *et al.*, 2006, 2003).

For the calculation of the activation state of transcription factors, a list of differentially regulated genes between NBS and normal fibroblasts was used as input for Ingenuity® Pathway Analysis (IPA®, QIAGEN Redwood City, www.qiagen.com/ingenuity).

2.9 REPROGRAMMING METHODS

2.9.1 *Viral Transduction*

2.9.1.1 *Virus production*

Phoenix amphotropic 293 (PA) cells were seeded onto a gelatin coated flask (75 cm^2) at a density of $2*10^5/cm^2$. On the next day each flask was transfected with retroviral packaging plasmids containing each of the four transcription factors for reprogramming (pMXs-hOCT4, pMXs-hSOX2, pMXs-hKLF4, pMXs-hC-MYC, pLIB-GFP; see Section A.10). Therfore, 12 µg retroviral vector were added to 1 ml of opti-MEM, gently mixed 5 times and then 30 µl FuGENE HD transfection reagent was gently mixed into that solution. The mixture was incubated at RT for 15 min and meanwhile the medium from PA cells was replaced with 9 ml fresh medium (DMEM w/o antibiotics). The transfection reagent/DNA complex was added to the cells in a dropwise

manner. The dish was then gently swirled to ensure even distribution over the entire plate surface. Afterwards the cells were incubated at 37°C, 5 % CO_2 for 14 hours, then the medium was changed and the supernatant discarded. The retrovirus-containing medium was collected 48 hours and 72 hours post-transfection and the virus was stored either at 4°C (for short term storage) or frozen at -80°C.

2.9.1.2 *Virus titer*

Virus containing supernatant was collected 48 h and 72 h after transfection. Different amounts of GFP containing virus were used to infect NBS-5 and HFF1 cells at different concentrations of virus and basic growth factor 2 (FGF-2) and were then measured for infection efficiency (GFF positive cells per total cells) by flow cytometry. Therfore, the cells were rinsed with PBS, trypsinized to generate single cells and quantified for the number of green fluorescent cells.

The biological titer, representing the transducing units (TU) per µl was calculated using following formula:

$$\frac{TU}{\mu l} = \frac{P * N}{100 * V} * \frac{1}{DF} \tag{1}$$

P= % GFP positive cells; N= number of cells at time of transduction in well; V= Volume of dilution added to each well; DF= dilution factor (1= undiluted)

2.9.1.3 *Infection with O/S/K/M loaded retrovirus*

Target cells (HFF1 and NBS cells) were seeded onto 12-well plates at a density of $6*10^4$cells per well (~60 % confluency). On the next day, medium was aspirated and replaced with retroviral infection medium (OCT4, SOX2, KLF4, C-MYC, or GFP) and 4 mg/ml polybrene were added to increase infection efficiency. The infection medium consisting of DMEM w/o antibiotics, contained 2.5 TUs of each factor per cell. Serving as a non-transduced control for the reprogramming process, one well was tranduced with empty vectors (pMXs backbone) and the same procedure was followed as for the four factors. The plates were centrifuged at 1000 g at 37°C for 99 min before further incubation at 37°C and 5 % CO_2 over night. On the following day the medium was aspirated and the infection process was repeated. Also, 6-wells plates were coated with matrigel and inactivated MEFs were seeded at a density of $1.5*10^5$ per well. On the next day, the plates with infected cells were washed twice, the infected cells trypsinized and seeded onto the MEF/Matrigel coated dishes at a density of $2*10^4$ per well of a 6-well plate (~ 1:4). On the next day, medium was aspirated and the plate was washed once with hESC medium and finally covered with hESC medium supplemented with 4 ng/ml FGF-2 for further cultivation.

2.9.1.4 *Transduction control*

A 24-well plate was seeded with HFF1 and NBS fibroblasts at a density of $5*10^3$/well. On the next and third day the cells were infected with O/S/K/M loaded retrovirus according the the chapter above. The infected cells were cultivated for 12 more days and then fixed with paraformaldehyde and subjected to immunocytochemistry (see 2.10.3) to detect OCT4, SOX2, KLF4 and C-MYC.

2.9.2 *Episomal Reprogramming with Small Molecules*

The reprogramming protocol of deriving hiPSCs free of transgene sequences from fibroblasts was adapted from (Yu *et al.*, 2009, 2011).

2.9.2.1 *Plasmid amplification*

The plasmids containing the transcription factors for reprogramming (pEP4EO2SEN2K, pEP4EO2SET2K, pCEP4-M2L) were purchased from addgene.org (see Section A.10) and amplified by transformation into heat-shock competent *E. coli* (DH5α) and subsequent isolation with the "NucleoBond® Xtra Maxi EF" Kit (Macherey-Nagel) according to the manufacturers instructions.

2.9.2.2 *Nucloefection*

HFF1 and NBS-8 fibroblas were split one day before transfection to stimulate a growth phase. The cells were then harvested by trypsinization and centrifugation (300 g, 5 min). According to the manufacturers instructions of "Cell Line Nucleofector® Kit R" (Lonza), $8*10^5$ cells were mixed with 3 µg of pEP4EO2SEN2K and pEP4EO2SET2K each, 2 µg of pCEP4-M2L, 82 µl nuceofection reagent R and 18 µl supplement per transfection. The mixture was transfered to the electroporation kuvette and the electroporation was utilized by program U-020 (Nucleofector® II Device; Amaxa). Immediately afterwards 500 µl prewarmed DMEM medium was added to the cuvette and the contents were mixed with additional 4 ml of medium before equal distribution into 4 wells of a 6-well plate.

2.9.2.3 *Aiding reprogramming by addition of small molecule inhibitors*

From the 1^{st} to the 6^{th} day after nucleofection the cells were grown in DMEM (containing FBS and Ampicillin/Streptomycin) supplemented with small molecule inhibitors (MEK inhibitor PD0325901: 0.5µM; GSK3-β inhibitor CHIR99021: 3 µM and TGF-beta/Activin/Nodal receptor inhibitor A-83-01: 0.5 µM (also see Section A.5)). On day 7 post nucleofection, the cells were split onto matrigel-covered 6-well plates with MEFs and cultivated with CM, 4 ng/ml FGF-2 and the cocktail of small molecules until day 15. Aftwards, the cells were cultivated with CM and 4 ng/ml FGF-2 until colonies appeared.

2.9.3 *Direct Delivery of Recombinant O/S/K/M*

The procedure was inspired by the publications of Lee *et al.* 2012; Zhou *et al.* 2009; Pan *et al.* 2010. Recombinant proteins and protocol were aquired from "Recombinant Human Protein Set: OSKM-11R" (Stemgent). 5*10^4 HFF1 cells per well (6-well plate) were seeded in 3 individual wells for 3 different treatment strategies, the day before the first treatment. In the following 20 days the cells were treated with recombinant OCT4, SOX2, KLF4 and C-MYC fused to a cell-penetrating peptide (CPP; CPP-O/S/K/M) at a concentration of 200 nM for the first 6 days and at 100 mM for the other days. Adapted from (Lee *et al.*, 2012), the reprogramming process was enhanced by activation of the TLR3 pathway, using poly-iosinic-polycytidylic acid (poly I:C) at 300 ng/ml for the first 6 days. The treatment was modified in 3 different ways (as shown in Table 6 on page 48). The first treatment required change of medium (hESC-medium supplemented with FGF-2) every day, for the second treatment plan the medium was replaced only every other day. In the third well, the medium was replaced every other day and a combination of small molecules were added (until day 20), which were used before in enhancing reprogramming with episomal plasmids (Yu *et al.*, 2011). Overview pictures of the whole well were taken with a digital camera through the microscope at 4-fold ocular, every other day from day 1 until day 30.

Table 6: **Reprogramming by recombinant proteins: treatment plan**

Plan 1	**Plan 2**	**Plan 3**
Replace medium every day	Replace medium every other day	Replace medium every other day
CPP-O/S/K/M, 200 nM Poly I:C, 300 ng/ml	CPP-O/S/K/M, 200 nM Poly I:C, 300 ng/ml	CPP-O/S/K/M, 200 nM Poly I:C, 300 ng/ml PD0325901, 0.5 µM CHIR99021, 3 µM A-83-01, 0.5 µM EDHB, 2.5 mM

2.10 CHARACTERIZATION OF PLURIPOTENT CELLS

2.10.1 *Morphology*

Pictures were taken through the ocular of the microscope at a 4- to 100-fold magnification with a digital camera (4.000 x 3.000 pixel; 180 dpi) to monitor the morphological changes (shape of colony, shape of cell, nucleus to cytoplasm ratio) during reprogramming and compare appearing colonies to hESC (standard cell lines H1 and H9).

2.10.2 *Alkaline Phosphatase Staining*

25 days post induction, the staining was perfomed according to the manufacturers instructions of the Stemgent® Alkaline Phosphatase Staining Kit. In brief: For preparation of the AP staining solution (suited for one well of a 6-well plate) 0.5 ml of AP staining solution A and 0.5 ml of AP staining solution B were mixed in a 15 ml conical tube prior to the staining. For optimal results, the AP Substrate Solution should be used within 5 minutes after preparation.

First, the culture medium was aspirated and the cells were washed twice with 2 ml of PBS-T. Secondly, 2 ml of Fix Solution was added and incubated at RT for 1 to 2 minutes. It is important to not over-fix the cells, because excessive fixation will result in the loss of AP activity. Afterwards the Fix Solution was removed and the cells washed with 2 ml of PBS-T. 1 ml of freshly prepared AP staining solution was applied to the cells and kept for 10 to 20 minutes at RT in the dark. The reaction was stoped when the color turned bright red, by aspirating the AP staining solution and washing the wells twice with 2 ml of PBS. Finally, the cells were covered with PBS for storage at 4°C. AP expression resulted in a red or purple stain, while the absence of AP expression resulted in no stain.

2.10.3 *Immunofluorescent Detection of Marker Proteins*

Plates with cells were rinsed with 0.05 % Tween-20 in PBS (PBS-T) and fixed with 4 % paraformaldehyde in PBS for 10 min at RT. Afterwards the cells were washed twice with PBS-T and permeabilized with 1 % Triton X-100 in PBS for 10 min at RT. The cells were washed twice again with PBS-T and a blocking solution (10 % FBS in PBS-T) was applied for 45 min at RT with gentle rocking. The primary antibody (total volume for a 6-well: 800 µl; 12-well: 500 µl; 24-well: 300 µl) was diluted in blocking solution and incubated over night at 4°C. The next day, unattached primary antibody was removed by 3 consequent washing steps (5 min each) with 0.1 % BSA in PBS-T. The secondary antibody was usually diluted 1/300 in blocking solution and applied for 1 h at 4°C in the dark. Afterwards the cells were washed several times in with 0.1 % BSA in PBS-T and incubated in a staining solution for the nulclei (DAPI 100 ng/ml in PBS-T) for 10 min. Last, the cells were washed again and pictures of fluorescent staining were taken with a LSM 510 Meta confocal microscope (Zeiss).

Primary and secondary antibodies which were used in this thesis are listed in Section A.4.

2.10.4 *Embryoid Body Differentiation*

For in vitro differentiation, embryoid body (EB) formation of NBS- and HFF1-iPSCs was induced in hESC medium lacking FGF-2 supplementation. Therfore, the colonies were mechanically removed from thier plates and split into small fragments. They were transferred to a conical tube and then left in a water bath at 37°C for 3-5 min to seperate greater fragments from single cells. The sedimented fragments were seeded to "Ultra Low Attachment Culture Dishes" and cultivated for 8 days until round aggregates were formed. Then, aggregates were transfered to gelatin-coated plates (12-well) containing cover slips. The cells were allowed to differentiate (in hESC medium w/o FGF-2) for 3 (early markers like SOX17 and Brachiury) to 14 days (FOXA2, AFP, Albumin, SMA NES and TUJ1) and were fixed and stained according to the immunofluorescent protein labeling procedure 2.10.3.

2.10.5 *Teratoma Formation in Mice*

The *in vivo* differentiation experiments (teratoma formation) were performed by EPO-Berlin GmbH (http://www.epo-berlin.de). Briefly, per injection, the contents of 3 wells (6-well plate) of near-confluent grown iPSCs were collected by combined type IV collagenase- treatment and 0.05 % Trypsin/EDTA-treatment. Cells were resuspended in Matrigel and immediately injected subcutaneously into NOD.Cg-Prkdc^{scid} Il2rg^{tm1Wjl}/SzJ mice, commonly known as NOD scid gamma (NSG) mice, which combine the features of the NOD/ShiLtJ background, the severe combined immune deficiency mutation (scid) and IL2 receptor gamma chain deficiency. Mice bearing teratomas were carefully monitored and sacrificed 78 days after injection. The teratomas were collected and processed by means of standard procedures for paraffin embedding and hematoxylin and eosin staining. Histological analysis was performed by a pathologist (Dr. med. vet. Wolfram Haider, Institut für Tierpathologie, Berlin).

2.10.6 *Karyotyping*

To detect potential karyotypic abnormalities in NBS fibroblasts and in the generated iPSC-lines, which may have resulted from the retroviral interference during the process of direct reprogramming, chromosomal analysis was performed after GTG-banding at the Praxis für Humangenetik, Berlin. For each line, between 15 and 20 metaphases were counted and 5 to 8 karyograms analyzed.

Part III

RESULTS

3 RESULTS

3.1 CHARACTERIZATION OF NBS CELL LINES

Nijmegen Breakage Syndrome is a rare genetic disorder that has a frequency of 1:866 in Germany (Carlomagno *et al.*, 1999) and a higher frequency of 1:177 in eastern Europe (Varon *et al.*, 2000) but is estimated to affect only 1 in 100000 worldwide. Therefore, relatively fresh cell samples from patients are difficult to obtain. Fibroblasts from patients with diagnosed Nijmegen Breakage Syndrome were kindly provided by Prof. Karl Sperling from Charité-Universitätsmedizin Berlin. In total, we received 8 NBS patient fibroblast lines of different age and sex as listed in Table 7 on page 53. With one exception (NBS-8), all lines (NBS 1-7) were previously cultivated in our lab, so the passage number was already greater than 5 when they were used for this project (see Table 9 on page 110). Only the line NBS-8 was obtained at passage 4 from a recent biopsy. Unlike immortalized cell lines which are often used for experiments in the lab, primary, somatic cells have a very limited life span in culture before they undergo senescence, an irreversible arrest in G1 phase. This phenomenon is caused by the gradually shortening of telomeres with each cell division and is also known as the Hayflick limit (HAYFLICK, 1965). The number of passages until this happens greatly depends on the tissue, age and the individual sample (Stanley *et al.*, 1975). For example, the neonatal reference cell line Human Foreskin Fibroblast line 1 (HFF1) can double around 50 times before senescence sets in (McFarland & Holliday, 1994).

Table 7: **Overview of NBS patient cell lines**

Cell line [NBS #]	Patient ID	Passage [#]	Gender	Age [Years]	657del5 (Exon 6) Mutation	Global Transcriptome Analysis
1	94P112	16	male	5	homozygeous	YES
2	94P469	11	male	9	homozygeous	NO
3	95P558	14	female	7	homozygeous	YES
4	89P319	20	female	7	homozygeous	NO
5	06P0565	10	female	32nd week of pregnancy	homozygeous	YES
6	2239	16	female		homozygeous	NO
7	94P027	16	male		homozygeous	YES
8	11P0037	4	male	7	heterozygeous	YES

The NBS cell lines 1-7 were thawed from frozen stocks and expanded in EMEM medium. The morphology of the different lines can be compared in Figure 16 on page 54. NBS-3 and NBS-5 proliferated similar to the reference cell line HFF1 and also had similar cell morphology. NBS-1 and -7 proliferated also well in the beginning, but cell morphology indicated a higher frequency of senescent cells, observed as wide spread, flattened cell body (Figure 16 on page 54, B). NBS-6 and NBS-4 had an even higher frequency of those cells and were terminated after several passages. NBS-2 had so few viable cells after thawing, that it could not be cultivated further. To perform global transcriptome analysis, RNA was isolated from the lines with high viability, and low frequency of senescent looking cells (NBS-1, -3, -5 and -7). The line NBS-8 was obtained at a later time point and was therefore not included in the global transcriptome analysis of NBS fibroblasts (Section 3.5). As expected from a fresh sample of primary cells at early passage, NBS-8 cells did not show signs of senescent cells and proliferated in similar manner as HFF1 cells.

Figure 16: **Morphology of NBS fibroblasts and HFF1**
(A) 4x magnification of fibroblast lines for evaluation of senescence. (B) 20x magnification of senescent fibroblasts .

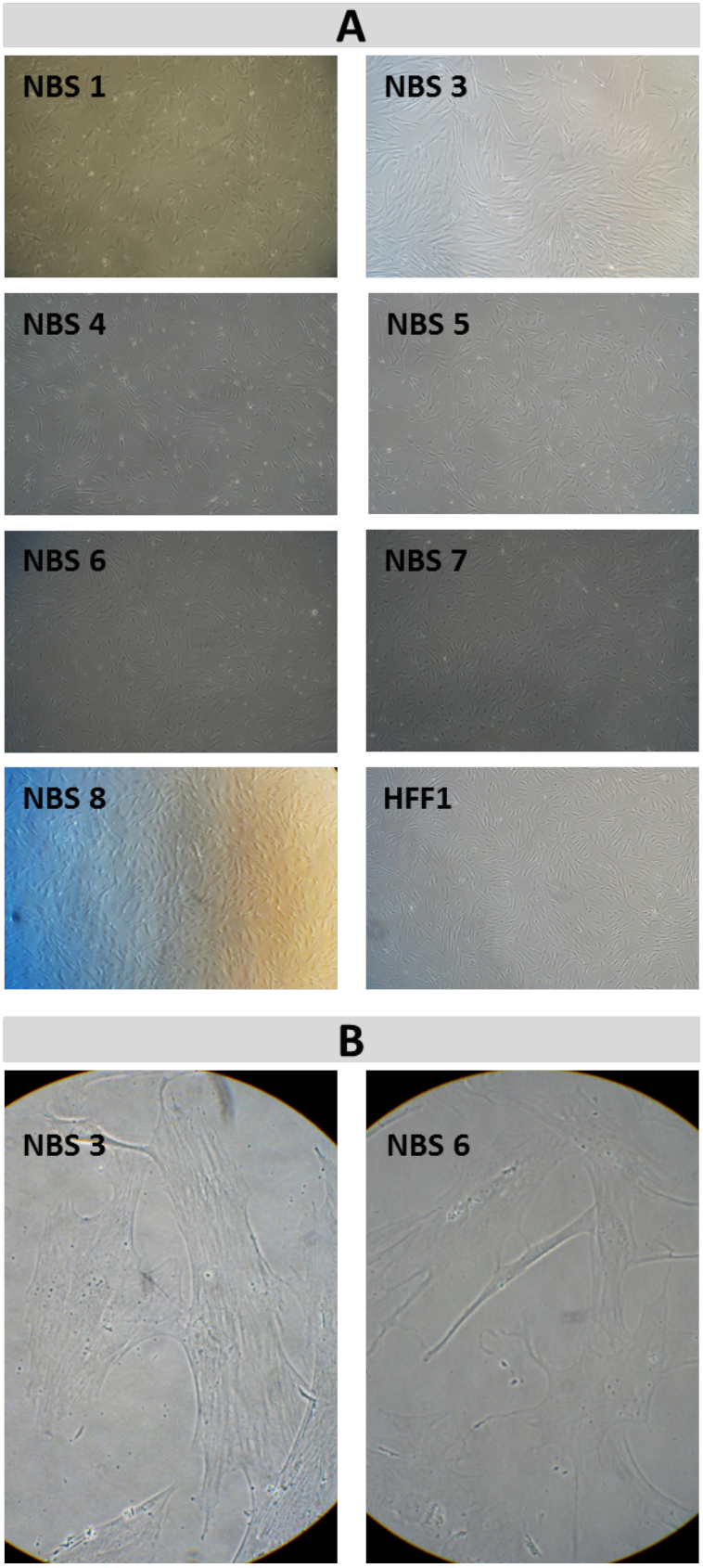
A
NBS 1
NBS 3
NBS 4
NBS 5
NBS 6
NBS 7
NBS 8
HFF1
B
NBS 3
NBS 6

3.1.1 *NBS Patient-derived Fibroblasts Lack Full-length NIBRIN*

The most frequent mutation in patients with Nijmegen Breakage Syndrome (NBS) is a 5 bp deletion in exon 6 of the NBN gene, called 657del5. This mutation causes truncated versions of NIBRIN (NBN protein), one short fragment P26 and one larger fragment, P70. It has been shown in knockout-mice, that homozygous deletion of NBN is lethal (Zhu *et al.*, 2001), but the P70 fragment of NBN retains some of the function, leading to the previously described phenotype of NBS. All patients used in this study were tested for the 657del5 mutation by PCR analysis, sequencing and western blotting.

3.1.1.1 *NBN is mutated at DNA level*

To confirm the presence of the 657del5 mutation within the NBN gene, a PCR-based analysis with primers flanking the 5 bp deletion in exon 6 was performed. The PCR product results in either a 60 bp (wild type) or 55 bp (657del5) amplicon and can be distinguished by resolving the bands in a high percentage (3 %) agarose gel, or a 10 % acrylamide gel (Figure 17 on page 58, A). Genomic DNA (gDNA) samples from NBS patient 1, 3, 5 and 7 show only one PCR product of 55 bp, confirming the loss of 5 bp in exon 3, whereas gDNA isolated from HFF1 cells show one PCR product of 60 bp. PCR of gDNA from NBS patient 8 results in amplicons of both sizes, implying a heterogeneous mutation for 657del5 in this cell line.

Sanger sequencing was performed to confirm the presence of mutations. A PCR product of primers flanking the whole exon 6 was sequenced, using the same primer set. The resulting sequences were analyzed employing CHROMAS, a free tool for illustrating and translating sequencing signals into sequences. Proof-reading of the sequences included matching the correct bases in cases when the program misinterpreted the signal curve. Each peak represents one base in the sequence and color identifies the kind of base, namely red, green, blue and black for Thymine, Adenine, Cytosine and Guanine respectively (Figure 17 on page 58, B). All NBS patient sequences (1, 3, 5, 7 and 8) were aligned to the sequence of non-mutated reference cell line HFF1 using BLAST (blast.ncbi.nlm.nih.gov) (Altschul *et al.*, 1990). BLAST finds regions of similarity between biological sequences and can either be used to align two sequences or find the nucleotide query in a genome database. All obtained sequences could be matched to the NBN gene using either the whole human mRNA database or the HFF1 exon 6 sequencing result. In NBS patient 1, 3, 5, 7 the sequences obtained from CHROMAS missed 5 bp at the 657 position of exon 6. When sequence from NBS patient 8 was analyzed from both strands, there were inconclusive nucleotide signals exactly at the 657-661 positions. With careful observation, the non-mutated sequence could be

spotted overlapping the mutated sequence. Therefore, NBS patient 8 is heterozygous for the 657del5 mutation.

3.1.1.2 *Expression of NIBRIN at protein level*

The translated NBN gene product, NIBRIN, consists of 754 amino acids and has a theoretical molecular weight of 84,959 kDa, but migrates at 95 kDa on SDS PAGE (sodium dodecyl sulphate polyacrylamide gel electrophoresis). The 657del5 mutation in NBS patients results in two truncated protein products. One N-terminal, shorter product, that terminates translation close at the mutation site and the longer C-terminal, hypomorphic version that initiates translation due to two cryptic ATG start codons that fall into frame after the 5 bp deletion. These proteins migrate at 70 kDa and 26 kDa and are therefore often called p70-NIBRIN and p26-NIBRIN respectively (Maser *et al.*, 2001a).

To confirm the expression of NIBRIN protein in all the cell lines used for this study, especially to confirm the absence of a full-length NIBRIN protein in cell line NBS-8, which is heterozygous for the 657del5 mutation, a western-blot-based immuno-detection of NIBRIN was performed. NIBRIN was not detected in NBS patient cell lines, but detected in the non-mutated control cell line, HFF1 (Figure 17 on page 58, C). There was a band observed of approximately 70 kDa, which could represent p70-NIBRIN, but the band occurred in the reference cell-line as well. This was not expected, because p70-NIBRIN protein initiation can only occur because of the 5 bp deletion as explained earlier. Therefore the p70 fragment was not further analyzed with this antibody and the observed band was regarded as non-specific. The p26 fragment was also not observed.

Figure 17: **Confirmation of the 657del5 mutation in patient cell lines by PCR and Western blotting**
(A) PCR-based analysis of genomic DNA with primers flanking the deletion, results in either a 60 bp (wt) or 55 bp (657del5) amplicon. (B) Sequencing by primers flanking the 657del5 mutation for HFF1 (wild-type), NBS-1 (representative for samples #3, #5, #7) and NBS-8. HFF1 was aligned against NBN mRNA, NBS-1 and NBS-8 were aligned against HFF1. The overlay of two sequences of the heterozygeous mutation in NBS-8 can be tracked by looking at the raw-data (Chromas). (C) Immunoflurescent detection of full-length (p95) NBN. Even loading of the SDS-gel is shown by house-keeping protein GAPDH.

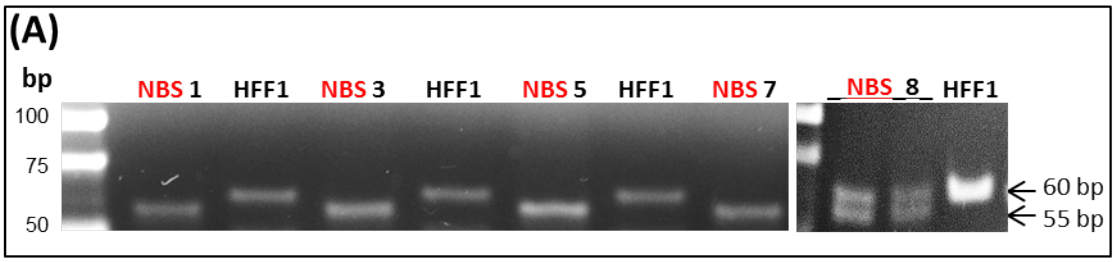

(B)

HFF1 Exon 6 (fw) against NBN mRNA (NM_002485.4)	Query 694 GTTTTTACCCACCTCTTGATGAACCATCTATTGGAAGTAAAAATGTTGATCTGTCAGGAC 753 Sbjct 26 GTTTTTACCCACCTCTTGATGAACCATCTATTGGAAGTAAAAATGTTGATCTGTCAGGAC 85 Query 754 GGCAGGAAAGAAAACAAATCTTCAAAGGGAAAACATTTATATTTTTGAATGCCAAACAG 812 Sbjct 86 GGCAGGAAAGAAAACAAATCTTCAAAGGGAAAACATTTATATTTTTGAATGCCAAACAG 144
NBS 1 Exon 6 (fw) against HFF1 Exon 6 (fw)	Query 21 ACTTTA-TTATTTTTACNGTTTTTACCCACCTCTTGATGAACCATCTATTGGAAGTAAAA 79 Sbjct 8 ACTTTAATTATTTTTACNGTTTTTACCCACCTCTTGATGAACCATCTATTGGAAGTAAAA 67 Query 80 ATGTTGATCTGTCAGGACGGCAGGAAAGAAA-----TCTTCAAAGGGAAAACATTTATAT 134 Sbjct 68 ATGTTGATCTGTCAGGACGGCAGGAAAGAAAACAAATCTTCAAAGGGAAAACATTTATAT 127
NBS 8 Exon 6 (fw) against HFF1 Exon 6 (fw)	Query 25 ACTTTANNTANTTTTACNGTTTTTACCCACCTCTTGNTGAACCATCTATTGGAAGTAAAA 84 Sbjct 8 ACTTTAATTATTTTTACNGTTTTTACCCACCTCTTGATGAACCATCTATTGGAAGTAAAA 67 Query 85 ATGTTGATCTGTCAGGACGGCAGGAAAGAAA 115 Sbjct 68 ATGTTGATCTGTCAGGACGGCAGGAAAGAAA... 98

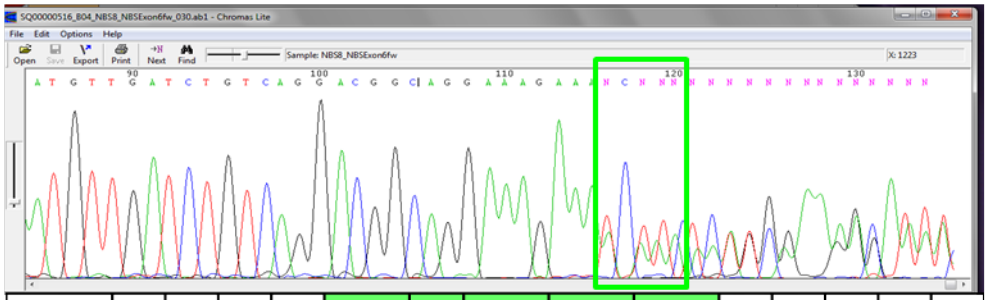

wt	G	A	A	A	A	C	A	A	A	T	C	T	T	C
mut	G	A	A	A	a/t	C	a/t	a/t	a/t					

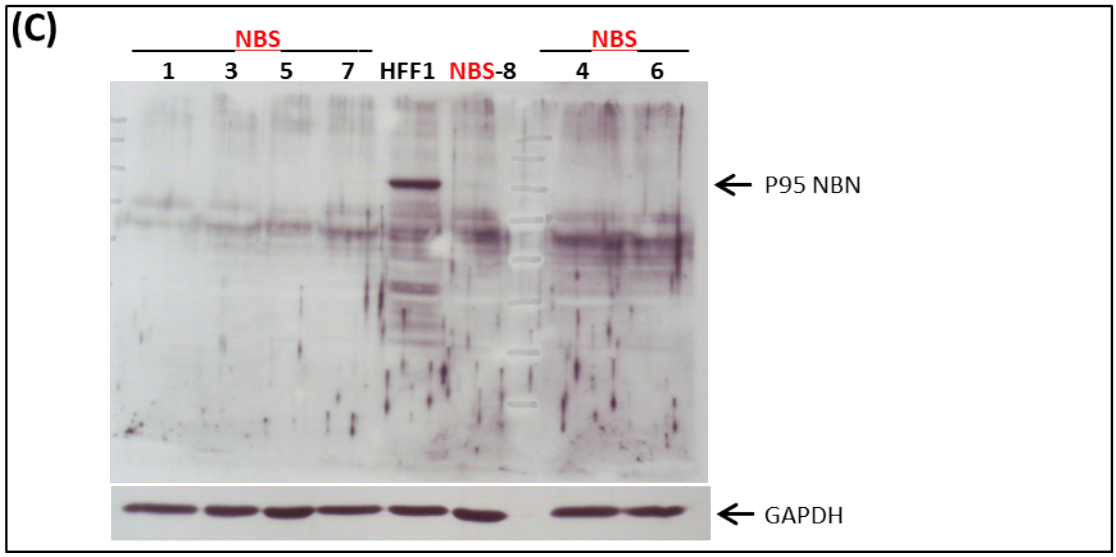

3.1.2 *Cellular Reprogramming: Fibroblasts from Patients with Nijmegen Breakage Syndrome Can be Reprogrammed into Induced Pluripotent Stem Cells (iPSCs)*

Reprogramming of mature cells into pluripotent stem cells is one of the most remarkable findings of this century and has been acknowledged with the Nobel Prize in Physiology or Medicine 2012 for the researchers responsible for the discovery, John B. Gurdon and Shinya Yamanaka (AB, 2012). This new technology might enable us to replenish lost cells or even tissues and organs in the body without the problem of transplant rejection that occurs when the donor is different from the host. It also enables us to make drug or toxicity testing more specific and enables the unraveling of disease mechanisms in a dish with unlimited material. However, like all new technologies that arise, reprogramming is still fraught with several difficulties. Problems, that were also encountered in this study, are for example the low efficiency (around 0,01 – 1 %, (Hasegawa *et al.*, 2010)), epigenetic memory, or long-term quality of genetic material. In addition, reprogramming efficiency was negatively influenced by defective repair mechanisms in NBS patient cells, which are crucial to ensure chromosomal stability during the process (Rocha *et al.*, 2013).

The benefit of reprogramming cells from NBS patients include for example, autologous transplantation of bone marrow cells after genetic correction of the mutation, because these patients have high incidence of immune deficiency and lymphoid malignancy. In this study, the focus lies in creating an unlimited supply of cells, namely induced pluripotent stem cells, to enable modeling the disease in different cell lineages, as the effect of the mutation has several severity and effects in different tissues. Till today, the most efficient method is viral delivery of the four transcription factors OCT4, SOX2, KLF4 and C-MYC (O/S/K/M). Unfortunately, it has the disadvantage that the virus integrates randomly into the genome of the cell, which can have unpredictable effects on the phenotype and can even make the cells susceptible to become malignant. There are other, non-integrating methods, which use e.g. mRNA, microRNA, proteins, episomal vectors or sendai virus for O/S/K/M delivery, but all yet go at the expense of reprogramming efficiency. Here, viral transduction as well as episomal vectors and cell-penetrating recombinant proteins were used to deliver O/S/K/M into NBS patient derived fibroblasts with the aim to generate stable iPSCs.

3.1.2.1 *Viral-based reprogramming*

Reprogramming somatic cells towards pluripotency by viral delivery of the four transcriptions factors OCT4, SOX2, KLF4 and C-MYC is efficient, highly reproducible and also cost effective. On the other hand, random integration of virus DNA can cause disruption or mis-

regulation of genes that are important to retain genomic stability or regulate cell cycle. Mis-regulations of so-called oncogenes could cause cancer. In addition, genes which are not expressed in stem cells can become mutated, their effects might be only observable after they get activated upon differentiation. This could result in a different phenotype of the cell than the wild-type, leading to false results when performing studies. Here, I show the successful production of virus particles and infection of cells from NBS patients and healthy donors.

O/S/K/M RETROVIRUS PRODUCTION To generate retrovirus for delivery of OCT4, SOX2, KLF4 and C-MYC, the packaging cell line PhoenixAmpho (encoding pol, env) was transfected with mammalian expression vectors (pMXs backbone) containing Retroviral Psi packaging element 2 (psi plus pack2), group specific antigen (gag) and one of the four transcription factors O/S/K/M or GFP. Virus containing supernatant was collected 48h and 72h after transfection. Assuming that virus production was similar for all five constructs, only GFP containing virus was used to determine the virus titer. Different amounts of GFP containing virus were used to infect NBS-5 and HFF1 cells at different concentrations of basic growth factor 2 (FGF2) and were then measured for infection efficiency (GFF positive cells per total cells) by flow cytometry (see Figure 18 on page 61).

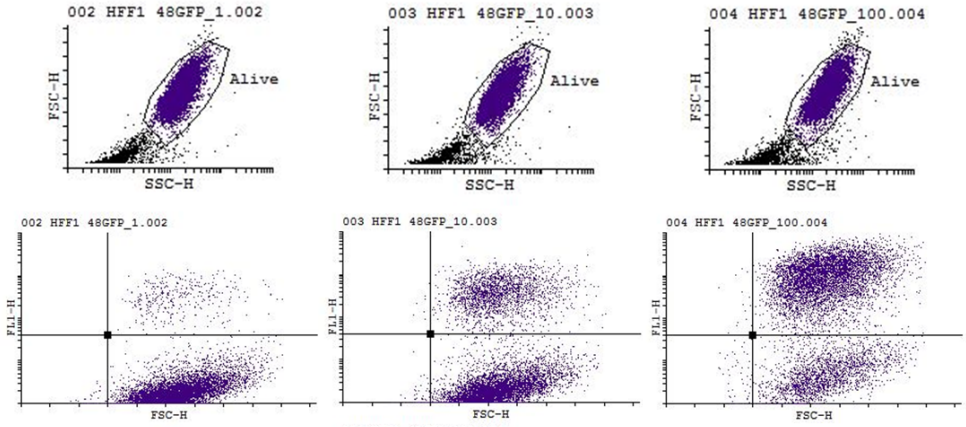

Figure 18: **Detection of GFP(+) cells by FACS analysis**
Representative analysis for all tested conditions (see Table 8 on page 62). Cells were infected with different amounts of virus supernatant (002: 1µl; 003: 10 µl; 004: 100 µl) to determine the biological titer. First the cells were discriminated by size (FSC-H) and granularity (SSC-H) to deselect dead cells and debris (not "Alive"). The gated ("Alive") cells were then further discriminated by green fluorescence (GFP, FL1-H) and size (FSC-H) and cells with fluorescence (upper right quadrant) were counted and used for calculation of the virus titer.

The biological titer, representing the transducing units per µl was calculated using following formula: $\frac{TU}{\mu l} = \frac{P*N}{100*V} * \frac{1}{DF}$ ((1))

P=% GFP positive cells; N=Number of cells at time of transduction in well; V=Volume of dilution added to each well; DF= dilution factor (1=undiluted)

In HFF1 cells, virus titer was 729 TU/µl after 48 h without addition of FGF2 and 594 TU/µl with addition of 8 ng/ml FGF2 (Table 8 on page 62). Therefore, FGF2 cannot be used to enhance infection efficiency in HFF1 cells. In NBS-5 cells, virus titer was 399 TU/ml after 72 h without FGF2. After 48 h it was 240 TU/µl without FGF2, 305 TU/µl with 8 ng/ml FGF2 and 481 TU/µl with 16 ng/ml FGF2. The overall infection rate in NBS-5 cells is therefore lower as in HFF1 cells, but can be enhanced by adding FGF2 or increasing incubation time.

Table 8: **Calculation of virus titer**

Cell line	Supplement	Vol [µl]	GFP$^{(+)}$ [%]	TU/µl	TU x 10^5/ml
NBS5	48h Virus	1	1,41		
NBS5	48h Virus	10	7,99	239,70	2,40
NBS5	48h Virus	100	38,52		
NBS5	72h Virus	1	1,93		
NBS5	72h Virus	10	13,31	399,30	3,99
NBS5	72h Virus	100	45,56		
NBS5	48h Virus + FGF2 (8 ng/ml)	1	1,88		
NBS5	48h Virus + FGF2 (8 ng/ml)	10	10,18	305,40	3,05
NBS5	48h Virus + FGF2 (8 ng/ml)	100	46,74		
NBS5	48h Virus + FGF2 (16 ng/ml)	1	2,36		
NBS5	48h Virus + FGF2 (16 ng/ml)	10	16,04	481,20	4,81
NBS5	48h Virus + FGF2 (16 ng/ml)	100	55,26		
HFF1	48h Virus	1	4,11		
HFF1	48h Virus	10	24,3	729,00	7,29
HFF1	48h Virus	100	73,66		
HFF1	48h Virus + FGF2 (8 ng/ml)	1	2,49		
HFF1	48h Virus + FGF2 (8 ng/ml)	10	19,8	594,00	5,94
HFF1	48h Virus + FGF2 (8 ng/ml)	100	78,51		

O/S/K/M RETROVIRUS QUALITY To ensure correct production and infection capabilities as well as an overview of infection efficiency, HFF1 and NBS-3, -5, -7, -8 cells were infected with 2,5x TU of all four viruses per cell which is the same condition as for the reprogramming experiment. Immunocytofluorescence staining was performed for each of the four transduced transcription factors (O/S/K/M) after 48 h (Figure 19 on page 63, A). All four factors could be observed in all transduced cell lines with high efficiency in HFF1 and NBS-8 cells, whereas NBS-3, -5, -7 showed low level transduction and cell morphology appeared senescence-like (Figure 19 on page 63, B). From

this result, it can be anticipated, that virus overall infection ability is sufficient for reprogramming, but infection of several NBS lines appeared more difficult and therefore also less efficient for reprogramming.

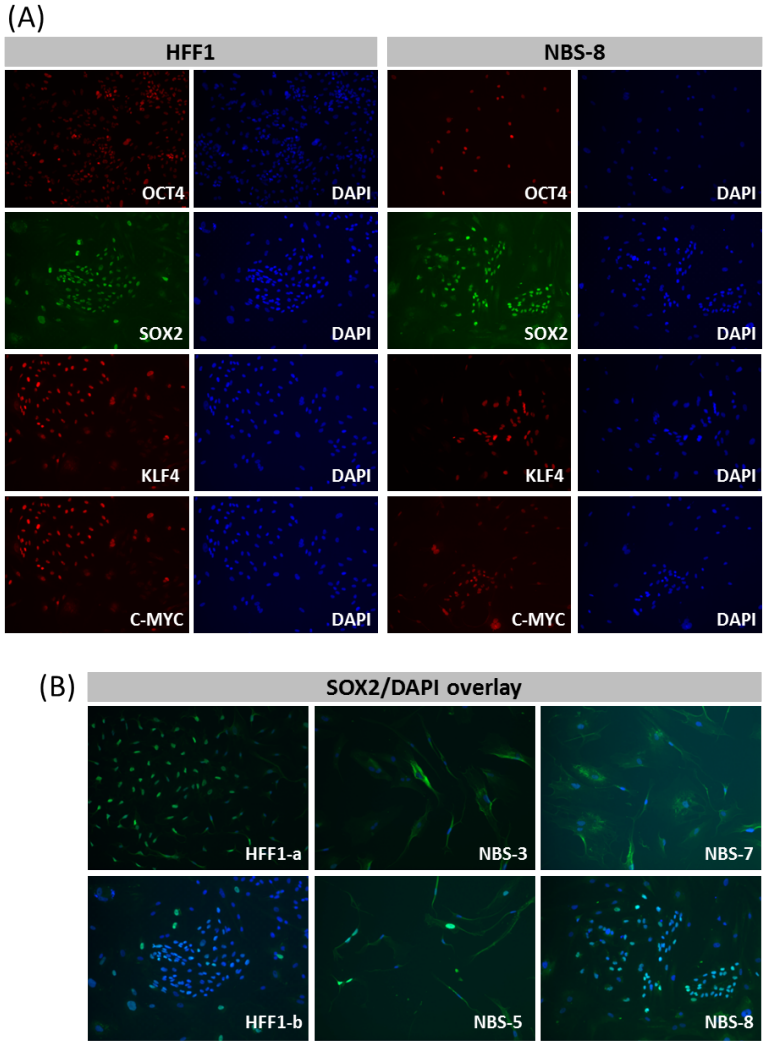

Figure 19: **Immunofluorescent detection of reprogramming factors 48h after infection**
(A) Paraformaldehyde-fixed fibroblasts were treated with the respective primary antibody and a fluorescent secondary antibody. The nuclei were stained with DAPI. Overview pictures show the cell confluency and approximate infection efficiency of each reprogramming factor. (B) Comparison of cell morphology and confluency after infection with reprogramming factor SOX2 of several NBS cell lines and HFF1.

3.1.2.2 *Reprogramming with episomal-based vectors*

As mentioned previously, there are great disadvantages in viral transduction of the four reprogramming factors O/S/K/M. Therefore, the field has been searching for procedures with better reproducibility and efficiency on the one hand and avoidance of exogenous material on the other hand. A publication from (Yu *et al.*, 2009) described the generation of "footprint-free" human iPSCs by transfection of oriP/EBNA-1 (Eppstain-Barr nuclear antigen-1) episomal vectors. Those vectors were designed on the basis of viral elements but without the virulent effects. The episomal vectors are present at low copy number per cell, minimizing DNA re-arrangement and genome integration and oriP/EBNA-1 improves import and retention of vector DNA in the nucleus. They replicate only once per cell cycle and are lost from cells at a rate of ~5 % per cell generation. Therefore, after several passages the iPSCs are free of exogenous DNA. A single transfection is sufficient for inducing pluripotency. With the aid of small molecule inhibitors, efficiency was reported at 220 iPSC colonies per $1*10^6$ input cells (0,02 %) (Yu *et al.*, 2011).

To obtain iPSCs without DNA integration, fibroblasts from a healthy donor (HFF1) and a NBS patient (NBS-8; heterozygous for the 657del5 mutation) were nucleofected with the 7F-2 vector combination (Figure 20 on page 66, A) containing two copies of OCT4, SOX2 and KLF4, plus one copy of NANOG, SV40LT (Simian Vacuolating Virus 40 large T antigen), C-MYC and LIN28. After transfection, the reprogramming efficiency was enhanced by supplementation with small molecule inhibitors of the following pathways for 15 days: MEK (PD0325901) pathway, GSK3beta (CHIR99021) pathway and TGF-beta/Activin/Nodal-receptor (A-83-01).

On day 15 (Figure 20 on page 66, B), HFF1 cells showed morphological changes at high frequency and even colony-like shapes. In between, there were many fibroblast-shaped cells at high density. In contrast, NBS-8 cells showed only a few clustered cells, otherwise the cell morphology appeared unaltered. The cells were trypsinized and seeded to gelatin coated plates with mouse embryonic fibroblasts (MEFs).

On day 55 (Figure 20 on page 66, C), HFF1 derived cells resulted in one single big hESC-like shaped colony, which was also similar to hESCs at single cell morphology level. NBS-8 cells grew in tightly packed cell humps with undefined edges, very dissimilar to the flat colonies inherent to hESCs with round defined edges (see Figure 20 on page 66, C). From both lines, cells were split (day 70) onto matrigel coated plates with feeders. The NBS-8 cells were terminated 3 weeks later, because they failed to reprogram to iPSCs. But also the promising looking colony derived of HFF1 cells failed to re-grow into hESCs shaped colonies. They were kept for some more weeks, but perished

eventually. Repeated attempts to reprogram NBS-8 fibroblasts to iPSCs by episomal plasmids also failed.

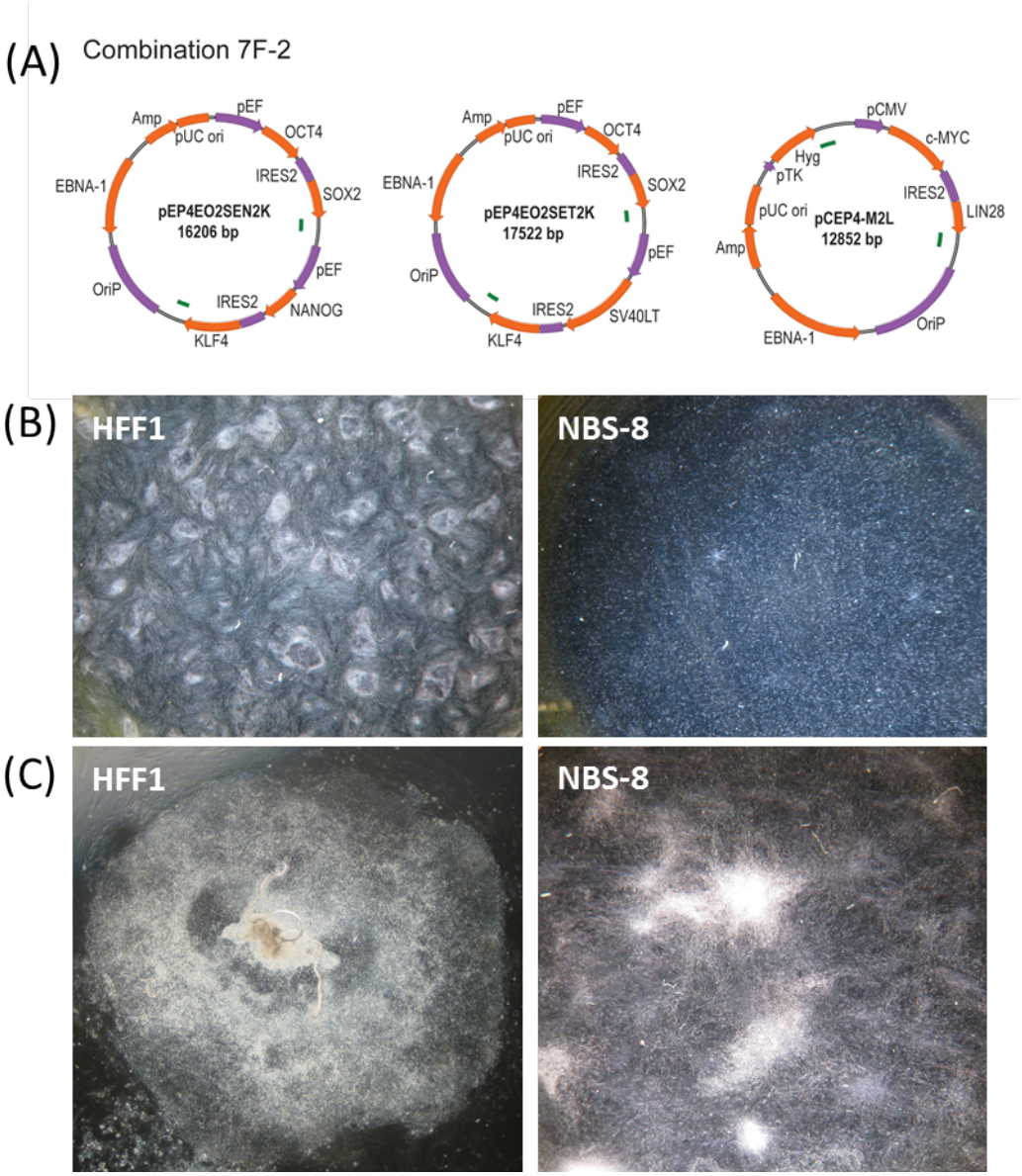

Figure 20: **Episomal reprogramming**
(A) Location of reprogramming factors on episomal plasmids. (B) Overview of cell growth 15 days after transfection (no magnification). (C) Colony morphology 55 days after transfection (5x magnification).

3.1.2.3 *Reprogramming by Cell-penetrating Recombinant Proteins*

One of the alternatives to viral-based reprogramming is the use O/S/K/M recombinant proteins. The proteins can be added to the medium and cross plasma membranes by a short cell-penetrating peptide, which is fused to each of the transcription factors. The transport into the nucleus is achieved by a nucleus localization signal that is already present in the natural sequence of the transcription factors. One of the advantages of reprogramming with cell-penetrating-proteins is, that there is no transfection required, which is otherwise time consuming and stressful for the cells.

In this study, we tried to reprogram HFF1 cells with the aid of recombinant O/S/K/M attached to cell-penetrating-peptides. The reprogramming procedure was performed with three different set-ups as described in 2.9.3. The process was monitored by taking pictures with a digital camera through the microscope every other day of 10x magnified cells.

After HFF1 fibroblasts were seeded, they set at a confluency of approximately 40 % on the day after (Day 1). They were quickly growing to 100 % confluency (Day 7) but no morphological changes of any kind whatsoever could be observed until day 14. Small accumulations of cells that had also grown into the z-axis had formed at that time but did not increase in number or size over the next two weeks. The course of reprogramming was similar for all three conditions. From the well with treatment condition (i) a small area was cut and removed from the well on day 30 (Figure 21 on page 68, A). The tissue-like fragment was trypsinized and plated into a new well with matrigel-coating and feeders. Some smaller tissue-like structures and some single cells attached the next day, but didn't grow further. Therefore, the experiment was terminated and all remaining cells were stored as frozen stocks for possible further studies.

To illuminate possible roadblocks that could have affected the reprogramming process, the most potent reprogramming protein OCT4 was incubated together with HFF1 cells for 24 hours, fixed and immunostained with OCT4 antibodies. Under the microscope it became apparent, that recombinant OCT4 protein neither entered the nucleus nor the cell itself (Figure 21 on page 68, B). By varying the z-axis, it could be observed that all detected OCT4 protein was localized in one layer that appeared to be the top surface of the cells (Figure 21 on page 68, C). The reprogramming experiment therefore failed because of possible quality defects in the recombinant proteins, incompatibility of HFF1 cells or other factors. Because of economic reasons, the problem could not be analyzed further and the experiment could not be repeated.

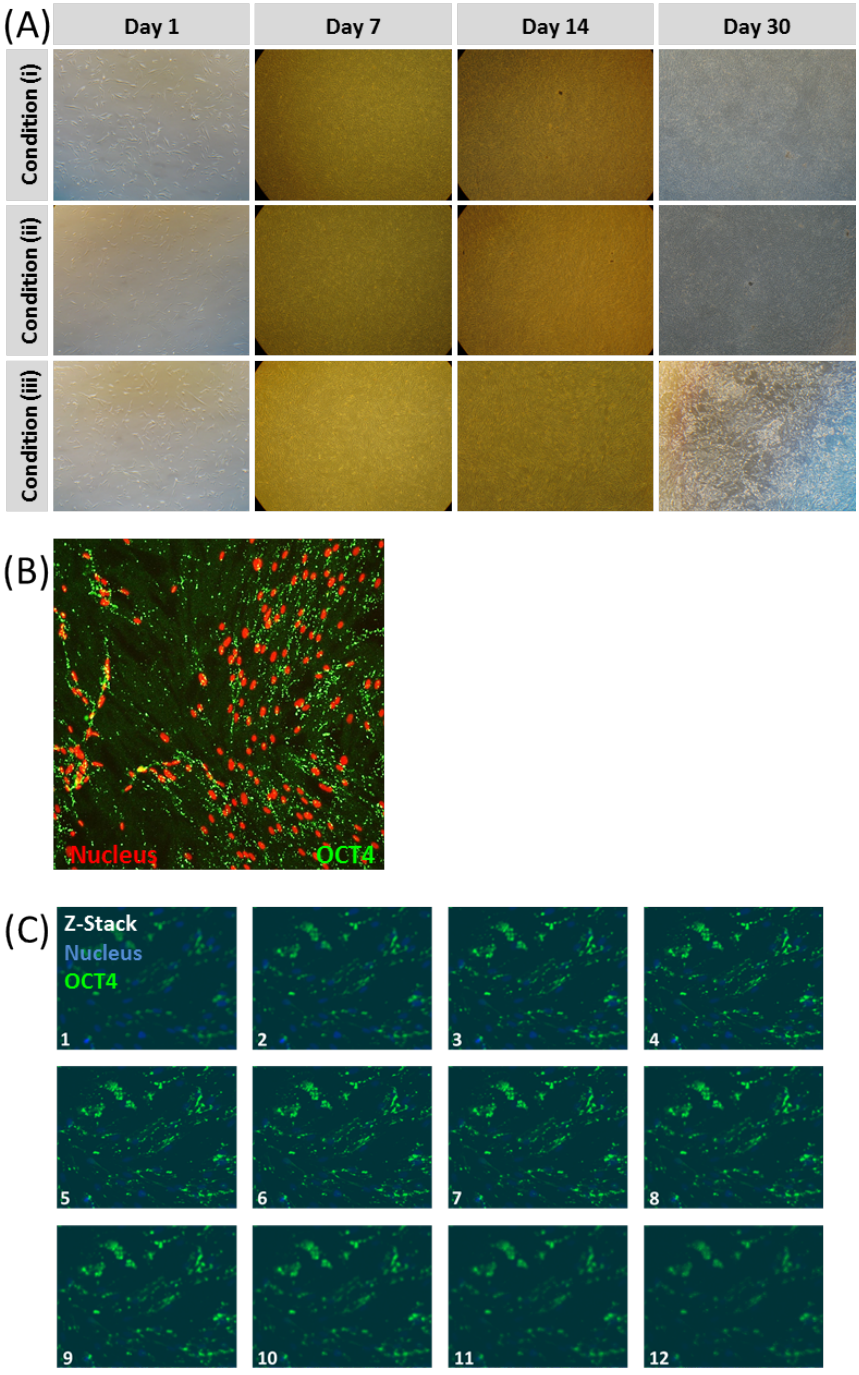

Figure 21: **Reprogramming with recombinant proteins**
(A) Overview of reprogramming progress after 1, 7, 14 and 30 days by means of morphological changes (10x magnification). (B) Localization of OCT4 recombinant protein 48 h after application (green) in comparison to nucleus (red). (C) Localization of recombinant OCT4 (green) and nuclei (blue) in a Z-stack series of 3,59 µm/slice and a total diameter of 39,50 µm (x-y-Area: 396 x 313 µm).

3.1.2.4 *Characterization of reprogrammed cell lines from viral transduction*

Observations of cell and colony morphology had already shown, that the original fibroblasts underwent drastically changes. But there are certain requirements to be met, before the cells can be called iPSCs and can be approved by other researchers in stem cell society. Several experimental setups to prove the pluripotent state and high similarity with hESCs emerged in the years after the first publication of human iPSCs by Yamanaka in 2007 (Takahashi *et al.*, 2007). Those methods include observation of certain morphology characteristics, detection of alkaline phosphatase (AP), a set of pluripotency markers on the surface and in the nucleus of the cells, a fingerprinting PCR to prove that source and reprogrammed cells are identical, differentiation of iPSCs to EBs (Embryoid Bodies), which include cells of all three germ layers, differentiation of iPSCs under the skin of immunodeficient, live mice into teratomas which comprise of tissues of all three germ layers and also the epigenetic state (methylation state of pluripotency gene promoters) can be analyzed and compared to hESCs. All of the above methods (except promoter methylation) were performed and confirmed the high similarity of the reprogrammed cells with hESCs. In the process of obtaining stable clones, one HFF1-iPSC clone (HFF1-iPSC-8) and two from NBS-8 cells derived clones were selected (NBS-8-iPSC-1 and NBS-8-iPSC-2) in which NBS-8-iPSC-2 is a subclone, derived from NBS-8-iPSC-1 at very early passage number. The selection was based on morphological characteristics. This viral-derived iPSCs from one NBS patient (NBS-8) and control HFF1 cells were subject to further characterization.

COLONY MORPHOLOGY Comparing cell and colony morphology is the first and fastest feature to determine the progression of cellular reprogramming from fibroblasts to iPSCs. Fibroblasts are mesenchymal cells, specialized in sequestering extracellular matrix like collagen. They often form a spindle-shaped cell body with branched cytoplasm and high cytoplasm to nucleus ratio (Figure 22 on page 70, A). Fibroblasts can migrate slowly and tend to spread out, forming loose contacts with neighboring cells *in vitro*, but can also grow tight if space is limited. To become iPSCs, fibroblast first have to undergo MET (mesenchymal-epithelial transition) resulting in cells that grow in a monolayer and in close contact to each other. They also have to lose their spindle-like structure with branched cytoplasm and gain a smaller, round but flat morphology, similar to cobblestones, with a high nucleus to cytoplasm ratio. Fibroblasts do not grow in colonies and rather spread out as much as possible. HESCs, on the other hand, form round-shaped colonies with very tight cell-cell con-

nections, that appear almost as a homogeneous area at lower magnification (10x) (Figure 22 on page 70, B). Another characteristic of the hESC colony is the defined and sharp periphery. With this in mind, several colonies were selected and transferred to isolated wells to observe their growth for several passages. During that time, many clones that were selected, lost their pluripotency and became differentiated or apoptotic. A fraction of picked clones resulted in stable iPSC-lines. Here, one HFF1-iPSC clone and two NBS-8-iPSC clones were obtained through picking and repeated passaging.

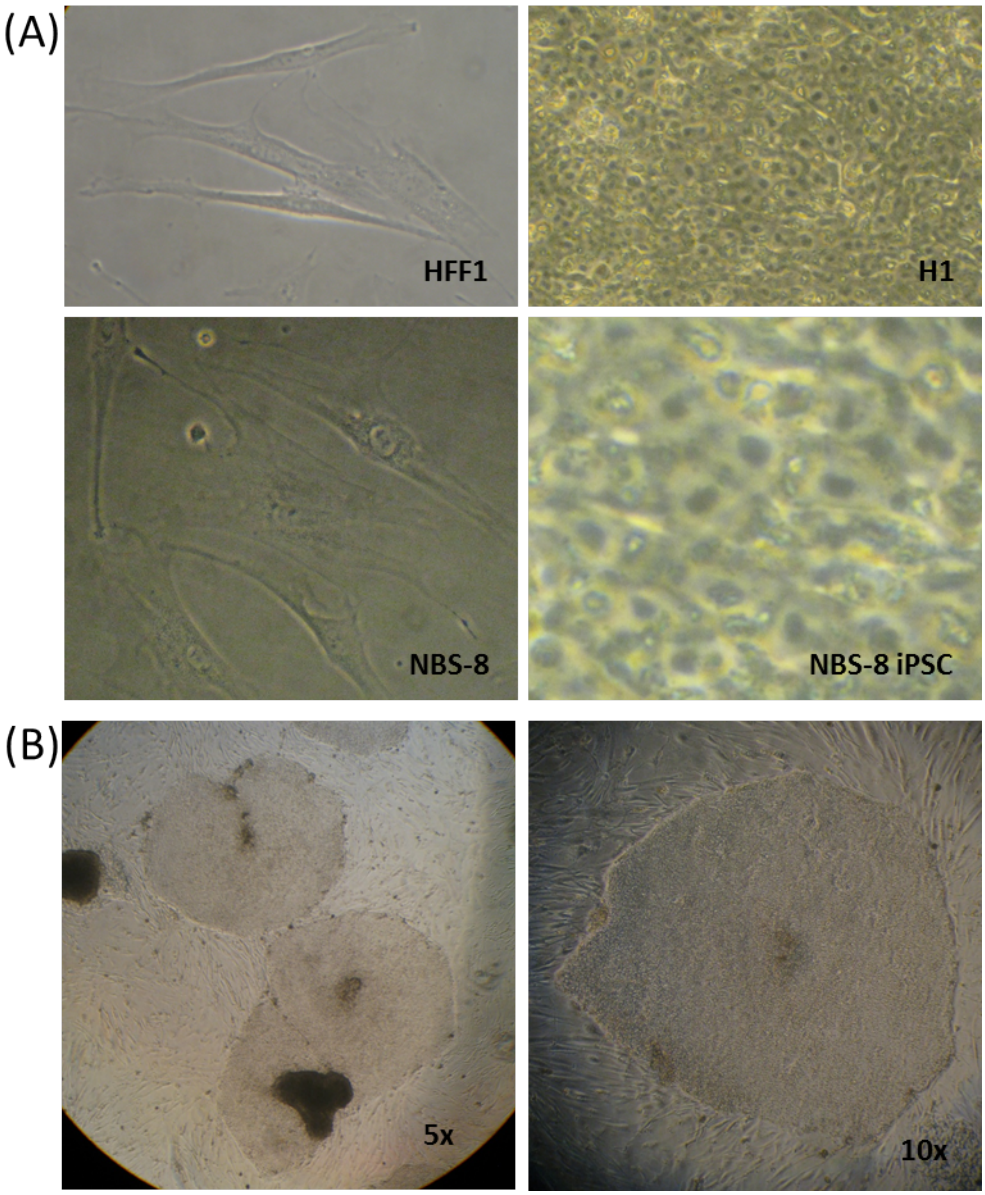

Figure 22: **Morphology of human embryonic stem cells**
(A) 60x magification of HFF1 and NBS-8 fibroblasts (right), hESCs (H1) and NBS-8-iPSCs (additional 3x digital zoom). (B) 10x magification of typical hESC-like colonies, here NBS-8-iPSCs, P2.

EFFECT OF OXYGEN TENSION ON THE MAINTENANCE OF PLURIPOTENCY NBS-8-iPSCs and HFF1-iPSCs were grown at both 21 % and 5 % oxygen levels and appeared to grow stably at both conditions. But when NBS-8-iPSCs were put from 5 % oxygen to 21 % oxygen, all cells died or differentiated during the next 24-48h. Notably, the change from high to low oxygen was no problem for the cells. The observation of oxygen sensitivity was solely made with iPSCs from the NBS patient. The change in oxygen concentration did not affect iPSCs from HFF1 cells or hESCs. Effects were judged on occurrence of visible changes, like differences in cell or colony morphology, increased differentiation or cell death. Fibroblasts of NBS patients were also grown at low and high oxygen concentration, but this did not lead to ultimate loss of the cells by apoptosis (see 3.3.2, Figure 29 on page 89). At this early stage of the study it was therefore already clear, that iPSCs from NBS patients have a greater sensitivity towards oxidative stress.

CONFIRMATION OF HESC MARKER EXPRESSION One of the very early markers for detecting pluripotency in cells that were reprogrammed is detection of alkaline phosphatase (AP) on the surface of these cells. It is therefore often used in the preliminary rounds of assays to discriminate the good from the bad colonies. HESCs have elevated AP in their membrane and by detection of AP negative cells and colonies in early reprogramming stages they can be separated from potential iPSCs. The AP positive cells can be stained with an assay where a non-colored synthetic substrate of AP becomes red or purple after hydrolysis by AP. There are also immunofluorescence-based live stainings available. The downside of this assay is, that AP can be also positive in partial reprogrammed cells and some somatic cells like liver, bone and placenta. Therefore it is necessary to perform further assays to analyze the iPSC lines. Here, a sufficient number of AP positive colonies were derived after reprogramming NBS-8 fibroblasts, to further cultivate them into stable iPSC-lines (Figure 23 on page 73, A).

Human ESCs serve as the gold standard when pluripotency is determined in iPSCs. Therefore, the expression of several known marker genes for hESCs have to be confirmed in iPSCs. There is a set of nuclear transcription factors like OCT4, SOX2 (which also belong to the reprogramming cocktail) and NANOG (a transcription factor that is endogenously transcribed). And there is a set of surface proteins that are specific to hESCs. They include TRA1-60, TRA1-81, TRA-2-49/6E, SSEA3, SSEA4 and negative expression for SSEA1. IPSCs from HFF1 and NBS-8 fibroblasts were immunocytologically stained for several of these markers. The colonies were grown on MEFs and pictures were taken in a way, so MEFs served as negative control for each staining. NANOG and OCT4 positive colonies were found at high

frequency and homogenously stained all nuclei of the colony. SOX2 was found at higher intensity in the middle of the colony and in the cells that make up the border of the colony. The fact, that there were cells in between (clonal cells of the colony), which had little or no SOX2 expression, could indicate that SOX2 is solely endogenously transcribed and virus DNA had been silenced. TRA1-60, TRA1-81 and SSEA4 antigens were all stained homogeneously on the surface of the iPSC colonies and the specificity of used antibodies is confirmed not only by negative staining of surrounding MEFs, but also by negative staining of small additional colonies (Figure 23 on page 73, B).

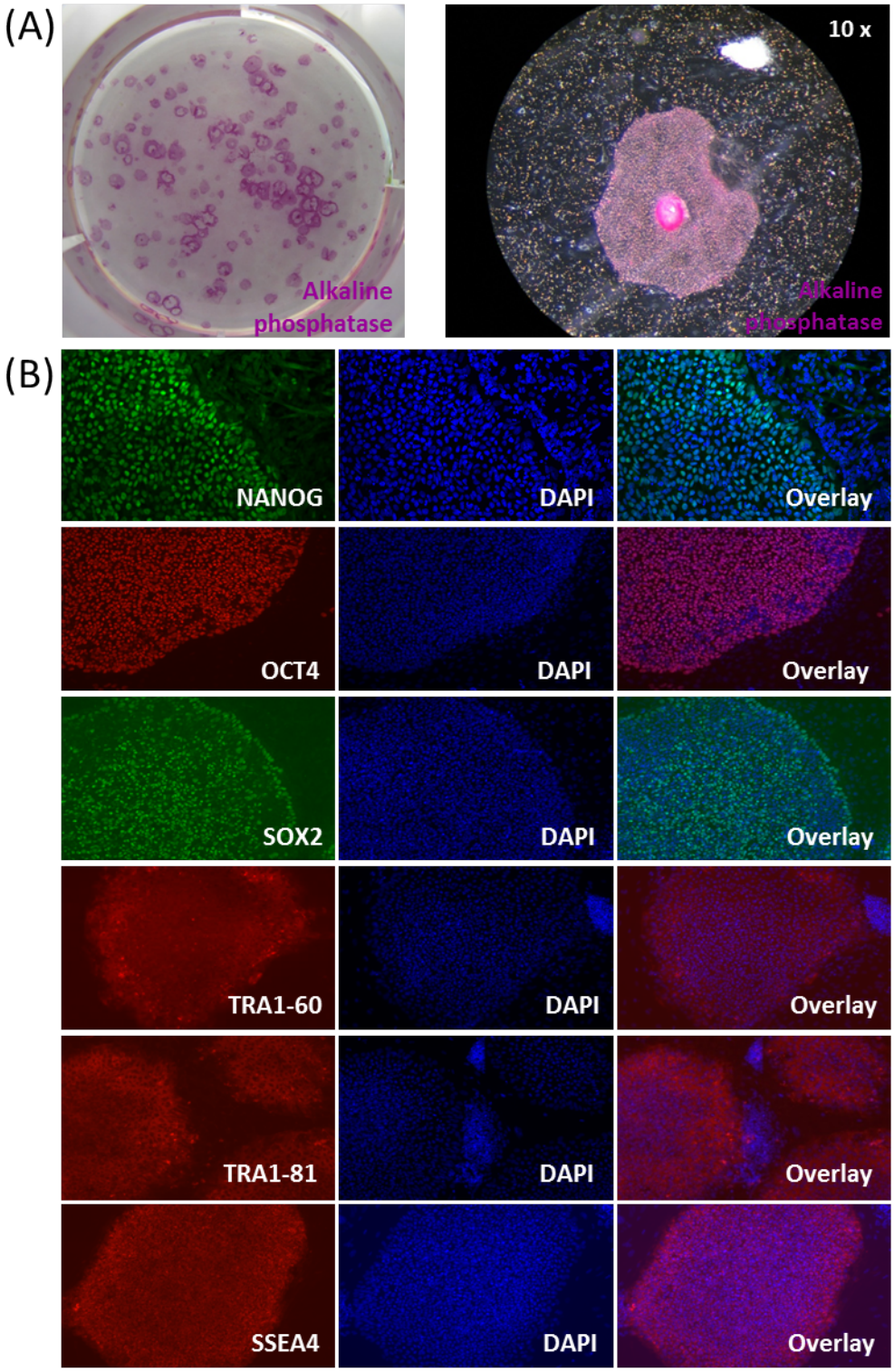

Figure 23: **Pluripotency marker**
(A) Alkaline phosphatase (AP) staining of NBS-8 iPSC-colonies in full-well overview and 10x magnification. (B) Immunofluescent detection of nuclear (NANOG, OCT4, SOX2) and surface (TA1-60, TRA1-81, SSEA4) pluripotency marker (green, red). Nuclei are stained with DAPI (blue).

Global transcriptome analysis was performed with cells from NBS-8 fibroblasts and NBS-8-derived iPSCs. In addition, samples from HFF1 fibroblasts, HFF1-iPSCs, BJ fibroblasts, BJ-iPSCs (Prigione *et al.*, 2011) and the hESC lines H1 and H9 were added to this analysis. The expression profiles were used to illustrate and compare the expression of NBN and several pluripotency related genes in this set of samples (Figure 24 on page 75, A). NBN expression in NBS fibroblasts and NBS-8-iPSCs was reduced by 50 % compared to control cells. This indicates that NBN is expressed from only allele, most likely from the allele with 657del5 mutation. The patient is heterogeneous at the genomic level for this mutation as was shown in part 3.1.1.1, but only expression of mutated mRNA could be confirmed by PCR of NBN mRNA and no full length NIBRIN could be found at the protein level (Figure 17 on page 58). The expression of pluripotency genes like NANOG, POU5F1 (OCT4), SOX2 and MYC was up-regulated in all iPSCs and hESCs whereas KLF4 was expressed at similar or lower level (Figure 24 on page 75, B).

DNA fingerprinting makes use of the 0,01 % of human DNA that differs in individuals (except monozygotic twins) to identify the individual. A PCR is performed with primers spanning so-called tandem repeats, which length and number varies from person to person. This method was used to confirm the somatic origin of the generated iPSC lines (Figure 24 on page 75, C). Four different primers were used to amplify different tandem repeats. PCR products of NBS-8 fibroblasts and the two NBS-8 derived iPSC lines (NBS-8-iPSC-1, NBS-8-iPSC-2) were separated by size on an acrylamide gel. They show the same pattern in number and size of bands. The strong bands are the expected main products of the PCR, but the weaker, unspecific bands show the same pattern in all NBS-8 samples as well and therefore strengthen the result. PCR products from HFF1 cells were loaded as a control and they show a different banding pattern than NBS-8 samples. The reprogrammed NBS-8-iPSCs were therefore proven to originate from NBS-8 fibroblasts and were not found contaminated by co-cultivated HFF1 cells.

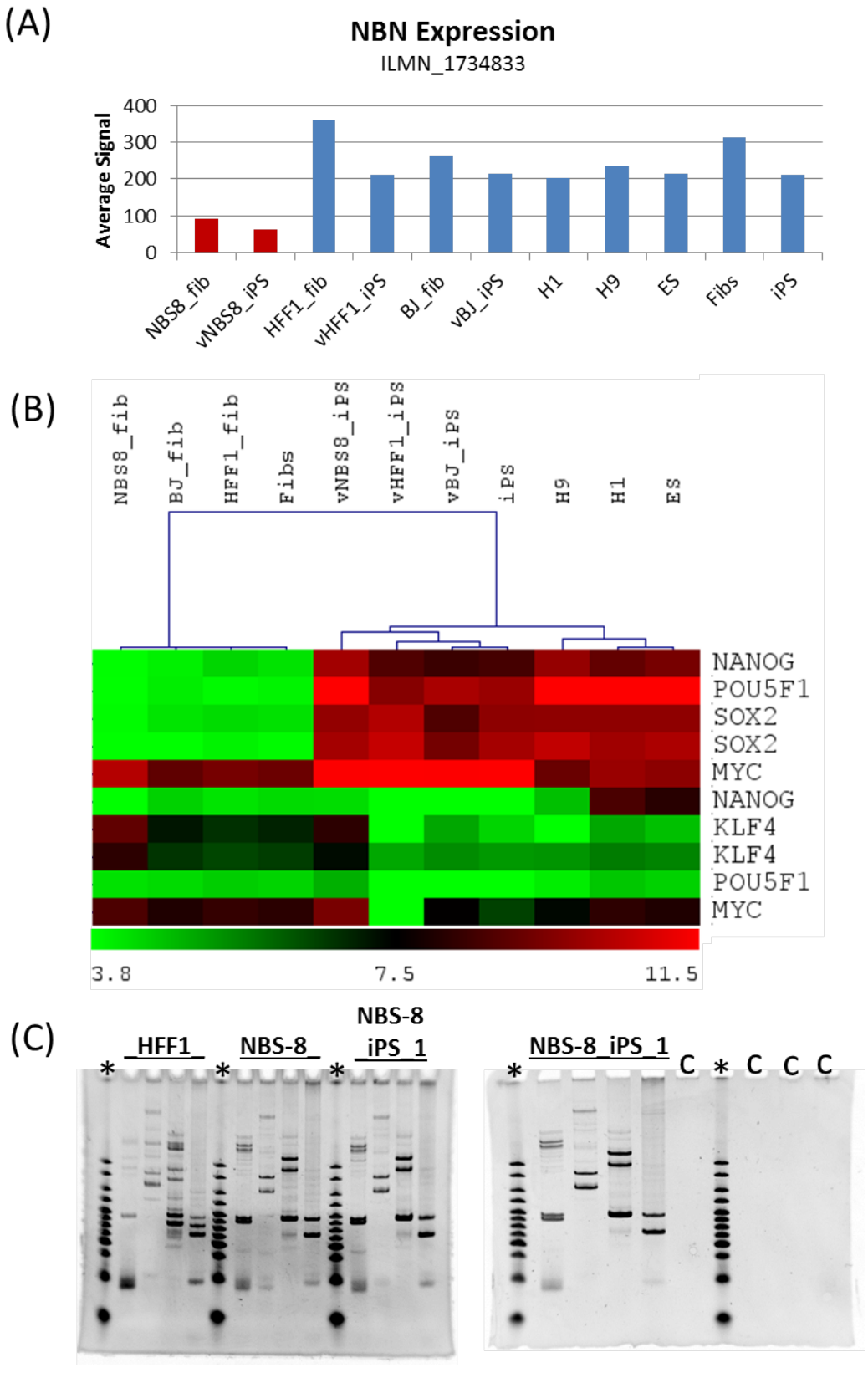

Figure 24: **Gene expression in NBS-iPSCs and fingerprinting**
(A) NBN mRNA average signal in different cell types. (B) Expression of pluripotency genes as heatmap before and after reprogramming and in comparison to hESCs (ES, H1, H9). Signal range of low (green) and high (red) expression is displayed as log2 of average signal. (C) Four different primers were used for fingerprint PCR (loaded on 10 % polyacrylamid gel) to compare banding pattern between iPSCs and their respective origin (*Hyper Ladder V; c: negative control).

Expression of NBN at the protein level was tested in NBS-8-iPSCs to confirm somatic origin and disease phenotype, lack of full-length NIBRIN. Expression of NIBRIN was detected by Western Blotting, with HFF1 fibroblast lysate as a positive control. Expression of full-length NIBRIN was not detected in NBS-8 fibroblasts and the NBS-8-iPSC lines (Figure 25 on page 77, B) even at high exposure time (not shown). Interestingly, it was difficult to obtain an even protein loading amount, due to unknown abundant proteins that contributed above average to the overall protein amount. Therefore, β-Actin, a structural protein that usually is uniformly expressed in most cells and little affected by altered conditions and serves as loading control, was detected at higher levels in HFF1 fibroblasts than in H1 or iPSC lines.

KARYOTYPE The karyotype of HFF1-iPSCs (P27), NBS-8-iPSCs (P29) and NBS-8 fibroblasts (P12) was tested for aberrations (Figure 25 on page 77, A). The parental line NBS-8 had one aberration in chromosome 4 with a frequency of 100% (46,XY,add(4)(p15)). NBS-8-iPSC-1 had one derivative chromosome 11 (46,XY,der(11)t(5;11)(q12;q25)). The second clone, NBS-8-iPSC-2, had two aberrant karyotypes. One, with trisomy 8 and a derivative chromosome 11 with the frequency of 12 in 15 counted metaphases (47,XY,+8,der(11)t(5;11)(q12;q25)). The second one occurred with a frequency of 3 in 15 counted metaphases and contained an isochromosome of the long arm of chromosome 1, a derivative chromosome 4 with additional material of unknown origin and different banding pattern, a deletion in 13q and additional material of unknown origin at 17p (47,XY+i(1)(q10),add(4)(p15),del(13)(q13),add(17)(p11)). The HFF1-iPSC-8 cell line derived from normal HFF1 fibroblasts was tested after the same cultivation time and reprogramming process and contained an unbalanced whole-arm translocation consisting of the long arm of chromosome 20 and 21 (45,XY,der(20;21)(q10;q10).

NBS-8-iPSC-1 (46,XY,der(11)t(5;11)(q12;q25)): As a result from the aberration, 628 genes distal from Chr.5q12 were gained. They enriched ($p \leq 0{,}05$) in pathways "Neuroactive ligand-receptor interaction" (18 genes), "Asthma" (5 genes) and "Fc epsilon RI signaling pathway" (8 genes). Enriched ($p \leq 0{,}0001$) with 297 genes in "Brain" as UP_TISSUE. Among the genes were some participating in the cell cycle (CCNH, CCNB1, CCNG1, CDK7, CDC25C, CDC23, PTTG1), some from repair pathways (XRCC4, UBE2B, MSH3, H2AFY), some involved in redox mechanisms (TXNDC15, ATOX1, GLRX, GPX3, GRXCR3, HIGD2A) and others (BTF3, CD14, HDAC3, SMAD5, PANK3). The growth of IPSC-colonies appeared normal in comparison to standard hESC-colonies and passed all pluripotency tests.

NBS-8-iPSC-2 (47,XY,+8,der(11)t(5;11)(q12;q25)): trisomy 8 is known for affecting a various features as observed from trisomy 8 mosaicism

(Riccardi, 1977). The cell line passed all pluripotency tests, but was instable and often suffered from reemerging non-ES sub-colonies of aggressively proliferating cells.

NBS-8 fibroblasts (46,XY,add(4)(p15)): One chromosome 4 gained additional material of unknown origin.

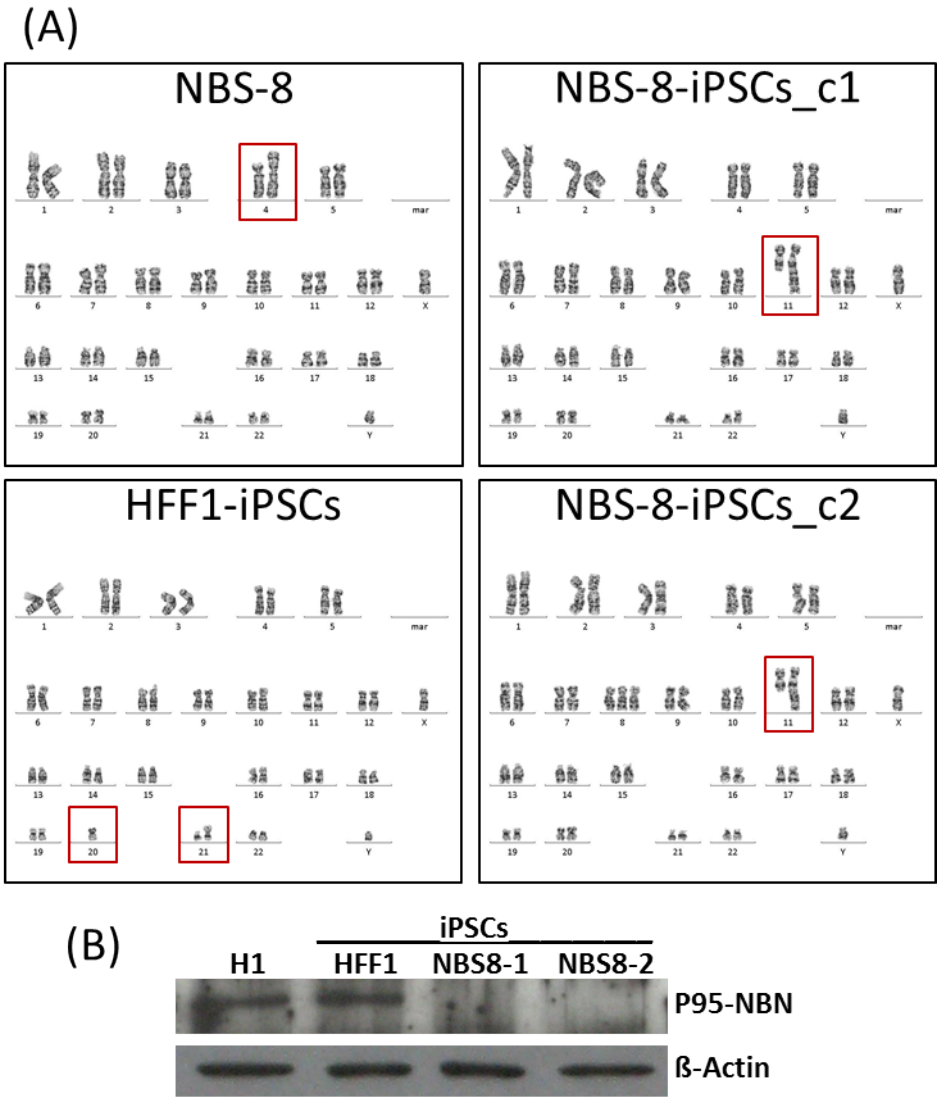

Figure 25: **Karyotype in NBS cells**
(A) Karyograms of NBS-8 fibroblasts and reprogrammed cell lines. Red boxes indicate chromosomes affected with aberrations. (B) Western Blot detection of p95-NBN in reprogrammed cells. ß-Actin serves as a loading control.

CONFIRMATION OF PLURIPOTENCY BY *in vitro* AND *in vivo* ASSAYS The major characteristic of hESCs is pluripotency, meaning that they can differentiate into cells of all three germ layers, mesoderm, endoderm and ectoderm. *In vitro*, this is tested by spontaneous

differentiation of hESC or iPSC colonies into so-called embryoid bodies (EBs), which further differentiate after attachment to the bottom of a culturing dish. The cells are then stained with fluorescently labeled antibodies for several markers representative of all three germ layers. The reprogrammed cell lines (HFF1-iPSC-8, NBS-8-iPSC-1, NBS-8-iPSC-2) were subjected to EB formation and then analyzed for the expression of (a) endoderm markers SOX17 and FOXA2, (b) ectoderm markers TUJ1 and NESTIN, and (c) mesoderm markers SMA (smooth muscle actin) and BRACHYURY (Figure 26 on page 79, A). Positive stained areas could be found in all cell lines. In some cases, typical morphologies of neurons could be seen (see TUJ1).

The most stringent test for pluripotency is the growth of teratomas in immundeficient mice. The tumors grow from injected iPSCs and should contain tissues of all three germ layers to confirm the similarity of iPSCs with hESCs. To reduce the use of animals, only one NBS-8-iPSC line was tested. The pathologist could confirm the growth of all three germ layers in NBS-8-iPSC-1 (Figure 26 on page 79, B). Three tumors in two mice were grown and reached the size of an average of 1,160 cm^3 on day 78. As ectoderm, focally small neuroectodermal tubular structures with several rows high prismatic epithelium were found. Endoderm was represented by few small tubular structures with iso- to high-prismatic epithelium, sometimes stocking with cilia, sometimes with goblet cells. And for mesoderm, the pathologist found large cysts with endothelial-like lining, some mucin gatherings and collagenous connective tissue. In total, tumors consisted largely of cystic structures and all represented tissues were found only in small portions, with least frequency of ectoderm.

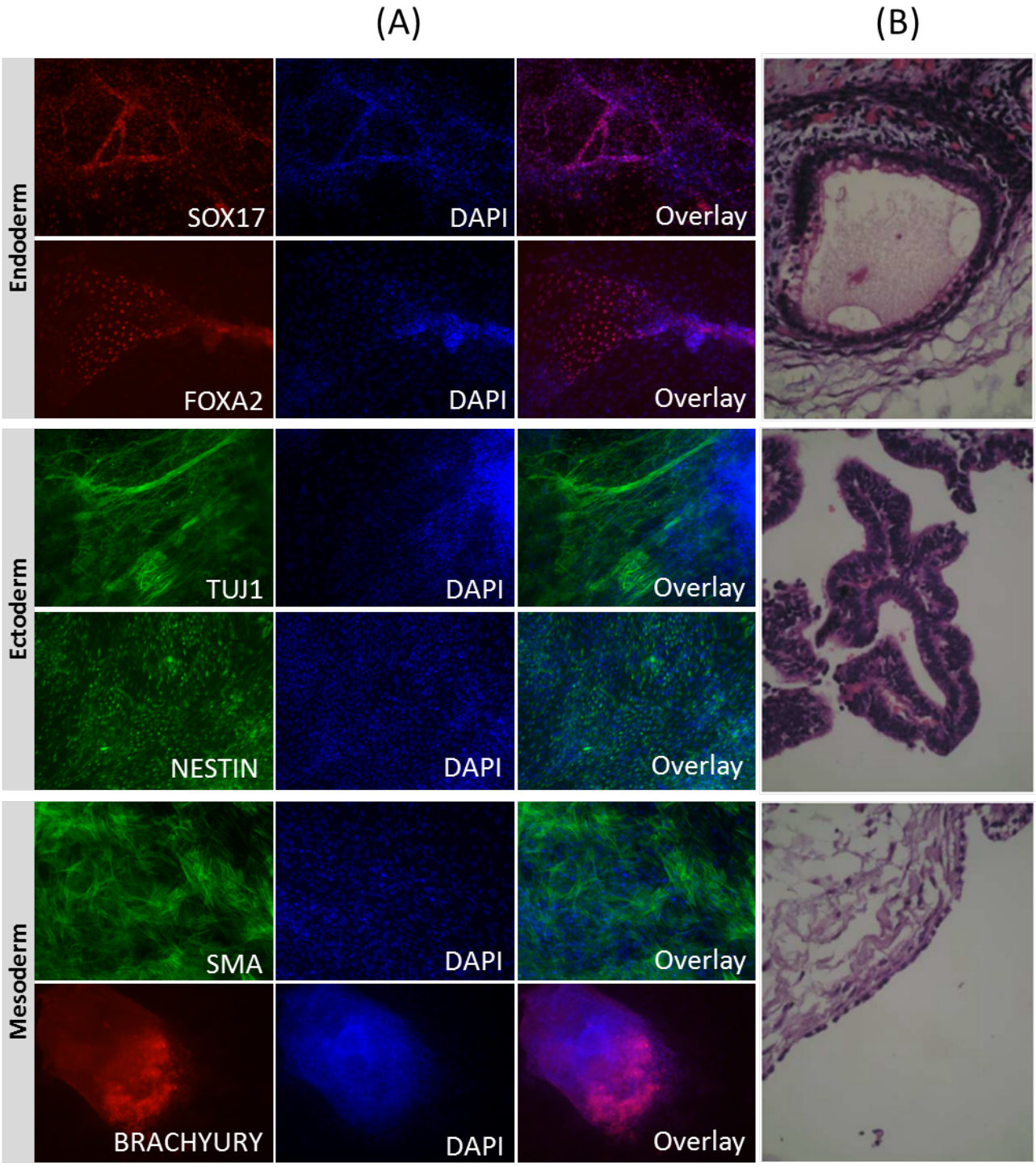

Figure 26: **Undirected differentiation with NBS-8-iPSCs**
(A) Immonufluorescent detection of endosomal, ectosomal and mesosomal marker proteins after embryoid body (EB) differentiation. (B) Histopathology of teratoma (hematoxylin and eosin staining) in immunodeficient mice after transplantation of NBS-8-iPSCs.

3.2 NBS RESCUE CLONING

During reprogramming cells undergo extensive changes in gene regulation, their epigenetic state and metabolism. It was shown, that this is stressful for the cells, especially with respect to increased incidences of DNA double-strand breaks. The cells react with activation of repair pathways, apoptosis and senescence (Müller *et al.*, 2012c). Therefore, it was anticipated, that reprogramming of NBS cells might encounter major roadblocks due to the NBS characteristic impairment of repair and checkpoint activation, or that NBS cells even might be impossible to reprogram. To compensate for this potentiality, a tetracycline inducible expression system for NBN was created in parallel to the reprogramming experiments, with the aim to rescue NBS-caused reprogramming failure. In addition, rescued NBS stable cell lines could serve as control in experiments, so patient specific effects can be ruled out and tetracycline-induced expression of NBN can serve as a tool, to directly compare NBS disease and rescued NBS.

3.2.1 *Overview of Cloning Strategy and Requirements to Establish a Stable Cell Line*

Technically, it is difficult to transfect hESCs with reasonable efficiency. Therefore, the NBS fibroblast lines were planned to be stably transfected with the constructs in advance to the reprogramming process. Advantages of a stable cell line are the long term expression and a stable copy number, whereas transient transfected cells can contain several variations of vector numbers and expression can be 10-100-fold higher. The tetracycline-inducible system requires two different plasmids, which have to be stably transfected into the target cells (Figure 27 on page 83, A). One plasmid contains the Tet-On 3G transactivator (pEFα-Tet3G), which is transcribed from an EF-1 alpha promoter. This promoter is derived from human EEF1A1 gene and provides long-term expression, especially in stem cells. The more frequent used CMV promoter is not suitable, because it can become silenced in many cell lines (Xia *et al.*, 2007; Qin *et al.*, 2010). The transactivator only induces expression when bound to its corresponding promoter together with tetracycline. The second plasmid (pTRE3G-BI-ZsGreen1) contains the response element for the transactivator, the P-TRE3F-BI bidirectional promoter, which induces expression of the green fluorescent protein, ZsGreen1, to the one direction and expression of a cloned gene (into MCS) in the other direction. The sequence of Myc-DDK tagged NBN was obtained from a commercially bought human cDNA ORF clone (NM_002485 in vector backbone RC214682). NBN-Myc was cleaved from the vector by restriction enzymes and cloned into the MCS of pTRE3G-BI-ZsGreen1. To obtain stable cell lines with both plasmids, the plasmids have to be transfected sequen-

tially. First, the pEFα-Tet3G has to be linearized (to increase chances of recombination into the genome) and is transfected into the target cells. The cells are treated with G418 for 2 weeks to isolate transfected cells. Clones are picked and treated further. The best clones are selected for transfection of the second vector. Best clones need to be selected according to the following characteristics: a) express the Tet-On 3G transactivator; b) result in high levels of induction from P-TRE3G; and c) exhibit low basal levels from P-TRE3G. To generate a double-stable cell line, linearized pTRE3G-BI-ZsGreen1-NBN-Myc has to be co-transfected with linearized hygromycin selection marker. Under selection of hygromycin, stable clones are also selected for G418 resistance. The resulting clones are then tested for maximal expression of NBN-Myc under tetracycline treatment and minimal expression of NBS-Myc in tetracycline depletion.

3.2.2 *Cloning Experiments to Generate a Tetracyclin-inducible NBN Expression Vector*

The commercially bought plasmids containing transactivator, bidirectional promoter for ZsGreen and a gene of interest (GOI), and NBN-Myc cDNA were transformed into *E. coli* bacteria (strain DH5alpha) to amplify the amount. Clones were tested by digesting with restriction enzymes at characteristic sequences and analysis of resulting specific DNA fragments by gel electrophoresis (Figure 27 on page 83, B). To clone NBN-Myc into the ZsGreen vector (pTRE3G-BI-ZsGreen1), the sequence of NBN-Myc was released from its vector (RC214682) by restriction enzymes. The same enzymes were used to cut the ZsGreen vector at the multiple cloning site (MCS) and produced sticky ends. Sticky end cloning (opposed to blunt ends) increases ligation events and ensures the correct orientation of the target sequence when different sequences are used for each restriction site. The digested DNA was separated by agarose gel electrophoresis (Figure 27 on page 83, C) and fragments of desired size were cut from gel with a razor blade. After DNA purification and concentration measurement of the fragments, a ratio of 1:3 (Backbone:Insert) was chosen for ligation. After the reaction, a small amount of the ligation mixture was tested in gel electrophoresis. The faint shifted bands above the size of backbone and insert alone indicated a successful ligation of the construct (Figure 27 on page 83, D). The ligation product was transformed into *E. coli* bacteria and plated on agarose plates containing ampicillin. Several clones were picked, plasmid DNA was isolated and digested with previously used set of restriction enzymes to test for positive clones of pTRE3G-BI-ZsGreen1-NBN-Myc (Figure 27 on page 83, E). Based on this result, one clone was selected for amplification (Lig2).

3.2.3 *Confirmation of Tetracyclin-inducible Expression of NBN in Cell Culture*

To create a stable cell line, cells have to be selected with the transfected construct and the corresponding antibiotic for at least 2 weeks to ensure integration of DNA into the host genome. Usually, the vectors used to transport the GOI carry selection marker resistance genes. In this case, G418 (Geneticin) and Hygromycin B were used to select transfected cells. But before treatment of the transfected cells, the optimal concentration of these antibiotics has to be determined for each cell line. Different concentrations of G418 and hygromycin were applied on HFF1 cells and optimal concentration was drawn from the minimal concentration that results in 99 % dead cells after 5 days, which was 500 µg/ml of G418 and 50 µg/ml of Hygromycin B. The cloned construct and the functionality of the tetracycline inducible expression system were tested in 293 cells, a cell line that can be transfected easily and with high efficiency. The vector containing transactivator and the vector containing ZsGreen and NBN-Myc were co-transfected by a non-liposomal reagent (FugeneHD) into 293 cells under either tetracycline (also called doxycycline) deprivation or supplementation (500 ng/ml). Pictures of ZsGreen expression were taken with a fluorescence microscope after 72 hours and cells were lysed in RIPA buffer (Figure 27 on page 83, F). Western blot analysis showed increased expression of NBN in transfected and doxycycline supplemented cells, compared to non-transfected control and tetracycline deprived cells (Figure 27 on page 83, G). In addition, expression of NBN-myc was specifically detected only in tetracycline supplemented cells. The construct was therefore considered functional and it was continued with creation of a stable NBS fibroblast cell line. For this, NBS8 fibroblasts were transfected first with the transactivation vector (pEFα-Tet3G) and selected with G418. After 5 days, only approximately 10 % of the cells did survive and were cultivated further. But even after several transfection attempts, a sufficient amount of cells was never reached to proceed with the second transfection/selection round (vector pTRE3G-BI-ZsGreen1-NBN-Myc). The cells stopped proliferating after 2 weeks, which was probably the result of cell cycle arrest or senescence, induced by stress of the transfection, or late initial passage of the cell line.

The stable inducible expression system is nevertheless a valuable tool, that can be used in future experiments with NBS cells, best with fresh patient samples or immortalized cell lines. It can also be used in transient expression experiments. Because this study is focused on hESCs and iPSCs, which are very difficult to transfect at high efficiencies, this was not pursued further.

Figure 27: **Cloning and transfection of doxycyclin-inducible NBN rescue plasmid**
(A) Overview of rescue strategy: NBS cells are transfected with transactivator construct (pEF1α-Tet3G) and selected for integrates with neomycin (G418). In a second round the cells are transfected with linearized hygromycin and the construct, carrying the inducible bidirectional promoter, green fluorescent protein ZsGreen1 and NBN, cloned into the MCS. (pTRE3G-BI-ZsGreen1-NBN). After selection, the NBS fibroblasts can express wild type NBN ectopically if induced by doxycyclin. (B) Agarose gel of control digest of commercially obtained plasmids (NBN-cDNA clone; pEF1α-Tet3G and pTRE3G-BI-zsGreen1). (C) Agarose gel of linearized destination plasmid pTRE3G-BI-zsGreen1 and NBN-cDNA seperated from vector backbone. Dotted boxes indicate fragments that were cut out and purified. (D) Agarose gel of successful ligation of pTRE3G-BI-zsGreen1 and NBN-cDNA (Lig), linearized pTRE3G-BI-zsGreen1 and NBN-cDNA fragment alone (pTRE3G, NBN) and unligated combination (pTRE3G + NBN). Arrows indicate successful ligation products. (E) Agarose gel of control digest of pTRE3G-BI-zsGreen1-NBN clones (L1-L7) and pTRE3G-BI-zsGreen1 vektor alone as control. Clone L2 (red) was selected for further upscaling. (B-E) * 1 kb DNA Ruler. (F) 293 cells were transfected with pTRE3G-BI-zsGreen1-NBN with or without addition of doxycyclin (Dox) to verify the inducible system. Left: Microscopy picture of ZsGreen1 fluorescence; right: Overlay of fluorescent with brightfield image. (G) SDS-PAGE with immunofluorescent detection of NBN and myc-tag in 293 cell lysates after transfection with pTRE3G-BI-zsGreen1-NBN with or without addition of doxycyclin (Dox). C = Control.

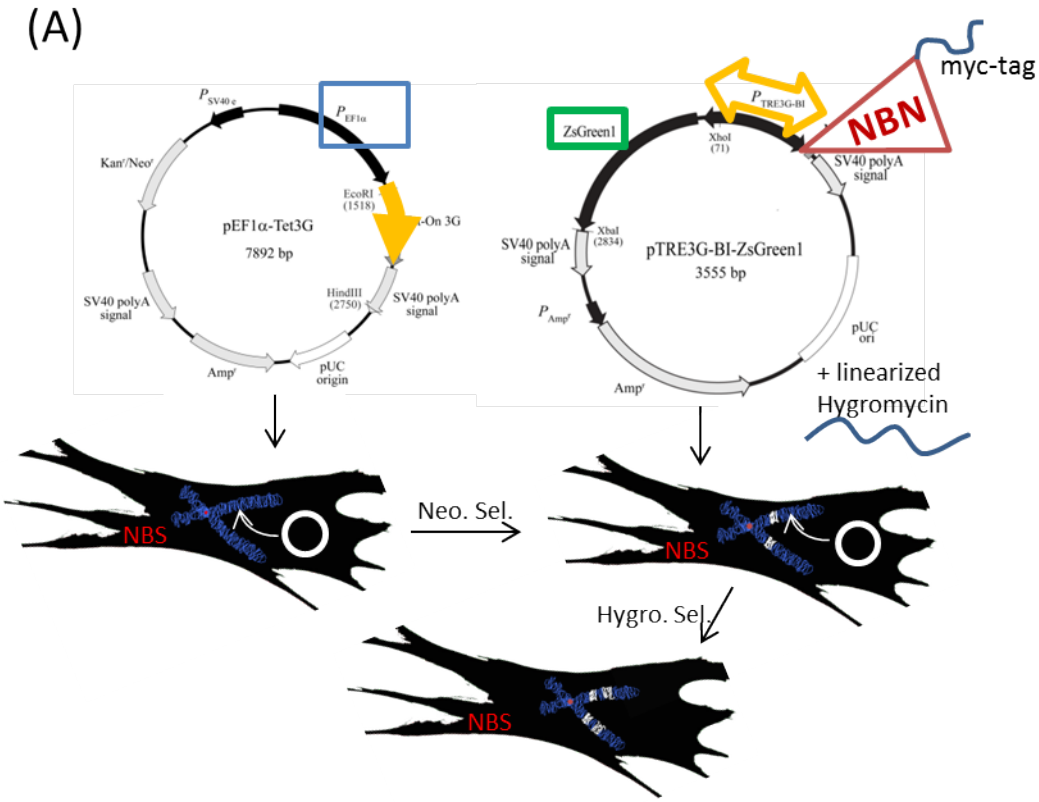
(A)
myc-tag
NBN
ZsGreen1
pEF1α-Tet3G
7892 bp
pTRE3G-BI-ZsGreen1
3555 bp
SV40 polyA signal
Kan^r/Neo^r
Amp^r
pUC origin
pUC ori
+ linearized Hygromycin
NBS
Neo. Sel.
Hygro. Sel.

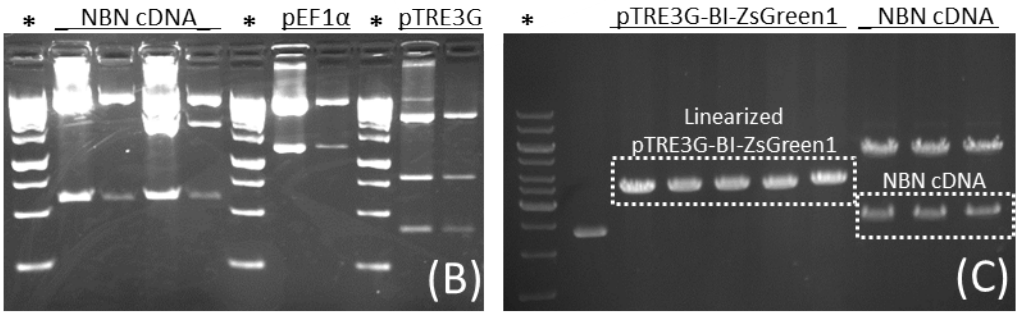
* NBN cDNA * pEF1α * pTRE3G
(B)
* pTRE3G-BI-ZsGreen1 NBN cDNA
Linearized pTRE3G-BI-ZsGreen1
NBN cDNA
(C)

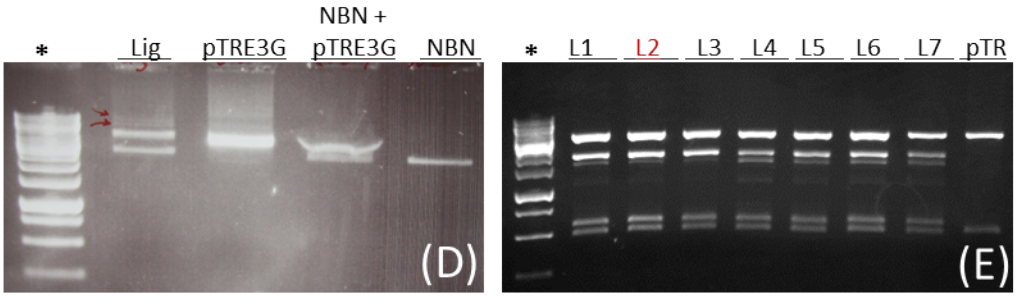
NBN +
* Lig pTRE3G pTRE3G NBN
(D)
* L1 L2 L3 L4 L5 L6 L7 pTR
(E)

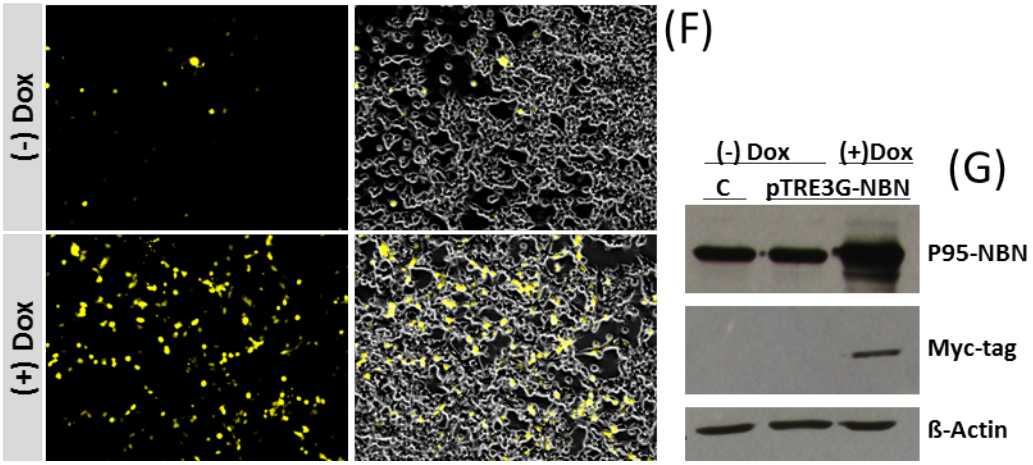
(-) Dox
(+) Dox
(F)
(-) Dox (+)Dox
C pTRE3G-NBN
(G)
P95-NBN
Myc-tag
ß-Actin

3.3 FUNCTIONAL LEVEL: ROS, DNA DAMAGE AND CELL CYCLE

3.3.1 *Cell Cycle and Proliferation*

NBS's prominent features are genetic instability and reduced growth as manifests by shortened body height and microcephaly (Chrzanowska *et al.*, 2012). Therefore regulation of proliferation and cell cycle might be generally effected by truncated NIBRIN, with measurable changes on physiological, transcriptional or translational level.

To compare proliferation speed of NBS fibroblasts to non-diseased fibroblasts (HFF1) a MTT assay was performed. This assay can reflect the number of viable cells present by employing cellular oxidoreductases to reducing the MTT reagent 3-(4,5-dimethylthiazol-2-yl)-2,5-diphenyltetrazolium bromide to its insoluble form formezan. Formezan has a purple color and can be measured in a colorimetric assay. The cells were seeded at three different starting concentrations, grown for 4 days and then stained with the typical MTT reagent. At all three conditions (resulting in different end-point confluence) the amount of viable cells was similar in HFF1 and NBS-8 containing wells (Figure 28 on page 87, A), therefore there was no difference in proliferation speed.

To obtain a broader view of the proliferation behavior, the cells were synchronized in G1-phase by sustaining 100 % confluence for several days, split 1:2 and then left to grow for 24 h. Cells were harvested at 100 % confluence and at growth phase (log-phase), stained with propidium iodide to quantify the DNA content and analyzed by FACS. HFF1 cells collected at 100 % confluence were observed to be mostly in G1 phase and almost none in S-G2/M-phase (Figure 28 on page 87, B, red outline). After 24 h, the cells had started proliferation again as observed by an increase in S-G2/M phase cells (black filling). The ratio of G1 to S and G2/M phase cells is similar to other often observed proliferating fibroblasts cells (Ryba *et al.*, 2011). NBS-8 cells on the other hand, showed a complete different ratio of proliferating cells (green outline). Here, almost all G1 cells entered S-G2/M phase at the observed time point. The difference between HFF1 and NBS cells may lie in variable resting points during confluence. While contact inhibition of HFF1 cells may result in early G1 phase arrest or even dormancy (Go phase), NBS-8 cells might have rested at the G1-S checkpoint at high frequency. So NBS-8 cells could progress into cell cycle much faster. Another explanation could be a slower passage of NBS-8 cells through S- and G2-phases due to DNA damage. It can be concluded that NBS-8 cells are different in their proliferation, not in doubling speed, but how they progress though the particular phases of the cell cycle.

As the last experiment already gave interesting insights into the cell cycle progression of NBS cells, it also raised some more questions. To

address this, the experiment was repeated with extended features. Two NBS lines were included instead of one, and the numbers of time points were increased to four. Comparing HFF1 with NBS-5 and NBS-8 cells at 100 % confluence showed common features like a high G1 peak and a small G2/M peak, reflecting the synchronization frequency in G1 phase (Figure 28 on page 87, C). But, as assumed before, there was a higher content of S-phase cells in both NBS cell lines, underlining the possibility that these cells deal differently with contact inhibition. After 22 h, NBS-8 cells showed the same behavior as before, a high number of S-G2/M phase cells in contrast to HFF1 cells, which only showed a small increase in these proliferating cells. At a closer look, the G2/M peak seemed to be missing in NBS-8 cells, leaving only the S-phase cells to consider. After 47 h the cell cycle profile of all three cell lines appeared to be similar, with only little variation in increased amount of S-phase cells in NBS-8 cells. Overall the cells seem to have fully entered their maximal ratio of proliferating cells, reaching the G2/M phase. After 67 h all cell lines had reduced their amount of dividing cells (S- and G2/M phase), in the cases NBS-5 and NBS-8 even to a level to the confluent cells (Figure 28 on page 87, F) and in the case of HFF1 cells, still on a moderate proliferating level (some S-phase cells and some G2/M-phase cells present). This leads to the same conclusion as the previous experiment, that overall proliferation speed of NBS-8 cells is similar to HFF1 cells, but differs in the frequency of cells the progress to the same cell cycle phase in the same time. There is specific evidence that the checkpoint between S and G2-phase might be activated and that is slowing the cell cycle progression. Interestingly, the progression of NBS-5 cells over the time course of 67 h is very similar to HFF1 cell and differs from NBS-8 cells. So in consequence, the proliferation properties only differ between the individual cell lines and are not necessarily associated with a NBS phenotype. But to answer this, experiments with more patient cell lines should be performed.

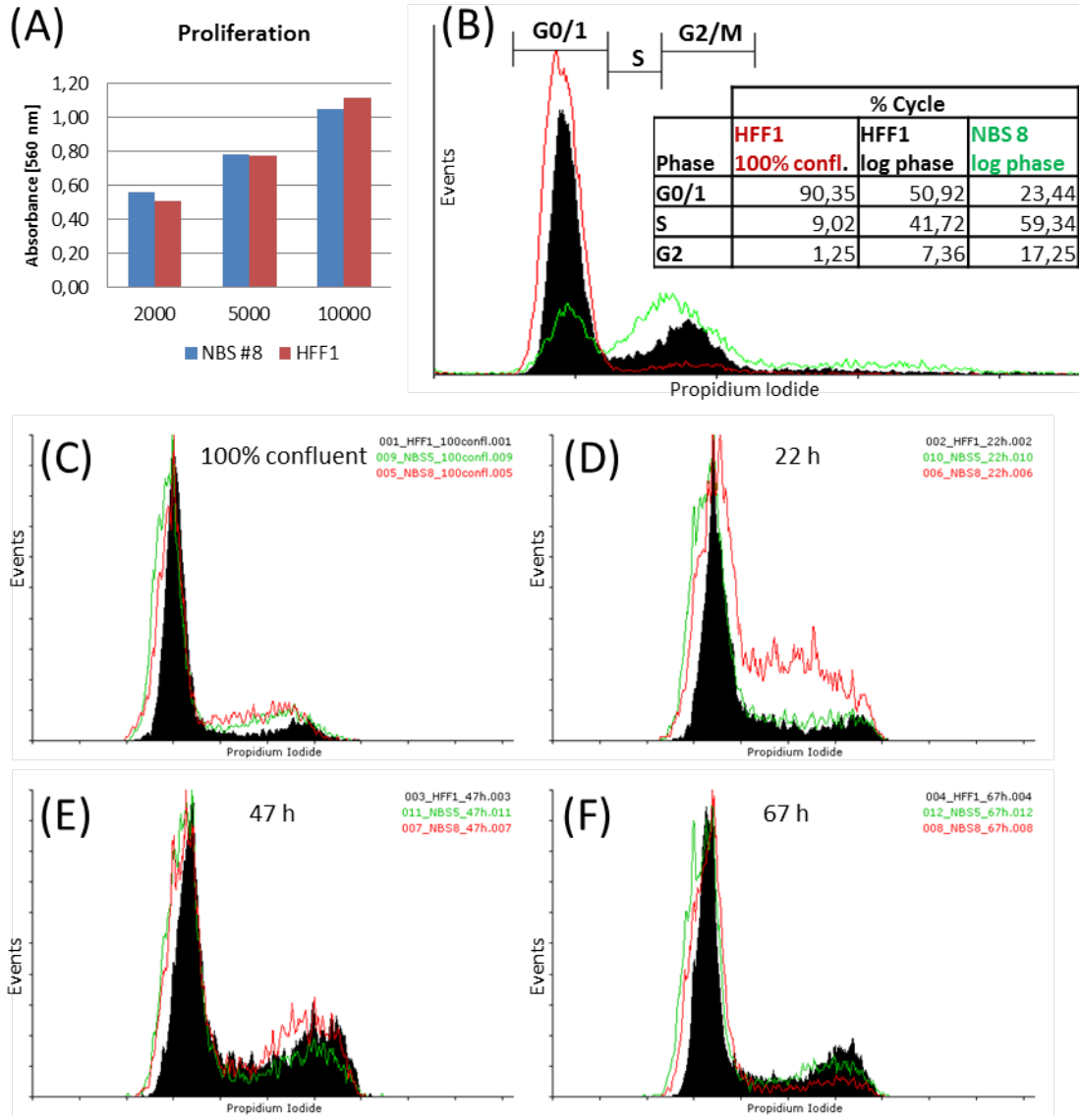

Figure 28: **Proliferation profile of NBS fibroblasts**

(A) MTT proliferation assay. Higher absorption stands for higher proliferation or greater cell number. X-axis shows different seeding densities (cell number per well). (B) DNA content of cells was stained with propidium iodide and sorted. Cell cycle phases (G1, S, G2/M) are indicated by bars above the peaks and relative cell number contribution to each phase was calculated. Black fill: HFF1 cells in logarithmic (log) phase; red outline: HFF1 cells at 100% confluence (not proliferating); green outline: NBS-8 cells in log-phase. (C)-(F) Fibroblasts were synchronized in G1-phase, than re-entered proliferation until harvest after 22, 47 and 67h. DNA content of cells was stained with propidium iodide and sorted. Black fill: HFF1; red outline: NBS-8; green outline: NBS-5.

3.3.2 *Oxygen Sensitivity*

As previously observed, NBS-8-iPSCs were highly sensitive towards oxidative stress and cells died or differentiated within 48 h after a switch from low (5 %) to ambient (21 %) oxygen. The same drastic effect could not be observed with NBS-8 fibroblasts. But in anticipation of a similar oxygen sensitivity that might show effect in a different phenotype, a comparative oxygen stress test between HFF1 and NBS-8 fibroblast was performed. Furthermore, the effect of the DNA double-strand-break inducer bleomycin was tested on the frequency of DNA damage under high and low oxygen partial pressures. The experiment was repeated three times, but at different confluence of the cells. The cells were grown under the respective oxygen concentration for the whole length of the experiment, but treated with bleomycin for 4 h before harvest, at either a 100 % confluence or in log phase 24 h and 48 h after splitting.

In HFF1 cells the difference in DNA damage, measured as phosphorylated histone 2AX (gamma-H2AX), was at low levels (around 0,55 % positive cells at 5 % O_2 and 1,03 % cells at 21 % O_2; p=0,093; Figure 29 on page 89). The natural frequency of DNA damage in NBS-8 cells was double as high as in HFF1 (1,78 % positive cells at 5 % O_2 and 1,92 % cells at 21 % O_2; p=0,338), and there was less difference in the comparison of 5 % vs. 21 % oxygen. When HFF1 cells were stressed with bleomycin, the damage increased 13-fold (13,04 %) at 21 % oxygen and only 6-fold (3,31 %) at 5 % oxygen. The induction of DNA damage in NBS-8 was even higher than in HFF1 (6-fold and 2-fold at 5 and 21 % oxygen, respectively). It was measured to be 11-fold higher at 5 % oxygen (20,16 %) and 14-fold higher at 21 % oxygen (26,16 %), as without bleomycin. Again, there was a smaller influence of oxygen on DNA damage in NBS-8 (p=0,128) than in HFF1 cells (p=0,023). In addition, cell cycle analysis was performed (not shown). In both, HFF1 and NBS-8 cells, there was an increased population of cells in S-phase after 24 h. This overlaps with a higher sensitivity for DNA damage at 24 h and bleomycin.

Taken together, the sensitivity of HFF1 cells towards induction to DNA damage by bleomycin can be greatly reduced, if cultured under low oxygen conditions. A similar result was found for NBS-8 cells, but the overall sensitivity for DNA damage was higher than in HFF1 cells. Furthermore, the phase of cell cycle might influence the sensitivity towards DNA damage as well.

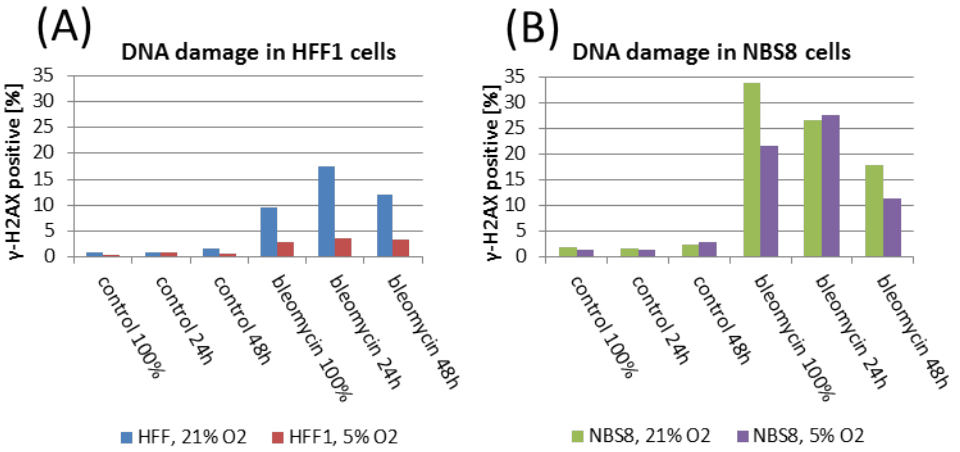

Figure 29: **Correlation between oxygen tension and DNA damage in HFF1 and NBS-8 fibroblasts**
Cells were synchronized in G1-phase (100% confluency) and released for 24h or 48h under high (21%) or low (5%) oxygen tension. Before harvest, cells were treated for 4h with radiomimetic bleomycin then released for 2h. DNA damage was detected by fluorescent γ-H2AX antibodies and analyzed via FACS. (A) HFF1 fibroblasts. (B) NBS-8 fibroblasts.

3.3.3 *Influence of Antioxidants on Cell Proliferation and Internal ROS Levels*

Oxygen concentration has an influence on DNA damage as presented in the previous paragraph. The repair of DNA damage, especially double-stand-breaks (DSBs) is impaired in NBS cells which ultimately lead to serious cell fates like apoptosis, arrest or accumulation of mutations that can result in cancer. Therefore, one of the possible options to increase the life span of NBS patients could be an environment with alleviated oxidative stress. There exist many components that have protecting effects, like vitamins, uric acid, or glutathione.

3.3.3.1 *Screening for antioxidants that have a modulating effect on internal ROS levels and increase resistance to DNA damage in cells with NBS*

To find a suitable agent that improves genetic stability of NBS cells, first, screenings for cell viability under addition of several antioxidants were performed. Glutathione and Vitamin C (ascorbic acid) are two of the well-known antioxidants. MTT assays were employed to analyze, if those could improve viability or increase proliferation in NBS cells. The working hypothesis was, if cells proliferate better, it is less likely that they encountered any DNA damage that in turn activated cell cycle checkpoints. HFF1 cells as the healthy control and NBS-8 fibroblasts were grown for 72 h with a high and low glu-

tathione/ Vitamin C combination (6,4 and 0,8 mM glutathione, 260 and 65 µM Vitamin C, Figure 30 on page 90, A). HFF1 cells responded to both treatment combinations with a 2-fold increase in proliferation, NBS-8 cells on the other hand did not respond to the high concentration and with a decreased proliferation to the low concentration. The experiment was repeated with addition of single component treatments (Figure 30 on page 90, B). Here, HFF1 cells again responded with 2-fold increase in proliferation to the high concentration combination of glutathione and vitamin C, but only with 1-5-fold increase when treated with glutathione alone and with reduced proliferation to vitamin C alone. In NBS-8 cells, there was no difference observed in all three conditions. Almost all HFF1 and NBS cells were lost, when treated with a 10-fold higher concentration of vitamin C. Also treatment with 1 mM EDTA was not supportive for fibroblast viability or proliferation. The effect of EDTA was tested, because it can stabilize the half-life of glutathione in aqueous solutions by 70-fold (Stevens *et al.*, 1983). But since the effect was negative on proliferation, it was not included in glutathione solutions.

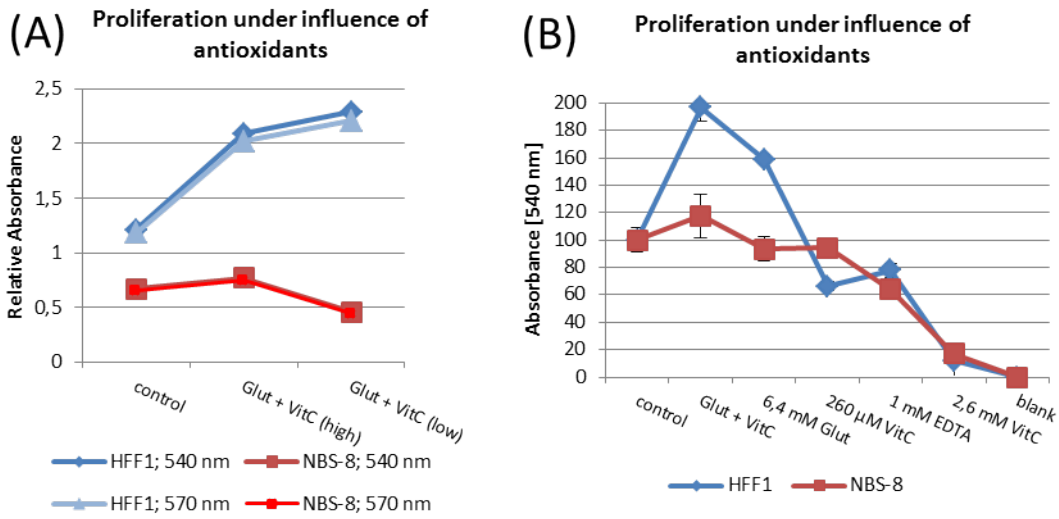

Figure 30: **Proliferation under influence of antioxidants**
MTT proliferation assays. Higher absorption stands for higher proliferation or greater cell number. (A) Cells were treated with a combination of glutathione (Glut) and ascorbic acid (VitC) either at high (6,4 mM Glut; 260 µM VitC) or low (0,8 mM Glut; 65 µM VitC) concentrations and measured at different absorptions (540 and 570 nm). (B) Cells were treated with different amounts of antioxidants as indicated.

Since the addition of glutathione and vitamin C had no beneficial effect on NBS cell proliferation, other components were considered. Two chemicals, disulfiram (DSF) and gallic acid (GA) were selected by

literature search. Microarray experiments with gallic acid had demonstrated its antioxidant and anti-mutagenic activities by inducing expression of antioxidant enzymes and repair genes (Abdelwahed *et al.*, 2007). DSF, usually used as a drug for treatment of alcohol abuse, also acts as a DNA methyltransferase (DNMT) inhibitor (Lin *et al.*, 2011). In theory, DSF treatment could keep repair genes activated, by preventing CpG methylation of their promoters. This could compensate for the impaired repair signaling in NBS cells. In addition, DSF was observed to protect cells against gamma-radiation (Gandhi *et al.*, 2003). Both reagents were tested for their toxicity at several concentrations in HFF1 fibroblasts to narrow down a concentration for treatment (Figure 31 on page 91, A, B). In a MTT assay, GA was found to be toxic at concentrations higher than 40 µg/ml. The increase of the curve at 100 µg/ml GA results from GA coloring the medium and disturbing MTT absorption spectrum. Disulfiram was found harmful to the cell at concentrations higher than 20 µM.

Figure 31: **Screening for effective antioxidants in NBS-8-iPSCs**
(A) MTT toxicity assay to determine optimal gallic acid concentration for fibroblasts. Different concentrations of gallic acid (range: 1 – 1000 µg/ml) were added for 48h. High absorption equals high viability. (B) Same study was performed for disulfiram (range: 1 – 1000 µM). (C) Various antioxidants were added alone or together with hydrogenperoxide (H_2O_2) and intracellular ROS levels of NBS-8-iPSCs were measured by FACS. (D-G) Pluripotency of NBS-8-iPSCs was determined by TRA1-60 immunofluorescence-staining. Cells were first sorted for viability (D), determined by size (FSC) and granularity (SSC) and second: viable cells were sorted for TRA1-60 positive cells (E, in yellow). In red: TRA1-60 negative population. (G) only TRA1-60 positive cells (used for ROS analysis).

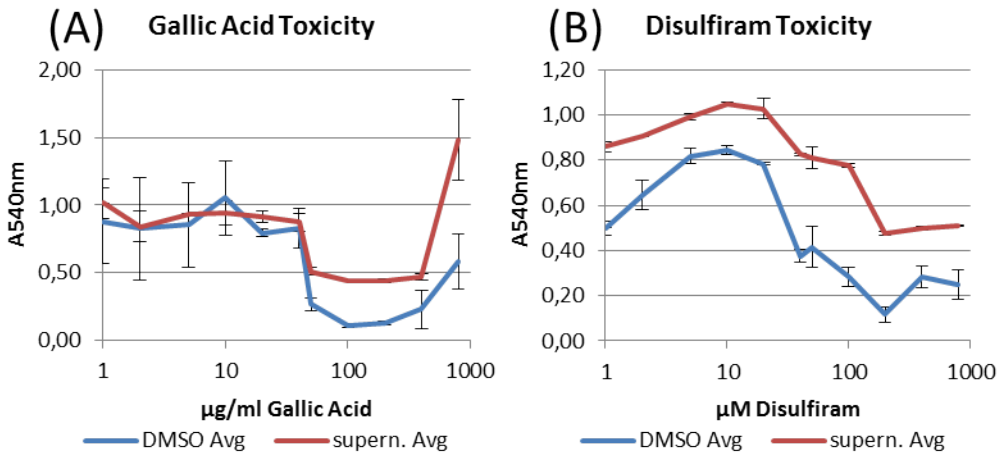
(A)
Gallic Acid Toxicity
A540nm
2,00
1,50
1,00
0,50
0,00
1
10
100
1000
µg/ml Gallic Acid
DMSO Avg
supern. Avg
(B)
Disulfiram Toxicity
A540nm
1,20
1,00
0,80
0,60
0,40
0,20
0,00
1
10
100
1000
µM Disulfiram
DMSO Avg
supern. Avg

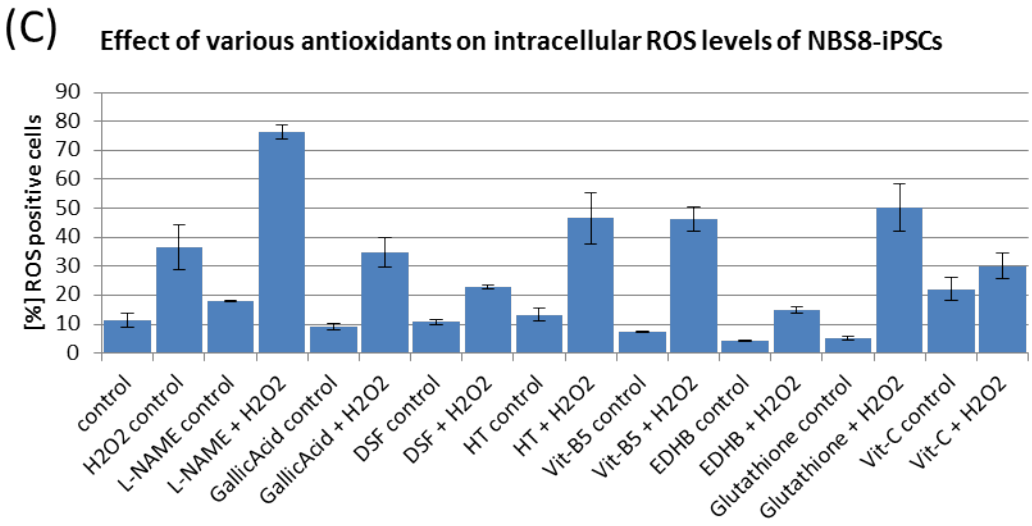
(C)
Effect of various antioxidants on intracellular ROS levels of NBS8-iPSCs
[%] ROS positive cells
90
80
70
60
50
40
30
20
10
0
control
H2O2 control
L-NAME control
L-NAME + H2O2
GallicAcid control
GallicAcid + H2O2
DSF control
DSF + H2O2
HT control
HT + H2O2
Vit-B5 control
Vit-B5 + H2O2
EDHB control
EDHB + H2O2
Glutathione control
Glutathione + H2O2
Vit-C control
Vit-C + H2O2

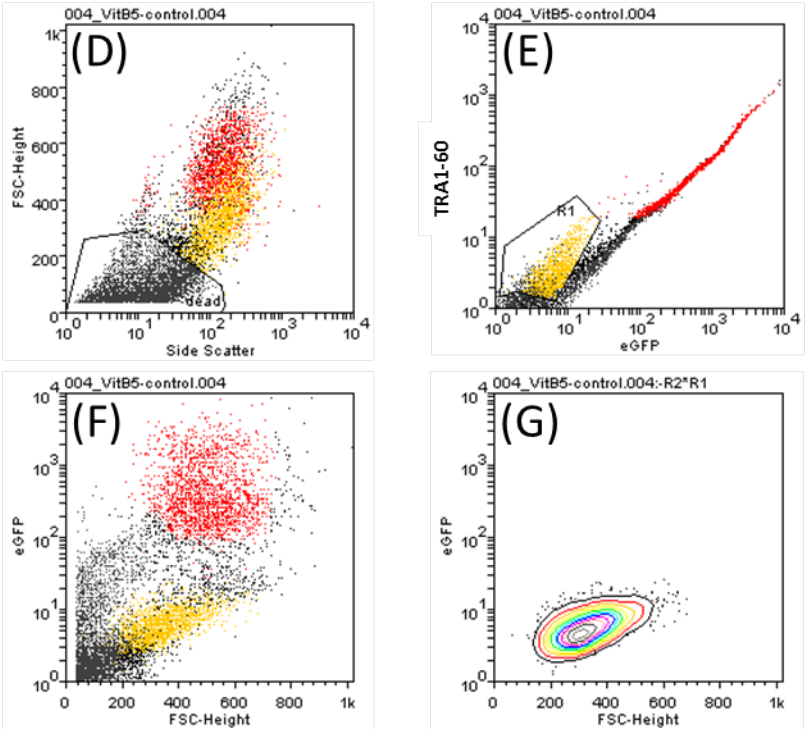
004_VitB5-control.004
(D)
FSC-Height
Side Scatter
dead
004_VitB5-control.004
(E)
TRA1-60
eGFP
R1
004_VitB5-control.004
(F)
eGFP
FSC-Height
004_VitB5-control.004:-R2*R1
(G)
eGFP
FSC-Height

Next, the question was addressed, which of a broad set of antioxidants and other components can actually decrease ROS levels in NBS-8-iPSCs. The iPSCs were each treated with the component alone or together with 20 µM H_2O_2. The following compounds were tested: L-NAME (L-NG-Nitroarginine methyl ester; nitric oxide synthase inhibitor), gallic acid, disulfiram, hydroxytryrosol (very high oxygen radical absorbance capacity), vitamin B5, EDHB (ethyl-3,4-dihydroxybenzoate; substrate analog and competitive inhibitor of prolyl 4-hydroxylases, which activates the HIF-pathway; (Chu *et al.*, 2010)), glutathione and vitamin C. Because of the difficult growing properties of stem cells, high-throughput screening of different concentrations was not possible. In most cases, the selected concentration was as high as possible, as tested in toxicity test or indicated by publications. Cells were loaded with the cell permeant reagent DCF-DA (2',7'–dichlorofluoresceindiacetate) where it becomes deacetylated by cellular esterases and oxidized by ROS into a non-cell permeant, fluorescent compound. Afterwards the cells were treated with H_2O_2 and antioxidants and analyzed by FACS. The amount of fluorescence corresponds to the amount of ROS inside the cells and the analysis shows that treatment with H_2O_2 increases the internal ROS levels by 3-fold (Figure 31 on page 91, C).

Some of the tested compounds contributed to the increased ROS level (L-NAME, vitamin C), some did not alter the internal ROS levels (GA, hydroxytyrosol, vitamin B5), some only decreased ROS without H_2O_2 (glutathione), some decreased ROS only in the presence of H_2O_2 (vitamin C) and some were able to decrease ROS levels under both conditions (DSF, EDHB). DSF and EDHB are therefore the most promising candidates to improve genetic stability of NBS cells. Cultivation of iPSCs often shows heterogeneous growth of hESC-like colonies mixed with differentiated areas. In order to obtain only undifferentiated cells for the measurement, they were counterstained with hESC-specific marker antibody TRA1-60 (Figure 31 on page 91, D-G).

The most effective ROS modulators (EDHB and DSF) in NBS-8-iPSCs were also tested in NBS fibroblasts and compared to HFF1 cells (Figure 32 on page 95, A). The ground level of ROS was around 84 RU (relative units) in HFF1 and around 57 RU in NBS cells (NBS-5, NBS-8). After incubation of 20 mM H_2O_2 in PBS (PBS to avoid ROS scavengers in FBS containing medium), HFF1 and NBS-8 cells showed a decrease in ROS by 26 and 19 RU, respectively and a slight increase in ROS by 9 RU in NBS-5 cells. After incubation with EDHB alone, ROS levels were similar to H_2O_2 treatment, but when treated with a combination of EDHB and H_2O_2 the ROS levels were decreased in all samples by at least 2,3-fold. Treatment with DSF alone lead to a decrease in ROS by 1,7-fold in HFF1 and NBS-8 cells and to a decrease of further 1,5-fold when DSF was combined with H_2O_2. Vitamin C on

the other hand, resulted in increased ROS levels when treated alone. Combination of Vitamin C and H_2O_2 reduced levels to around 2-fold in comparison to control and to around 2,5-fold in comparison to Vitamin C treatment. Interestingly the overall intensity of ROS was always higher in HFF1 cells than in NBS-8 fibroblasts. Here we see that EDHB and DSF both were able to modulate internal ROS levels in HFF1 and NBS fibroblasts to below the ground state.

From the previous experiments EDHB emerged as the most potent ROS modulator on NBS fibroblasts and iPSCs. To solidify these findings, EDHB, H_2O_2 and the combination of both were tested for internal ROS concentrations in NBS-8-iPSCs in comparison to hESCs. To discriminate the often heterogeneous growth of stem cells and their descendent differentiated cells, FACS analysis was performed, measuring the ROS intensity and immuno-detected, TRA-1-60 (stem cell marker) positive cells simultaneously (Figure 32 on page 95, D-E). With this setup, the cells clustered into two populations, the smaller cells, with low ROS intensity and high signal for the hESC-marker TRA-1-60 and the bigger, TRA-1-60 negative cells with higher ROS intensity. The TRA-1-60 positive population was considered to represent homogenous hESCs and iPSCs. The basal ROS level of hESCs and NBS-8-iPSCs was similarly low (around 2 RU) and was raised by H_2O_2 treatment by 10-fold in hESCs and 6,4-fold in NBS-8-iPSCs (Figure 32 on page 95, C). Treatment with EDHB alone resulted in ROS levels below the ground state (to around 1,5 RU). Were the cells stressed with H_2O_2 and treated with EDHB at the same time, the internal ROS levels could be leveled down by 2,9-fold in hESCs and 2,4-fold in NBS-8-iPSCs. Similar to the experiment with fibroblasts (Figure 32 on page 95, A) the "healthy" hESCs were more sensitive to oxidative stress than NBS-8-iPSCs. Looking at the TRA-1-60 negative population of cells revealed a similar response to the given conditions but with higher overall ROS levels (Figure 32 on page 95, B). The ground state level of ROS in hESCs is at 64 RU and at 121 RU in NBS-8-iPSCs. That range is similar to the ground state of ROS measured in fibroblasts.

It can be concluded that EDHB can be used as a potent modulator of internal ROS levels that works both in NBS fibroblasts and iPSCs.

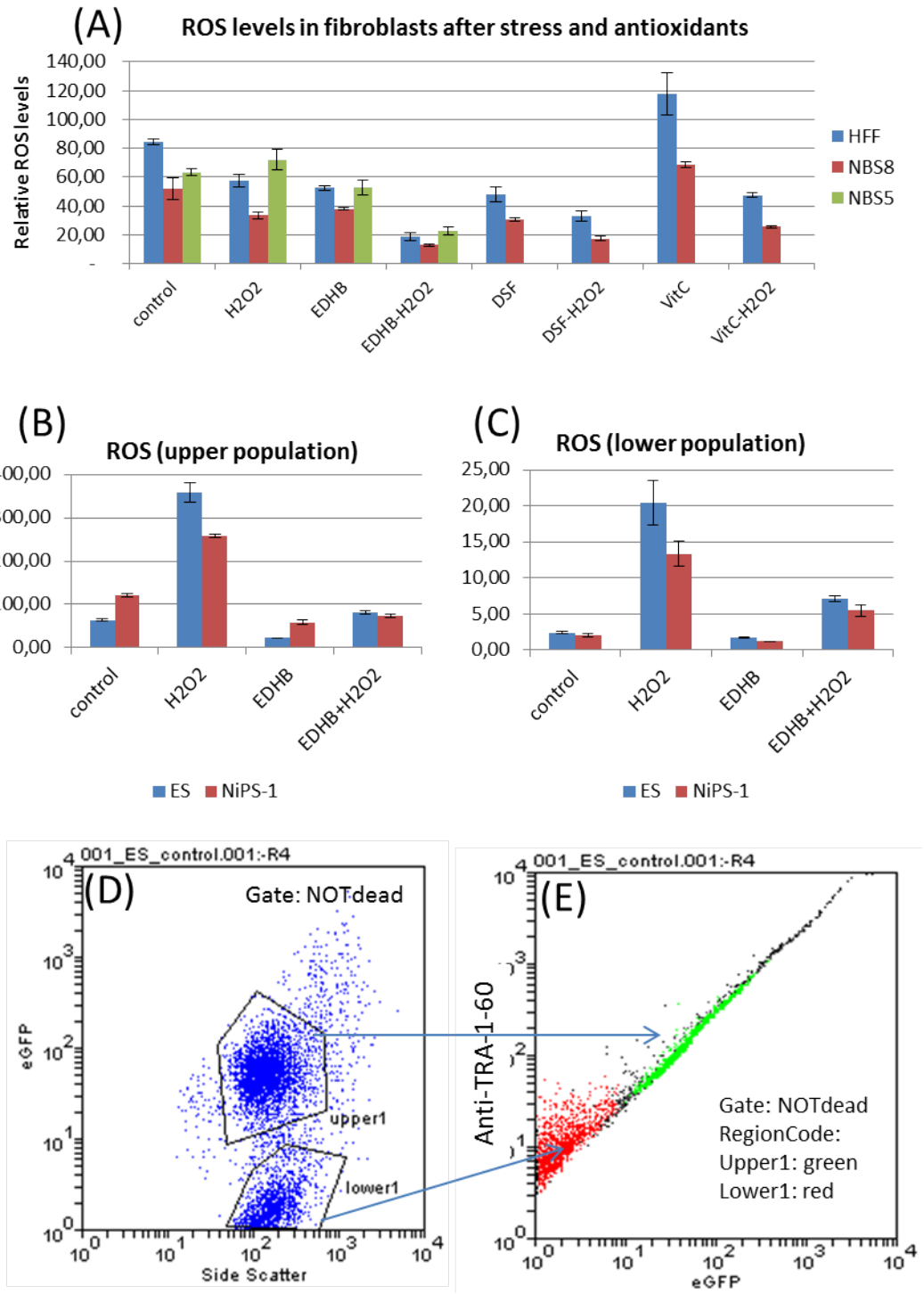

Figure 32: **Effect of EDHB on ROS Levels in Fibroblasts and iPSCs**
(A) Intracellular ROS levels in fibroblasts were determined by FACS analysis. Cells were either treated with hydrogen peroxide (H_2O_2) or the antioxidant alone, or together (e.g. EDHB-H_2O_2). There was no data on DSF, DSF-H_2O_2, VitC, VitC-H_2O_2 for NBS5. (B, C) Intracellular ROS levels were measured in hESCs and NBS-8-iPSCs. Cells were either treated with hydrogen peroxide (H_2O_2) and EDHB alone, or together (e.g. EDHB+H_2O_2). (D+E) Cells in B+C were also tested for pluripotency by detection of the surface marker TRA1-60. In red: TRA-1-60 positive cells; in green: TRA1-60 negative cells. All populations shown, were already subtracted of dead cells and debris.

3.3.4 *Influence of Bleomycin and Antioxidants on DSBs*

One of the earliest events in DNA double strand break (DSB) recognition is the phosphorylation of histone H2AX (called gamma-H2AX) around the area of the break position (Reinhardt & Yaffe, 2009). This process is facilitated by the ATM kinase and is enhanced by the recruitment of NIBRIN as part of the MRN complex (Czornak *et al.*, 2008). Immunfluorescence-based detection of gamma-H2AX can be used to measure the frequency of DSBs in cells. In NBS, patients suffer from frequent incidents of cancer due to chromosomal instability. Several chemicals were tested for their ability to reduce internal ROS levels (previous paragraph), one of the major natural causes of DNA damage in NBS cells. Next, we addressed the question if agents, with a focus on EDHB, can also decrease the amount of damage in NBS cells. To further challenge this question the cells were either stressed with H_2O_2 or the DSB-inducer bleomycin.

HFF1 and NBS-8 fibroblasts were treated with various antioxidants, then exposed to bleomycin and finally treated with the antioxidants again. This treatment conditions were selected to include protective actions and repair-supporting actions of the antioxidants. Afterwards the cells were analyzed by FACS and measured for the percentage of gamma-H2AX positive cells; representing cells with DSBs (Figure 33 on page 98, A). Cells without treatment or with treatment of the antioxidants glutathione and vitamin C showed less than 4 % damaged cells. Treatment with bleomycin increased the amount of damaged cells to 15 % in HFF1 cells and to 60 % in NBS-8 cells. Treatment with glutathione, vitamin C or glutathione and vitamin C together, did not notably reduce the bleomycin-induced DNA damage. But treatment with gallic acid reduced this damage to less than 1 % in HFF1 cells and by 2,2-fold to 27 % in NBS-8 cells. Taken together, NBS-8 cells appeared to be greatly more sensitive towards DNA damaging agent, bleomycin than HFF1 cells. The commonly known antioxidants glutathione and vitamin C failed to protect the cells from the damage. Gallic acid was able to reduce the amount of DNA damage very efficiently in HFF1 cells but only to some extent in NBS-8 cells.

A similar experiment was conducted focusing on the action of EDHB in connection to DSB-protection (Figure 33 on page 98, B). Cells without treatment or treatment with EDHB alone showed less than 1,5 % damaged cells in HFF1 and NBS-8 and around 5 % damaged cells in NBS-5. When stressed with H_2O_2, both NBS lines responded with higher DNA damage (approx. 20 %) than HFF1 cells (approx. 10 %) which was rescued to less than 5 % by EDHB treatment in all three lines. Treatment with bleomycin, resulted in 47 % damaged HFF1 fibroblasts, 36 % NBS-8 cells and 66 % NBS-5 cells. Treatment with EDHB reduced bleomycin inflicted damage 1,4-fold in all three cases. Therefore EDHB can efficiently protect fibroblasts from

DSBs caused by oxidative damage. EDHB also has protecting properties when DNA damage was inflicted by DSB-inducer bleomycin.

The same experimental conditions were conducted on hESCs (H1) and NBS-8-iPSCs (Figure 33 on page 98, C). Here the damage induction by H_2O_2 did not show a difference between the cell-lines, but was with 35-39 % higher than in fibroblasts (10-20 %, Figure 33 on page 98, B). EDHB decreased the oxidative DNA damage 1,6 to 1,9-fold but did not affect the amount of damaged cells when damage was induced with bleomycin (approx. 45 % positive cells).

In contrast to fibroblasts (HFF1 vs. NBS-5 and NBS-8), H1 and NBS-8-iPSCs did not react with different sensitivity to oxidative stress or bleomycin. In addition, the protecting effect of EDHB was smaller in stem cells than in fibroblasts.

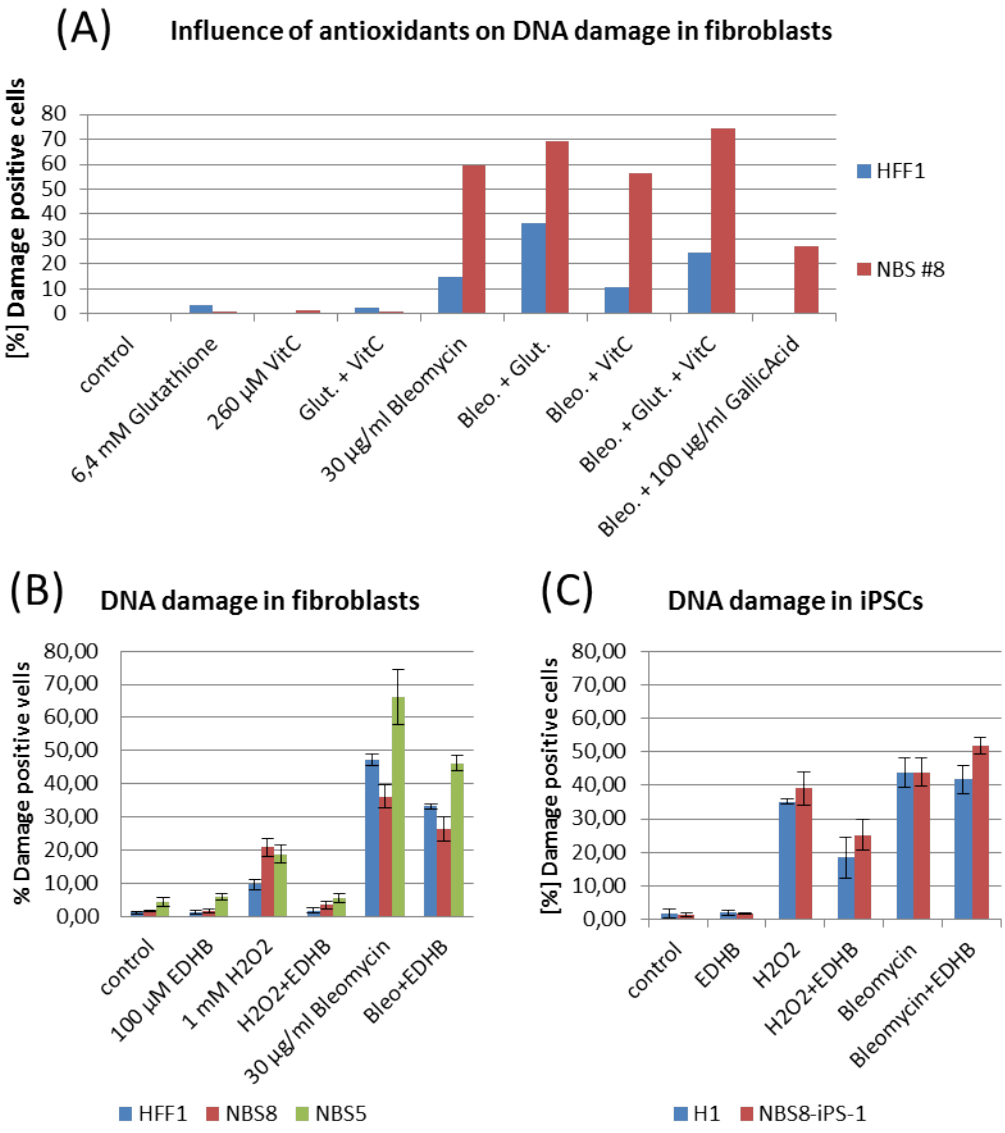

Figure 33: **Effect of EDHB on DNA damage in fibroblasts and iPSCs** (A) DNA damage was detected by immunofluorescent staining of γ-H2AX and quantified by FACS analysis. Cells were treated with the radiomimetic bleomycin (Bleo) alone, or together with antioxidants as indicated. VitC: ascorbic acid. (B) Same assay was performed with EDHB and bleomycin on normal fibroblasts (HFF1) and two NBS cell lines. (C) DNA damage after treatment with bleomycin and EDHB was measured in hESCs (H1) and NBS-8-iPSCs.

3.4 DETECTION OF PHOSPHORYLATED DAMAGE SIGNALING PROTEINS

DNA damage signaling and repair is primarily regulated on post-translational protein level at a time range of minutes (Reynolds *et al.*, 2012) and is typically studied at that level by western blotting and immunocytofluorescence. This study aims to understand the long term effects of impaired repair in NBS cells by global transcriptome analysis (Section 3.5), but the short time effects cannot be neglected. With regard to the creation of iPSC-lines as a disease model of NBS, it is important to analyze the changes that occurred in repair signaling in comparison to their somatic origin, the NBS fibroblasts. In NBS, mutations in the gene NBN are responsible for the disease phenotype. NIBRIN, the NBN gene product is one of the first proteins that are recruited to DSBs. Together with MRE11 and RAD50 it forms the MRN complex. It binds ATM which stimulates ATM itself, which in turn phosphorylates H2AX and others to amplify the damage signaling (Reynolds *et al.*, 2012). Binding of FHA and BRCT domains of NIBRIN to other repair and signaling proteins, brings them in proximity to each other and the DSB. These domains are specifically missing in the investigated patient cells. Here, we tested the effect of oxidative stress (H_2O_2) and induction of DSBs (bleomycin) on repair signaling by detection of phosphorylated (= activated) versions several damage response proteins (CHEK1, CHEK2, P53, ATM, ATR, BRCA1, gamma-H2AX). Furthermore the influence of EDHB, a protector from the oxidative damage and DSBs, on repair signaling is monitored.

Previous experiments using FACS analysis revealed that EDHB can decrease DNA damage caused by H_2O_2 in fibroblasts and iPSCs, but only moderately reduce the damage in fibroblasts caused by bleomycin (3.3.4, Figure 33 on page 98). Western Blot analysis of gamma-H2AX after treating hESCs and NBS-8-iPSCs with H_2O_2 and bleomycin confirmed these measurements (Figure 34 on page 101, B). It also showed that the application of H_2O_2 can indeed result in DSBs as indicated by the increased detection of gamma-H2AX. But it is important to keep in mind that in comparison (gamma-H2AX measurement, Figure 33 on page 98), H_2O_2 induced approx. the same level of DNA damage in hESCs as bleomycin, but 2-fold lower DNA damage in fibroblasts than in ESCs.

CHEK1 (S345) phosphorylation is mostly facilitated by ATR and required for the G2/M DNA damage checkpoint (Zhao & Piwnica-Worms, 2001; Liu *et al.*, 2000). Upon DNA damage, CHEK1 becomes activated and phosphorylates and inhibits CDC25C, thereby preventing activation of the cyclin B/CDK2 complex responsible for mitotic entry (Sanchez *et al.*, 1997). Here, DNA damage was induced by oxidative stress in the form of H_2O_2 and by the DSB-inducer bleomycin (Figure 34 on page 101). HFF1 cells only showed a slight increase in

phospho-CHEK1 after treatment with bleomycin, but NBS-8 fibroblasts on the other hand exhibited CHEK1 activation without any treatment (Figure 34 on page 101, A). This was decreased, but not eliminated upon treatment with EDHB. Bleomycin did not cause stronger activation than in control and this was not challenged by EDHB treatment. Interestingly, the supplementation with H_2O_2 completely diminished CHEK1 phosphorylation but not in the presence of EDHB. In hESCs and NBS-8-iPSCs phospho-CHEK1 was detected in control and EDHB, with higher amounts in the iPSCs (Figure 34 on page 101, B). There was no increase after bleomycin treatment, but an efficient decrease was observed when bleomycin was administered together with EDHB. Similar to NBS-8 fibroblasts, CHEK1 phosphorylation was abolished after H_2O_2 treatment, but there was no discrimination between hESCs and iPSCs and no effect by EDHB addition.

CHEK2 (T68) phosphorylation: In response to ionizing radiation, CHEK2 is known to be phosphorylated and activated in an ATM-dependent manner (Matsuoka *et al.*, 1998; Blasina *et al.*, 1999; Brown *et al.*, 1999; Chaturvedi *et al.*, 1999). This event has been linked to the regulation of TP53 stability and maintenance of G2 cell cycle arrest. CHEK2 also associates with and phosphorylates the BRCA1 breast cancer gene product (Ahn *et al.*, 2000). Activated CHEK2 phosphorylates TP53 at serine-20 (Hirao *et al.*, 2000; Chehab *et al.*, 2000; Shieh *et al.*, 2000), CDC25A at serine-123 (Falck *et al.*, 2001), and CDC25C at serine-216, contributing to the G1/S, S, and G2/M checkpoints, respectively (Xu *et al.*, 2002). In HFF1 cells treated with H_2O_2, CHEK2 became phosphorylated and this increased after combined application of H_2O_2 and EDHB (Figure 34 on page 101, A). The same effect was observed in NBS-8 fibroblasts. Bleomycin did not activate CHEK2 in HFF1 cells, but the activation was strong in NBS-8 cells. In hESCs and NBS-8-iPSCs the activation of CHEK2 was rather leveled, except for an increased signal in NBS-8-iPSCs treated with H_2O_2 and EDHB, bleomycin and bleomycin and EDHB (Figure 34 on page 101, B). EDHB increased CHEK2 phosphorylation in combination with H_2O_2, but reduced it in combination with bleomycin. Thus, CHEK2 phosphorylation is specifically induced in NBS cells suffering from DSBs, independently from their cellular state.

TP53 (S15) phosphorylation: TP53 is a major tumor suppressor which plays a huge role in regulating cellular responses to DNA damage. Phosphorylation of TP53 can occur on many different sites and dependent on that, TP53 activation can result in different cell fates like G1 arrest, repair, senescence and apoptosis (Vousden & Prives, 2009). DNA double-strand breaks induce phosphorylation of TP53 S15 by ATM or DNA-PK (Banin *et al.*, 1998; Shieh *et al.*, 1997). The activated TP53, which induces transcription of the cyclin-dependent kinase inhibitor p21CIP1, leads to arrest in the G1 phase of the cell cycle (Deng *et al.*, 1995). This study shows, that in HFF1 cells, TP53

S15 phosphorylation was observed after treatment with bleomycin, but not after H_2O_2 administration. In addition, the level of induction was lowered by addition of EDHB in the bleomycin treatment. In NBS-8 cells, the same effect was observed, but the TP53 activation by bleomycin was lower and was almost abolished after EDHB treatment (Figure 34 on page 101, A). In hESCs and NBS-8-iPSCs TP53 was only phosphorylated at S15 after bleomycin treatment as well. But here, phospho-TP53 was higher in NBS-8-iPSCs and EDHB treatment did not show a clear effect (Figure 34 on page 101, B).

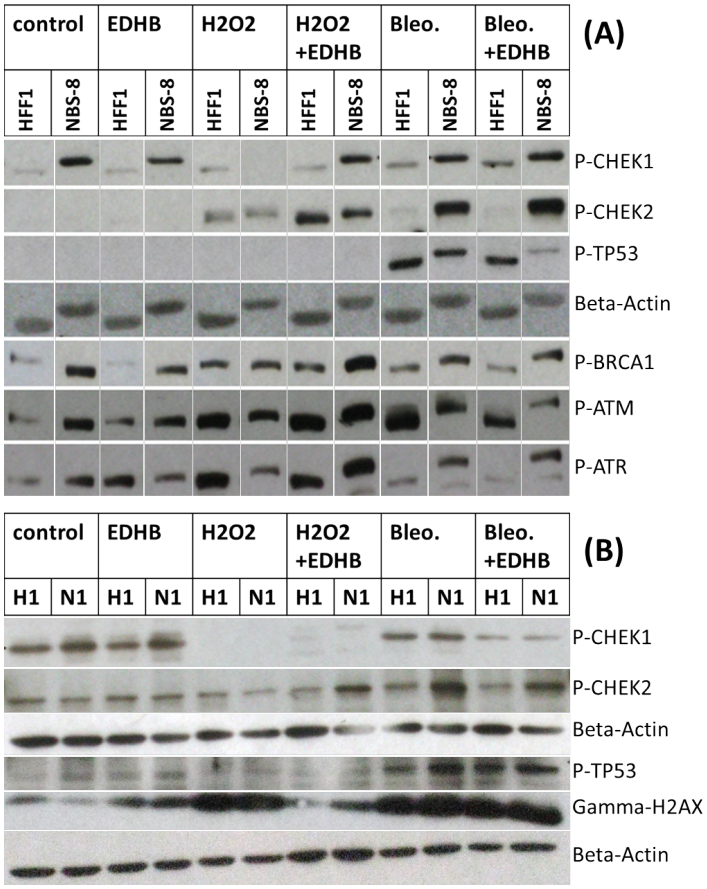

Figure 34: **Influence of DNA Damage and EDHB on Phosphorylation of DNA Damage Signaling Proteins**

Cells were treated with EDHB (antioxidant and inducer of HIF-pathway), hydrogen peroxide (H2O2) and radiomimetic bleomycin (Bleo). (A) Immunofluorescent detection of phosphorylated signaling proteins in fibroblasts (HFF1, NBS-8) after SDS-PAGE. For reasons of better comparison, the order of lanes was digitally rearranged. (B) Immunofluorescent detection of phosphorylated signaling proteins in hESCs (H1) and NBS-8-iPSCs (N1) after SDS-PAGE. Each lane of β-Actin corresponds to the lanes directly above and β-Actin is always unphosphorylated.

ATM (S1981), ATR (S428) phosphorylation: ATM is activated by auto-phosphorylation after chromatin changes resulting from IR-induced DSBs or shortened telomeres (Iijima *et al.*, 2008). ATM phosphorylates a huge set of proteins involved in damage signaling and repair, including CHEK2, NBN, H2AX, TP53 and BRCA1, therefore amplifying the initial unique, limited damage signal. There is an overlap in substrates between ATM and ATR, but it is believed that ATM primarily targets CHEK2 and ATR the CHEK1 kinase (Ashwell & Zabludoff, 2008). ATR is activated by ssDNA that result at a later stage in HRR, or result from stalled replication forks. In NBS, repair from HR is impaired, so ATR signaling is rather activated by stalled replication forks. In NBS-8 cells, phosphorylated ATM exhibited a similar level without or after treatment with H_2O_2 or bleomycin (Figure 34 on page 101, A). EDHB on the other hand increased the signal in cells treated with H_2O_2 (oxidative stress) and decreased the signal in cells treated with bleomycin (DSB inducer). Control cells, HFF1, exhibited lower basal levels of P-ATM than in NBS-8 cells but got strongly activated after H_2O_2 and bleomycin treatment. EDHB decreased the ATM activation by bleomycin as well. In contrast to ATM, ATR was not activated in HFF1 and NBS-8 cells by bleomycin. It was phosphorylated after treatment with EDHB or H_2O_2 in HFF1 cells, but not in NBS-8 cells. Here it only became activated after treatment with H_2O_2 and EDHB together. Comparison of ATM activation with activation of its target CHEK2, did not show the expected similar expression level in the western blot, neither did CHEK1 as target of ATM.

BRCA1 (S1524) phosphorylation: BRCA1 is involved in HRR and repair signaling. S1524 can be catalyzed by ATM or ATR and is responsible for G2 checkpoint activation, whereas S988 is catalyzed by P-CHEK2 and is important in HR via the connection of NBN-CtIP-BRCA1 (Zhang *et al.*, 2004; Chen *et al.*, 2008). Here, BRCA1 S1524 phosphorylation appeared on a similar level of activation as ATR in NBS-8 cells, but different in HFF1 and also different in both cases in comparison to ATM (Figure 34 on page 101, A). In detail, BRCA1 was slightly activated by H_2O_2 and bleomycin in HFF1 cells with no difference after addition of EDHB in any case. Again, there was a high level of phosphorylated protein in the control in NBS-8 cells, which was only further raised after treatment with H_2O_2 and EDHB. EDHB alone, H_2O_2 alone, bleo alone and bleo plus EDHB did show a similar expression of phopho-BRCA1, which was lower than in control.

The important finding here is the ability of EDHB to decrease the amount of DSBs caused by oxidative stress (administered by H_2O_2). EDHB showed a reduction of P-CHEK1 and P-CHEK2 in hESCs and iPSCs after bleomycin treatment, and an induction of P-CHEK1 and P-CHEK2 in fibroblasts after treatment of H_2O_2. Interestingly, the important tumor suppressor TP53 was less activated in NBS-8 fibrob-

lasts as in control cells (HFF1) and exhibited an even lower signal after treatment with bleomycin.

The pattern in activation of TP53, CHEK-1 and CHEK-2 is similar, but not identical in NBS-8 fibroblasts and iPSCs and differs in comparison to their healthy counterparts. The most prominent difference is the response of CHEK-1 to EDHB in NBS-8 fibroblasts in comparison to NBS-8-iPSCs (activated in response to H_2O_2 only in the presence of EDHB). Furthermore, the relative activation of CHEK-2 to bleomycin is a lot stronger in NBS-8 fibroblasts compared to iPSCs.

3.5 GLOBAL TRANSCRIPTOME ANALYSIS

3.5.1 *Global Gene Expression Analysis Comparing Nomal Fibroblast Lines with Fibroblast Lines from four NBS Patients*

DNA repair and signaling is executed and regulated mostly on post-translational level and within relative short time periods. However, in patients with NBS the repair and repair signaling mechanisms underlie a permanent modification. This might also reflect to long-term or permanent alterations in transcriptional regulation of these processes. By employing microarray technology, changes in the global transcriptome can be identified and show the effect of NBS mutation on repair or other intracellular pathways.

3.5.1.1 *Hierarchical cluster analysis*

RNA of four patients with confirmed NBS, 2 male (NBS-1, NBS-7)and 2 female (NBS-3, NBS-5) was isolated from *in vitro* cultured fibroblasts. The RNA quality was assessed by electrophoretic means (Figure 35 on page 104, A). Biotin-labeled cRNA was produced by linear amplification. After hybridization on the microarray, bound cRNA was detected by Cy3-streptavidin staining. Whole genome gene expression analysis of the Illumina human-8 Bead Chip employing the manufacturer's software, GenomeStudio, was used to profile the transcriptomes of these samples which were loaded in technical duplicates. Data reproducibility is demonstrated by sample correlation (Figure 35 on page 104, C). As expected, technical duplicates cluster close together (pVal < 0,03) and all NBS patient lines cluster closer together (pVal < 0,065) than against normal fibroblasts (pVal < 0,09). The same is true for sample correlation coefficients that were calculated by clustering the whole genome data of each group to each other (Figure 35 on page 104, B). NBS-1, -3, -5 and -7 show higher correlations between each other (R^2 = 0,92-0,95) than with normal fibroblasts (R^2 = 0,89-0,91). The patients which have the highest level of correlation are NBS-3 and -7 (R^2 = 0,95) and of all samples, NBS-7 also correlates the closest to healthy fibroblasts (R^2 = 0,91).

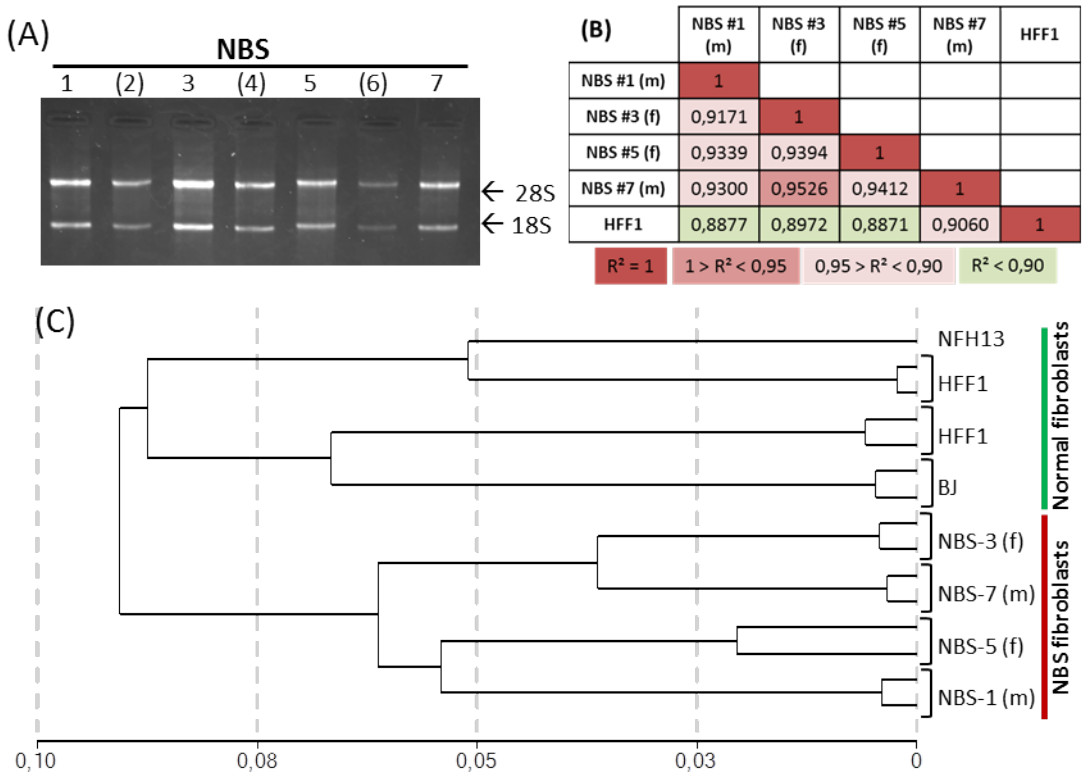

Figure 35: **Microarray sample analysis**
(A) Total RNA of individual NBS samples (1-7; in brackets: not hybridized) separated on agarose gel showing main products of 28S rRNA and 18S rRNA as indicated by arrows. (B) Calculated correlation coefficent (R^2) between hybridized samples. (C) Dendrogram of sample clustering of NBS patient fibroblasts and normal fibroblasts (BJ, HFF1, NFH13).

3.5.1.2 *Confirmation of relevant genes by real-time PCR*

Quantitative real-time PCR was used to verify microarray results for a selection of genes from cell cycle and DNA damage response where expression was significantly regulated in NBS patients. In all cases, there was agreement in terms of general orientation of expression change between microarray data and the real-time PCR data (Figure 36 on page 105). As microarrays require linear amplification of RNA, it is not surprising that the absolute fold values did not match exactly between the two methodologies (PCR and microarray) and are substantially higher in the PCR experiment. The pattern of expression between the patients is comparable in both methods with exception of GSK3B in NBS-3, CHEK1 in NBS-1 and RB in NBS-3 and -5.

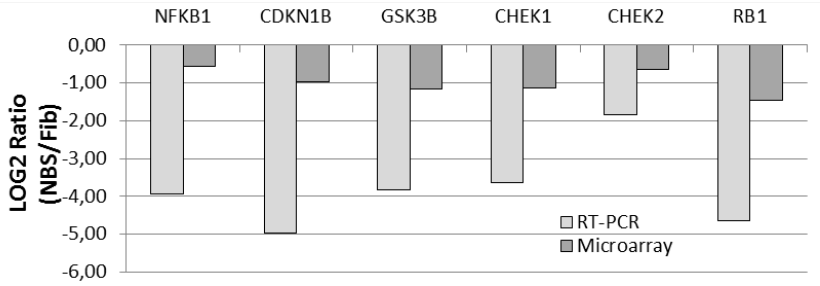

Figure 36: **qPCR confirmation of selected genes**

3.5.1.3 *Global data analysis*

All humans share 99.9 % of the same genome sequence, but the 0,01 % that vary, can make a huge impact on the phenotype of the individual person (Rosenberg *et al.*, 2002). The Illumina human-8 Bead Chip enables 24525 individual sequences (ILLUMINA_ID) to be analyzed simultaneously, which represent a total of 18415 gene products (GENE_SYMBOL). The expression patterns of four patients were compared to each other and each patient was found to have at least 199 genes that were uniquely expressed (Figure 37 on page 107, A). The genes specific to each patient were analyzed using the Gene Annotation Tools – DAVID (http://david.abcc.ncifcrf.gov/) (Da Wei Huang & Lempicki, 2008) to identify cluster of common gene functions. In NBS-1 genes grouped at the terms related to cell adhesion, taxis and inflammation, NBS-3 were related to folic acid metabolism, cell polarity and endocytosis, NBS-5 related to muscle processes and development, and protein phosphorylation in response to DNA damage, NBS-7 related to endocrine system and transcription. The variations cover several areas and can already give hints to the patient's specific conditions. All patients share 8690 of the 11088 total genes that are expressed at least in one of them. That makes approx. 2 % individual genes of the whole array.

3.5.1.4 *Detailed analysis to identify NBS specific expression patterns*

For further analysis, the samples were organized in groups of technical duplicates, a group that included all NBS samples and a group of all healthy fibroblast samples as the reference group. Raw data was derived of average signal, detection p-value and differential p-value of those group-sets by performing differential expression analysis in GenomeStudio (Illumina) (full data available as supplementary file "S01" and "S02" in online version). Expressed genes were judged by an expression pValue $\leq$ 0,001. First, individually expressed genes of the different patients were eliminated by finding overlapping genes of all four lines (Figure 37 on page 107, A). This list was then used to illustrate differences on the expression level between NBS and normal fibroblasts. Common and distinct genes were found to be ex-

pressed in both groups by creating a Venn diagram. By this analysis, 129 genes, irrespective of patient source, were found to be exclusively expressed in fibroblasts with mutated NBS-1 and 2167 genes to be exclusively expressed in healthy fibroblasts (full lists of exclusive gene expression in NBS group and healthy fibroblast group are provided in supplementary file "S03"). The gene lists were further analyzed using the "Gene Annotation Tools" - DAVID (david.abcc.ncifcrf.gov) to identify altered KEGG pathways and Gene Ontologies. The use of pathways has the advantage, that it can show well known gene functions instead of mere gene clustering in the same category. But there were no significant KEGG pathways in the DAVID output of the 129 genes specific for NBS. Instead enriched annotations were found, as shown in Figure 37 on page 107, B, which lists significant (pValue $\leq$ 0,05) GOTERM_BP_FAT ontologies in the NBS group. The most significant groups were cholesterol and sterol metabolic process, but the groups with highest gene count of significant enriched terms were related to cell death and regulation of proteolysis. KEGG annotated pathways specific for healthy fibroblasts were found in the analysis and replace GOTERM_BP_FAT annotations (Figure 37 on page 107, C). Pathways in cancer have the highest gene count and the highest significance. Apoptosis, cell cycle, progesterone-mediated oocyte maturation, DNA replication and O-glycan biosynthesis all fall under the top category of highly significant (p value $\leq$ 0,01) targeted pathways.

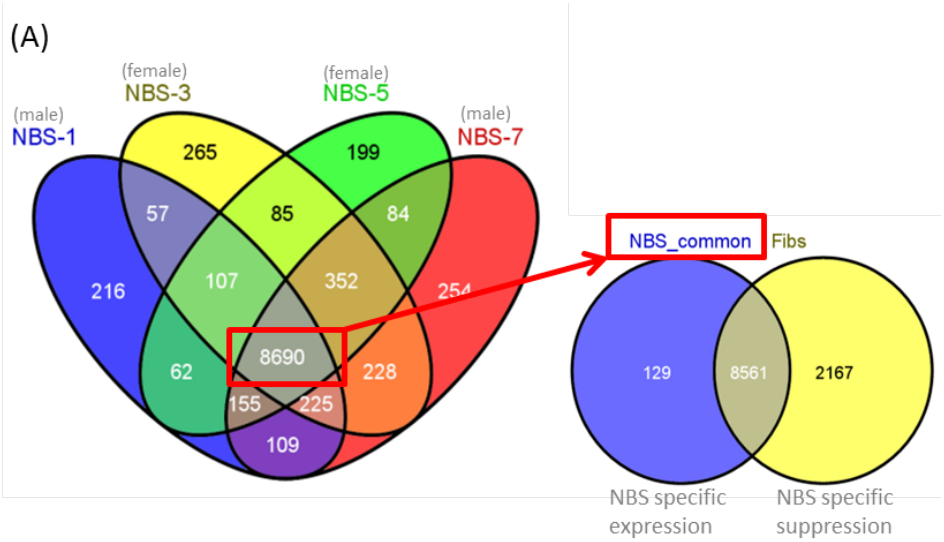

Elements only in "NBS_common":			(B)
Category KEGG_PATHWAY: no significant results			
Category GOTERM_BP_FAT:			
Term	**Count**	**%**	**PValue**
cholesterol metabolic process	4	3,13	0,023
sterol metabolic process	4	3,13	0,029
negative regulation of cellular protein metabolic process	5	3,91	0,031
ceramide metabolic process	3	2,34	0,031
negative regulation of protein metabolic process	5	3,91	0,035
sphingoid metabolic process	3	2,34	0,035
membrane organization	7	5,47	0,040
steroid metabolic process	5	3,91	0,044
cell death	10	7,81	0,046
regulation of transcription	25	19,53	0,047
regulation of proteolysis	3	2,34	0,047
death	10	7,81	0,048

Elements only in "Fibs":			(C)
Category KEGG_PATHWAY:			
Term	**Count**	**%**	**PValue**
Pathways in cancer	64	3,17	0,000
Small cell lung cancer	19	0,94	0,001
Apoptosis	19	0,94	0,002
Cell cycle	24	1,19	0,003
Colorectal cancer	18	0,89	0,004
Progesterone-mediated oocyte maturation	18	0,89	0,005
DNA replication	10	0,50	0,008
O-Glycan biosynthesis	9	0,45	0,008
Melanoma	15	0,74	0,010

Figure 37: **NBS specific gene expression**
(A) Venn diagram of significantly expressed genes (pVal < 0,001). The genes common to all hybridized NBS samples were compared to gene expression in normal fibroblasts (Fibs) to identify NBS specific genes. (B) Table of annotations for genes only expressed in NBS fibroblasts. Count: Number of genes; %: of total input list (129); Pvalue: significance value for the term. (C) Table of signifcantly enriched pathways for genes only expressed in normal fibroblasts (= suppressed in NBS).

3.5.1.5 *Sex differences in the expression profile of NBS*

It is known, that sex influences the biology of cells beyond the sex specific tissues like cervical epithelial cells or prostate cells (Shah *et al.*, 2014). In NBS exists a sexual dimorphism affecting development in puberty and hormone concentrations ((Chrzanowska *et al.*, 2010) 1x male, 1x female). In principle, males develop normally, whereas females show very little pubertal development. To identify possible expression patterns resulting from sex in NBS, significantly expressed genes (detection pVal $\leq$ 0,001) of the two male and the two female patients were compared (Figure 38 on page 109). 670 male-specific genes were found and enriched in pathways like ECM-receptor interaction, Inositol phosphate metabolism and Basal cell carcinoma. The female-specific counted only 222 individual genes and enriched in Melanoma, Regulation of actin cytoskeleton, Viral myocarditis, Axon guidance, Pathways in cancer and Prostate cancer. Especially the female-specific pathways were, although significant (pVal $\leq$ 0,05), represented by a low number of genes (4-8). Unfortunately, there was no female control cell line available as microarray data. So, the identification of both, the NBS- and sex-specific genes in the cells, was limited to males. After the comparison of male and female NBS cells with the male control line, HFF1, there were 354 male- and NBS-specific genes found which enriched in nearly the same pathways as before. Despite the male phenotype of HFF1 cells, still 101 of 222 genes overlapped with the female NBS group. Therefore 121 genes were female- and NBS-specific and showed overlapping pathways with the previous group (Melanoma, Viral myocarditis, Pathways in cancer). Additional pathways were Calcium signaling, Neuroactive ligand-receptor interaction and Endcytosis. 356 genes remained specific to NBS but independent to sex.

The sex of each cell line was not confirmed experimentally during this study, but the information was obtained from the suppliers. Evidence for clearly male-specific expression could be detection of Y-chromosome genes on the microarray. After screening the whole array for sex-specific genes, there was high expression of some Y-specific genes in all the NBS samples (eg. CD99, VAMP7, GTPBP6, ZBED1), but also some Y-specific genes, which were only expressed in the male-denoted samples (eg. RPS4Y1, CYorf15A, CYorf14, JARID1D). There were 7 Y-expressed genes in the male specific list and only 1 Y-expressed gene in the female-specific list, supporting the designated phenotype.

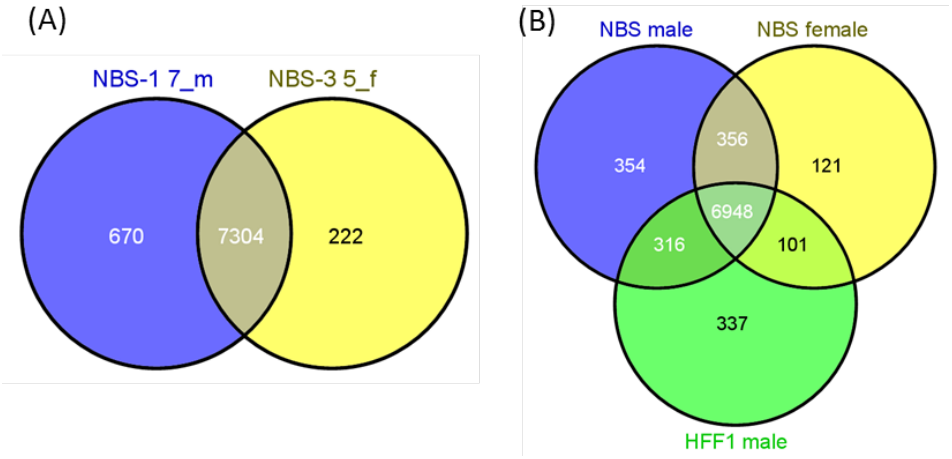

Figure 38: **Gender specific gene expression**
(A) Venn diagram of significantly expressed genes (pVal < 0,001) in NBS fibroblasts, grouped as male (NBS-1+7_m) and female (NBS-3+5_f) populations. (B) Venn diagram of significantly expressed genes (pVal < 0,001) comparing male (NBS male) and female (NBS female) NBS fibroblasts with HFF1 cells (HFF1 male).

3.5.1.6 *Significant pathway enrichment of regulated genes in NBS*

Comparing the data on the level of expressed genes vs. non-expressed genes only gives a rough picture of the global transcriptome differences in healthy and diseased fibroblasts. Gene expression is also modulated by strength of expression and RNA stability. So, the differential expression level of genes was analyzed as well. Genes were considered differentially regulated when differential pValue $\leq$ 0,05 and the ratio between healthy and NBS fibroblast $\geq$ 1,5 (or $\leq$ 0,6667). Several KEGG pathways (Table 9 on page 110) obtained by DAVID analysis are significantly regulated by this list of genes (list of differentially regulated genes available as supplementary file "S04"). As NBS is a disease of genomic instability, it was not surprising that closely related pathways like cell cycle, TP53 signalling, apoptosis and cancer were targeted with high probability (pVal $\leq$ 0,01). But also genes that are involved in lysosomal degradation were found at high number and likelihood (pVal $\leq$ 0,0001, 36 IlluminaIDs, 13 up-, 23 down-regulated). Some pathways broadly overlap with other pathways, like oocyte meiosis and progesterone-mediated oocyte maturation with cell cycle. But also other pathways show up with high significances (pValue $\leq$ 0,05), which are rather unexpected in relation to NBS. To name a few, there are for example MAPK signaling, axon guidance, purine metabolism, aminoacyl-tRNA biosynthesis and circadian rhythm.

Table 9: **KEGG pathways of regulated genes in NBS fibroblasts**

Term	Count	%	PValue
Cell cycle	37	1,5	0
Lysosome	34	1,38	0
Oocyte meiosis	29	1,18	0,001
p53 signaling pathway	19	0,77	0,005
Progesterone-mediated oocyte maturation	22	0,89	0,007
Apoptosis	22	0,89	0,009
Pathways in cancer	63	2,55	0,009
RNA degradation	16	0,65	0,011
MAPK signaling pathway	52	2,11	0,014
Chronic myeloid leukemia	19	0,77	0,015
Axon guidance	28	1,13	0,022
Prostate cancer	21	0,85	0,022
Purine metabolism	32	1,3	0,023
Aminoacyl-tRNA biosynthesis	12	0,49	0,024
Circadian rhythm	6	0,24	0,027
Bladder cancer	12	0,49	0,029
Amyotrophic lateral sclerosis (ALS)	14	0,57	0,031
Ribosome	20	0,81	0,033
Endocytosis	36	1,46	0,039
Colorectal cancer	19	0,77	0,044

3.5.1.7 *TOP25 regulated genes and their annotations*

The full list of significantly (differential pValue $\leq$ 0,05) regulated genes ($\geq$ 1,5-fold) in the combined NBS patients group contained 1586 down-regulated sequences (1510 genes) and 1053 up-regulated sequences (980 genes). A selection of the top 25 down- and top 25 up-regulated genes in NBS patients from the microarray transcriptional profile were plotted in a heat map with a horizontal dendrogram showing the differences in gene expression between the NBS patients themselves and healthy fibroblasts. NBS-7 and -5 cluster most closely together followed then by NBS-1 and last NBS-3. But overall, all patients show a similar expression pattern that is distinct from normal fibroblasts. The top 3 up-regulated genes (8 to 12-fold) are CCND2, BMP6 and C11orf87. Cyclin D2 (CCND2) forms a complex with and functions as a regulatory subunit of CDK4 or CDK6, whose activity is required for cell cycle G1/S transition. It also has been shown to interact with and be involved in the phosphorylation of tumor suppressor protein RB. The bone morphogenetic protein 6 (BMP 6) belongs to the family of bone morphogenic proteins (BMPs) which are secreted signaling molecules that can induce ectopic bone growth. BMP 6 has a proposed role in early development and it is the key regulator of hepcidin, a small peptide secreted by the liver which is the major regulator of iron metabolism in mammals ((Andriopoulos *et al.*, 2009)). Chromosome 11 open reading frame 87 (C11orf87) is a yet uncharacterized protein of 197 amino acids and 20,6 kDa. The top 3 down-regulated genes (14 to 63-fold) are KRT34, BEX1 and ALDH1A1. Aldehyde dehydrogenase 1 family, member

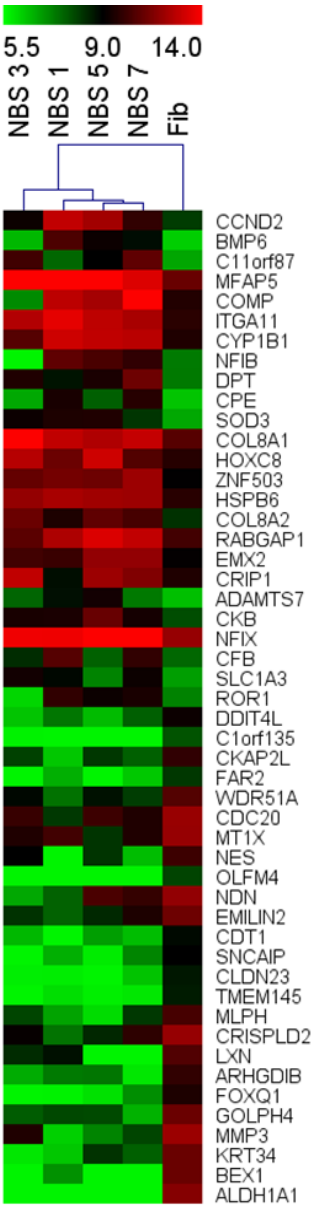

Figure 39: **The top-25 regulated genes in NBS fibroblasts**
Heatmap of top 25 up- and down-regulated genes in NBS compared to normal fibroblasts. Log2 of average expression is shown in green for low and in red for high expression.

A1 (ALDH1A1) is the second enzyme of the major oxidative pathway of alcohol metabolism. The gene encodes the main cytosolic isoform, which has a lower affinity for aldehydes than the mitochondrial isoform. Brain-expressed X-linked protein 1 (BEX1) is an adapter molecule involved in NGFR signaling and plays a role in cell cycle progression and neuronal differentiation. In response to nerve growth factor (NGF) it inhibits neuronal differentiation. Keratin 34 (KRT34) is a member of the keratin gene family. As a type I hair keratin, it is an acidic protein which hetero-dimerizes with type II keratins to form hair and nails. The full list of all top 25 regulated genes is available as supplementary file "S05", which also provides gene-related annotations. In summary, most of the up-regulated genes can be classified as extracellular matrix and secreted signaling molecules and most of the down-regulated genes belong to cell structure and cell cycle control.

3.5.1.8 *Prediction of transcription factor activity by Ingenuity® via analysis of downstream targets*

Identification of interaction networks, like pathways, which are affected by mutated NIBRIN, gives a good understanding of possible mechanisms that underlie the disease. But instead of analyzing complex networks, it is also possible to gain plenty of relevant information by targeting single genes. Activation or repression of transcription factors can be the switch for expression of a whole batch of target molecules. Of course, expression is only one parameter of cellular control over a protein, there is also translation regulation, protein stability and activity by posttranslational modifications as well as localization that results in changed regulation of target proteins. These regulations cannot be measured by microarray data directly, but the Ingenuity prediction tool of transcription factor regulation uses the overlap of known targets (that are significantly regulated in the microarray experiment) of one particular transcription factor to identify the transcriptional regulators that are able to explain observed gene expression changes and infer their activation state. Ingenuity therefore calculates a certain z-score that will reflect the overall predicted activation state of the regulator (<0: inhibited, >0: activated). In practice, z-scores greater than 2 or smaller than -2 can be considered significant and only if there are at least 4 genes in the data set that have an expected direction of regulation in the knowledgebase for the TF, a z-score for a particular TF is calculated. The analysis also produces a simple overlap score (Fisher's Exact Test p-value) that does not consider the direction of expression in the dataset and only seeks to find cases of statistically significant overlap between a transcriptional regulator and the list of targets whose expression is perturbed in experiment vs. control. Based on these grounds, it is possible that

regulation for a transcription factor is judged differently in the microarray experiment than in the Ingenuity TF analysis.

As shown in Table 10 on page 114 the transcription factor with the highest z-score and therefore activated is TP53, the most important tumor suppressor gene and central element in DNA damage signaling and apoptosis. Other activated TFs with a z-score higher than 2,00 are an inducer of cell cycle arrest in G1 and G2 phases, CDKN2A; a component of the CREST-BRG1 complex, SMARCA4; a component of the neural progenitors-specific chromatin remodeling complex (npBAF complex) and the neuron-specific chromatin remodeling complex (nBAF complex), SMARCE1; a factor involved in initiation of neuronal differentiation, TCF3; a group of TFs surrounding RB1, a key regulator of entry into cell division that acts as a tumor suppressor; GATA1, which has a role in erythroid development; an activator for transcription of the p21 promoter, TP63; and GLI3, that is known for having a dual function as a transcriptional activator and a repressor of the sonic hedgehog pathway.

TFs that have a z-score below -2,00 and are therefore judged as inhibited are v-myc myelocytomatosis viral related oncogene (MYCN); TBX2, that is required for mesoderm differentiation, E2F1 as a member of E2F family plays a crucial role in the control of cell cycle; SREBF2 and SREBF1 which are transcriptional activators required for lipid homeostasis; the receptor for retinoic acid, RXRA and SMAD7 an antagonist of signaling by TGF-beta through binding the E3 ubiquitin ligase SMURF2. Interestingly, these TFs hold key roles or reflect the pathways that were found regulated in NBS cells, especially TP53-signaling pathway and cell cycle.

Table 10: **Regulated transcription factors in NBS patient fibroblasts judged by differential expression of their target molecules**

Transcription Regulator	Predicted Activation State	Fold Change	Regulation z-score	p-value of overlap	Number of target molecules
TP53	Activated	1,484	4,321	2,04E-06	175
CDKN2A	Activated	1,045	3,930	6,69E-06	46
SMARCA4	Activated	-1,486	3,695	4,91E-01	34
SMARCE1	Activated	1,236	2,449	3,79E-02	6
TCF3	Activated	2,020	2,388	7,72E-02	35
Rb	Activated		2,260	9,29E-03	14
GATA1	Activated	-1,088	2,243	5,05E-01	11
TP63	Activated	-1,002	2,233	6,79E-02	27
GLI3	Activated	1,648	2,111	3,56E-01	4
SMAD7	Inhibited	-1,628	-2,126	3,05E-01	16
SREBF1	Inhibited	-1,259	-2,306	4,32E-01	22
RXRA	Inhibited	1,084	-2,457	7,76E-03	17
SREBF2	Inhibited	1,159	-2,482	3,77E-02	15
E2F1	Inhibited	1,363	-2,597	5,03E-04	63
TBX2	Inhibited	-1,721	-2,772	3,29E-05	24
MYCN	Inhibited	-1,074	-4,406	2,49E-01	33

3.5.1.9 *Detailed pathways analysis of transcriptional changes caused by mutated NIBRIN*

CELL CYCLE RELATED GENES ARE EXTENSIVELY DOWN-REGULATED IN NBS The repair of double strand breaks (DSB) is strongly connected to the cell cycle. In most cases they are either repaired by non-homologous end joining (NHEJ) or homologous recombination repair (HRR), whose relative contributions are cell cycle dependent (Wu *et al.*, 2008b). In addition, coordination of repair processes with cell cycle progression is important for cell cycle checkpoints which are induced by proteins from the repair machinery, several with or via involvement of TP53.

The cell cycle is represented with high number of regulated genes and one of the most significantly targeted KEGG pathways in the DAVID analysis of regulated genes as shown in Table 9 on page 110. 42 of 124 KEGG pathway genes were significantly regulated (Diff.p-Value $\leq$ 0,05). Of those only 6 genes were up-regulated (EP300, GADD45B, YWHAE, CDC14B, CCND2). An overview of the pathway is given in Figure 41 on page 117. An overview how to read pathways is given in Figure 40 on page 116.

What stands out, is the immediate responsible genes for cell cycle progression, which are the CDKs and their cyclins, were all down-regulated, except for the early G1 phase complex cyclin D(2)/ CDK4/6, which were significantly up-regulated. This situation can be interpreted as an on-going G1-S checkpoint which may be induced by

TP53 signaling (see Figure 44 on page 123, A), down-regulated MYC (c-MYC, MYCN) signaling or pRB activation. Another contributor or even initiator of this G1 arrest can be CDC25A which is required for progression from G1 to the S phase of the cell cycle by its activation of the cyclin-dependent kinase CDC2. CDC25A is specifically degraded in response to DNA damage by phosphorylation from CHEK1 and CHEK2. Phosphorylation creates binding sites for YWHAE/14-3-3 epsilon which inhibits CDC25A. All CDC25 genes (A, B and C) were down-regulated in NBS patients, but CDC25A appeared on the border of significant regulation and was therefore not colored on Figure 41 on page 117.

One of the few up-regulated genes in this pathway was EP300, which possesses histone acetyltransferase activity and is a transcriptional co-activator of TP53. TP53 was not found regulated via expression data, but was reviewed activated by Ingenuity analysis of TP53 downstream targets. TP53 activation can lead to cell cycle arrest, senescence or apoptosis. For example, downstream of TP53, we find an up-regulated gene as well: GADD45B (GADD45A: 1,2-fold up, Diff.p-Val = 0,06; GADD45G: significantly 1,14-fold down), which can induce growth arrest.

Cyclin D2 was with a 12-fold up-regulation the most up-regulated gene in this transcriptional analysis. Cyclin Ds, which are important for connecting nutrient availability and hormones to cell division are inhibited upon nutrient deficiency amongst others by GSK3B. Here, enough growth factors may have caused inhibition of GSK3B that can enable increased transcription Cyclin D2 by transcription factors like FOXO4, TCF3 and STAT5A which were found up-regulated in this array as well.

In normal healthy cells, pRB (here 2-fold down-regulated, but judged activated by Ingenuity analysis) blocks cell cycle progression in G1, and phosphorylation of RB is required for S-phase entry. The kinases that inactivate pRB are CDK4, 6/Cyclin D1, 2 in early G1 which were here up-regulated. But for late G1 and during S-phase Cdk2/Cyclin E and Cdk2/Cyclin A are responsible which were here down-regulated. The primary targets of pRB binding are the E2F transcription factors (here down-regulated) which, upon phosphorylation of pRB, dissociate from it and activate the transcription of S-phase genes including cyclin E.

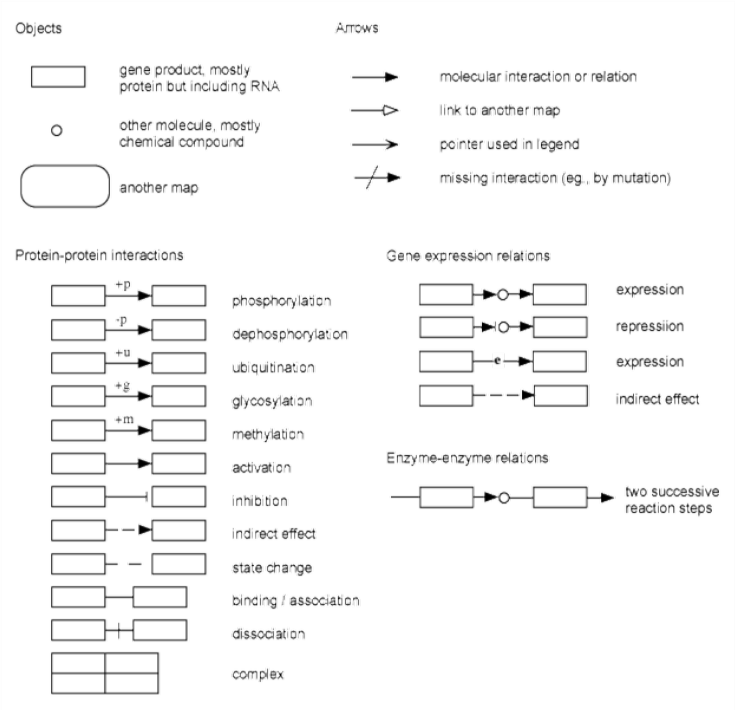

Figure 40: **KEGG pathway key**

The KEGG PATHWAY database is a collection of manually drawn graphical diagrams, called KEGG pathway maps, representing molecular pathways for metabolism, genetic information processing, environmental information processing, other cellular processes, human diseases, and drug development. Each pathway is identified by a five-digit number preceded by one of: map, ko, ec, rn, and three- or four-letter organism code. The pathway map is drawn and updated with the notation shown above. http://www.genome.jp/kegg/pathway.html

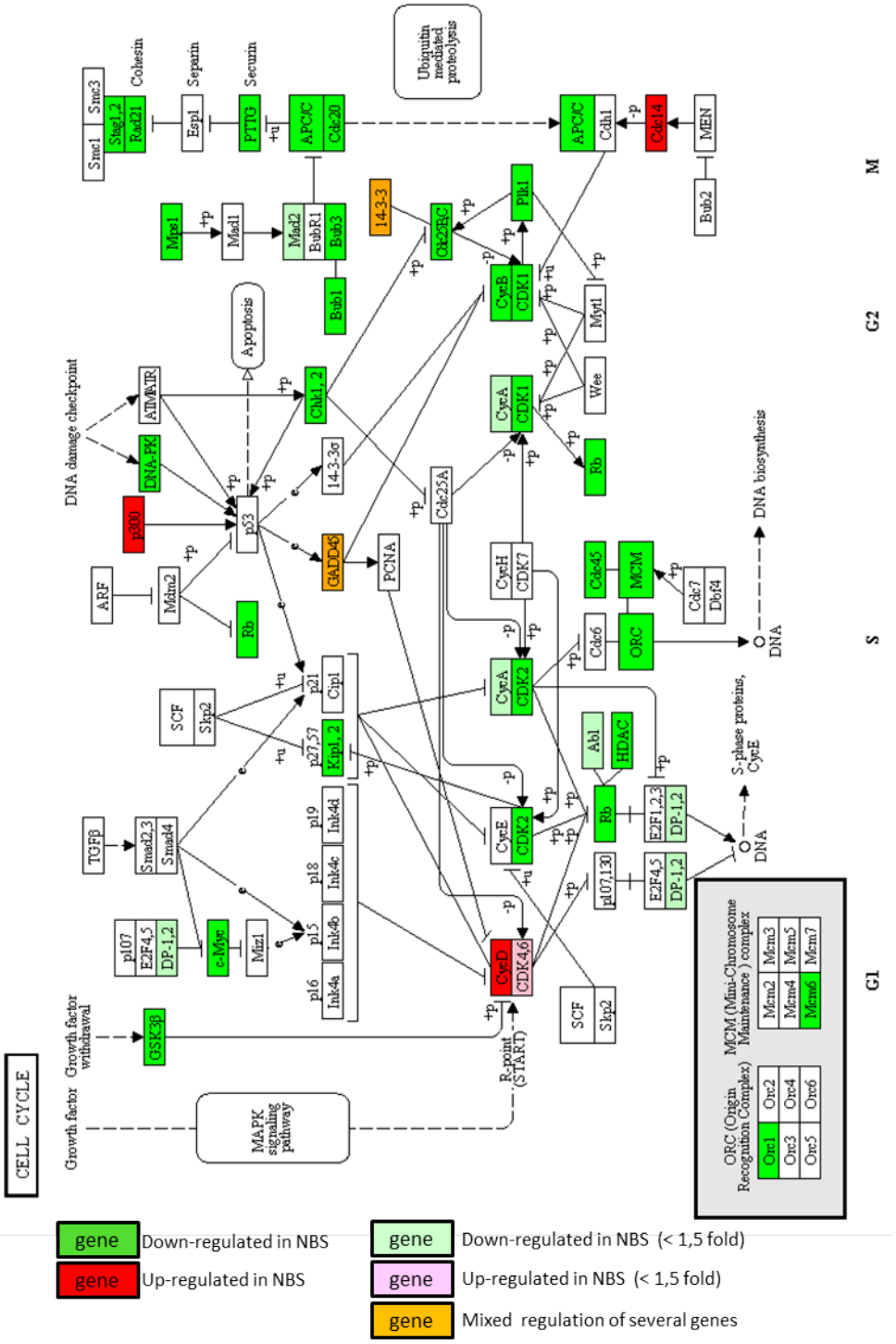

Figure 41: **Regulated genes of the cell cycle signaling pathway in NBS patients**

The DAVID output shows regulated genes in cell cycle signaling using KEGG pathways. Regulated genes are selected by diff. p-value </= 0,05 and >/= 1,5 fold ratio. Expression levels of NBS patients relative to healthy fibroblasts are indicated by green and red boxes for decreased and increased expression respectively. Some boxes represent several genes, so in some cases up-regulated and down-regulated are found together in the same box, which is indicated with orange color.

OOCYTE MEIOSIS AND MATURATION divisions to create a haploid genome. The first division is started during embryonic development but is halted in prophase I until puberty. With each menstrual cycle a few cells complete this step and enter meiosis II which is halted in metaphase II until fertilization. NBS was found to be linked with this process. In a mouse model with N-terminal exon disruption of NBN gene (modeling NBS) leads to infertility due to oogenesis failure (Kang *et al.*, 2002). In a study with NBS patients, 37 females were found to have primary ovarian insufficiency (POI) resulting in infertility (Chrzanowska *et al.*, 2010). Here, the transcriptional profile showed a high percentage of genes involved in oocyte meiosis and progesterone-mediated oocyte maturation, which were differentially regulated in NBS fibroblasts (Figure 42 on page 119). It is notable, that there is a high overlap with the cell cycle pathway (10 of 28 genes from meiosis; 8 of 22 genes from maturation), possibly drawing a link to DNA damage signaling. Similar to the cell cycle, most of the genes were down-regulated. The few up-regulated genes were specific to the oocyte pathway: Rsk1/2 (RPS6KA2, RPS6KA3), a serine/threonine-protein kinase that acts downstream of ERK (MAPK) signaling; B56 (PPP2R5D, PPP2R5B) that is part of Ser/Thr phosphatases and implicated in the negative control of cell growth and division; CAMK2G, a calcium/calmodulin-dependent protein kinase. The genes which were down-regulated in oocyte meiosis and did not overlap with cell cycle contained the following genes: AC (ADCY3), Aurora-A (AURKA), CPEB1, Plk1, Plkk1 (SLK), Cdc2 (CDK1), Sgo (SGOL1), PP2A (PPP2CA), CaN (PPP3CA, PPP3R1) and IP3R (ITPR3). The key process driving meiosis is the maturation-promoting factor (MPF), a complex of CDC2 and cyclin B, which were both down-regulated (3 to 3,5-fold) in this context. In addition, the factor responsible for activating this complex, the CDC25C phosphatase, was down-regulated to a level that it is not considered an expressed (detection pValue > 0,01) gene.

Progesterone-mediated oocyte maturation depicts a similar pathway, but from a different angle (Figure 42 on page 119, B). Therefore a high overlap with genes from oocyte meiosis occurred (15 of 22 genes). 22 genes were found down-regulated and 6 up-regulated. The genes which don't overlap with meiosis and cell cycle were: Akt/PKB (AKT1), a serine/threonine-protein kinase which regulates many processes including metabolism, proliferation, cell survival and growth; G (GNAI2, GNAI3), subunits of guanine nucleotide binding proteins; Raf (RAF1, ARAF) kinase which play a part in MAP kinase cascade and ERK signaling; and CDC25A which is required for progression from G1 to the S phases of the cell cycle and is specifically degraded in response to DNA damage (not expressed in NBS, but in non-diseased fibroblasts).

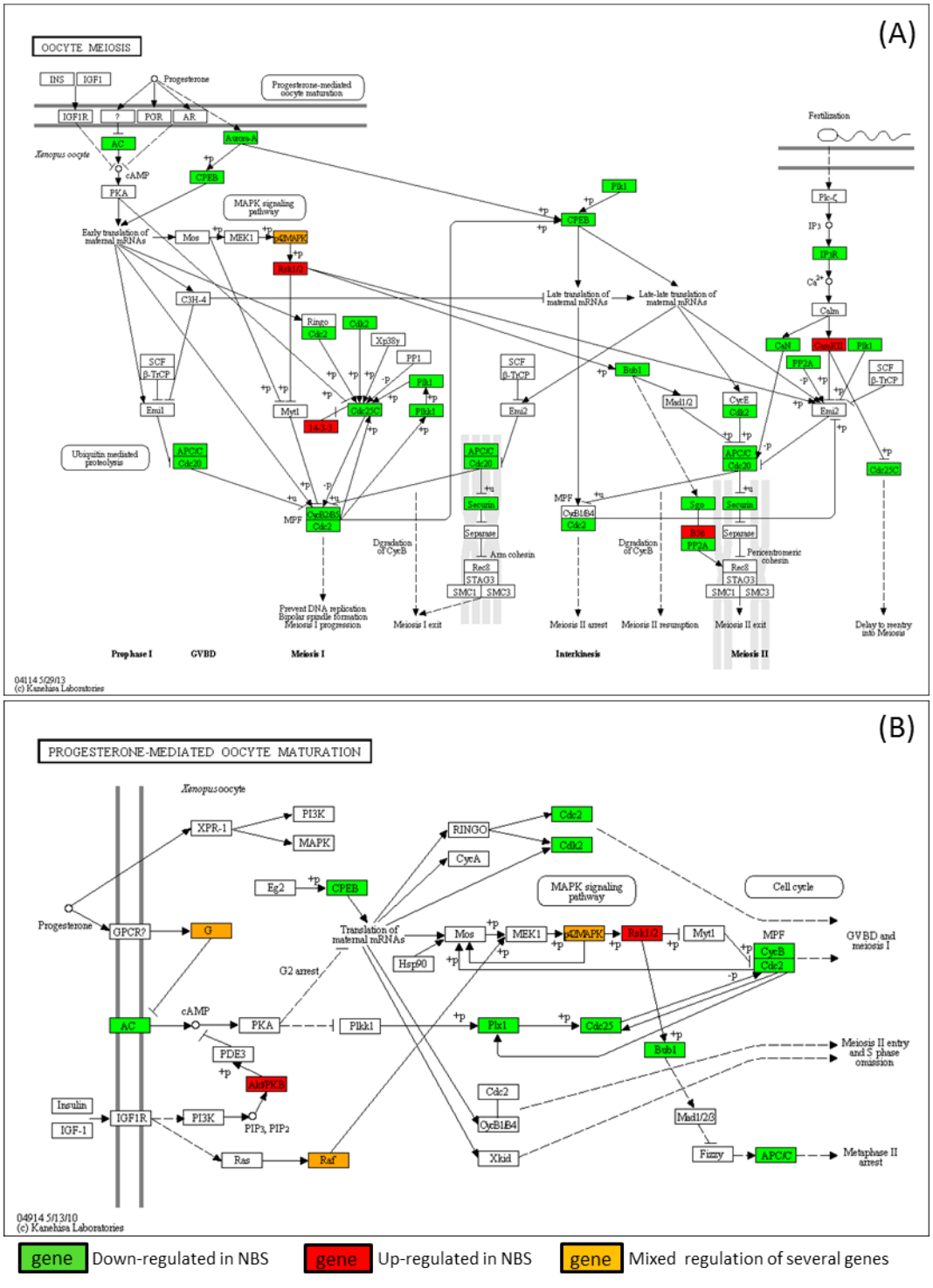

Figure 42: **Regulated genes of the oocyte related signaling pathway in NBS patients**

The DAVID output shows regulated genes in (A) oocyte meiosis and (B) maturation signaling using KEGG pathways. Regulated genes are selected by diff. p-value </= 0,05 and >/= 1,5 fold ratio. Expression levels of NBS patients relative to healthy fibroblasts are indicated by green and red boxes for decreased and increased expression respectively. Some boxes represent several genes, so in some cases up-regulated and down-regulated are found together in the same box, which is indicated with orange color.

LYSOSOME Lysosomes are cell organelles which are used to digest all sorts of macromolecules. They are created by endocytosis, phagocytosis or autophagy. The digest is mainly executed by many different hydrolases in an acidic environment which is maintained by active proton transport from the cytosol by V-ATPases (Vacuolar-type H+-ATPase). Mutations in lysosomal genes result in lysosomal storage diseases (LSD) where un-degraded target molecules accumulate in the cell and can cause severe disorders. In this study, several lysosomal genes were found differentially regulated in NBS fibroblasts. The lysosome pathway encompassed 120 genes in total, of those, 13 genes were found up-regulated and 21 genes down-regulated (Figure 43 on page 122). The regulation occurred in all classes of lysosomal proteins. In the class of acid hydrolases, 3 cathepsin proteases were down-regulated (CTSO, CTSL1, CTSB) and 2 up-regulated (CTSD, CTSF), 2 glycosidases were down-regulated (GLA, NEU1) and 4 up-regulated (IDUA, NAGLU, HEXA, MAN2B1), 1 sulfatase was down-regulated (GNS), 1 lipase was down-regulated (LIPA), 1 sphingomyelinase was up-regulated (SMPD1) and 1 apartylglucosaminidase was down-regulated (AGA). Of other lysosomal enzymes, 2 were down-regulated (GM2A, CLN1/PPT1). LAMP2, a major lysosomal membrane protein was down-regulated, but CD68 was up-regulated. Other membrane proteins consisted of 5 down-regulated (NPC1, CTNS, CD164, LAPTM4B, MFSD8) and 2 up-regulated genes (LAPTM4A, ABCA2). The proton-pumping V-ATPase was represented with 1 up- (ATP6V0C) and 2 down-regulated (ATP6V0A2, ATP6V0B) subunits. Lysosomal degradation was therefore affected by the NBS phenotype in a broadly manner.

THE TP53 PATHWAY IS REGULATED IN NBS PATIENT FIBROBLASTS In NBS fibroblasts the TP53 transcription factor was activated as predicted by Ingenuity®, which analyses downstream targets of TP53. The TP53 pathway is also a target when regulated genes in NBS are analyzed with DAVID 6.7. The corresponding KEGG pathway is displayed in Figure 44 on page 123, A and shows significantly regulated genes (Diff. p-Val < 0,05) with fold changes higher than 1,5. CHEK1 and CHEK2 are mediators of DNA damage signal and trigger cell cycle checkpoints. Both mRNAs were down-regulated in NBS patients. Usually CHEK1 and 2 are able to phosphorylate and therefore stabilize TP53, but TP53 can also be activated and stabilized by other factors. Among them are e.g. MAPK family members, DNA-PKCs, ATM, ATR, and p14ARF (CDKN2A) which in this case, don't show expression changes in NBS (data available as supplementary material "S04"). But it is known, that TP53 is mostly regulated on a post-translational level which is not accessible by microarray analysis. There are three Cyclin Ds of which CCND2 was 12-fold up-regulated and CCND3 was 2-fold down-regulated. CDK6 is part of the Cyclin D/CDK4/6 complex and was significantly up-regulated

by 1,46 in this analysis. The complex is usually required for G1-S transition. Cyclin E (CCNE2) and CDK2 were both down-regulated in NBS which can lead to G1-S arrest. The interaction of GADD45 (GADD45B up-regulated) with the CDC2/Cyclin B1 kinase complex is responsible for the G2/M cell cycle arrest through dissociation of the kinase complex. In addition, CCNB1 and 2 were also down regulated. B99 (GTSE1) leads to cycle arrest in G2/M phase but was down-regulated in NBS fibroblasts. PIGs (P53 inducible genes) can promote ROS generation and therefore also promote apoptosis, like TP53I3, which was up-regulated in NBS. According to the KEGG pathway ZMAT3 is associated with apoptosis and is up-regulated as well, but down-regulation of SIAH1, PERP and NOXA (PMAIP1) is antagonizing this. IF-BP3 was up-regulated in NBS and therefore able to inhibit IGF1, a protein that protects from apoptosis and is part of the IGF-1/mTOR pathway. DNA damage repair and prevention proteins GADD54B and SESN1 were up-regulated, p53R2 (RRM and RRM2B) were down-regulated. TP53 negative feedback proteins like Cop1 (RFWD2) and SIAH1 were down-regulated. In summary, most of the regulated genes that are connected to TP53 result in cell cycle arrest, regulation of apoptosis and repair .

REGULATION OF APOPTOSIS IN NBS Regulation of apoptosis is of special importance to cells with genomic instability because it can be the last barrier preventing arising tumor cells from manifesting in the body. Apoptosis is tightly connected to DNA damage signaling by TP53 as an intrinsic mediator. But it is also regulated by other intrinsic or extrinsic factors like ER stress, cytokines like TNFalpha, or lack of survival factors.

The intrinsic decision for apoptosis comes from a balance of pro- and anti-apoptotic factors. Expression chances in some of these factors occurred in NBS cells e.g for anti-apoptotic factors: BCL-XL/BCL2L1 (up), PKA (down), NIK/MAP3K14 (down), IKK/IKBKB (down), NFKB1 (down), RELA (up), IAP (BIRC2/8) down. Pro-apoptotic factors were also regulated, e.g. BAD (up), ENDOG (up), CHP and PPP3CC (up), BID (down), CASP3 (down), AIFM1 (down), PPP3R1 and PPP3CA (down) (Figure 44 on page 123, B).

In this analysis many adaptors for extrinsic signaling like FADD and TRADD or IRAK were regulated, but very mixed in up- or down-regulation. In summary, it was not really clear from this result if apoptosis was rather up-, or down-regulated in NBS cells compared to healthy cells. But judged from the expression status of most apoptosis executing enzymes like caspases, that are rather down-regulated or not especially regulated, there was not substantially more apoptosis in NBS.

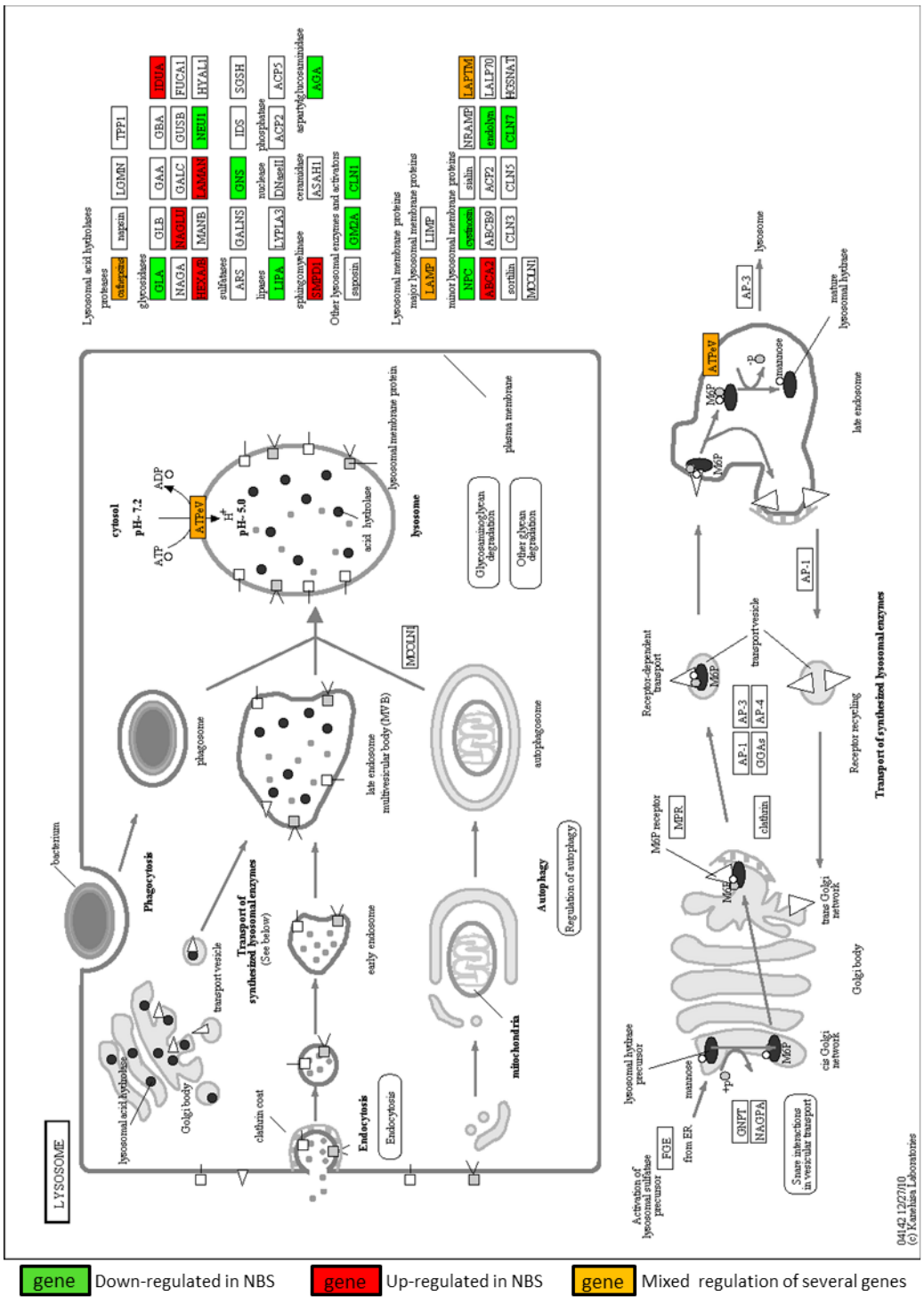

Figure 43: **Regulated genes of lysosome signaling pathway in NBS patients**

The DAVID output shows regulated genes in lysosome signaling using KEGG pathways. Regulated genes are selected by diff. p-value </= 0,05 and >/= 1,5 fold ratio. Expression levels of NBS patients relative to healthy fibroblasts are indicated by green and red boxes for decreased and increased expression respectively. Some boxes represent several genes, so in some cases up-regulated and down-regulated are found together in the same box, which is indicated with orange color.

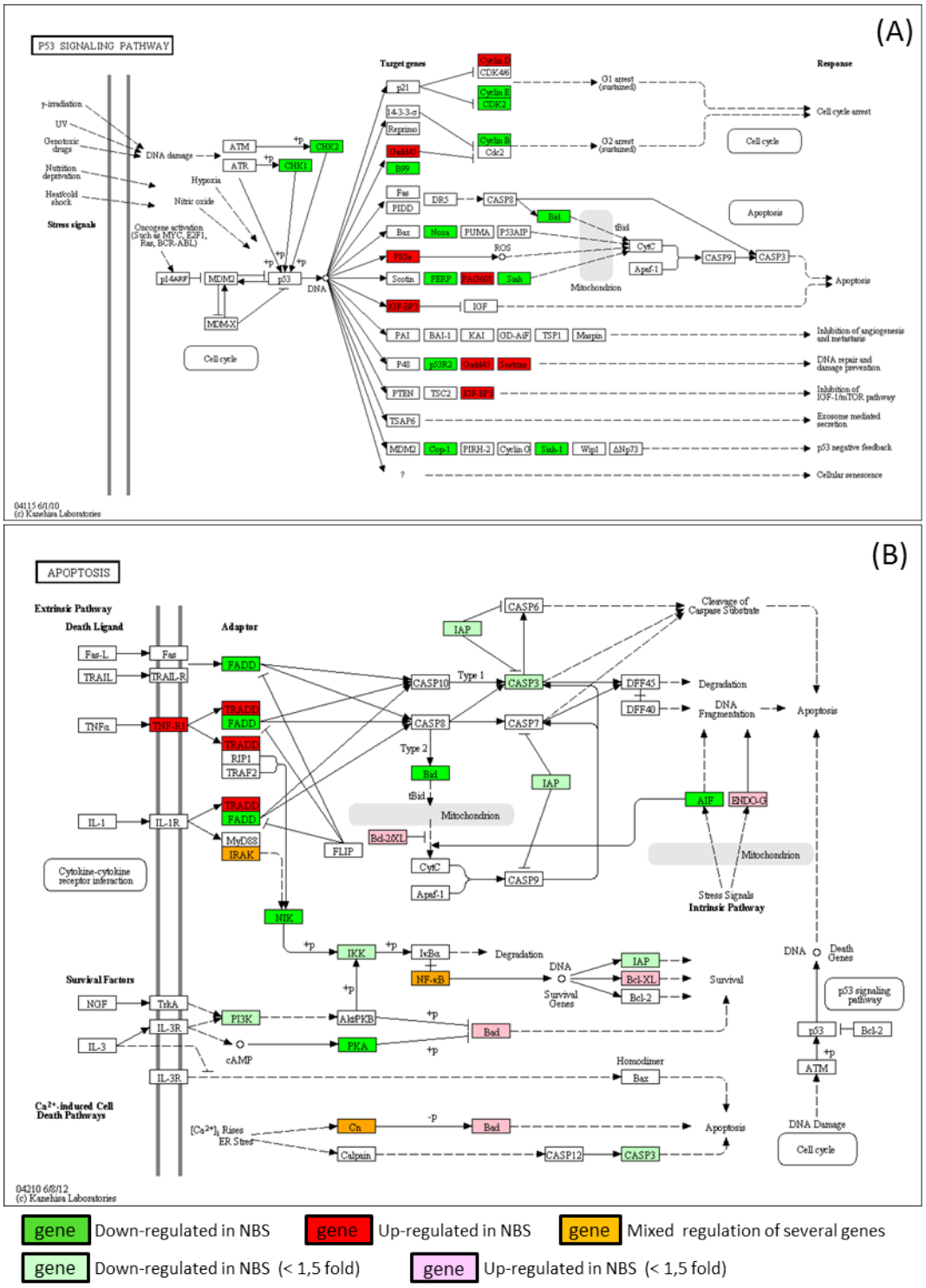

Figure 44: **Regulated genes of the TP53 and apoptosis signaling pathway in NBS patients**

The DAVID output shows regulated genes in (A) TP53 and (B) apoptosis signaling using KEGG pathways. Regulated genes are selected by diff. p-value </= 0,05 and >/= 1,5 fold ratio. Expression levels of NBS patients relative to healthy fibroblasts are indicated by green and red boxes for decreased and increased expression respectively. Some boxes represent several genes, so in some cases up-regulated and down-regulated are found together in the same box, which is indicated with orange color.

3.5.1.10 *Pathways in cancer*

In the genomic instability disease NBS, a high frequency of cancer is the major concern for patients, who often die from it before they have grown into adulthood. Therefore, it was not astonishing that many paths in different cancer key positions were found regulated in NBS cells (Figure 45 on page 124). The major elements for tumorigenesis are: (a) evading apoptosis, (b) proliferation, (c) sustained angiogenesis, (d) failed repair of genes, (e) insensitivity to anti-growth signals, (f) genomic damage, (g) resistance to chemotherapy, (h) block of differentiation, (i) tissue invasion and (j) metastasis.

In total, there were 26 genes up- and 37 genes down-regulated. Concentration of up-regulated genes occurred in "failed repair of genes" (BAX, MSH3, TGFBR2) and "sustained angiogenesis" (TCEB2, ARNT, EP300, VEGFB, MMP2). Concentration of down-regulated genes occurred in "proliferation" (RB1, CDK2, CDKN1B, SKP2, MYC). Pathways which were most affected by modified gene regulation included "VEGF signaling" (EGLN2, TCEB2, ARNT, EP300, VEGFB, MMP2), "Wnt-signaling" (FZD1, FZD9, GSK3B, CTNNB1, AXIN1, BIRC5, MYC), "Focal adhesion" (LAMA2, LAMA3, LAMB2, PTK2) "PI3K-Akt signaling" (NKX3-1, AKT1, CDKN1B, BCL2L1, NFKB1, NFKB2, RELA, TRAF3), "Jak-STAT signaling" (STAT1, STAT5A, BCL2L1, VEGFB) and "MAPK signaling" (GRB2, NCOA4, RAF1, ARAF, MAPK1, MAPK3, MYC, ETS1, RALB, CDC42, DAPK2). (see Figure 45 on page 124)

Figure 45: **Regulated genes of cancer pathways in NBS patients**
The DAVID output shows regulated genes in cancer signaling using KEGG pathways. Regulated genes are selected by diff. p-value </= 0,05 and >/= 1,5 fold ratio. Expression levels of NBS patients relative to healthy fibroblasts are indicated by green and red boxes for decreased and increased expression respectively. Some boxes represent several genes, so in some cases up-regulated and down-regulated are found together in the same box, which is indicated with orange color.

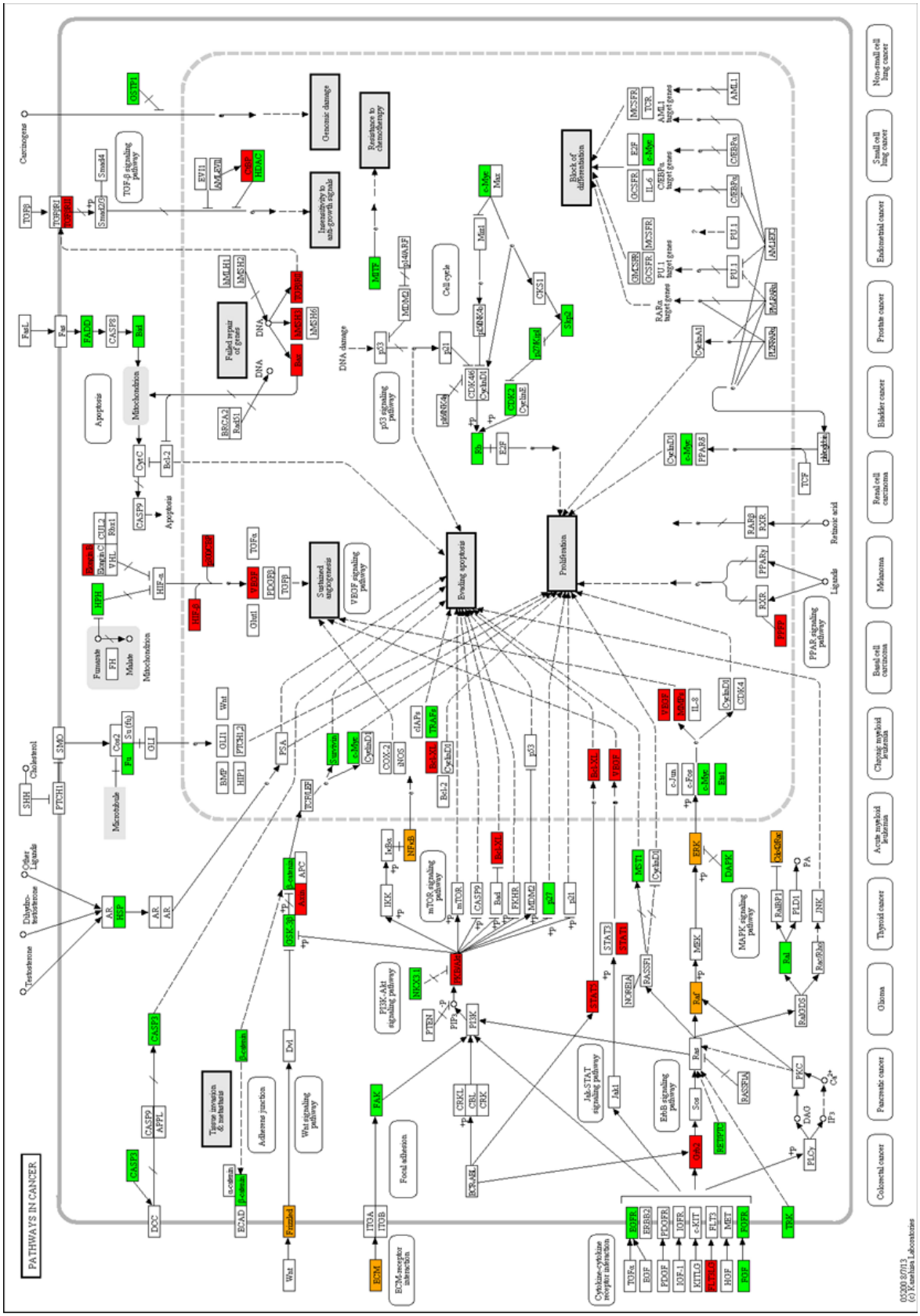
PATHWAYS IN CANCER
gene Down-regulated in NBS
gene Up-regulated in NBS
gene Mixed regulation of several genes

FANCONI ANEMIA PATHWAY IN NBS Fanconi anemia (FA) is caused by mutations in one of at least 13 FA genes. FA and NBS share several clinical features like developmental delay, microcephaly, and cancer predisposition. To discriminate both diseases, the clinic has relied on diagnosing chromosomal instability following exposure to DNA cross-linking agents in FA and to ionizing radiation (IR) in NBS.

The Fanconi anemia pathway is required for the efficient repair of damaged DNA, especially interstrand cross-links (ICLs). Monoubiquitination of the Fanconi anaemia protein FANCD2 is a key event leading to repair of ICLs. It was already reported that FANCD2 colocalizes with NBN and that inhibition of NBN leads to a decrease of FANCD2. Here we show, that in cells with truncated NIBRIN, several FA genes have reduced expression levels as depicted in a KEGG pathway of FA (Figure 46 on page 126, A), or in a diagram of FA and FA-related genes (Figure 46 on page 126, B). In fact, all FA genes appear to be down-regulated, or show at least a tendency towards down-regulation, but not all with a high probability (diff. p-val < 0,05). Several of these genes (eg. FANCD2, RPA3, UBE2T, FANCG) were confirmed by real-time PCR as shown in Figure 46 on page 126, C.

Figure 46: **The Fanconi Anemia (FA) pathway is affected in NBS patients** (A) The KEGG pathway shows regulated genes in FA signaling. Regulated genes are selected by diff. p-value </= 0,05 and >/= 1,5 fold ratio. Expression levels of NBS patients relative to healthy fibroblasts are indicated by green boxes for decreased expression. (B) A list of FA related genes obtained from SABioscience PCR array shows Log2 ratios (array data) of average expression in NBS vs. normal fibroblasts. The genes are sorted according to their fold differences and marked in green and grey for high and low differential p-Val respectively. (C) Real-Time-PCR confirmation of FA and FA related genes.

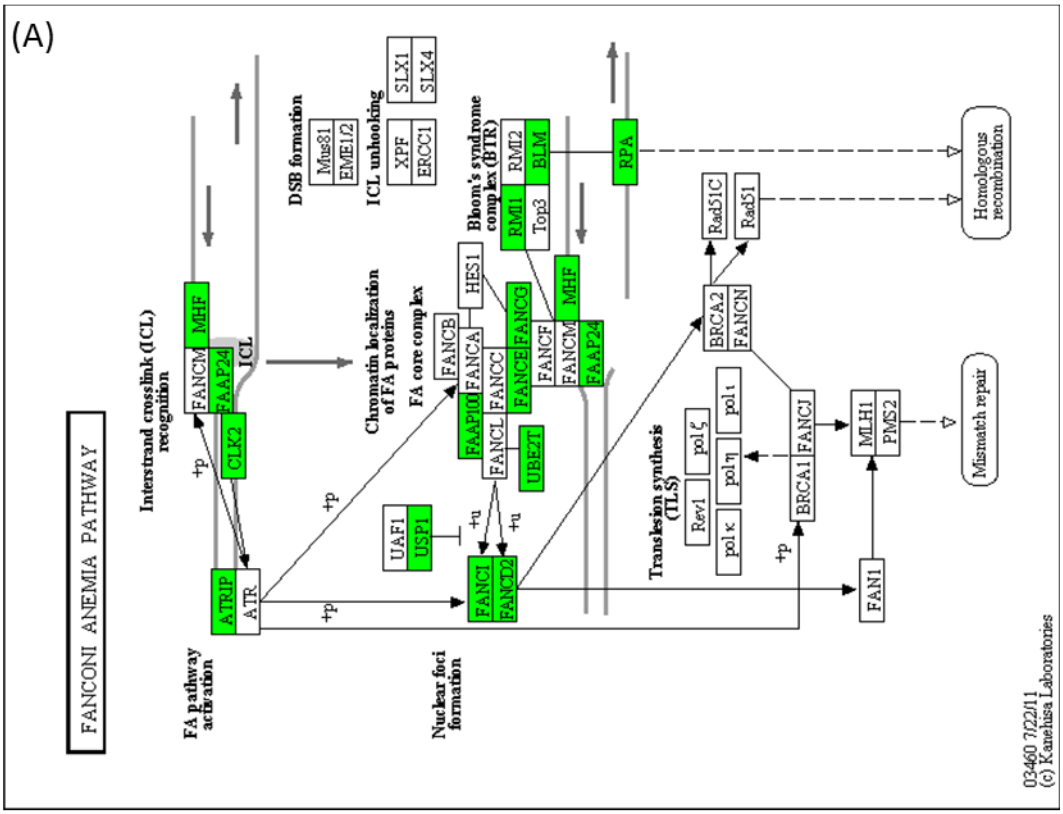
(A)
FANCONI ANEMIA PATHWAY
Interstrand crosslink (ICL) recognition
FA pathway activation
DSB formation
ICL unhooking
Chromatin localization of FA proteins
FA core complex
Bloom's syndrome complex (BTR)
Nuclear foci formation
Translesion synthesis (TLS)
Homologous recombination
Mismatch repair
FANCM
MHF
FAAP24
ICL
CLK2
ATRIP
ATR
Mus81
EME1/2
SLX1
SLX4
XPF
ERCC1
HES1
FANCB
FANCA
FANCC
FAAP100
FANCL
UBE2T
FANCG
FANCE
FANCF
UAF1
USP1
FANCI
FANCD2
RMI2
BLM
RMI1
Top3
RPA
Rad51C
Rad51
BRCA2
FANCN
Rev1
pol ζ
pol ι
pol η
pol κ
BRCA1
FANCJ
MLH1
PMS2
FAN1
+p
+u
03460 7/22/11
(c) Kanehisa Laboratories

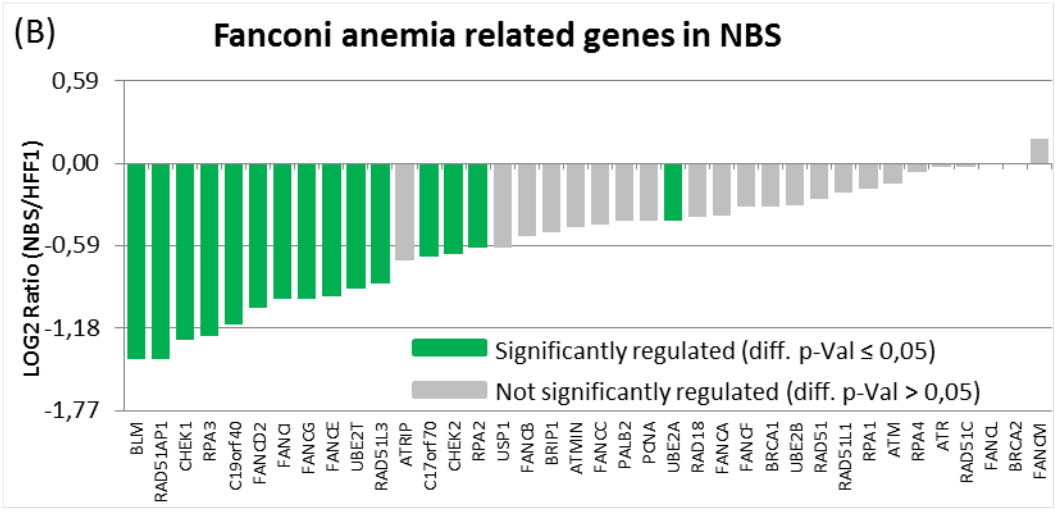
(B)
Fanconi anemia related genes in NBS
LOG2 Ratio (NBS/HFF1)
0,59
0,00
-0,59
-1,18
-1,77
Significantly regulated (diff. p-Val ≤ 0,05)
Not significantly regulated (diff. p-Val > 0,05)
BLM
RAD51AP1
CHEK1
RPA3
C19orf40
FANCD2
FANCI
FANCG
FANCE
UBE2T
RAD51L3
ATRIP
C17orf70
CHEK2
RPA2
USP1
FANCB
BRIP1
ATMIN
FANCC
PALB2
PCNA
UBE2A
RAD18
FANCA
FANCF
BRCA1
UBE2B
RAD51
RAD51L1
RPA1
ATM
RPA4
ATR
RAD51C
FANCL
BRCA2
FANCM

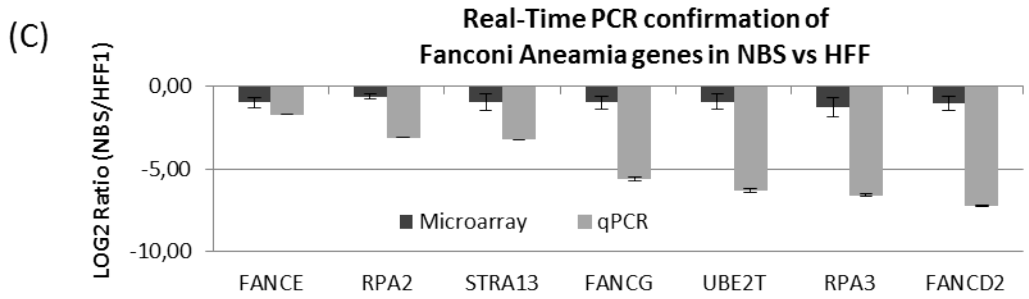
(C)
Real-Time PCR confirmation of
Fanconi Aneamia genes in NBS vs HFF
LOG2 Ratio (NBS/HFF1)
0,00
-5,00
-10,00
Microarray
qPCR
FANCE
RPA2
STRA13
FANCG
UBE2T
RPA3
FANCD2

3.5.1.11 *Summary of the findings for NBS fibroblasts*

By performing global transcriptome analysis of fibroblasts of 4 NBS patients it was shown, that NBS patients had a distinct profile compared to non-diseased fibroblasts and that previously observed phenotypes of the disease were mirrored in the expression profiles of related pathways. Furthermore, other pathways and biological functions were affected by the NBS transcriptome, which were not yet known or poorly related to NBS. The identification of strongly regulated genes and transcription factors enabled deeper insight in the mechanisms behind the disease and might be targets in future studies and therapies.

3.5.2 *Global Gene Expression Analysis Comparing hESCs with Fibroblast-derived iPSCs from NBS Patients*

After reprogramming of NBS-8 fibroblasts to NBS-8iPSC-lines 1 and 2, the parental cell line and the reprogrammed lines plus non-diseased fibroblasts, iPSCs and hESCs were loaded onto a HumanHT-12_V4 microarray (Illumina). The samples were analyzed and compared to samples of HFF1 and BJ fibroblast cells, HFF1 and BJ derived iPSCs and H1 and H9 hESCs, loaded to the same array type. The manufacturer's software, GenomeStudio, was used to profile the transcriptomes of these samples which were loaded in technical duplicates except for sample H9, loaded as single sample, and NBS-8-iPS1/2 plus NBS-8_Fib_a/b which were loaded in biological duplicates. All samples originated from male cells, except H9, which was derived from female cells. Data reproducibility is demonstrated by sample correlation (Figure 47 on page 129, B). As expected, technical duplicates cluster close together (pVal < 0,03) and all pluripotent lines cluster closer together (pVal < 0,08) than against fibroblasts (pVal < 0,13). Non-diseased fibroblasts cluster closer together than NBS-8 fibroblasts, but interestingly, hESCs correlate more to NBS-8-iPSCs than to the other fibroblast-derived iPSCs. The biological replicate of NBS-8 fibroblasts clustered rather far to each other in comparison to other fibroblasts. The difference between the two NBS-8 samples was extraction of RNA from different passage numbers (a: 08/2011, b: 11/2011). To compare the similarity of sample type groups, correlation coefficients were calculated by clustering the whole genome data from expressed genes (detection pValue $\leq$ 0,01) of each group to each other (Figure 47 on page 129, A). Of course, fibroblasts and pluripotent cells correlated apart from each other (R^2 between 0,6711 and 0,7607) and with high correlation (R^2 between 0,7925 and 0,9588) among each other. The highest correlation appeared between HFF1 and BJ fibroblasts (R^2 = 0,9588), followed by hESCs and BJ-iPSCs (R^2 = 0,9038). NBS-8-iPSCs correlated highest with hESCs (R^2 = 0,8984), than with BJ-iPSCs (R^2 = 0,8534) and lowest with HFF1-iPSCs (R^2 =

0,7925). NBS-8 fibroblasts correlated similar with HFF1 (R^2 = 0,8555) and BJ (R^2 = 0,8619) fibroblasts.

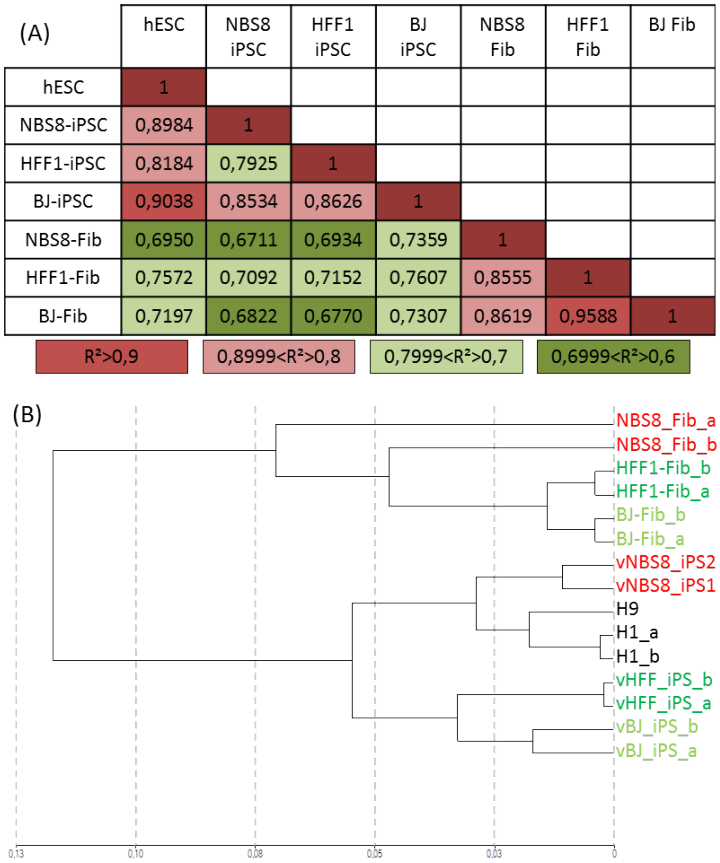

Figure 47: **Microarray sample analysis of reprogrammed cells** (A) Calculated correlation coefficent (R^2) between hybridized samples. High R^2 indicates high similarity. (B) Dendrogram of sample clustering of NBS patient cells (in red), normal cells (in green) and hESCs (in black).

3.5.2.1 *qPCR confirmation*

Quantitative real-time PCR was used to verify microarray results for a selection of genes from cell cycle and DNA damage response which expression was significantly changed in NBS patients (Figure 48 on page 130). The relative expression of NBS-8-iPSCs to hESCs was confirmed in 5 of 9 tested genes (NFKB1, CKN1B, CHEK1, RB1, TP53I3; Figure 48 on page 130, A). There were different expression of GSK3B, CHEK2, CREB1 and SESN1 for both NBS-8-iPSC replicates and different CDKN1B expression for NBS-8-iPS-1. The same set of genes was tested to calculate the LOG2 ratio of NBS-8-iPSCs to NBS-8 fibroblasts (Figure 48 on page 130, C). Here, 6 out of 9 genes were confirmed (NFKB1, CDKN1B, CHEK1, CHEK2, RB1, TP53I3). The RNA level of GSK3B CREB1 and SESN1 differed in qPCR from microarray analysis. When the gene set was tested to compare RNA expression in

NBS-8 and HFF1 fibroblasts, the LOG2 ratios of qPCR did not match the range or orientation of the microarray values (Figure 48 on page 130, B). This was caused by a different type of RNA input, which was RNA isolated from HFF1 cells directly and cRNA from NBS-8 fibroblasts (same cRNA was also used for the microarray). In summary, microarray data was confirmed by a selection of genes, but array or qPCR data lacked accuracy when expression of genes was close to detection limit.

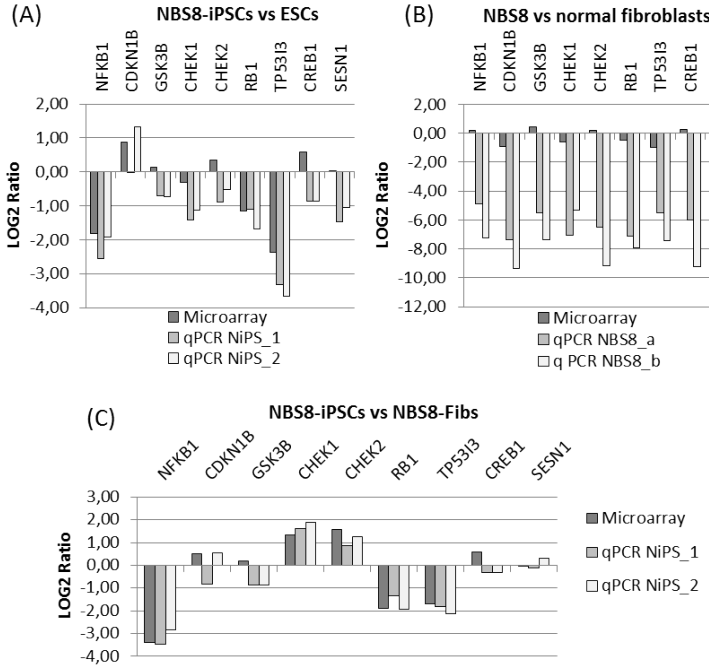

Figure 48: **Real-time confirmation of selected genes from array data** NiPS_1/2: NBS-8 iPSCs clone 1/2; NBS8_a/b: NBS-8 fibroblasts sample a/b

3.5.2.2 *NBN expression detected by microarray*

NBN expression was analyzed from microarray data in all sample-groups (Figure 24 on page 75, A). The background average signal was around 13. The average expression of NBN in NBS-8 fibroblasts and iPSCs ranged between 64 and 92, whereas in all other samples (non-diseased) the expression ranged between 204 and 360 which is approximately 3- to 4-fold higher. The DNA sequence on the array was aligned to the RefSeq RNA database (NCBI-BLAST) and matched the C-terminal area of NBN mRNA. Therefore the sequence was able to detect the non-mutated part of NBN mRNA.

3.5.2.3 *Assessment of human pluripotent stem cells with PluriTest*

After reprogramming a cell line from somatic to pluripotency it is good laboratory practice to perform extensive tests for validation as described in 3.1.2.4. The transcriptome data of the iPSC-lines and their parental cells provides additional assurance and quality control. Core pluripotency genes were analyzed for their expression levels in somatic (HFF1, BJ, NBS-8) and stem cell lines (HFF1-iPSCs, BJ-iPSCs, NBS-8-iPSCs, H1, H9, Figure 49 on page 132, A). Correlation of pluripotency genes alone resulted in the same clustering pattern as global transcriptome clustering (Figure 47 on page 129, B). In addition, using the Euclidean metric, the pluripotency genes clustered in three different settings, a group with high ratios between fibroblasts and stem cells, a group with similar high expression and a group with similar low expression. Among the group with exclusive expression in stem cells were genes like NANOG, OCT4, SOX2, LIN28, NODAL, DNMT3B, PODXL and other typical stem cell marker genes.

Müller *et al.* created a program, based on a collection of validated hESCs and iPSCs, which calculates the level of pluripotency based on their gene expression profiles and not the non-standardized teratoma assay which is costly and time consuming and therefore not amenable to high throughput derivation and characterization of iPS cells. The quality of the stem cell line is judged by calculation of a pluripotency and novelty score. The pluripotency score gives an indication if a sample contains a pluripotent signature, the higher the value, the more likely the stemness. But partially differentiated pluripotent cells, teratocarcinoma cells or karyotypically abnormal embryonic stem cells often have a high pluripotency score as well. Because they differ in their expression profiles the group employed a novelty score, which describes the similarity of the samples with samples from the database and should be low in order to show high similarity. So, a very high quality stem cell cell should have a high pluripotency in combination with a low novelty score. After analysis of all microarray samples, all fibroblast lines were found to have low pluripotency and high novelty scores (Figure 49 on page 132, B-C). NBS-8-iPSC-1 showed the highest pluripotency score, BJ-iPSC-a, H1-a, H1-b, H9 and NBS-8-iPS-2 had a lower score but were within the border that contains approx. 95% of validated pluripotent cells from the database. HFF1-iPS-a/b and BJ-iPS-b were outside this region and HFF-1-a/b also failed the novelty tests. All other stem cell lines passed this test.

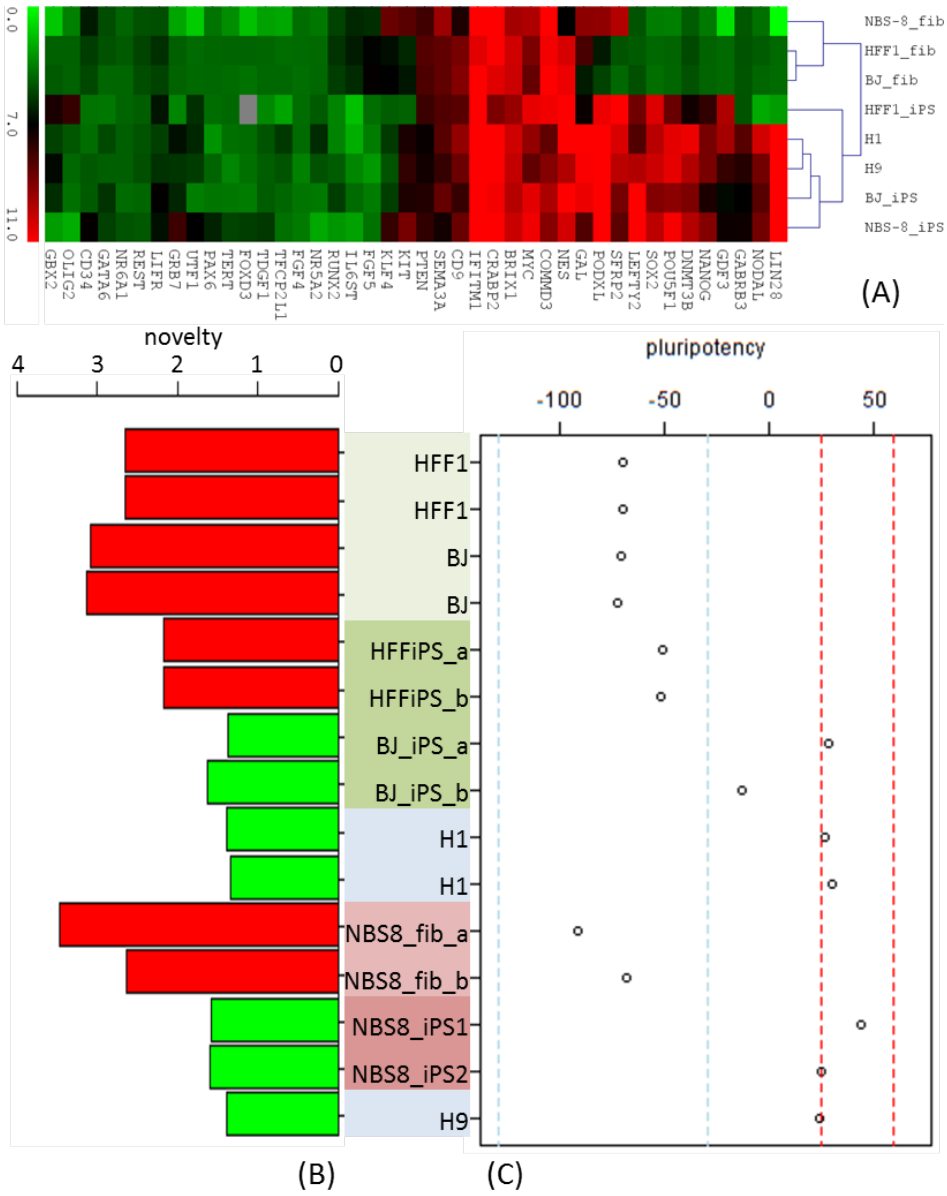

Figure 49: **Evaluation of pluripotency in reprogrammed NBS cells** (A) Heatmap of pluripotency genes. LOG2 of average signal shows low (green) and high (red) expression. (B) Novelty Score: A score that is based on well-characterized pluripotent samples in the stem cell model matrix. Samples are color-coded green (pluripotent), orange, red (not-pluripotent) based on the probabilities given from the logistic regression model. A low Novelty Score indicates that the test sample can be well reconstructed based on existing data from other well-characterized iPSC and ESC lines. A high Novelty Score indicates that there are patterns in the tested sample that cannot be explained by the currently existing data from well-characterized, karyotypic normal pluripotent stem cells (http://www.pluritest.org). (C) Pluripotency Score: A score that is based on all samples (pluripotent cells, somatic cells and tissues) in the stem cell model matrix. Samples with positive values are more similar to the pluripotent samples in the model matrix than to all other classes of samples in the matrix. The area between the red lines indicates the range that contains approximately 95 percent of the pluripotent samples tested. The blue lines indicate those scores that was observed in approximately 95 percent of the non-pluripotent samples (http://www.pluritest.org).

3.5.2.4 *Expression comparison between NBS samples and their healthy counterparts to identify NBS specific gene targets*

The Illumina HumanHT-12_V4 array detected 47223 individual sequences (Illumina IDs) which correspond to 34688 genes. The 15 samples were grouped into 5 different classes according to their replicates (ES, iPS, NBS-8-iPS, NBS-8-Fib, Healthy-Fib). In each group contained a distinct set of expressed genes as judged by the expression pValue $\leq$ 0,01. NBS-8-iPSCs were represented by 18989 (40,21 %) expressed IDs, of which 877 were exclusively expressed, 626 were shared only with ESCs, 675 were shared only with iPSCs and 16811 were shared with both of them (Figure 50 on page 135, A). By comparing NBS-8 fibroblasts and NBS-8-iPSCs, 1808 IDs were found to be exclusively expressed in NBS-8-Fib and 3814 in NBS-8-iPSCs (Figure 50 on page 135, B). In fibroblasts, 995 IDs were found only in NBS-8 cells and 2781 IDs only in the group of non-diseased fibroblasts (Figure 50 on page 135, C). To identify genes which were specific to NBS cells in general, expressed IDs were tested for distinct and overlapping IDs in all groups (Figure 50 on page 135, D). 41 unique Illumina IDs were found in this group, whereas 612 IDs remained to be specific in NBS-iPSCs and 296 in NBS-8 fibroblasts.

Further analysis of NBS specific IDs which referred to 41 unique genes revealed "neuron differentiation" as an enriched annotation (GOTERM_BP_FAT) and CRE/BP1 as the most significant TFBC (determined by DAVID; see methods Section 2.8) which included 75 % of the gene list as possible target genes (Table 11 on page 133, Table 12 on page 134). Genes exclusively expressed in NBS-8-iPSCs were enriched in the pathway "B cell receptor signaling pathway" and in the annotation "ion transport" (GOTERM BP_FAT) and others (suppl. file "S08"). The group of genes solely expressed in NBS-8 fibroblasts clustered for "cytokine-cytokine interaction as the most significant pathway and "extracellular matrix organization" as the most significant functional annotation (Table 13 on page 134, Table 14 on page 134).

Table 11: **Annotations of NBS specific gene expression**

GOTERM BP_FAT:	Count	%	PValue
neuron differentiation	4	12,5	0,037
positive regulation of macromolecule metabolic process	5	15,6	0,054
determination of left/right symmetry	2	6,3	0,069
determination of symmetry	2	6,3	0,071
determination of bilateral symmetry	2	6,3	0,071
pattern specification process	3	9,4	0,075
secretion	3	9,4	0,091
excretion	2	6,3	0,094

Table 12: **NBS specific gene expression cluster together under certain transcription factor binding sites (TFBS)**

UCSC TFBS:	Count	%	PValue
CREBP1	24	75	0,000
NGFIC	18	56,3	0,000
LMO2COM	25	78,1	0,002
ROAZ	21	65,6	0,003
MYOGNF1	21	65,6	0,004
SOX5	21	65,6	0,005
GATA	20	62,5	0,006
AP1	24	75	0,007
ATF6	20	62,5	0,008
FREAC3	19	59,4	0,009

Table 13: **Fibroblast dependent NBS specific gene expression summarized in pathways**

KEGG Pathway	Count	%	PValue
Cytokine-cytokine receptor interaction	11	5,73	0,001
ABC transporters	4	2,08	0,016
Complement and coagulation cascades	4	2,08	0,051
Calcium signaling pathway	6	3,13	0,062
ECM-receptor interaction	4	2,08	0,082
Hematopoietic cell lineage	4	2,08	0,087

Table 14: **Fibroblast dependent NBS specific gene expression summarized in common functional annotations**

GOERM BP_FAT	Count	%	PValue
extracellular matrix organization	9	4,69	0,000
cell adhesion	21	10,94	0,000
biological adhesion	21	10,94	0,000
response to wounding	17	8,85	0,000
positive regulation of cell-substrate adhesion	5	2,6	0,000
extracellular structure organization	9	4,69	0,000
positive regulation of cell adhesion	6	3,13	0,000
cellular calcium ion homeostasis	9	4,69	0,000
regulation of growth	12	6,25	0,001
calcium ion homeostasis	9	4,69	0,001
wound healing	9	4,69	0,001
cellular metal ion homeostasis	9	4,69	0,001
metal ion homeostasis	9	4,69	0,001
homeostatic process	18	9,38	0,001
regulation of cell-substrate adhesion	5	2,6	0,001
regulation of survival gene product expression	4	2,08	0,001
multicellular organismal homeostasis	6	3,13	0,001
chemical homeostasis	14	7,29	0,001

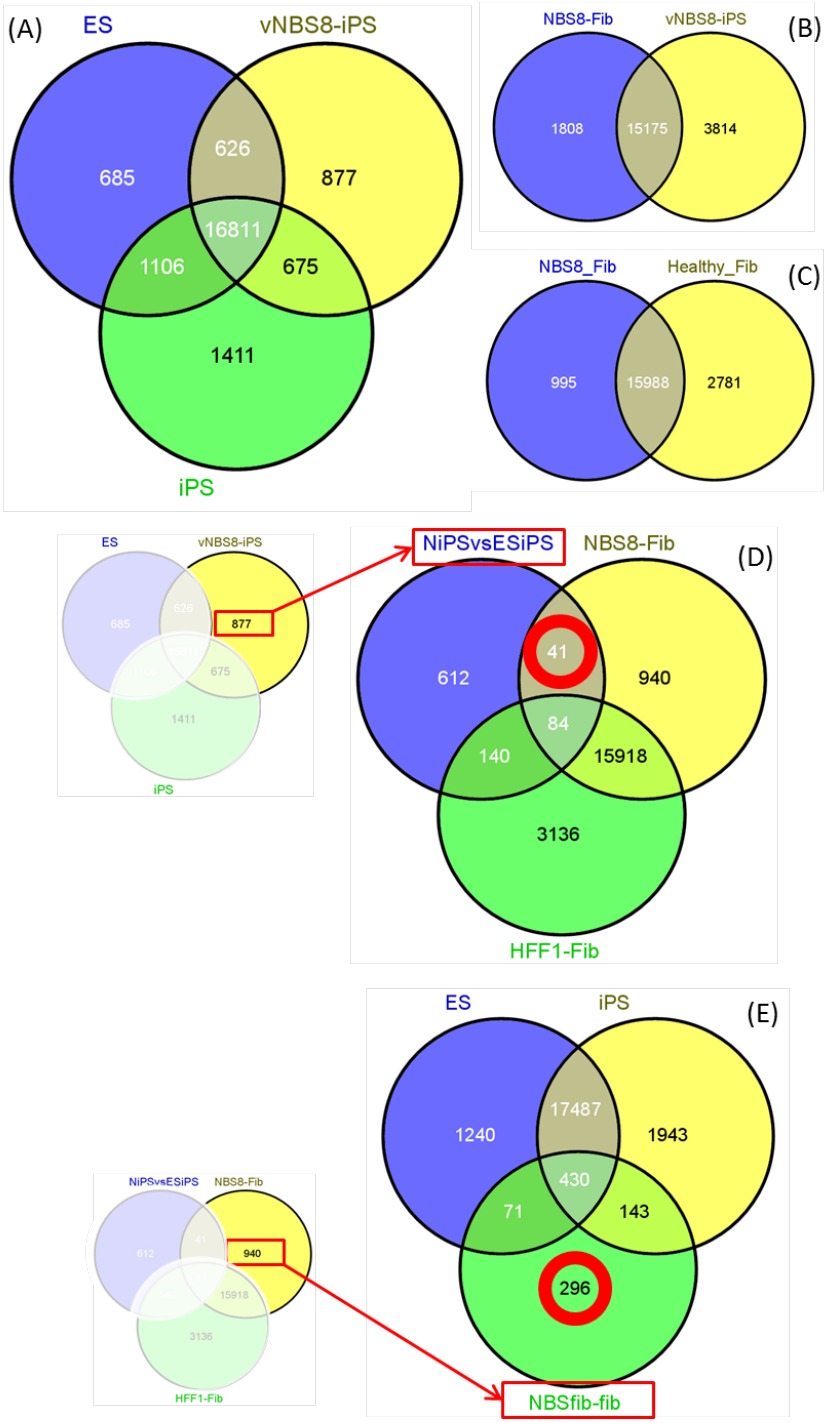

Figure 50: **Comparison of gene expression between normal and NBS cells** (A) Venn diagram comparing expressed genes (pVal < 0,01) of hESCs (ES), normal viral and fibroblasts derived iPSCs (iPS) and viral derived NBS-iPSCs (vNBS8-iPS). (B) Comparison of gene expression (pVal < 0,01) between NBS fibroblasts (NBS8-Fib) and NBS-iPSCs (vNBS8-iPS). (C) Comparison of gene expression (pVal < 0,01) between NBS fibroblasts (NBS8-Fib) and normal fibroblasts (Healthy_Fib). (D) The subpopulation (red box) of distinct expression in NBS-iPSCs (compared to hESCs and normal iPSCs) was used to isolated NBS-specific gene expression (red circle) by further comparison to NBS and normal fibroblasts. (E) NBS-specific gene expression limited to NBS fibroblasts (red circle) was isolated by comparison of the subpopulation (red box) of NBS fibroblasts from (D) with hESCs and normal iPSCS.

3.5.2.5 *Identification of enriched pathways in NBS cells by significant regulated genes*

To compare expressed to not-expressed genes is a very stringent way of comparing data. Especially when the gene set, which is distinct in each group, is small, further analysis of integrated biological functions is hard to determine. In addition, a large dataset ensures better calculation of significance. Comparing the biological functions of expressed or regulated genes should give a similar result, because the exclusive expressed genes were a subpopulation of regulated genes. Expression in a yes/no background would resolve to strong transcription factor activation, or epigenetic changes, but regulation can also include secondary regulation methods like mRNA stability. In addition, classification of up-regulated and down-regulated genes can be used to specify the regulation networks. Here, regulated genes were judged by a differential pValue $\leq$ 0,05 and a ratio of sample expression $\geq$ 1,5-fold. By this, the number of genes representing a certain group was increased. For example, 1552 genes were specifically expressed in NBS-8-iPS compared to hESCs and 2194 were significantly regulated.

PATHWAYS ENRICHED IN NBS-8 FIBROBLASTS Differentially regulated genes between NBS-8 and HFF1 fibroblasts were determined by statistical analysis (GenomeStudio) and by manual threshold settings (Diff pValue $\leq$ 0,05; fold-ratio $\geq$ 1,5). There were 1178 down- and 149 up-regulated IDs found which were further analyzed by "DAVID Functional Annotation". A combined list of up- and down-regulated genes was used to find enriched pathways. The top 3 significant pathways were "Focal adhesion", Regulation of actin cytoskeleton" and "Renal cell carcinoma" (Table 15 on page 137, A). There were pathways overlapping with the analysis of 4 NBS patients (see 3.5.1.6) in significant range below 0,05 (pValue) of "Cell cycle", "Pathways in cancer" and "Amyotrophic lateral sclerosis (ALS)". When gene lists were analyzed separated from their regulation form, up-regulated genes enriched in pathways like "Focal adhesion", "ECM-receptor interaction" and "TGF-beta signaling". Down-regulated genes enriched in pathways like "Splicosome", "Steroid biosynthesis" and "Regulation of actin cytoskeleton" (Table 15 on page 137, B).

Table 15: **Pathway analysis of differentially regulated genes between NBS-8 fibroblasts and normal fibroblasts**

(A) KEGG Pathway (regulated)	Count	PVal
Focal adhesion	31	0
Regulation of actin cytoskeleton	29	0
Renal cell carcinoma	14	0
Steroid biosynthesis	7	0
Pathogenic Escherichia coli infection	12	0
Pathways in cancer	37	0
Spliceosome	19	0
Leukocyte transendothelial migration	17	0
ECM-receptor interaction	13	0,01
Adherens junction	12	0,01
Biosynthesis of unsaturated fatty acids	6	0,01
Terpenoid backbone biosynthesis	5	0,01
Wnt signaling pathway	18	0,02
Inositol phosphate metabolism	9	0,02
Proteasome	8	0,03
Cell cycle	15	0,03
Colorectal cancer	11	0,04
Phosphatidylinositol signaling system	10	0,05
Amyotrophic lateral sclerosis (ALS)	8	0,05
Cysteine and methionine metabolism	6	0,07
Dilated cardiomyopathy	11	0,07
Fc gamma R-mediated phagocytosis	11	0,09
Small cell lung cancer	10	0,09
Hypertrophic cardiomyopathy (HCM)	10	0,1

(B) KEGG Pathway (up or down)	Count	PValue
Focal adhesion	9	0
ECM-receptor interaction	6	0
TGF-beta signaling pathway	5	0,01
Primary bile acid biosynthesis	3	0,01
Dilated cardiomyopathy	5	0,01
Metabolism of xenobiotics by cytochrome P450	4	0,02
Colorectal cancer	4	0,04
Hypertrophic cardiomyopathy (HCM)	4	0,04
Steroid hormone biosynthesis	3	0,07
Pathways in cancer	7	0,08
Spliceosome	19	0
Steroid biosynthesis	7	0
Regulation of actin cytoskeleton	25	0
Pathogenic Escherichia coli infection	11	0
Focal adhesion	22	0
Renal cell carcinoma	11	0
Leukocyte transendothelial migration	15	0,01
Biosynthesis of unsaturated fatty acids	6	0,01
Pathways in cancer	30	0,01
Terpenoid backbone biosynthesis	5	0,01
Inositol phosphate metabolism	9	0,01
Adherens junction	11	0,01
Proteasome	8	0,01
Phosphatidylinositol signaling system	10	0,02

PATHWAYS ENRICHED IN NBS-8-IPSCS The same analysis as above was performed with NBS-8-iPSCs and hESCs. Here, the top 3 significant pathways of combined regulated genes were, "DNA replication", "Pyrimidine metabolism" and "Glycolysis/Gluconeogenesis" (Table 16 on page 138, A). In the group of significant pathways (pValue $\leq$ 0,05) there were the same overlaps with NBS-8/Fib as with NBS-1-3-5-7/Fib (Cell Cycle, Pathways in Cancer). The most significant pathways enriched for up-regulated genes were "Glycolysis/Gluconeogenesis", "Fructose and mannose metabolism" and "Circadian rhythm". The most enriched pathways for down-regulated genes were "DNA-

replication", "Mismatch repair" and "Pyrimidine metabolism" (Table 16 on page 138, B).

Table 16: **Pathway analysis of differentially regulated genes in NBS-8 iPSCs and hESCs**

(A) KEGG Pathway (regulated)	Count	PVal
DNA replication	11	0
Pyrimidine metabolism	19	0
Glycolysis / Gluconeogenesis	14	0
Cell cycle	22	0,01
Endocytosis	29	0,01
Fructose and mannose metabolism	9	0,01
Mismatch repair	7	0,02
Pathways in cancer	43	0,03
Pentose phosphate pathway	7	0,03
Arginine and proline metabolism	10	0,06
Maturity onset diabetes of the young	6	0,08
Purine metabolism	21	0,09
RNA degradation	10	0,09
Galactose metabolism	6	0,09
Chronic myeloid leukemia	12	0,1
Small cell lung cancer	13	0,1

(B) KEGG Pathway (up or down)	Count	PValue
Glycolysis / Gluconeogenesis	12	0,000
Fructose and mannose metabolism	8	0,001
Circadian rhythm	4	0,019
Pentose phosphate pathway	5	0,025
Galactose metabolism	5	0,028
Starch and sucrose metabolism	6	0,040
Ribosome	9	0,043
Arginine and proline metabolism	6	0,091
DNA replication	10	0,000
Mismatch repair	6	0,005
Pyrimidine metabolism	12	0,007
Proteasome	8	0,008
Epithelial cell signaling in Helicobacter pylori infection	9	0,018
Cell cycle	13	0,020
Pathways in cancer	25	0,033
Endocytosis	16	0,038
Spliceosome	12	0,047
ECM-receptor interaction	9	0,055
Melanoma	8	0,061
Pancreatic cancer	8	0,064
Chronic myeloid leukemia	8	0,077
B cell receptor signaling pathway	8	0,077
Fc epsilon RI signaling pathway	8	0,090
Base excision repair	5	0,093

PATHWAYS ENRICHED FOR NBS SPECIFIC GENES The previous lists of regulated genes in somatic cells (NBS-8 vs HFF1 fibroblasts) and pluripotent cells (NBS-8-iPS vs ES) of NBS patients were compared to each other (Figure 51 on page 139). 151 terms overlapped, 2043 were specific to NBS-8-iPS and 1176 specific to NBS-8 fibroblast

cells. Elements specific to the NBS-8-iPS group still enriched in nearly the same pathways as the full list and elements specific to NBS-8 fibroblasts did the same (see Table 17 on page 139, Table 15 on page 137). Here, the list of core NBS dependent regulation changes was extended to 151 IDs (143 genes). The list was not sufficient to obtain significant regulated pathways, but several significant (pValue $\leq$ 0,05) GOTERM annotations were found: "positive regulation of cell proliferation" (e.g. VEGFA, CAPN1, TNS3, NBN), "camera-type eye development" (e.g. CASP6, ABI2, TWSG1), "immune system development" (e.g. LYN, KITLG, NBN) and "eye development" (e.g. VEGFA, CASP6, TWSG1) (Table 17 on page 139).

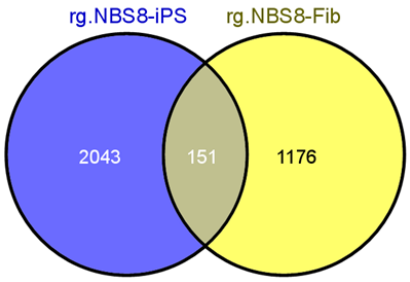

Figure 51: **Comparison of gene regulation between NBS fibroblasts and NBS iPSCs**
Venn diagram of gene lists comparing significantly (diff pVal < 0,05) regulated genes in NBS fibroblasts (vs. normal fibroblasts) (yellow) against significantly (diff pVal < 0,05) regulated genes in NBS iPSCs (vs. normal hESCs) (blue).

Table 17: **Pathway analysis of differentially regulated genes that occur common to NBS-8 iPSCs and NBS-8 fibroblasts but are specific in comparison to their normal counterparts**

GOTERM BP_FAT	Count	PValue
positive regulation of cell proliferation	8	0,02
camera-type eye development	4	0,03
immune system development	6	0,03
eye development	4	0,05
hemopoiesis	5	0,06
regulation of pigmentation during development	2	0,07
vesicle-mediated transport	8	0,07
mesoderm development	3	0,08
hemopoietic or lymphoid organ development	5	0,08
response to abiotic stimulus	6	0,08
reproductive developmental process	5	0,08
regulation of transcription from RNA polymerase II promoter	9	0,09
intracellular protein transport	6	0,09
RNA stabilization	2	0,09
mRNA stabilization	2	0,09
cell migration	5	0,1

3.5.2.6 *Detailed pathways analysis of transcriptional changes caused by mutated NIBRIN in pluripotent NBS cells*

As mentioned before, highlighting transcriptional changes in pathways is the most robust way of reading global transcriptomes. In section 3.5.1, several NBS fibroblast lines were analyzed in comparison to normal fibroblasts (HFF1). Here, the focus is laid to the comparison of NBS-8-iPSCs to non-diseased hESCs, but the parental cell line (NBS-8 fibroblasts) is integrated as well. The major finding was that "Glycolysis" was strongly and specifically up-regulated in NBS-iPSCs compared to hESCs, which itself already had strong activation of the pathway in comparison to somatic cells like fibroblasts. Secondly, the HIF1A-pathway was not statistically enriched in DAVID analysis, but contained high percentage of regulated genes in all scenarios. Other pathways, especially cell cycle and cancer, were affected in all scenarios as well and were compared to the 1st analysis (NBS-1-3-5-7 vs. HFF1).

GLYCOLYSIS IS UP-REGULATED IN NBS-8-IPSCS AND SHOWS A FOCUS TO ANAEROBIC METABOLISM Enrichment analysis of differentially regulated genes in NBS-8-iPSCs compared to hESCs revealed "Glycolysis" as the most significant up-regulated pathway (Table 16 on page 138 B, Figure 52 on page 141). In more detail, the group of enzymes, responsible to convert (HK2, GPI) glucose sugars (alpha-D-Glucose, alpha-D-Glucose-6P, beta-D-Glucose, beta-D-Glucose-6P) to beta-D-fructose-6P were 2 to 4-fold up-regulated. Especially interesting is the next reaction from beta-D-fructose-6P to beta-D-fructose-1,6P which is rate-limiting step in glycolysis and is carried out by phosphofructokinase (PFKL, PFKM). The phosphofructokinase was 2-fold up-regulated and the gene transcribing for the enzyme of the reverse conversion (FBP1), responsible for gluconeogenesis, was 2,5-fold down-regulated further solidifying the glycolysis direction. Also most of the other enzymes (ALDOA, ALDOC, TPI1, GAPDH, PGK1, ENO2), which further convert the sugars to from beta-D-fructose-1,6P to phosphoenolpyruvate, were found up-regulated. The next irreversible step from phosphoenolpyruvate to pyruvate, catalyzed by pyruvate kinase (PKM2) was not significantly regulated. Interestingly, AKR1A1 (1,5-fold) and LDHA (3,5-fold), which catalyze aldehydes to alcohols and pyruvate to lactate, respectively, were found up-regulated as well, giving evidence for anaerobic glycolysis. Citrate cycle independent energy production was further indicated by down-regulation of IDH1 and IDH3A, responsible for the conversion of isocitrate, oxalosuccinate and 2-oxoglutarate, as well as, SUCLA2, which catalyzes the reaction of succinyl-CoA to succinate.

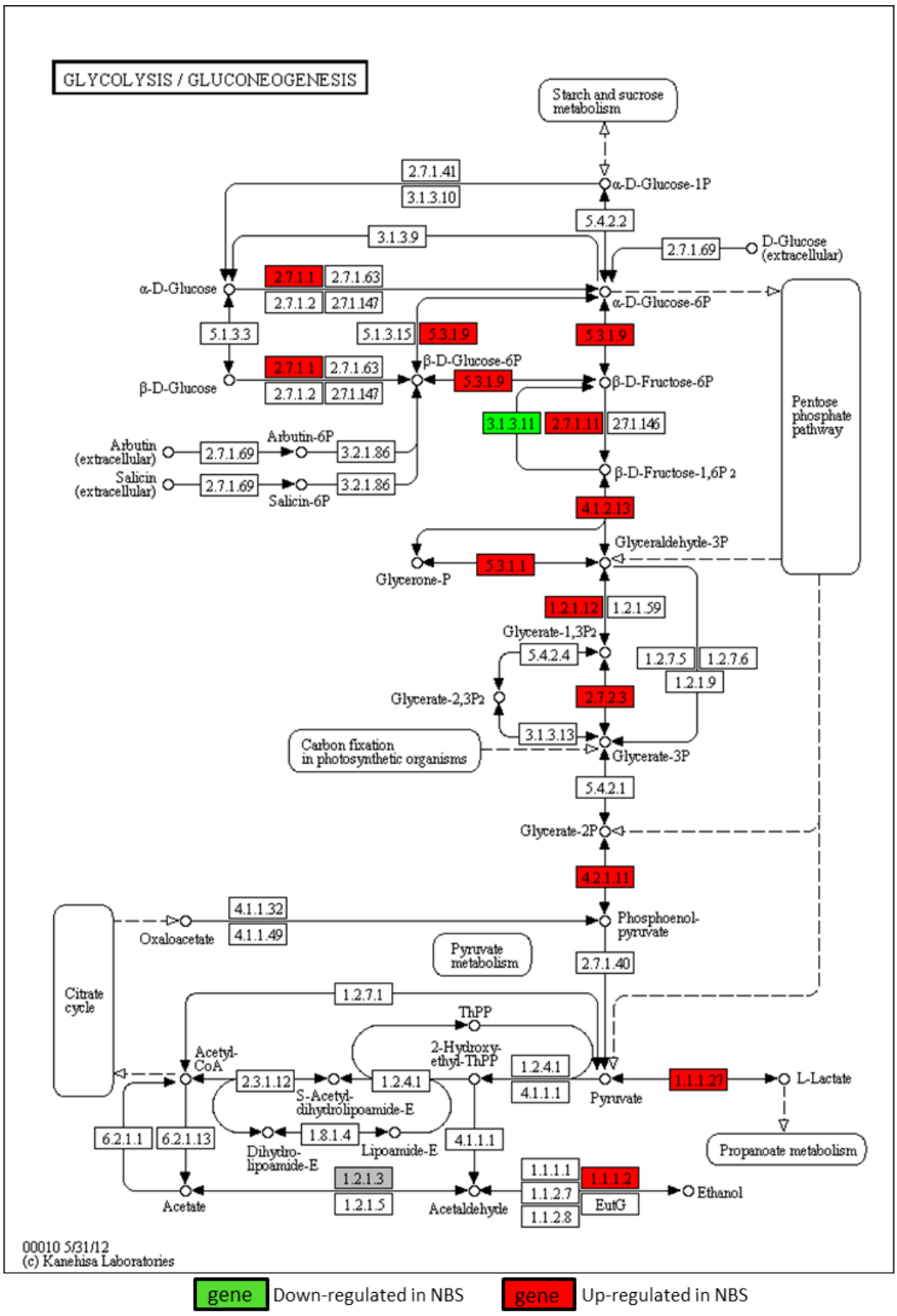

Figure 52: **Regulated genes of glycolysis pathway in NBS iPSCs**
The DAVID output shows regulated genes in glycolysis signaling using KEGG pathways. Regulated genes are selected by diff. p-value </= 0,05 and >/= 1,5fold ratio. Expression levels of NBS iPSCs relative to normal hESCs are indicated by green and red boxes for decreased and increased expression respectively.

HIF1A-PATHWAY REGULATION IN NBS CELLS The HIF1 pathway regulates the cells response to changing oxygen concentrations. It is activated by HIF1alpha stabilization which acts as an activating transcription factor to several genes in the response to hypoxia. In this study the pathway is highlighted in respect of the notably response of NBS cells to the HIF1-pathway activator EDHB, which was tested previously (Section 3.3). The pathway is analyzed towards expression changes under control conditions between NBS-8 fibroblasts, normal fibroblasts, NBS-8-iPSCs and normal hESCs. Array data including EDHB treatment was not yet generated.

The fate of HIF1-pathway results in "Increased oxygen delivery" and/or "Reduce oxygen consumption (Figure 53 on page 143). Genes which promote anaerobic metabolism in NBS-8-iPSCs compared to normal hESCs were already described by "Glycolysis" pathway. In addition, glucose transporter SLC2A1 was up-regulated, further supporting a positive response to hypoxia. VEGFA, responsible for oxygen delivery, was 5-fold up-regulated. EGLN1 (PHD) is the oxygen sensor and usually primes HIF1A for ubiquitin-based degradation. Though it was found up-regulated, the ubiquitin ligase complex itself was down-regulated (VHL, TCEB2). NFKB1 is known to regulate HIF1alpha basal levels and was found down-regulated. PIK3R1 and TEK were also down-regulated.

In contrast to NBS-8-iPSCs, NBS-8 fibroblasts showed a complete different regulation of the HIF1-pathway compared to their healthy counterparts (HFF1, Figure 53 on page 143, B). With one exception of VEGFA, only down-regulated genes were found: HIF1A, RBX1, EIF4E, PLCG1, PDHA1, SLC2A1, PFKFB and CDKNA1B. It can be concluded, that hypoxia was most likely activated in NBS-8-iPSCs and very unlikely activated in NBS-8 fibroblasts.

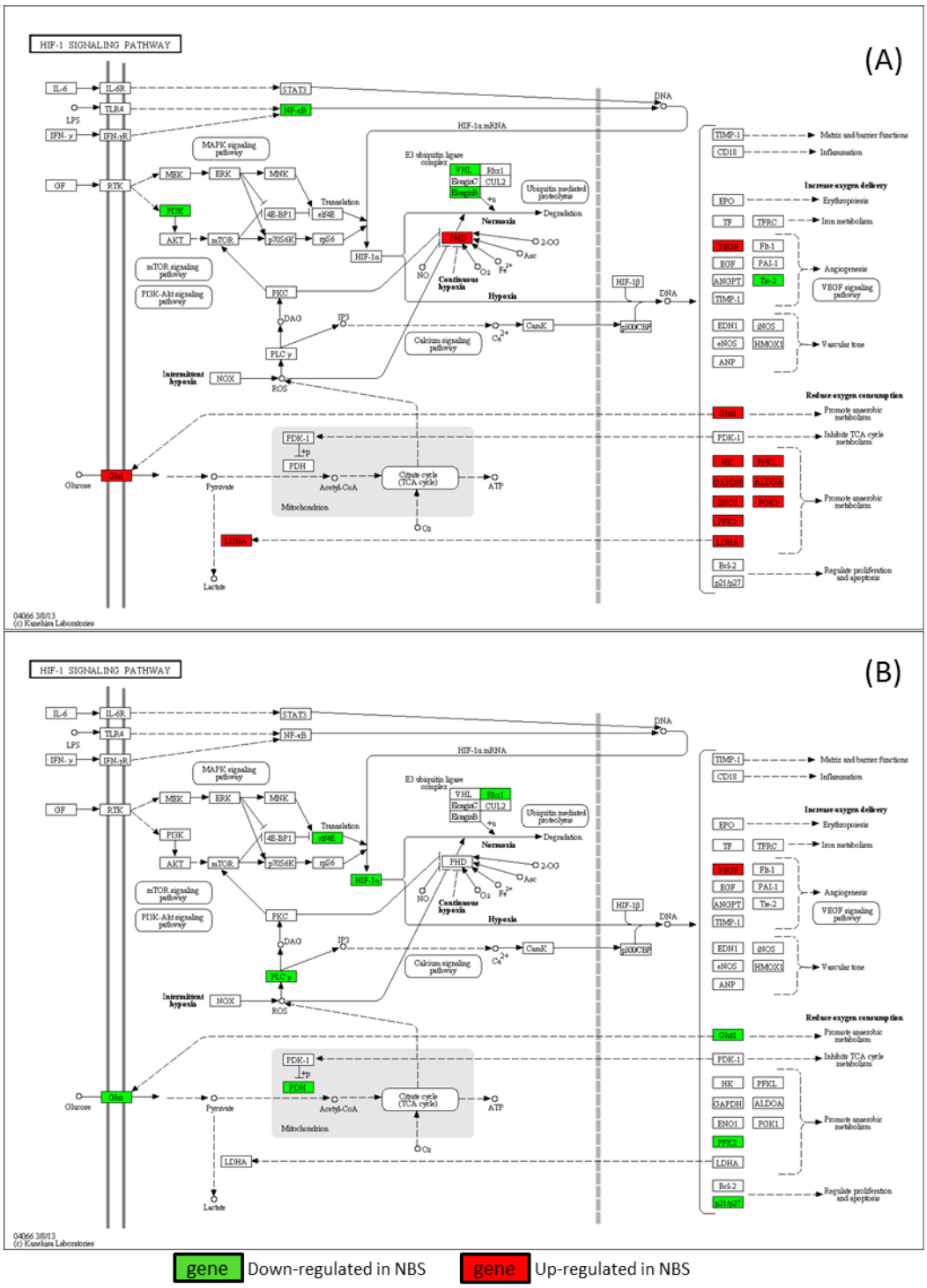

Figure 53: **Regulated genes of HIF1 pathway in NBS iPSCs**
The DAVID output shows regulated genes in HIF1 signaling using KEGG pathways. Regulated genes are selected by diff. p-value $\leq$ 0,05 and $\geq$ 1,5fold ratio. Expression levels of NBS iPSCs relative to normal hESCs (A) and NBS-8 fibroblasts relative to normal fibroblasts (B) are indicated by green and red boxes for decreased and increased expression respectively.

COMPARISON OF OVERLAPPING PATHWAYS BETWEEN NBS-1-3-5-7/FIB AND NBS-IPS/ES The main question behind the global transcriptome analysis was, which are the common and distinct features between NBS cells and their non-diseased counterparts and if they are maintained after massive regulatory changes which occur during cellular reprogramming. There were different regulatory changes in both analyses, NBS fibroblasts and NBS-8-iPSCs but there were also overlap of pathways, indicating NBS specific traits in cell cycle and cancer. But also apoptosis and p53 were reviewed, to enable comparison of NBS footprints between somatic and pluripotent cells.

Even though the cell cycle was significantly regulated in NBS-fibroblasts and NBS-iPSCs, there is almost no overlap between the single genes in this pathway (Figure 41 on page 117, Figure 54 on page 146). In NBS-fibroblasts was a high frequency of down-regulated genes, but in NBS-iPSCs was a balanced frequency of up- and down-regulated genes. Specifically up-regulated in NBS-iPSCs were MYC, SKP2, CCNH/CDK7, WEE1, PPTG1, STAG2, CDC23 and CDC25C. The few up-regulated genes in NBS-1-3-5-7 were specific to them and are called EP300, YWHAE (14-3-3), CDC14B, CCND2/CDK6 and GADD35B. What seemed especially targeted in fibroblasts were the cyclins and CDKs, whereas in iPSCs the regulation of E2F proteins and their dimerization partner seemed most consistent. CCND2 was extremely up-regulated in NBS fibroblasts (NBS-1-3-5-7: 12-fold; NBS-8: 100-fold), in control cells the gene was on the border to non-expression. CCND2 was down-regulated in NBS-8-iPSCs compared to their parental cells, but not in comparison to ESCs.

Interconnecting pathways that are involved in cancer supporting processes were found significantly regulated in both cell-type scenarios. Even though the specific gene regulation differed greatly, the frequency of regulated genes for several processes was similar (Figure 45 on page 124, Figure 55 on page 147). Under present factors which are involved in sustained angiogenesis, only VEGFA is shared, others even changed their orientation of regulation like HPH (EGLN), Enlongin B (TCEB2). Overall, that process was rather represented by up-regulated genes in both cases. Factors that result in evading apoptosis are mostly related to PI3K-AKT and JAK-STAT signaling. Those processes were more affected in NBS fibroblasts than in NBS-8iPSCs, but showed overlap in expression of Survivin (BIRC5) and NFKB1. Proliferation is mostly affected by cell cycle related genes and was discussed above. Other processes modulating proliferation were not overrepresented. Tissue invasion and metastasis were little affected in NBS-iPSCs except for down-regulation of Wnt-genes and up-regulated frizzled-genes. Wnt-signaling was more affected in NBS-fibroblasts, where frizzled, GSK-3ß, ß-catenin and Axin were regulated. Failed repair of genes was more represented by up-regulated genes in NBS fibroblasts. Insensitivity to anti-growth signals and ge-

nomic damage by carcinogens was only targeted by genes in NBS fibroblasts. Cytokines and receptors were differentially regulated in both analyses (ECM, TGFA, KITLG, FGFs, WNTs, FLT3LG), but without overlap in distinct genes.

Even though endocytosis was significantly regulated in NBS-8-iPSCs and lysosome was significantly enriched in NBS fibroblasts, they can be regarded as similar biological background, because endocytosis is needed to form lysosomes. In fact, several genes in endocytosis were regulated in NBS fibroblasts as well, but did not significantly enrich in DAVID analysis. Overlapping with NBS-8-iPSCs were the genes for E3 ligase, ArfGEF and endophilin.

Apoptosis was extensively regulated in NBS fibroblasts in the area of adapter proteins in ligand induced apoptosis. NBS-8-iPSCs on the other hand, only down-regulated genes were found, except for 3-fold up-regulated FLIP (CFLAR). BID, CASP6 and NFKB1 were down-regulated in both cases.

Similar to apoptosis, in NBS fibroblasts the TP53 pathway was strongly enriched in regulated genes with similar frequency of up- and down-regulated transcripts. NBS-8-iPSCs showed only down-regulated genes, except for 2-fold up-regulated Noxa (PMAIP1). BID, p53R2 (RRM2) and Cyclin E (CCNE) were down-regulated in both cases (see Figure 57 on page 231Figure 58 on page 232Figure 59 on page 233).

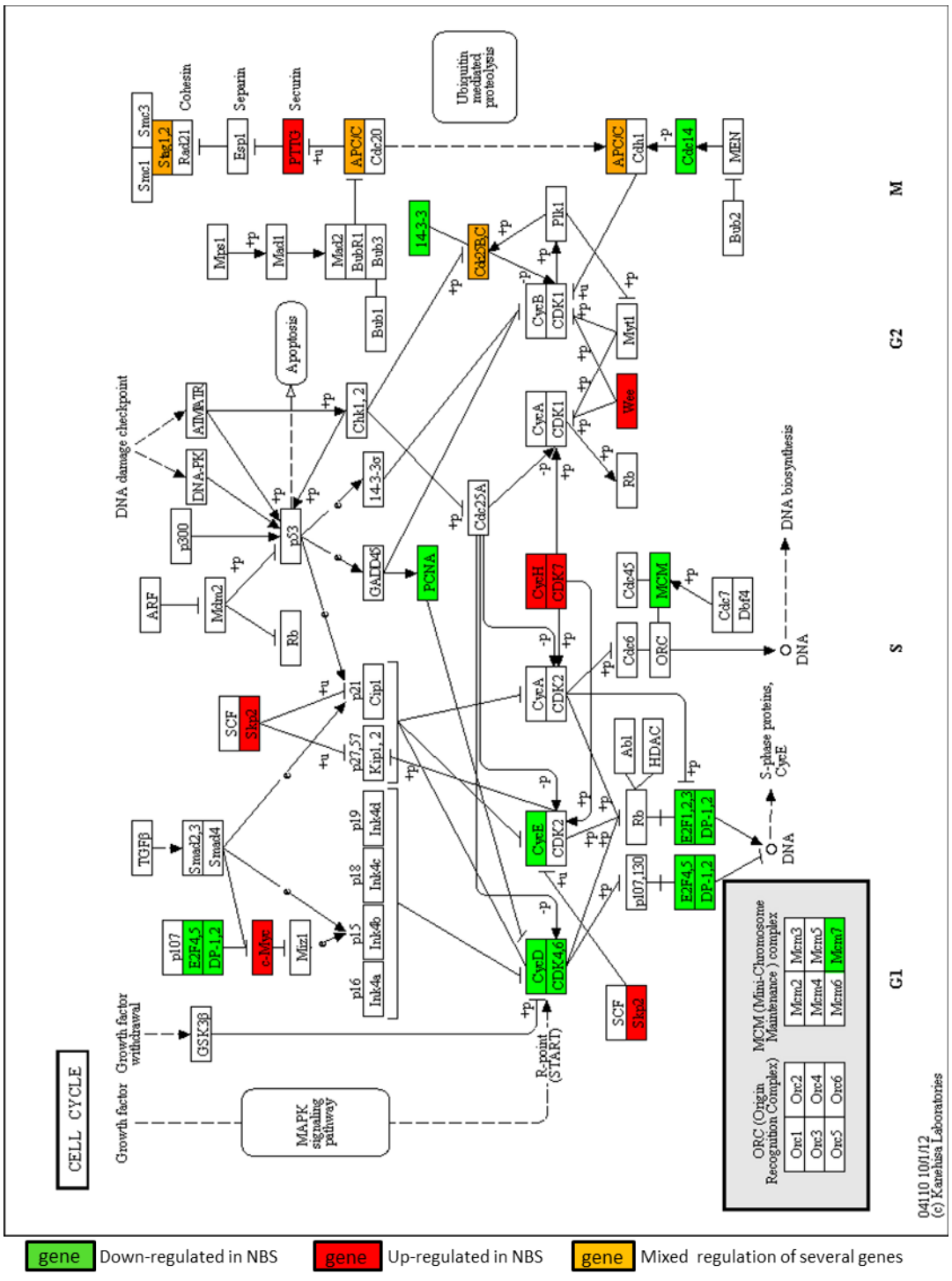

Figure 54: **Regulated genes of cell cycle pathway in NBS iPSCs**
The DAVID output shows regulated genes in cell cycle signaling using KEGG pathways. Regulated genes are selected by diff. p-value $\leq$ 0,05 and $\geq$ 1,5fold ratio. Expression levels of NBS iPSCs relative to normal hESCs are indicated by green and red boxes for decreased and increased expression respectively. Some boxes represent several genes, so in some cases up-regulated and down-regulated are found together in the same box, which is indicated with orange color.

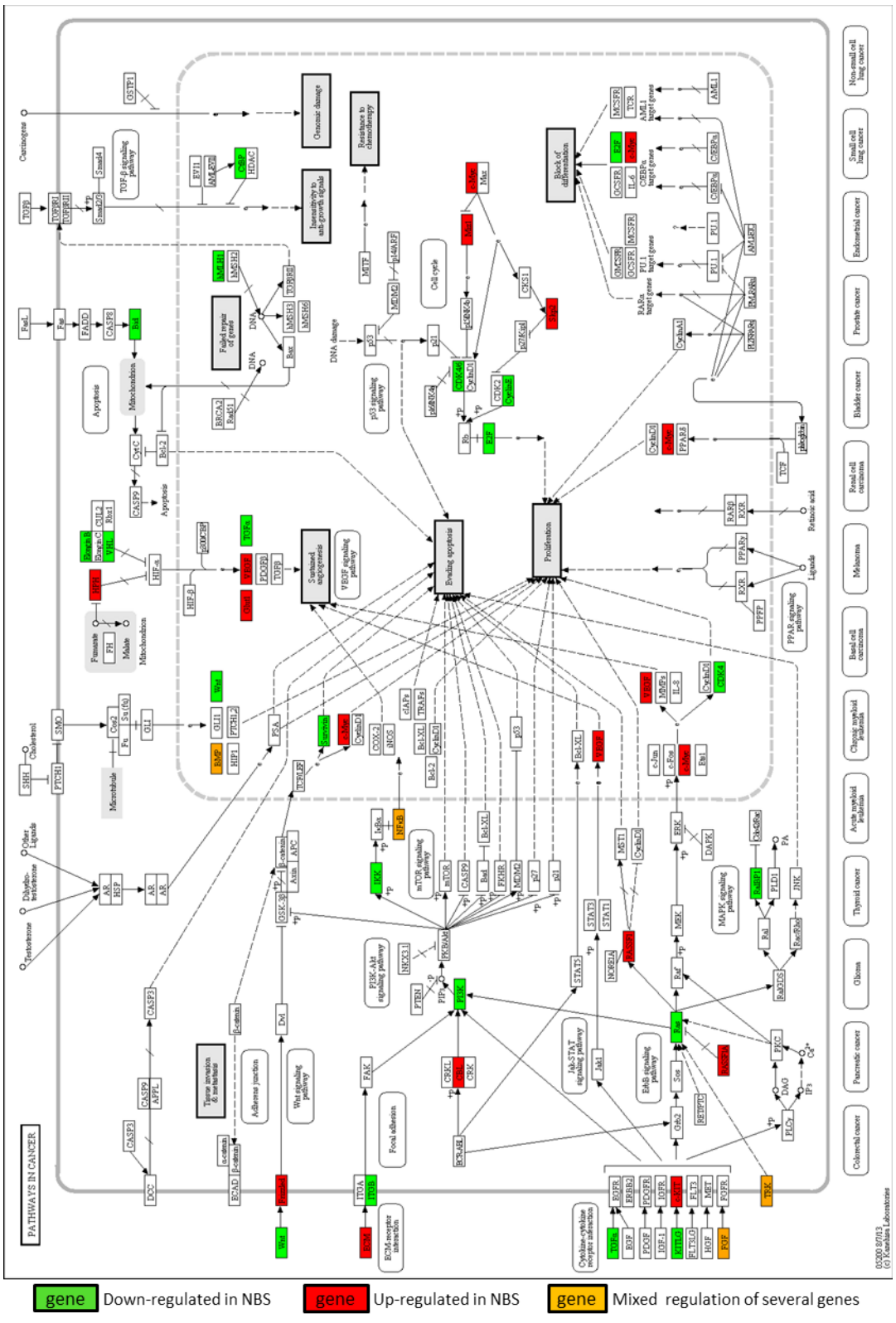

Figure 55: **Regulated genes of cancer related pathways in NBS iPSCs** The DAVID output shows regulated genes in cancer signaling using KEGG pathways. Regulated genes are selected by diff. p-value $\leq$ 0,05 and $\geq$ 1,5fold ratio. Expression levels of NBS iPSCs relative to normal hESCs are indicated by green and red boxes for decreased and increased expression respectively. Some boxes represent several genes, so in some cases up-regulated and down-regulated are found together in the same box, which is indicated with orange color.

3.5.2.7 *Summary of the findings for global transcriptome analysis of NBS-8 iPSCs*

Global transcriptome profiling was performed in order to illuminate the intrinsic regulatory mechanisms which are affected in NBS cells. The focus was set on pathways which enriched in significant regulated genes. It was found, that NBS cells, reprogrammed towards pluripotency, shared common transcriptional regulations with their parental and other NBS cell lines. To those pathways belonged the cell cycle, cancer, endosome/lysosome and a few genes in circadian rhythm. Shared regulations were also found on single gene level, like VEGF and E2F1, which were affected in all tested NBS samples. Cluster analysis showed that the reprogrammed NBS cells were highly similar to hESCs. PluriTest, a tool for assessing the pluripotency of cells was used to confirm a high level of pluripotency and close relation to hESCs in other labs. A comparison of all expressed genes in NBS-8 iPSCs and fibroblasts against hESCs and normal fibroblast was performed to identify NBS-specific genes. 41 genes were found to be exclusively expressed in the NBS-8 patient. Some of them might be candidates for NBS specific regulated genes.

Part IV

DISCUSSION

4 DISCUSSION

4.1 CHARACTERIZATION OF CELL LINES

4.1.1 *NBS Patient-derived Fibroblasts Lack Full-length NIBRIN*

For this study, 8 fibroblast lines from patients with NBS were obtained and compared to control cells (HFF1) in terms of proliferation and morphology. Several NBS lines proliferated slowly and exhibited a high frequency of senescent-like cells. 3 lines appeared similar to HFF1 cells with respect to proliferation (NBS-3, -5 and -8; see Section 3.1, 3.3.1 and Figure 28 on page 87, A). This variation could be explained by patient individual proliferation, passage number or a patient specific NBS phenotype. Most of these features are commonly known to occur in cells that are derived directly from a subject, also known as primary cells.

It is clear that the age of cultured cells depends on the age of the patient, but also on the time the cells aged outside the patient in a cell culture dish, which is mostly characterized by the number of passagings. Primary cells reach their Hayflick limit because of several reasons, mostly by the shortening of telomeres but also by other reasons, like accumulation of mutations within the genome and mitogenome (HAYFLICK, 1965). There was evidence that fibroblasts from NBS patients age faster than neonatal fibroblasts from healthy donors judged by the loss of NBS cell lines in early passage numbers or the higher frequency of senescent-looking cells. The occurrence of senescence in NBS cells should be studied further, e.g. by staining the cells with β-Galactosidase, a well-known marker for senescence. This could also lead to a better understanding of premature aging which is one characteristic of NBS. Premature senescence is also one of the major obstacles in this study, because it limits the number of experiments that can be done with one particular cell line and possibly also blocks the process of reprogramming the cells to pluripotency. For example, most reprogramming protocols need dividing cells with low TP53 levels to bring the cells through the process (Marión *et al.*, 2009). One possibility to circumvent senescence is to establish an immortalized cell line from primary cell material. It requires random mutations or can be induced by virus-mediated delivery of telomerase to artificially increase the length of telomeres. The latter one was tried on two NBS cells lines (NBS-3 and 5), but with no success (data not shown). This method also has the disadvantage of random integration of exoge-

nous DNA which can have unpredictable effects and influence future studies.

The most frequent mutation in the NBN gene is 657del5 and causes truncation due to the creation of a premature stop codon. In addtion, the mutation causes an alternate ribosomal entry site which results in the translation of a second NBN fragment (Maser *et al.*, 2001a). This might be also the reason for the high frequency among other possible mutations, because null or missense mutants of NBN are lethal (Zhu *et al.*, 2001). Other mutations in the NBN gene are known (Chrzanowska *et al.*, 2012), but not all cause a similar phenotype like NBS. In the 657del5 mutation variant, the longer NBN fragment is missing the FHA and one BRCT domain (see Figure 3 on page 5) and still retains many of its original functions. The shorter version consists only of the FHA and the first BRCT domain and its function is not explicitly described so far. In this study, the 657del5 mutation was confirmed by PCR and sequencing and the lack of full-length NBN expression was confirmed by western blot detection (Figure 17 on page 58). The shorter versions of NBN were not detected which could be explained by the specificity of the employed antibody. According to the manufacturers website (Biologicals, 2011), a partial length human NBS1 protein was used as immunogen for rabbit whole antisera. If the immunogen only encompassed the N-terminal region (eg, aminoacid 100-143) of NBN, it cannot detect the p70 variant. Other groups raised their own antibodies to detect p70 and p26 NIBRIN (Maser *et al.*, 2001b,a). According to Maser et al. (2001), p70 NBN was found in NBS LCLs but not in NBS fibroblasts, but the mechanism remains unclear. There are only few publications with reported p70 expression, eg. chicken B cell line DT40 (Nakahara *et al.*, 2009), and even fewer in fibroblasts (eg. 1 NBS patient with little p70, one without in (Yanagihara *et al.*, 2011)). One reason for low or absent p70 could be inefficient translation due to secondary mRNA structures close to the internal ribosomal entry site. Further tests should clarify if p70 expression is exclusive in certain cell types and if NBS-iPSCs are among those. So far, there is nothing known of the effect of p26 NBN on the cell and repair mechanism. Since it is detected in most NBS cell lines, it is possible that it is folded in its proper domains, FHA and BRCT. Both domains are common in many DNA repair mechanisms and it would be possible for such a peptide to interfere with this mechanism.

The NBS-8 patient was heterozygous for the founder mutation, but lacked full-length NBN on protein level (Figure 17 on page 58). This was tested in fibroblasts and their respective iPSCs. It is possible, that there is a mutation in NBN of the second allele, inhibiting either expression or translation. There is only 50 % NBN mRNA expression in the patient compared to wild-type cells (Figure 24 on page 75, A) indicating that one of the NBN gene copies could be silenced, which can

be caused e.g. by a mutation in NBN promoter. For confirmation, the whole NBN, including some area up- and downstream of the gene, has to be sequenced.

4.1.2 *Fibroblasts from Patients with Nijmegen Breakage Syndrome Can Be Reprogrammed towards Induced Pluripotent Stem Cells (iPSCs)*

4.1.2.1 *General remarks on stem cell culture*

The initial goal of this project was to bypass senescence and use the resulting pluripotent cell lines as a model system for studying disease mechanisms. Based on publications of iPSC-generation from other diseases like FA (Müller *et al.*, 2012b,c), reprogramming of NBS cells was anticipated to succeed only under the aid of exogenous expression of wild-type NIBRIN. As observed from culturing NBS fibroblasts, these cells senescence much faster than the reference HFF1 cells and also showed an abnormal passage through the cell cycle (Figure 28 on page 87).

Of four distinct NBS cell lines, only one was reprogrammed successfully. Because the general aim was realized, reprogramming in combination with ectopic expression of wild-type NIBRIN was not pursued further. But the reason why only one of five lines succeeded should be further evaluated. The most likely reason could be the early passage number, as all other cells, which also came from primary sources, were already passaged for more than 5 times and in addition, at least frozen and thawed for two times. In addition, they already showed evidence of senescence during normal culturing. Evidence of full-length NBN translation was not found, but the only successful reprogrammed cell line was heterozygous for the 657del5 mutation. There might be additional mutations in NBN preventing expression or translation. But this was not tested. As there are reports on selective expression of NBN in different cell types (Yanagihara *et al.*, 2011), it cannot be 100 % ensured that small amounts of NIBRIN enabled reprogramming.

Reprogramming cells is difficult because some labs struggle with the expensive maintenance costs of stem cells and this new technology is not performed by standard procedures, yet. The methods are rather adapted to each different cell type and aim. Another limitation is the cytokine supplementation in the stem cell medium, which is important and has to be kept constant. This can be a challenge if self-made conditioned medium (CM) is used to replace defined medium for economic reasons, because CM quality can vary from batch to batch.

Reprogramming NBS cells is especially difficult because the stress of the procedure can induce TP53 signaling and promote senescence. Evidence for TP53 activation in NBS cells was found by global transcriptome analysis (3.5.1). Another roadblock in reprogramming NBS

cells is gene integration of O/S/K/M, which requires DNA recombination. This process is impaired in NBS cells and the cells already showed impaired proliferation, which is disadvantageous for retroviral infection and reprogramming. A recent publication showed that there is still much to be uncovered in order to understand the mechanistic of reprogramming. They achieved a near 100 % reprogramming efficiency by knock-out of a single gene, MBD3 (Rais *et al.*, 2013). If this can be used to improve reprogramming protocols, also cells, which are difficult to reprogram might succeed.

Here, three different approaches were used for delivery of the transcription factors O/S/K/M for induction of pluripotency: retroviral transduction 3.1.2.1, expression from episomal plasmids 3.1.2.2 and transcription factor proteins itself, tagged to a cell-penetrating peptide 3.1.2.3. The retrovirus approach resulted in two stable iPSC-lines and the episomal approach generated one iPSC-colony in control fibroblasts (HFF1) which was lost after several passages. The cell-penetrating proteins did not result in any reprogrammed cells and were found not to accumulate in the nucleus as expected because they apparently failed to penetrate the cells.

4.1.2.2 *Comparison of reprogramming methods*

Since the first reports on reprogramming somatic cells to pluripotency in 2006 by Takahashi and Yamanaka (Takahashi *et al.*, 2007; Takahashi & Yamanaka, 2006) a lot of research has been published based on this method. Many focused on finding alternatives to viral-based methods, improving the efficiency or resolving the mechanism underlying the reprogramming process (Tavernier *et al.*, 2013). While all of this directions are important, this study focused on non-integrating alternatives of O/S/K/M delivery in context to make the resulting iPSCs potentially clinical relevant.

Viral delivery is the most robust method up to today, but integration of exogenous DNA into the host genome has several disadvantages. Most importantly, the integration happens randomly and can cause disruption or misregulation of host genes. Furthermore, the copy number of the reprogramming factors is random as well and can result in partial reprogrammed cells that have to be distinguished from fully reprogrammed cells by a complex evidence trail. Integration of the four factors leads to their stable expression which supports the reprogramming process, but it has been shown that viral-based genes are not always silenced, or can be even reactivated (Kane *et al.*, 2010), which limits down-stream experiments like differentiation.

Therefore it is necessary to look for alternative methods to induce pluripotency. One of the approaches uses sendai virus, a non-integrating, single-stranded RNA virus, to deliver O/S/K/M to target cells (Fusaki *et al.*, 2009). The advantage is clear, but the use of sendai virus is still considered a risk class II (§ 3 Biostoffverordnung; http://www.gesetze-

im-internet.de) virus and in addition, showed low reprogramming efficiency. There are also a multitude of DNA-transfection based systems like minicircle DNA (Jia *et al.*, 2010), plasmids (Okita *et al.*, 2008) and episomes (Lin *et al.*, 2009) or RNA-based systems like mRNA transfection (Warren *et al.* 2010; Drews *et al.* 2012), or microRNA (Anokye-Danso *et al.* 2011; Lin *et al.* 2008; Miyoshi *et al.* 2011). They are considered low risk for integration events and only stay transiently in the cell. But also here efficiency is a huge problem. For this study, the episomal approach was tested to reprogram NBS and HFF1 cells according to a detailed publication on this matter (Yu *et al.*, 2011, 2009). As described in the results (see 3.1.2.2), only HFF1 fibroblasts were reprogrammed to iPSCs, however NBS-8 fibroblasts repeatedly failed, even though the process was assisted by supplementation of small molecule inhibitors: MEK (PD0325901) pathway, GSK3beta (CHIR99021) pathway and TGF-beta/Activin/Nodal-receptor (A-83-01). It was anticipated, that the episomal approach might even work better in NBS cells than the retrovirus, because it does not require integration into the host genome. Retrovirus use DSB repair enzymes for integration (Sakurai *et al.*, 2009) which ae disordered in NBS cells. Sakurai et al, showed that ATM and DNA-PKcs had more impact on transduction efficiency of HIV than NBN and MRE11, but also observed variable results from different types of retrovirus. The reason for failure of episomal-based reprogramming of NBS cells remains unsolved. Probable reasons are stress-intolerance caused by the transfection method (electro-nucleoporation), an abnormal cell cycle preventing maintenance of the plasmids, a late passage number of the cell line, or resistance to electroporation by modified ECM (extracellular matrix) (it was observed that NBS-8 cells were more difficult to trypsinize than HFF1 cells). Overall it could be a combination of moderate factors that simply reduced the reprogramming efficiency to a rate, so it did not succeed in the limited number of experiments performed.

Another alternative to viral-based reprogramming is the use of O/S/K/M recombinant proteins. The proteins are simply added to the medium and get absorbed by the cell due to a short cell-penetrating peptide, which is fused to the transcription factors (O/S/K/M). They are transported into the nucleus by a nucleus localization signal that is already present in the natural sequence of the transcription factors. Advantages of reprogramming with cell-penetrating-proteins are, that there is no transfection required (which is time consuming and stressful for the cells). The medium just has to be supplemented with the proteins and combination and concentration can be varied anytime throughout the process. This could improve reprogramming protocols to a point where they can be adjusted to maximum efficiency for any cell type. In addition, ratios of O/S/K/M to each other can be varied and it was shown before that distinct ratios of O/S/K/M can

influence the efficiency of reprogramming (Papapetrou *et al.*, 2009). On the other hand, transcription from an unknown number of transfected or transduced vectors leads to an uncontrolled expression ratio of the reprogramming factors. By employing recombinant proteins there will be no integration of exogenous material into the genome. Instead it permits xeno-free reprogramming, which will be interesting for clinical applications of iPSCs. Disadvantages of this method are the low efficiency and also the costs and time to generate the recombinant proteins. In addition, the construction and purification of the proteins might still require some advanced bioengineering before it reaches a maximum in availability for the cells. Here, this method was especially chosen as an alternative to *in vitro*-derived O/S/K/M mRNAs, because mRNAs require multiple transfections. From other studies it was known, that exogenous ssRNA activates immune responses which can induce apoptosis in cells and also decreases mRNA stability (Kawai & Akira, 2007; Diebold *et al.*, 2004). But a recent publication by (Lee *et al.*, 2012), describes how activation of a special kind of the innate immunity, namely by TLR3 stimulation, causes chromatin remodeling that supports reprogramming by recombinant proteins. PolyI:C (Poly-iosinic-polycytidylic acid), a synthetic analog of dsRNA was used to stimulate TLR3 and was also used in this study.

Several groups found a connection between immunity and reprogramming, whether it was supporting the process or not. My group did transcriptional profiling on reprogramming events as early as 24, 48 and 72 h post retrovirus transduction and found activation of the innate immune response in combination with "oxidative stress", "apoptosis", "proliferation" and "cell cycle", but not after plasmid transfection, suggesting viral responses as an early reprogramming roadblock (Mah *et al.*, 2011). With reference to mRNA delivery, it is clear that immune response has to be minimized in order to achieve notable reprogramming efficiencies (Drews *et al.*, 2012; Warren *et al.*, 2010).

Lin *et al.* found in 2008, that not only mRNA can be employed to reprogram somatic cells but also ectopic expression of the embryonic microRNA cluster, mir-302, can generate pluripotent cells. Two other groups adopted this strategy in 2011 and extended mir-302 by the mir-369 family (Miyoshi *et al.*, 2011; Anokye-Danso *et al.*, 2011).

Where all above mentioned publications and others were highly methodical and were mostly aimed at the generation and efficiency of iPSCs, it also generated a better understanding to the mechanistics of the reprogramming process. Several pathways and enzymes were discovered which supported reprogramming when inhibited by small molecules (Li *et al.*, 2009; Lin *et al.*, 2009; Yu *et al.*, 2011). A few of them are: MEK inhibitor (PD0325901), GSK3b inhibitor (CHIR99021), TGF-b/Activin/Nodal receptor inhibitor (A-83-01), human leukemia in-

hibitory factor (hLIF), ROCK inhibitor HA-100, FGFR inhibitor (PD173074) (Ying *et al.*, 2008), G9a histone methyltransferase inhibitor (BIX-01294) (Shi *et al.*, 2008), histone deacetylases (HDACs) inhibitor (valproic acid) (Huangfu *et al.*, 2008) and others. As some of these molecules were used to replace one of the reprogramming factors (eg. (Ichida *et al.*, 2009)), it is possible, that reprogramming can be achieved by the sole application of small molecules in the future.

A recent publication showed a very different approach in the attempt to reprogram somatic cells to pluripotency. Obokata et al. showed that CD45+ lymphocytes from postnatal mice spleens can acquire pluripotency by a sub-lethal acid-bath and called them "stimulus-triggered acquisition of pluripotency" (STAP) cells (Obokata *et al.*, 2014b). The method was discussed controversially, because several labs failed to reproduce this data and Obokata had to retract two papers due to inconsistencies (Obokata *et al.*, 2014a). But still, there is evidence that at least some of the methodical part of this research was true and provides a chance to learn more about the process. In addition, it also got many researchers all over the world to try and modify this relatively simple and cheap method to reprogram cells, so there might already be an improved version in the making. The idea goes back to research in 1947 by Holtfreter (HOLTFRETER, 1947), who found that amphibic embryonic cells can be forced to differentiate into cells of one germ layer or another, simply by different pH environments.

So far, an optimized method for efficient reprogramming is yet to be found. Maybe several approaches have to be combined, or methods have to be adapted to the different cell types. But it is clear that the methods must eliminate the use of virus and preferably exogenic DNA as well, in order to become clinically relevant. In addition to efficiency, also the safety and control of iPSCs in terms of genomic and epigenomic integrity and efficient differentiation protocols are necessary. A more detailed description of reprogramming methods is given in my review "Current Methods for Inducing Pluripotency in Somatic Cells" (Tavernier *et al.*, 2013).

4.1.2.3 *Characterization of reprogrammed lines*

Reprogramming is still a very inefficient process with efficiency rates ranging from 0,0001 to 0,002 % for most methods and cell lines (Hasegawa *et al.*, 2010) and with only one positive exception (90 % by MDB3 knockout (Rais *et al.*, 2013)) to date. The fact, that there is always a mixture of different cells in the dish during the reprogramming process, consisting of the original somatic cells, partially reprogrammed cells, iPSCs and others that might gone a complete different direction or acquired mutations, makes it necessary to isolate and control the quality of the obtained iPSCs. This is accomplished by morphologic characterization and other experimental methods like immune-

fluorescence-based detection of alkaline phosphatase (AP) and other pluripotency markers, fingerprinting PCR, embryoid body differentiation, teratoma formation in live mice and also the epigenetic profile of the cells. For the acquired iPSCs made from NBS-8 and HFF1 fibroblasts in this study, all requirements were met to be accepted as such by other scientists in this field (see 3.1.2.4). Because the cells were reprogrammed by retrovirus and in addition, showed some genetic aberrations, they cannot be considered for clinical use, but can be employed as a tool to study the disease or for drug testing. The current methods which are used to compare iPSCs with hESCs are suitable to describe their high similarities, but there are differences especially in the epigenome (Nishino *et al.*, 2011; Müller *et al.*, 2012a), which questions the predictability of iPSCs in differentiation experiments and potential clinical applications. In the future, quality control for iPSCs has to be fast, cheap, high-throughput, automated, reproducible in all labs and also has to encompass genetic profiling. Most likely this can be achieved by bioinformatic means as this technology is evolving quickly. It would also have the benefit, that this kind of data is less likely used for broad interpretation as it can happen with e.g. cell stainings. It can happen that publications show only one unspecific stained cell as proof (which is easily missed in the reviewing process) or that AP staining is used as only proof for stemness, neglecting the fact that AP is not only expressed in stemcells (Moss, 1982). A very promising quality control could be a combination of a transcriptional profile like pluritest.org with a full genome sequencing to cover both the dynamic status of the cell and its genetic stability.

The iPSCs generated in this study passed all sufficient tests for pluripotency, but also some anomalies were noted. E.g. in some cases pluripotency factor staining was not evenly distributed over the colony like e.g. SOX2, or NANOG in Figure 23 on page 73. Interesting for SOX2 is the specific expression at the outmost borderline and the low expression between the middle and the border. This is evidence, that iPSC-colonies are not as homogenous as they look from morphology, but might also be regulated by gradients in their microenvironment. As there were both forms of colonies, homogenous expression of pluripotency markers and uneven distribution, it raises the question, if this is a normal phenomenon in the expression of pluripotency genes, or if there are quality differences in a monoclonal culture of iPSCs. As this is merely an observation which apparently does not disturb the overall pluripotency statement, it was difficult to find similar cases in the literature. At least it is evidence, that not everything that looks like a pluripotent stem cell, fulfills all the characteristics of a stem cell.

It might even relate to a general fluctuation problem in pluripotency and homogeneity that occurred during hESCs and iPSCs culturing, which might be explained by general cultivation procedures. To

passage the colonies, they had to be broken down to small cell aggregates, small enough to attach again, but big enough to gain a survival support by paracrine signaling of their neighboring cells. During this passaging process, only a small part of cells survived, attached and formed new colonies. The resulting number of surviving colonies was also subjected to big variations and limited the size and possibility for uniform repetitions of experiments. The use of conditioned medium (CM) is in preference to defined medium for economic reasons and enables the cultivation of hESCs and iPSC without feeders, which is important for most experiments that require pure material. But ESC-growth-supporting cytokines in self-made conditioned medium can fluctuate and cannot be monitored precisely. Only the concentration of Activin A, one of the major cytokines, was monitored after each charge of produced CM. The cytokine fluctuations were believed to be responsible for reduced colony survival and quality. It seemed, that with each new charge of CM, the cells first had to adapt to the changed composition for 2-3 weeks before they became stable again. This was the reason, that experiments could be only performed on occasions in between different CM charges and limited the number of overall experiments.

In vitro cultivation of hESCs is always different from *in vivo* conditions because the microenvironment has high impact on gene expression. Also, embryonic stem cells (*in vivo*) are not maintained, but are fated to differentiate eventually. Adult stem cells as well grow in a microenvironment and do not grow in a homogeneous cluster, but as few or single cells in a niche among somatic cells *in vivo* (Clevers *et al.*, 2014). Therefore it took some time until hESCs were cultured in a dish and also acknowledged as such (Thomson *et al.*, 1998). Cultivation of hESCs cannot match *in vivo* conditions but it should match it as close as possible. Publications indicated, that tissues which grow *in vivo*, are exposed to oxygen concentrations around 5 %, unlike most mammalian cells which are cultivated at 21 % oxygen *in vitro* (Konigsberg *et al.*, 2013). That means, optimizing physiological conditions for cells *in vitro*, requires reduced oxygen concentration in the incubator to a level around 5 %, but not less, because an oxygen range of 3-1 % O_2 induces hypoxia (Carreau *et al.*, 2011). It was already shown, that low oxygen increases reprogramming efficiency (Szablowska-Gadomska *et al.*, 2011) and genomic stability due to reduced stress by ROS (Tello *et al.*, 2011). During the generation of iPSCs, the original fibroblast cells as well as early iPSC clones were grown in a standard culturing incubator for mammalian cells, with 37°C, 5 % CO_2 and ambient oxygen (21 % O_2). But shortly after reprogramming, oxygen levels were set to 5 % O_2 to approximate *in vivo* conditions and minimize oxidative stress. The radical reaction of NBS-8-iPSCs to a change from 5 % to 21 % and the increased susceptibility to DNA damage at 21 % oxy-

gen in both HFF1 and NBS-8 fibroblasts, confirmed the importance of that culture condition (3.3.2).

Genomic instability is one of the key features of NBS and the reason why most patients die from cancers at early age. Therefore, it was anticipated, that the relatively fast proliferating NBS-8-iPSCs exhibit a high frequency of mutations including genomic aberrations as a result from impaired DNA repair and signaling. In contrast to that theory, NBS-8-iPSCs generated only one aberration in clone 1 and one aberration plus one trisomy in the second clone in passage 29, which relates to approximately 40 weeks of culturing. Also the parental line (reprogrammed at passage 4) which was analyzed for aberrations at passage 12, exhibited only one translocation and that was different from the ones in NBS-8-iPSCs (Figure 25 on page 77). It could be hypothesized, that translocation events result from failed HR which is inhibited in NBS cells. Instead, the cells turn to NHEJ and other repair pathways which are more error-prone than HR (Ohara *et al.*, 2014). This could lead to a higher rate of point-mutations, weak mosaicism, microdeletions or other disorders, which cannot be detected by karyotyping, but would contribute to genetic instability. In future experiments the quality of HR could be measured with STGC (short tract gene conversion) and LTGC/SCE (long-tract gene conversion/-sister chromatid exchange) and mutation frequency could be monitored by full-genome sequencing.

It has to be kept in mind, that aberrations and other mutations can severely affect the phenotype of cells. But in this case there was a high correlation of NBS-8-iPSCs to hESCs, which supports usefulness of the cell line for experimental studies.

4.2 FUNCTIONAL LEVEL

4.2.1 *ROS-induced Damage and Cell Cycle Assays*

The aim of this analysis section was to look for effects of NBN on cell cycle and to measure the impact of oxidative stress and antioxidants on DNA damage in NBS fibroblasts in comparison to NBS-derived iPSCs and control cells. It was found, that cell cycle progression showed abnormalities and that NBS cells are highly susceptible to DNA damage under oxidative stress.

4.2.1.1 *Proliferation-based obervations*

The main aspects of NBS are genetic instability and reduced growth as manifested by shortened body height and microcephaly (Chrzanowska *et al.*, 2012). These effects might be derived from an abnormal proliferation and cell cycle which could be generally effected by truncated NIBRIN. This was confirmed at the transcriptional level (Table 9 on

page 110), but showed mixed result in assays measuring proliferation and cell cycle.

As described in Section 3.1, proliferation of NBS fibroblasts varied depending on patients and not specifically because of the disease influence. This was also solidified by a proliferation assay in the comparison of HFF1 and NBS-8 fibroblasts, which showed no difference in proliferation (Figure 28 on page 87, A). In contrast, the ratio of cells in S/G2 phase in NBS-8 cells after G1 synchronization was different from HFF1 cells. G1 arrested populations contained approximately 90 % cells in G1, which shifted to 51 % after 24 h in log phase in HFF1 and to 23 % in NBS-8 cells. A similar experiment with two NBS lines in comparison to HFF1 cells and over a time course of 67 h showed that fewer NBS cells arrested in G1, than moved with a high quantity through S phase at either 22 h or 47 h and matched cell cycle phases with HFF1 cells after 67 h. Similarly to proliferation, the time cells spend at each cell cycle stage, seemed to depend more on the individual cell line than the disease. On the other hand, global transcriptional analysis of 4 different NBS patient cell lines showed a strong inhibitory effect on cell cycle genes (Figure 40 on page 116). The specifically strong difference in S and G2 phase ratio occurring only in NBS-8 cells (the line which was used for reprogramming, see Figure 28 on page 87), could be explained by either a stronger response to a growth stimulus, ineffective S-phase checkpoint, or triggered G2/M phase checkpoint.

Microcephaly and other defects resulting in decreased cell mass were observed as a phenotype of the disease (Chrzanowska *et al.*, 2012), but it is not yet entirely clear which effect is responsible. Proliferation deficiency specifically, is rarely mentioned in clinical reports on NBS or *in vitro* cultivated NBS cells. E.g. a humanized mouse model of NBS657del5, did not find growth defects in these mice except in testis and ovaries (Difilippantonio *et al.*, 2005). Apart from defects in proliferation, also misregulated apoptosis (TP53 signalling is affected in NBS cells, see 3.5.1.9) or developmental processes could be responsible (Frappart *et al.*, 2005).

Proliferation or apoptotic issues could play a part during developmental processes but might not affect general proliferation. Instead, proliferation might be only affected in a few cells per population where there are cases of unrepaired DNA damage. Statistically, DSB occur as frequent as 50-times per cell cycle (Vilenchik & Knudson, 2003). With this high statistics of possible DSB, and the fact that one unrepaired DSB can be lethal for a cell (Blöcher, 1982) the damage must be repaired in NBS cells somehow, even if HR and NHEJ is strongly impaired in this cells (Howlett *et al.*, 2006). This increases the possibility of less frequent repair mechanisms like MMEJ and alt-NHEJ, which produce small nucleotide errors during the process (McVey & Lee, 2008) in contrast to error-free HR. The shift to MMEJ

might accumulate so many small errors in the long run, that it results in senescence, apoptosis or malignancy. This is also overlapping with the aging theory of Jicun Wang et al, 2011, who describe aging as a consequence of misrepair of DNA (Wang *et al.*, 2012).

4.2.1.2 *Is DNA damage susceptibility dependent on cell cycle phase?*

The measurements of cell cycle and DNA damage can also be viewed under the focus of damage susceptibility in a certain cell cycle phase. Even though (Potter *et al.*, 2002) found no difference between the susceptibility of G1, S and G2/M phase cells to DNA damage induced by gamma-radiation or H_2O_2, or in the rate of repair of this damage, similar to the observations in control cells under 5 % oxygen in this study, the high DNA damage variations for cells at oxygen tension, must be related to different cell phase populations. The experiments under 5 and 21 % oxygen and bleomycin were analyzed at 100 % confluence, where most cells remained at G1 phase and after a 24 h growth phase, where a high portion of cells were caught in S and G2 phase (not shown). It was found, that cell cycle phase made no difference in HFF1 cells at 5 % oxygen but showed higher damage in cells after 24 h growth phase at 21 % oxygen and bleomycin, than at total confluence (Figure 29 on page 89). NBS cells were most susceptible at total confluence (G1 phase) at 21 % oxygen and bleomycin, but the highest damage at 5 % oxygen was at the 24 h growth phase. Interestingly, the lowest damage after bleomycin treatment occurred in NBS cells in the 48 h growth phase, which exhibited a similar cell cycle distribution than the confluent cells. This indicates that cell cycle phase might not be the only factor responsible for different damage susceptibilities. In summary, the results suggest that oxidative tension and S-phase cells are more susceptible to DNA damage in normal cells, but NBS cells are more susceptible in G1 phase. An analysis of the same cells, where each cell cycle was separated and measured for the amount of gamma-H2AX positive cells (not shown), revealed that untreated control cells showed most damage in S-phase, which is likely caused by stalled replication forks. NBS-8 cells on the other hand additionally exhibited strong DNA damage in G2/M phase. After bleomycin treatment the frequency of DNA damage in G1 and G2/M phase was similar to S-phase in both cell lines. But in HFF1 cells S-phase damage was stronger in non-proliferating cells and in NBS-8 cells the amount of S and G2/M phase DNA damage was higher than in G1 in all cases. So, NBS cells not only show a higher total susceptibility to DNA damage but they are particularly sensitive in the proliferative phases. As the experimental set-up consisted of 6 hours total time of treatment, including 2 hours release from the damage-inducer bleomycin, the question remains, how many cells were measured because they arrested or moved into a particular cell cycle phase, or how much impact the time for repair had caused. To

resolve this, future experiments where measurements immediately after and several time points later from bleomycin treatment should be performed. The cell cycle phase effect could also be related to the repair choices of the cell as e.g. it was shown that homologous recombination preferentially repairs DNA double-strand breaks in the S phase of the cell cycle in human cells (Saleh-Gohari & Helleday, 2004).

4.2.1.3 *Relationship between ROS levels and DNA damage*

ROS can basically oxidize all components of the cell, from proteins to lipids and RNA. But the most dangerous damage is caused by DNA oxidation, which often results in 8-oxoguanine (8-oxoG), but can also result in DSBs. These DSB, arising from SSBs after oxidization of the sugar backbone are in particular difficult to repair, because they do not have a "clean" ending (Woodbine *et al.*, 2011).

Long ago, a theory was established, that links oxidative stress with aging through accumulation of DNA damage (Schulz *et al.*, 2007; Harman, 1981; Bernstein & Bernstein, 1991; Sohal & Weindruch, 1996). That is why there are so many potions, creams, etc. on the consumer market, claiming that antioxidants as part of the composition slows the aging process. While there is direct link between ROS and aging, the answer is not that simple, because ROS has also important biological functions like antiviral defense mechanism (West *et al.*, 2011), signaling of cell cycle progression and others (Havens *et al.*, 2006; Burdon, 1995; Sauer *et al.*, 2001). Therefore, it should be considered not to achieve elimination of ROS, but obtaining an optimal ROS balance as e.g. postulated by theory of caloric restriction (Sohal & Weindruch, 1996). As NBS patients are very susceptible to genetic instability, a clinical approach to prolong life span of those patients could be a more balanced ROS homeostasis. To address this, I tried to identify antioxidants with the best ability to decrease DNA damage under stress conditions. A screening was carried out on NBS-8-iPSCs for the antioxidants L-NAME, gallic acid (GA), Disulfiram (DSF), hydroxyl tyrosol (HT), vitamin B5, EDHB, vitamin C and glutathione. The most effective reduction of ROS levels was observed with DSF and EDHB (Figure 31 on page 91, C). One study (Gatz & Wiesmüller, 2008) found, that the well-known antioxidant resveratrol which is also studied for its possible use in cancer therapy and anti-aging, surprisingly inhibited HR and NHEJ and additionally MMEJ in NBS lymphocytes in an ATM/ATR–NBN dependent manner. With respect to NBS, the destabilizing effects on DNA by resveratrol (Stopper *et al.*, 2005) would maybe outweigh the anti-oxidative protection. There is a broad spectrum of antioxidants used as prevention of DNA damage and aging which were analyzed elsewhere and could be suited for treatment of NBS patients as well. Most of these substances were tested as dietary supplementation in animal models: polyphenol-rich strawberry

extracts (Giampieri *et al.*, 2014); butylated hydroxyanisole (BHA) and oltipraz (Lawson & Stohs, 1985); melatonin (Reiter, 1997); β-carotene, α-tocopherol and ascorbic acid (Zhang & Omaye, 2001); selenium (Waters *et al.*, 2003); Vaccinium ashei berries (Barros *et al.*, 2006); fermented papaya (Aruoma *et al.*, 2006); hyaluronate (Zhao *et al.*, 2008); synthetic nitrogen compounds and quercetin (Silva *et al.*, 2009); hermetic levels of Curcumin (Lima *et al.*, 2011); salidroside (Mao *et al.*, 2010); N-acetyl-L-cysteine (NAC) (Gu *et al.*, 2011; Liu *et al.*, 2012). But there were also studies following a similar approach like this report: Pascucci B. et al. (2012) described cockayne syndrome cells to be hypersensitive to oxidative stress. But the addition of an antioxidant in the culture medium was able to partially rescue alterations in intracellular ROS content, oxidative DNA damage, and metabolic profile (Pascucci *et al.*, 2012).

Here, two substances, DSF and EDHB, proved to be potent for decreasing intracellular ROS levels and partly, also DNA damage in NBS cells. Their mechanism of action remains speculative as not much is known of these substances. DSF was originally used in alcohol use disorders, but is also used as an anti-tumor therapeutic (Brüning & Kast, 2014). But it is also known to inhibit DNA methyltransferases (Paranjpe *et al.*, 2014), the proteasome (Cvek & Dvorak, 2008) and supports an oxidized environment (Nagendra *et al.*, 1991; Paranjpe & Srivenugopal, 2013), which all contradict DNA protection. But Nemavarkar P. et al (2004) screened for antioxidants as radioprotectors in yeast cells and found that DSF decreased DNA damage at 100 µM (Nemavarkar *et al.*, 2004). A possible explanation for my results would be a hormetic effect of DSF which efficiently induced the intracellular antioxidant defense system. It is also possible that DSF interfered with the hypoxic pathway as noted in Park HJ. et al (2013) where DSF (0.3 to 2 µmol/L) inhibited hypoxia-induced gene expression and HIF activity in a dose-dependent manner (Park *et al.*, 2013). The hypoxia pathway is also targeted by EDHB, which is a prolyl-hydroxylase inhibitor (Sasaki *et al.*, 1987) which in turn leads to induction of the hypoxic pathway by accumulation of HIF1-alpha (Li *et al.*, 2008). EDHB can also be used to enhance cellular reprogramming by promoting the shift from oxidative phosphorylation (high oxygen tension) to glycolysis (low oxygen tension) (Prigione *et al.*, 2014). A low level of oxidative phosphorylation is a characteristic of hESCs (Prigione & Adjaye, 2010) which require an optimal stable environment for maintanance of DNA integrity. The same system may therefore also benefit NBS cells when the glycolytic shift is mimicked by EDHB. To substantiate this theory, metabolic assays should be performed in the future. In summary, it was shown in NBS cells, that genomic stability is influenced by an oxidative environment which was stabilized by the two small molecules DSF and EDHB. Both tar-

get the hypoxic pathway, but it is uncertain that this is the mechanism of action in NBS cells.

4.2.1.4 *Comparison between hESCs and somatic cells*

NBS is rare disease and therefore there is only limited access to tissues for experiments. In the past, studies were limited to observations in patients or *in vitro* cultures of cells from patients, mostly fibroblasts or lymphocytes. To escape the dependence on patients, humanized mouse-models were introduced (Difilippantonio *et al.*, 2005), but of course there is a limit on the comparability to human physiology and pathway signaling. *In vitro* cell culturing of NBS cells has a disadvantage which is deduced directly from the features of the disease, which is genomic instability and aging. Cells from patients therefore often acquire additional mutations or become senescent, limiting and interfering with the studies. By reprogramming somatic cells from NBS patients to iPSCs, senescence was circumvented and also de-novo aberrations were minimal, even after long-term culturing. Treatment with antioxidants and low-oxygen (5 %) culturing could even further reduce risks of genetic instability and enable reproducible studies on this disease. Here, I started discriminating differences between NBS fibroblasts and iPSCs by analysis of their sensitivity towards ROS and DNA damage (Figure 32 on page 95, Figure 33 on page 98). Interestingly, NBS fibroblasts reacted differently to stress than iPSCs when compared to their healthy counterparts. NBS fibroblasts showed higher DNA damage than HFF1 cells when stressed with H_2O_2 or bleomycin, but NBS-iPSCs showed the same level of DNA damage as hESCs (Figure 33 on page 98). The difference between fibroblasts and stem cells became also visible when the cells were treated with EDHB. EDHB almost completed protected fibroblasts (HFF1 and NBS) from DNA damage caused by oxidative stress and approx. 20 % from damage by bleomycin. But in stem cells the protection was lower. DSBs from oxidative stress were only decreased by 50 % and bleomycin induced damage was not affected at all. So, one could argue that the NBS phenotype is either not pronounced in pluripotent stem cells, or is counteracted by mechanisms only in stem cells. Both theories are supported by the normal embryonic development of NBS children. Apart from lower birth weight, NBS children are normal and problems start with birth and aging (Chrzanowska *et al.*, 2012). Further studies should be performed in the future to discriminate NBS-related differences between somatic cells and stem cells. It would be interesting to see if e.g. induction of apoptosis or proliferation speed is the common factor in NBS-iPSCs and hESCs, or if the mechanism is found in the time per cell cycle phase, repair, antioxidant defense system or other signaling pathways. One possible explanation could be the metabolic effect. In hESCs, glycolysis is up-regulated and oxidative phosphorylation reduced due to the

immature nature of the mitochondria (Prigione & Adjaye, 2010; Prigione *et al.*, 2014). This is supported by the fact, that the working agent EDHB affects the hypoxic pathway and global transcriptome analysis revealed "glycolysis" as the most significant up-regulated pathway in NBS-iPSCs even against hESCs (3.5.2.6). Another theory could be that hESCs focus on a different repair mechanism (eg. NHEJ or MMEJ) which does not involve or depend on NBN. Also cell cycle phase progression could be related to that, because cell cycle analysis showed different DNA damage sensitivity in S-phases than in others. The NBN-dependent homologous recombination repair requires a sister chromatid as template which is only available in S and G2-phases. In a third theory, hESCs are more sensitive to apoptosis and rather sacrifice cells before carrying the errors further and therefore establish genomic stability under moderate stress conditions.

4.2.1.5 *Technical observations*

Performing ROS and DNA damage studies raised a few technical questions. When ROS was measured by the fluorescent-releasing oxidation of DCF-DA in pluripotent cells, the cells were also immunofluorescently stained with the pluripotency marker TRA-1-60. The cell populations of hESCs and NBS-iPSCs then clearly showed two distinct populations in FACS analysis, when resolved by size (FCS) and granularity (SSC) or ROS levels (Figure 32 on page 95). The cells in the population with more base level ROS were bigger and TRA-1-60 negative and the other vice versa. But from colony morphology, the cells looked mostly homogenous. The reaction to treatments was very similar in both populations, but the question remains which cell type is present in these populations. Most likely, the upper population represents cells with an early differentiation stage. Also the low base ROS level in the lower populations would point to hESCs, since hESCs shift their metabolism to anaerobe and have smaller mitochondria. But it also indicates that homogeneous-looking hESC-populations can be far from it, which should always be kept in mind, when experiments are performed.

Another technical issue results from the time-frame of repair mechanisms. Repair of DSBs can occur in little as 8 min (Reynolds *et al.*, 2012), whereas experiment set-ups were performed over time-periods of several hours. In detail, most experiments were treated for 3 hours and then released from the damaging agent for 1 hour to allow the cells not only to acquire damage but also repair it to a certain extent. So cells with less damage either got less damage, or were more effective in repair. This enabled to see a definitive difference between NBS and control cells and also showed that at least one hour was not enough time to repair all the DSBs in all the cells. But it does not discriminate if the cells were more sensitive to damage, or, which is more likely, if cells had more effective repair than others. So, differ-

ent methods, like live-imaging could give deeper insights into repair and ROS mechanisms. Also a time course experiment with different recovery times could resolve repair-rates in NBS and non-NBS cells ((Shahar *et al.*, 2011); http://www.youtube.com).

4.2.2 *Detection of Phosphorylated DNA Damage-associated Signaling Proteins*

Cell cycle checkpoints enable the cells to delay cell cycle progression and take time to repair DNA damage and to prevent damage transmission to the daughter cells. NBS is known for its intra-S checkpoint failure (Falck *et al.*, 2002), so it was important to monitor regulation of checkpoint proteins like CHEK1, CHEK2 and TP53. While all related proteins are more or less interconnected, CHEK2 is mainly activated by ATM (after DSBs) in combination with the MRN complex and results in G1-arrest via the TP53 pathway. CHEK1 on the other hand, is mostly activated by ATR (after SSBs) and results in S-phase or G2/M arrest via activation of CDC25a and CDC25c, respectively (Bartek & Lukas, 2001).

Western Blotting is an effective tool for detecting and analyzing changes in signaling pathways or cascades. The effect of oxidative stress (by H_2O_2) and induction of DSBs (by bleomycin) on repair signaling was monitored by detection of phosphorylated (= activated) versions of several damage response proteins (CHEK1, CHEK2, P53, ATM, ATR, BRCA1, H2AX). Furthermore, the cells were treated with EDHB, an agent which proved to protect from the oxidative damage and DSBs in previous experiments and is also known as an activator of the HIF pathway. The western blot experiments confirmed that H_2O_2 can induce DSBs which is reversed or prohibited by EDHB, but DBSs caused by bleomycin were not prevented by EDHB (Figure 34 on page 101). EDHB therefore acts more likely as an antioxidant or activator of cellular antioxidative defense mechanisms and has no influence on repair itself. EDHB also influenced activation of checkpoint proteins (CHEK1, CHEK2) and TP53. E.g. in fibroblasts, there was only a low activation of CHEK2 by H_2O_2, but together with EDHB the activation was at least 3-fold. EDHB alone did not activate CHEK2 nor CHEK1. In NBS fibroblasts, oxidative stress-induced damage did not lead (as expected) to CHEK1 phosphorylation, which were further contrasted by CHEK1 activation under control conditions. Oxidative stress therefore inhibited CHEK1 (which was also seen in hESCs and iPSCs), but inhibition was reversed by EDHB. This results in a potential direct connection between the oxidative state or hypoxia and cell cycle checkpoints. It remains unresolved why CHEK1 is dephosphorylated (or eliminated altogether), but one possible explanation is suggested by Willis J, et al. 2012. They showed that CHEK1 is activated by H_2O_2, but this was reversed by overall decrease of CHEK1 after

80 min (Willis *et al.*, 2012). It is also known that hypoxia induces G1-arrest (Hubbi *et al.*, 2011; Box & Demetrick, 2004; Koshiji *et al.*, 2004; Gordan *et al.*, 2007) and overexpression of HIF1alpha is already sufficient to induce the checkpoint (Hackenbeck *et al.*, 2009). Others report that hypoxia activates CHEK1 and CHEK2 via ATR in the absence of detectable DNA damage and independent from the MRN complex (Freiberg *et al.*, 2006). If this is also true in NBS cells, then activation of the hypoxia pathway by EDHB not only prevents from oxidative damage, but might also restore abrogated checkpoints. CHEK1 activation usually leads to S-phase arrest, which is known to fail in NBS cells. The perpetual activation of CHEK1 in NBS fibroblasts under normal conditions indicates an impaired mechanism downstream of CHEK1, because proliferation appears normal in these cells. For example, truncated NBN could interfere with CDC25a phosphorylation or its proteolysis and thus prevent the checkpoint. But the question remains how CHEK1 is phosphorylated in the first place in the absence of detectable DNA damage? It is possible that other stressors activated the signaling pathway (e.g hypoxia mediated or hypotension (Kanu & Behrens, 2007)), or that NBN itself plays a greater role in maintenance of cell cycle related processes, which are then destabilized by truncated NBN.

CHEK proteins are not the only checkpoint regulators in the cell. TP53 plays a major role in all pathways dealing with maintenance of the genomic integrity. Its complex regulation functions as a switch that can decide the cell fate depending how severe the damage is (Kruse & Gu, 2008; Appella & Anderson, 2001). It can induce cell cycle checkpoints but can also induce apoptosis or senescence or, decide survival for the cell. TP35-S15 is phosphorylated by ATM, ATR or DNA-PK and results in TP53 accumulation in response to DNA damage (Tibbetts *et al.*, 1999; Shieh *et al.*, 1997). In NBS fibroblasts with induced DNA damage (by bleomycin) TP53-S15 phosphorylation was decreased after EDHB treatment by approx. 90 %. This raises two questions: a) why did it only occur in NBS fibroblasts and not in normal; and b) how did EDHB influence TP53-S15 phosphorylation? It is possible that transient activation of HIF-pathway (by EDHB) lead to destabilization of TP53 in contrast to severe hypoxia which leads to TP53 mediated apoptosis (Schmid *et al.*, 2004). With regards to the use of EDHB as a protective agent from DNA damage, this result shows the danger of ignoring severe damage and maybe failing to induce apoptosis where it would be needed. The fact that only NBS cells react this strongly to this treatment cannot be explained in that context. Again, a different ground state regulation of cell cycle processes inflicted by truncated NBN might be responsible.

Very unpredicted was the failing TP53 activation in all tested cells upon H_2O_2treatment, despite prominent DNA damage (judged by gamma-H2AX). Das & Dashnamoorthy explicitly showed in 2004,

that TP53-S15 phosphorylation was induced by $H_2O_2$and only failed in ATM knockout cells. Since it occurred in all tested cells under the same conditions it indicates an off-target effect, possibly by a too high H_2O_2 concentration.

After comparison of all tested factors and cells it can be summarized that there was a more similar level of checkpoint proteins between NBS and normal in pluripotent cells than in fibroblasts. A similar phenomenon was already observed in experiments monitoring DNA damage and ROS by FACS. This again supports the theory that NBS is a disease of somatic cells and the pathological effects is avoided naturally in pluripotent cells. One possible mechanism could be the dependence of pluripotent stem cells on glycolysis instead of Ox-Phos as discussed above.

The second last aspect reveals how important it is to critically review the technical aspects of an experiment. To determine if the H_2O_2 concentration was suited to address DNA damage signaling, it would have been beneficial to find an optimal concentration for each cell type beforehand. E. g. fibroblasts appeared to be less sensitive against DNA damage by ROS than pluripotent cells and it was not tested if the chosen concentration resulted in apoptosis. But there were also other technical issues that revealed itself only after the complete set of western blots was analyzed. Most of the issues were related to availability of time and cell material, like low number of repetitions or a missing gamma-H2AX western blot for fibroblast cells. To compensate, the DNA damage capabilities of H_2O_2 in fibroblasts, gamma-H2AX levels were translated from FACS experiments. There, H_2O_2 caused less damage in fibroblasts compared to stem cells. To analyze differences in fibroblasts and pluripotent cells it would have been more reliable, to compare samples from the same blotting membrane. Even though displayed, I did not analyze some of the proteins in detail. ATM, ATR and BRCA1 are very high weight proteins (200 kDa and above) and were therefore difficult to resolve, especially ATM and ATR, which were detected at the same height on the blot. Therefore results have to be taken with caution. They were only included in this work, because the pattern was clearly different from each other, supporting a specific detection of the respective protein. Another technical question that arose from conflicting results of the experiment, were the phosphorylation of H2AX to gamma-H2AX upon DNA DSBs which is rather generally accepted in the scientific community. But is H2AX really only phosphorylated at DNA-breaking points, or also other damages? Some publications claim that ATR phosphorylates H2AX in response to single-strand breaks (Ward *et al.*, 2004) and DNA-PK phosphorylates it under hypertonic conditions and during apoptosis (Reitsema *et al.*, 2005; Mukherjee *et al.*, 2006). So the evidence line for DNA damage might be more complex than thought. Another issue is the type of damage that is induced. De-

pending on the agent (e.g. oxidization, UV, X-rays) it can produce several types of broken DNA endings, which undergo different types of repair pathways (overview of the chemical types of clean and dirty ends by Andres *et al.*). In relation this study it could be also of relevance that H_2O_2 causes mainly SSBs and bleomycin a mixture of SSB and DSBs with increasing DSB by increased concentration (BENÍTEZ-BRIBIESCA & SÁNCHEZ-SUÁREZ, 1999). At last I want to mention that my previous experiments on DNA damage had shown that cell cycle stage might also be important for repair processes, but here the different proteins were not analyzed in a cell cycle stage dependent manner.

4.3 MICROARRAY-BASED TRANSCRIPTOME ANALYSES

Microarrays are an exceptional tool to look inside the mechanisms of the cell on a global context. By measurement of total mRNA of a cell population and comparing it to another population, the differences between the two gives direct insight into regulation mechanisms on the transcriptional level which can also include splicing variants. The disadvantage is, that the transcriptome is only one level of cellular control and it does not include protein amount and posttranslational modifications, localizations or epigenetic modifications. But nevertheless it enables a good overview what is going on inside the cells and there is no limit to the experimental conditions to explore specific mechanisms. NBS is a disease which mostly affects pathways like cell cycle, DNA repair and cell fate which all are regulated in a short time frame and on post-translational and protein-interaction level. But, while in healthy cells DNA damage is resolved quickly, the missing interactions of NBN in NBS cells cause a continuous effect on repair and related pathways. So analysis of the whole transcriptome can reveal if the cells react to this condition not only with short time responses but also with long time, transcriptional, responses as a product to the disease or maybe even to compensate for some effects. Here, I compared two sets of samples. First, I wanted to highlight general mechanisms between NBS and normal fibroblasts by pooling several patients together to eliminate patient-specific expression patterns. The aim was to identify pathways that directly translate to the known phenotypes of the disease but also find pathways which reveal novel involvement of NIBRIN in certain pathways (3.5.1). Second, I compared reprogrammed NBS cells (NBS-iPSCs) with hESCs and to their somatic counterparts to see if there is a NBS specific expression pattern that persists in all cell types and to see if pluripotent cells react differently to the disease than somatic cells (3.5.2).

All samples were loaded in technical duplicates and depending on the analysis there were at least two biological duplicates in each set of groups. The microarray technology is still rather expensive so sample

repetition must be carefully planned. The nature of the ILLUMNA array setup already includes internal controls, replicates and mathematical calculations to relativize background staining, so technical replicates are less important when a global picture is analyzed. On the other hand, too many biological replicates can increase the noise to signal ratio so that some lower transcriptional changes are lost during analysis. In either way, on the single transcript level, array data is very unreliable as it can be seen by detection of Y-chromosomal genes in female samples. In consequence, if single transcript data is used, it always has to be validated by other means like e.g. real-time PCR. Another minor technical bias is generated by the limit of samples that can be loaded onto a single chip or chip-set. As each chip might contain small modifications during its creation, it is best to compare samples from one chip or if several chips are used, spread technical replicates among the different chips. It is unknown how high the error is by comparing one chip to another and may also vary, but it might be minor in comparison to the diversity of biological replicates. Since the technology is always evolving it happed that my first samples were analyzed on an 8-chip and the second samples on a 12-chip. Even though many of the probes overlap it made it impossible to directly compare the first to the second set.

Different from *in vivo*, *in vitro* or *in silico* experiments, bioinformatics often does not produce a yes or no answer to scientific questions but probabilities weighted by size and reproducibility of the samples, creating a pValue for the null hypothesis. The threshold value which is used to mark a hypothesis secured is created artificially and in agreement of most mathematicians is mostly used a pValue of at least 0,05 for fairly save (meaning in 95 % of cases your hypothesis will be right) but the result is more significant the smaller pValue is given or produced. Here, I selected genes which were considered to be expressed in the sample population if their pValue for expression was smaller than 0,01. This means in 1 of 100 cases you will find a gene in your selection which is not truly expressed. This value is also widely used in publications using microarrays (Wang *et al.*, 2010; Wei *et al.*, 2004; Firoved *et al.*, 2004; Wolfrum *et al.*, 2010). But during analysis of the data, I often questioned that threshold because many genes were selected close the background detection signal (eg. BAX: 0,009; 37,4; background signal: 30). If I used a pVal of 0,001 instead, I rarely selected those kinds of genes and therefore enriched the number of genes expressed clearly above threshold. Especially when the selection encompassed several thousand genes the absolute number of false-positive number of genes were very different between a pValue of 0,01 and 0,001. E.g. in NBS-iPS there was a total of 47223 ILUMMINA-IDs and of those 18989 were selected as "expressed" for pVal < 0,01 and 14083 for a pVal < 0,001 which results in a difference of 4951 (26 %) IDs. Of those 97 % had an expression level below "300",

which was tested as the detection limit for real-time PCR. Therefore for genes that are expressed at a significant amount, the pVal threshold of 0,001 seems to be the better choice, but raises the question how relevant are genes (apart from transcription factors) that are very low expressed. As this might be a study of a different kind, I focused on the pVal of 0,01 as other researchers did before me. But all this critical consideration is necessary when dealing with bioinformatics, because the pure mathematical tools must be chosen in a way that it reflects the real biological condition. So, as a form of internal control of microarray analysis, I recommend to analyze the data for results already known, before using the mathematical model to generate new information. Here, I achieved this kind of control in finding pathways overlapping with the known conditions of NBS (like regulation of cell cycle and oocyte genes) and also newly discovered pathways based on the same conditions. Another way to eliminate false-positive genes was the analysis of differentially regulated genes which rather focused on significant differences in expression instead of absolute expression. Another advantage is, that it not only shows regulation but also discriminates between up- and down-regulated genes which than can be used to predict the status of certain transcription factors, which are the key elements in pathway regulation.

To find regulated pathways only two different tools were used: in majority the free online tool, the "DAVID" (Huang *et al.*, 2009a; Da Wei Huang & Lempicki, 2008) database, but also the commercial program "Ingenuity". Both tools showed similar results from the same data source, but the focus was put to DAVID as this has more options and is more transparent. One critical aspect in these tools is, that it is based on information which is already known and published, therefore if some transcripts from the array are unknown in the database, they are also not incorporated in the analysis. Usually only a few genes from the input list were missing in the DAVID database (~ 10 %), but in some analyses the amount was up to 67 % which results in poor significance for the outcome of the analysis.

Another source for errors are the sample conditions which sometimes cannot improved otherwise. It is unknown if the fibroblast extraction site was always from the same localization of the patient's body or if this material contained malignant cells. Further, the comparison of NBS fibroblasts with HFF1 and BJ cells could be biased by the fact that HFF1 and BJ are neonatal cells whereas the NBS fibroblasts are from patients of several ages. But this error might be minor because most NBS patients are very young. In addition, NBS-iPSCs had to be compared to a normal counterpart and hESCs were chosen instead of HFF1-iPSCs. The choice was made, because NBS-iPSCs clustered closer to hESCs than to HFF1-iPSCs, but preferably the compared samples should have a similar background (here the reprogramming process and the viral constructs) and most preferably

the exact background (e.g. NBS cells vs. genetically corrected NBS-cells).

One of the aims was to find genes which are specifically regulated in NBS cells. In the first array analysis several patients were combined and compared to normal fibroblasts and lead to a gene list of presumably NBS specific genes. But, as only one cell type was analyzed the result could also be fibroblast-specific. In the second array analysis, reprogrammed NBS cells were compared to hESCs and NBS fibroblasts to overcome the cell-type bias. But unfortunately only one patient was able to be reprogrammed, so the results from this analysis could be biased by patient-specific gene regulation.

4.3.1 *NBS Fibroblasts*

In a first attempt to describe the effects of NBS fibroblasts on a level of cellular control, four fibroblast lines with NBS (2 male, 2 female) were grouped together and compared to normal fibroblasts (HFF1, BJ) by means of a global transcriptional profile (ILLUMINA array, 3.5.1). The hierarchical cluster analysis showed that the complete transcriptomes of NBS fibroblasts could be clearly discriminated from normal fibroblasts and highlighted that the effect by truncated NBN was stronger than gender and biological variation (Figure 35 on page 104). Interestingly, gender seemed to have little effect on the transcriptional profile because the two male and two female samples clustered not together. This might be explained by normal biological diversity, but it could also mean that the effects of NBS can be grouped in different transcriptional outcomes.

The diversity of each patient was emphasized by selection of individual expressed genes which were than subjected to annotation cluster analysis (Figure 37 on page 107). This kind of analysis might give clues to patients-specific response to drugs or treatments, or give insight to the condition of the sample as e.g. one patient showed enriched expression in inflammation or one patient enriched in folic acid metabolism. In this case it was used to show, that all patients had a similar number of specific genes and no extreme outliers.

A selection of expressed genes that were common in all NBS samples but differed from normal fibroblasts was used to determine disease-specific genes. A total of 129 genes were found, which is a small number in relation to the full set of genes of the array (18415). So despite a great general difference between NBS and normal cells, as seen by the hierarchical clustering, it was hard to pinpoint these. The 129 specifically expressed genes did not cluster significantly in any pathway or any annotation that was related to known NBS phenotypes. So in turn, truncated NBN most likely did not activate any specific expression pattern. Interestingly, many pathways related to NBN were significantly enriched in the opposite group of genes, the genes that

were only expressed in normal fibroblasts and therefore missing in NBS cells. Thus, truncated NBN somehow leads to inhibition of several important players in cellular control such as CDK2, CyclinB, pRB and others. This shows how important it is to adapt the form of bioinformatics to the biological question instead of standardized tools, to discover new information.

Profiling of cell populations by whether genes are expressed or not, shows certainly very significant differences. But it is very artificial in comparison to the fine-tuned dynamics of a cell which is often not a question of on/off, but moderate regulation of transcript amount. Therefore the analysis of effects by truncated NBN was focused on genes that were differentially expressed (diff pVal <0,05; fold-ratio >1,5). The results of pathway analysis partially overlapped with the analysis of specifically expressed genes in normal fibroblasts and also matched many known features of the disease like abnormal cell cycle, cancer, TP53, apoptosis and oocyte regulation (Table 9 on page 110). These may be directly related to the physical phenotypes of NBS like radiation sensitivity, cancer, microcephaly and infertility in females. Especially female infertility is striking because it may be linked to abnormal oocyte maturation as seen by transcriptional profiling in fibroblasts. Mechanistically the problem might be caused by general misregulation of the cell cycle as most genes overlap in these pathways. Also, a gene of the cell cycle, CCND2, is one of the most upregulated (12-fold) genes in the whole array. But the exact mechanism how cell cycle and oocyte maturation is affected is unknown. The direct connection between NBN and female fertility was observed before in clinical studies of females (summarized by (Chrzanowska *et al.*, 2012)) and in a humanized mouse-model (Difilippantonio *et al.*, 2005), that showed loss of oocytes before birth as the cause for infertility. As male sexual maturation is normal, it clearly shows that NBS can have gender specific effects. Therefore a gender specific analysis was performed to reveal further differences. But the affected pathways were only moderately significant, contained few regulated genes and did not match any general mechanism. According to a very recent review (Shah *et al.*, 2014) there can be profound influence of gender on experimental results. Already in 2001, a report of the institute of medicine (Pardue *et al.*, 2001) suggested that researchers should take better care of documentation and influence of the sex of their cells used in studies.

The central question regarding NBS is in what way truncated NBN affects specific targets and subsequently alters pathways and phenotypes. Global transcriptional analysis identified pathways that were significantly regulated in NBS fibroblasts. But are they all connected by a few key players or affects truncated NBN a broad spectrum of targets? There is evidence for both theories. The action of truncated NBN must be of course based on the abrogated interaction

of the missing FHA-BRCT domain with specific targets. Many NBN-FHA-BRCT interaction partners are already identified like Lif1/DNA LigaseIV, Mdc1, Ctp1, gamma-H2AX, WRN/TRF2, DNMT1 (Hayashi *et al.*, 2013; Williams *et al.*, 2009; Kobayashi *et al.*, 2002, 2010) and can be translated to several cellular functions like DNA detection and repair, telomere maintenance or epigenetic modification. In addition, FHA and BRCT domains are a common motive in a variety of repair mechanisms (Mohammad & Yaffe, 2009), so the smaller fragment of truncated NIBRIN (P26-NBN) might also act as an inhibitor in these proteins which usually have a phosphothreonine (FHA) or phosphoserine (BRCT) response element. In fact, using DAVID analysis on all regulated genes in NBS fibroblasts revealed protein domain clustering in TOP hits (p=0,00004) like "Serine/threonine protein kinase-related", "Protein kinase, core", "Protein kinase, ATP binding site", "Serine/threonine protein kinase, active site" and "Serine/threonine protein kinase" (Lloyd *et al.*, 2009; Williams *et al.*, 2009; Chapman & Jackson, 2008; Melander *et al.*, 2008; Spycher *et al.*, 2008; Wu *et al.*, 2008a). This means mostly phosphorylated serine and threonine domains were affected in NBS fibroblasts thus supporting a broad spectrum of targets. On the other hand, there were a few gene names that reappeared frequently in many different analyses of the data and pathways. One of those was TP53, which is known to regulate many functions of the cell related to cell cycle, DNA repair and apoptosis. It was not only found significantly affected in NBS fibroblasts trough DAVID pathway analysis (Table 9 on page 110) but also through Ingenuity analysis of regulated transcription factors (Table 10 on page 114). TP53 is also connected to another central gene, E2F1 (Martin *et al.*, 1995). E2F1 is not only a key activator in cell cycle progression, but was also found to be a binding partner of the N-terminus of NBN (Maser *et al.*, 2001b). Maser et al. postulated that E2F1 binds to phosphorylated NBN after DNA damage during replication and is responsible for the intra-S checkpoint activation (which is missing in NBS cells). The broad down-regulation of cell cycle genes NBS fibroblasts may be incriminated to E2F1 which was also found inhibited by Ingenuity transcription factor analysis. Furthermore the E2F1 is also involved in Fanconi Anemia pathway regulation (Tategu *et al.*, 2007) which is closely related to NBS and many genes from FA pathway were significantly down-regulated in NBS fibroblasts.

Among the regulated pathways in NBS fibroblasts were besides anticipated targets like cell cycle also several which were unexpected or unknown in relation to NBS. Especially proteins connected to lysosomal pathways clustered with a high significance. In NBS-iPSCs, endosomal proteins and proteasome were significantly down-regulated, indicating a possible mechanism connecting all three pathways together. It was previously reported, that mutated NIBRIN levels were affected by proteasomal degradation and lysosomal microautophagy

(Salewsky *et al.*, 2013). It was also reported, that low intracellular amounts of mutated NIBRIN accompanied with a higher risk of early cancer onset (Krüger *et al.*, 2007). The total amount of NBN protein in was not measured here, but it was observed that NBS-8 fibroblasts and NBS-8-iPSCs had lower transcript levels compared to normal cells. Specific regulation of NBN protein amounts may therefore be an additional modifier of the clinical phenotype. Also, autophagy in general (lysosome-dependent) was reported to affect genomic integrity especially in the response to DNA damage and mitophagy (autophagy of mitochondria) of injured organelles might prevent a vicious cycle of ROS generation (Vessoni *et al.*, 2013). A similar theory was reported by (Schröter & Adjaye, 2014) which highlighted the role of the proteasome as a clean-up tool necessary to maintain pluripotency (Buckley *et al.*, 2012).

4.3.2 *Reprogrammed NBS Cells*

Before deriving reprogrammed NBS-iPSCs, I compared the global transcriptomes of four fibroblast lines of NBS patients to normal fibroblasts to identify NBS specific genes pathway regulation. Reprogramming of NBS cells was challenging because of NBS dependent reasons (as discussed in 4.1.2) and only two iPSC-lines of the same patient was obtained. As this patient was not available in the early analysis (8-chip), transcriptomes could not be compared to each other the expression level, but on the bases of the results itself. The analysis aimed to identify NBS specific gene expression which was not limited to a single cell type and discover if the influence of NBN in pluripotent cells was a different kind as in somatic cells.

Interestingly, one of the obtained NBS-iPSC-lines clustered more closely to hESCs as other (non-diseased) iPSCs and also obtained the highest score for pluripotency in comparison even with the hESC-lines (Figure 47 on page 129, Figure 49 on page 132). This indicates that p70-NBN does not interfere with maintenance of pluripotency. It can be speculated that the translocation found in the karyotype of the NBS-iPSC-line (Figure 25 on page 77) may have been supportive in achieving pluripotency, but different qualities of pluripotency are also often established by stabilization of an epigenetic profile which may be purely random (Pasque *et al.*, 2011; Lluis & Cosma, 2013).

Apart from actual partners that bind to the N-terminus of NBN, indirect targets of NBN might serve as therapeutic angle as well. Therefore, by eliminating all genes which overlap in expression with the same (fibroblasts) or other cell types (iPSCs) from normal patients, 41 genes that were distinct for NBS were identified (Figure 50 on page 135). Unfortunately, the gene list contained mostly genes with low expression intensities and was not overlapping with the NBS specific gene list of 4 different patient fibroblasts. Because the list was de-

rived only from one NBS patient, the identified genes might be also purely patient-specific and thus NBS-unspecific. To identify indirect targets of NBN, I propose to repeat a global transcriptome analysis with populations of minimized background, as can be achieved by comparing e.g. a patient cell line with a genetically corrected counterpart in a future study. Nevertheless, the overlap of several regulated pathways in NBS-iPSCs (vs. hESCs) and NBS fibroblasts (vs. normal) indicated, that there is a common effect of p70-NBN which is independent from cell type. Though, the effect might be indirect, because only the pathways but not the regulated genes overlapped (see e.g. cell cycle: Figure 41 on page 117, Figure 54 on page 146).

During the study of NBS, the question arose how a disease with genomic instability, activated TP53 and abnormal cell cycle regulation can produce a NBS-iPSC-line with a stable karyotype and normal proliferation. The distinct transcriptional profile of NBS-iPSCs might offer some clues to address this question. Most striking was the highly elevated glycolysis pathway in comparison to hESCs. It was shown before that a switch from oxidative phosphorylation to glycolysis is an essential trait of hESCs and iPSCs, caused by morphological changed, smaller mitochondria. The function is most likely to decrease the amount of ROS produced by mitochondria and therefore protection of the genome (Cairns *et al.*, 2011; Prigione *et al.*, 2014). NBS cells may have enhanced the switch to glycolysis, to compensate for their elevated sensitivity for ROS, as seen in this study. Prigione et al. showed that the HIF1-pathway plays a significant role during reprogramming to achieve the glycolytic shift. NBS cells may require additional effort to achieve this switch as indicated by the upregulation of genes responsible for decreasing oxygen consumption in NBS-iPSCs in comparison to hESCs. Even before reprogramming, NBS fibroblast showed evidence to have modified energy metabolism as seen by regulated genes for insulin signaling and mitochondria.

What was puzzling was the significant regulation in NBS cell of circadian clock genes not only in NBS fibroblasts but also in the reprogrammed cells. This might be caused by abnormal cell cycle regulation, connected to metabolism control, but can also be caused by a response or prevention of oxidative stress. It is known that clock genes regulate metabolism and availability of ROS scavenger (Hardeland *et al.*, 2003), but the clock gene clustering might also be attributed to the limited number of samples (one patient, two cell-lines).

In summary, global transcriptome analysis of NBS fibroblasts and iPSCs was a capable tool to narrow down the complex mechanistic of the disease to a few pathways (cell cycle, cancer, TP-53, HIF) and common functions (ROS, metabolism), which seem responsible for the NBS phenotype. Surprisingly, the focus settled less on direct repair mechanisms, as was expected from N-terminal binding

partners of NBN, but may be explained by the short-lived and non-transcriptional regulated nature of DNA repair.

Part V

CONCLUSION

5 CONCLUSION

Aim of this work was, to reprogram fibroblasts from NBS patients to iPSCs in order to bypass senescence and create a model system for the disease. The process failed for four cell lines from NBS patients despite using the most reliable method (viral transduction of O/S/K/M), but succeeded in one case of fibroblasts from a recent skin biopsy. Characterization of those cells however, showed that they were heterozygous for the founder mutation, which is contradictory to the recessive character of NBS. But evidence pointed to a possible second mutation in the gene or promoter of NBN, as indicated by lack of full-length NIBRIN in the cells and the fact, that the patient was actually diagnosed with the disease. In addition, microarray analysis of those NBS cells showed a NBN mRNA signal reduction by 50 % in comparison to normal cells which could also point to silencing of one NBN allele (probe sequences did not overlap with the site of 657del5 mutation). Some publications show that NBN is not detectable in NBS cells on protein level (Maser *et al.*, 2001a), and this should be tested for this study as well, to exclude the possibility that some cells do not require NBN at all.

Whether or not due to the heterozygous mutation, NBS cells can be reprogrammed to iPSCs without ectopic expression of full-length NBN. In comparison, cells of a similar disease, Fanconi anemia, were only reprogrammed after correction of the pathological mutation (Raya *et al.*, 2010), or hypoxic conditions (Müller *et al.*, 2012c). Why the NBS cells from other patients failed to reprogram (late passage, homozygous mutation, high TP53, ?) should be identified next and attempts of reprogramming more NBS cell lines should be made. By bypassing senescence, an immortal, pluripotent NBS cell line was established, which can serve as a tool to model the disease, or serve as an *in vitro* screen for drug testing.

A second aim of this work was to detect genomic instability in NBS cells before and after reprogramming, which was solved by karyotyping and toxicity tests. Surprisingly, the karyotype of NBS cells showed only few aberrations, which were stable over a long cultivation period (see 3.1.2.4). This contributed to the question of how stem cells maintain genomic stability, especially as NBS-iPSCs and normal hESCs alike, were found to be more susceptible to DNA DSBs than somatic cells in this study (Section 3.3). The answer was not in the focus of this study, however, a few theories can be extracted: a) the fate of damaged somatic cells may be shifted to an arrested but alive state, in contrast to hESCs that rid themselfs of unrepaired cells via apoptosis; b) hESCs are more susceptible to DNA damage, because they have

more open chromatin and proliferate; c) hESCs have up-regulated repair-genes and thus compensate better after DNA damage.

Assays that determined the sensitivity of NBS cells to oxidative and genotoxic stress revealed, that NBS-iPSCs and hESCs were equally sensitive towards DNA damage and more sensible than fibroblasts (Section 3.3). But NBS fibroblasts were more sensitive towards DNA damage than normal fibroblast. A small chemical compound was found, EDHB, a competitive inhibitor of prolyl 4-hydroxylase, which activates the HIF-pathway. EDHB was found to effectively decrease DNA damage caused by oxidative stress which shows potential for further studies and might be relevant in future clinical applications to increase survival in NBS patients. It was also revealed that *in vitro* cultivation of cells at 21 % oxygen is not optimal for maintenance of genomic stability in cells (especially for NBS cells), because oxygen tension increases susceptibly to genotoxic agents (3.3.2). Microarray analysis and immuno-detection of post-translational modifications of checkpoint proteins showed that most cell cycle genes were down-regulated and some checkpoint proteins were always active in NBS cells (see Section 3.4). Thus, NBS cells seem to work under a constant pressure, even under normal conditions (no substantial oxidative or damaging stress).

That *in vitro* cultivated NBS cells are suited to model characteristics of the disease was tested by comparing the transcriptome to clinical phenotypes. After of global transcriptome analysis with total RNA of NBS patients, several of the NBS phenotypes were represented by affected pathways and gene networks. E.g. female NBS patients have impaired or loss of fertility, which could be caused by global down-regulation of cell cycle genes that also take part in oocyte meiosis and maturation (Figure 42 on page 119).

5.1 OUTLOOK:

Despite many interesting findings during this study, this work also left a few areas open for more experiments, raised many new angles and possible new projects for further studies on Nijmegen Breakage Syndrome, DNA repair mechanisms, stem cell identity and aging.

For example, the measuring of genomic instability was performed by karyotyping and detection of gamma-H2AX in this study, but could be improved to a higher quality and better quantification by measuring homologous recombination events in STGC (short tract gene conversion) and LTGC/SCE (long-tract gene conversion/sister chromatid exchange) via the SCneo reporter as done in (Tauchi *et al.*, 2002). For the same reason, NGS (next generation sequencing) on the genome of early passage and late passage NBS fibroblasts and NBS-iPSCs could be performed to discuss genomic stability on point mutation level, which would possibly also indicate to how the mutation

was introduced (e.g. by inaccurate repair). In addition, full genome sequencing can also serve as quality control in the case of iPSCs, when introduced as a disease model, or for clinical applications.

NBS is also known as a disease of premature aging and NBN was found to be involved in telomere maintenance. Therefore it would be interesting to measure telomerase length and activity in NBS-iPSCs (and other cell types), to see whether reprogramming is also able to "rejuvenate" cells from a NBS patient and why.

While working on this project, I often came across the question, if there might be a pathological influence of p26-NBN. It was reported, that in patients with the 657del5 mutation in NBN, both fragments of the protein can be translated (Maser *et al.*, 2001a), but studies almost exclusively focus on the bigger, p70-NBN fragment. The review of Mohammad & Yaffe highlighted, that FHA domains and BRCT domains play a huge role as a general feature in cell cycle processes and DNA damage response. The small, p26 fragment of NBN is comprised of one FHA and one BRCT domain and in theory, if folded correctly, p26-NBN could act as competitor for these processes. A very recent publication, focused on NBN interaction partners and found evidence that p26-NBN exerts an inhibitory effect on PARP1 (Cilli *et al.*, 2014). Therefore, it is very likely that more of these cases can be found.

Part VI

APPENDIX

BIBLIOGRAPHY

AB, Nobel Media. 2012. The 2012 Nobel Prize in Physiology or Medicine - Press Release. *Nobelprize.org*, **1**, 1. (Cited on pages 25 and 60.)

Abdelwahed, Afef, Bouhlel, Ines, Skandrani, Ines, Valenti, Kita, Kadri, Malika, Guiraud, Pascal, Steiman, Régine, Mariotte, Anne-Marie, Ghedira, Kamel, Laporte, François, *et al.* 2007. Study of antimutagenic and antioxidant activities of Gallic acid and 1, 2, 3, 4, 6-pentagalloylglucose from Pistacia lentiscus: Confirmation by microarray expression profiling. *Chemico-biological interactions*, **165**(1), 1–13. (Cited on page 91.)

Adjaye, James, Huntriss, John, Herwig, Ralf, BenKahla, Alia, Brink, Thore C., Wierling, Christoph, Hultschig, Claus, Groth, Detlef, Yaspo, Marie-Laure, Picton, Helen M., Gosden, Roger G., & Lehrach, Hans. 2005. Primary differentiation in the human blastocyst: comparative molecular portraits of inner cell mass and trophectoderm cells. *Stem Cells*, **23**(10), 1514–1525. (Cited on page 23.)

Ahn, J. Y., Schwarz, J. K., Piwnica-Worms, H., & Canman, C. E. 2000. Threonine 68 phosphorylation by ataxia telangiectasia mutated is required for efficient activation of Chk2 in response to ionizing radiation. *Cancer Res*, **60**(21), 5934–5936. (Cited on page 100.)

Albert, M. H., Gennery, A. R., Greil, J., Cale, C. M., Kalwak, K., Kondratenko, I., Mlynarski, W., Notheis, G., Führer, M., Schmid, I., & Belohradsky, B. H. 2010. Successful SCT for Nijmegen breakage syndrome. *Bone Marrow Transplant*, **45**(4), 622–626. (Cited on page 29.)

Alper, Joe. 2009. Geron gets green light for human trial of ES cell-derived product. *Nature biotechnology*, **27**(3), 213–214. (Cited on page 26.)

Altschul, S. F., Gish, W., Miller, W., Myers, E. W., & Lipman, D. J. 1990. Basic local alignment search tool. *J Mol Biol*, **215**(3), 403–410. (Cited on page 56.)

Amit, Michal, Carpenter, Melissa K, Inokuma, Margaret S, Chiu, Choy-Pik, Harris, Charles P, Waknitz, Michelle A, Itskovitz-Eldor, Joseph, & Thomson, James A. 2000. Clonally derived human embryonic stem cell lines maintain pluripotency and proliferative potential for prolonged periods of culture. *Developmental biology*, **227**(2), 271–278. (Cited on page 25.)

Ammazzalorso, Francesca, Pirzio, Livia Maria, Bignami, Margherita, Franchitto, Annapaola, & Pichierri, Pietro. 2010. ATR and ATM differently regulate WRN to prevent DSBs at stalled replication forks and promote replication fork recovery. *EMBO J*, **29**(18), 3156–3169. (Cited on page 7.)

Andres, Sara N, Schellenberg, Matthew J, Wallace, Bret D, Tumbale, Percy, & Williams, R Scott. 2014. Recognition and repair of chemically heterogeneous structures at DNA ends. *Environmental and molecular mutagenesis*, **1**, 1. (Cited on pages 9, 12, and 170.)

Andriopoulos, Jr, Billy, Corradini, Elena, Xia, Yin, Faasse, Sarah A., Chen, Shanzhuo, Grgurevic, Lovorka, Knutson, Mitchell D., Pietrangelo, Antonello, Vukicevic, Slobodan, Lin, Herbert Y., & Babitt, Jodie L. 2009. BMP6 is a key endogenous regulator of hepcidin expression and iron metabolism. *Nat Genet*, **41**(4), 482–487. (Cited on page 111.)

Anokye-Danso, Frederick, Trivedi, Chinmay M., Juhr, Denise, Gupta, Mudit, Cui, Zheng, Tian, Ying, Zhang, Yuzhen, Yang, Wenli, Gruber, Peter J., Epstein, Jonathan A., & Morrisey, Edward E. 2011. Highly efficient miRNA-mediated reprogramming of mouse and human somatic cells to pluripotency. *Cell Stem Cell*, **8**(4), 376–388. (Cited on pages 155 and 156.)

Antoccia, A., Sakamoto, S., Matsuura, S., Tauchi, H., & Komatsu, K. 2008. NBS1 prevents chromatid-type aberrations through ATM-dependent interactions with SMC1. *Radiat Res*, **170**(3), 345–352. (Cited on page 6.)

Appella, Ettore, & Anderson, Carl W. 2001. Post-translational modifications and activation of p53 by genotoxic stresses. *European Journal of Biochemistry*, **268**(10), 2764–2772. (Cited on page 168.)

Armstrong, Lyle, Tilgner, Katarzyna, Saretzki, Gabriele, Atkinson, Stuart P, Stojkovic, Miodrag, Moreno, Ruben, Przyborski, Stefan, & Lako, Majlinda. 2010. Human induced pluripotent stem cell lines show stress defense mechanisms and mitochondrial regulation similar to those of human embryonic stem cells. *Stem Cells*, **28**(4), 661–673. (Cited on page 25.)

Arosio, Daniele, Cui, Sheng, Ortega, Claudia, Chovanec, Miroslav, Di Marco, Stefania, Baldini, Giancarlo, Falaschi, Arturo, & Vindigni, Alessandro. 2002. Studies on the mode of Ku interaction with DNA. *Journal of Biological Chemistry*, **277**(12), 9741–9748. (Cited on page 18.)

Aruoma, Okezie I, Colognato, Renato, Fontana, Ilaria, Gartlon, Joanne, Migliore, Lucia, Koike, Keiko, Coecke, Sandra, Lamy, Evelyn, Mersch-Sundermann, Volker, Laurenza, Incoronata, *et al.* 2006. Molecular effects of fermented papaya preparation on oxidative damage, MAP Kinase activation and modulation of the benzo [a] pyrene mediated genotoxicity. *Biofactors*, **26**(2), 147–159. (Cited on page 164.)

Ashwell, Susan, & Zabludoff, Sonya. 2008. DNA damage detection and repair pathways–recent advances with inhibitors of checkpoint kinases in cancer therapy. *Clin Cancer Res*, **14**(13), 4032–4037. (Cited on pages 9, 10, and 102.)

Aylon, Yael, & Kupiec, Martin. 2004. New insights into the mechanism of homologous recombination in yeast. *Mutation Research/Reviews in Mutation Research*, **566**(3), 231–248. (Cited on page 17.)

Bakkenist, Christopher J., & Kastan, Michael B. 2003. DNA damage activates ATM through intermolecular autophosphorylation and dimer dissociation. *Nature*, **421**(6922), 499–506. (Cited on page 8.)

Banfi, Andrea, Muraglia, Anita, Dozin, Beatrice, Mastrogiacomo, Maddalena, Cancedda, Ranieri, & Quarto, Rodolfo. 2000. Proliferation kinetics and differentiation potential of ex vivo expanded human bone marrow stromal cells: implications for their use in cell therapy. *Experimental hematology*, **28**(6), 707–715. (Cited on page 26.)

Banin, S., Moyal, L., Shieh, S., Taya, Y., Anderson, C. W., Chessa, L., Smorodinsky, N. I., Prives, C., Reiss, Y., Shiloh, Y., & Ziv, Y. 1998. Enhanced phosphorylation of p53 by ATM in response to DNA damage. *Science*, **281**(5383), 1674–1677. (Cited on page 100.)

Barhoumi, Rola, Bowen, Jeffery A, Stein, Lisa S, Echols, Jana, & Burghardt, Robert C. 1993. Concurrent analysis of intracellular glutathione content and gap junctional intercellular communication. *Cytometry*, **14**(7), 747–756. (Cited on page 22.)

Barros, Daniela, Amaral, Olavo B, Izquierdo, Ivan, Geracitano, Laura, do Carmo Bassols Raseira, Maria, Henriques, Amélia Teresinha, & Ramirez, Maria Rosana. 2006. Behavioral and genoprotective effects of Vaccinium berries intake in mice. *Pharmacology Biochemistry and Behavior*, **84**(2), 229–234. (Cited on page 164.)

Bartek, Jiri, & Lukas, Jiri. 2001. Mammalian G1-and S-phase checkpoints in response to DNA damage. *Current opinion in cell biology*, **13**(6), 738–747. (Cited on page 167.)

Baxter, Melissa A, Wynn, Robert F, Jowitt, Simon N, Wraith, J, Fairbairn, Leslie J, & Bellantuono, Ilaria. 2004. Study of telomere length reveals rapid aging of human marrow stromal cells following in vitro expansion. *Stem cells*, **22**(5), 675–682. (Cited on page 26.)

BENÍTEZ-BRIBIESCA, LUIS, & SÁNCHEZ-SUÁREZ, PATRICIA. 1999. Oxidative damage, bleomycin, and gamma radiation induce different types of DNA strand breaks in normal lymphocytes and thymocytes: a comet assay study. *Annals of the New York Academy of Sciences*, **887**(1), 133–149. (Cited on page 170.)

Bernstein, Carol, & Bernstein, Harris. 1991. *Aging and Sex, DNA Repair in*. Wiley Online Library. (Cited on page 163.)

Bhoumik, Anindita, Takahashi, Shoichi, Breitweiser, Wolfgang, Shiloh, Yosef, Jones, Nic, & Ronai, Ze'ev. 2005. ATM-dependent phosphorylation of ATF2 is required for the DNA damage response. *Mol Cell*, **18**(5), 577–587. (Cited on page 6.)

Biologicals, Novus. 2011. NBS1 Antibody. *www.novusbio.com*, **1**, NB100–143. (Cited on page 152.)

Blasina, A., de Weyer, I. V., Laus, M. C., Luyten, W. H., Parker, A. E., & McGowan, C. H. 1999. A human homologue of the checkpoint kinase Cds1 directly inhibits Cdc25 phosphatase. *Curr Biol*, **9**(1), 1–10. (Cited on page 100.)

Blöcher, D. 1982. DNA double strand breaks in Ehrlich ascites tumour cells at low doses of x-rays. I. Determination of induced breaks by centrifugation at reduced speed. *Int J Radiat Biol Relat Stud Phys Chem Med*, **42**(3), 317–328. (Cited on pages 14 and 161.)

Bondy, Stephen C. 1992. Ethanol toxicity and oxidative stress. *Toxicology letters*, **63**(3), 231–241. (Cited on page 20.)

Box, Adrian Harold, & Demetrick, Douglas James. 2004. Cell cycle kinase inhibitor expression and hypoxia-induced cell cycle arrest in human cancer cell lines. *Carcinogenesis*, **25**(12), 2325–2335. (Cited on page 168.)

Boyer, Laurie A, Lee, Tong Ihn, Cole, Megan F, Johnstone, Sarah E, Levine, Stuart S, Zucker, Jacob P, Guenther, Matthew G, Kumar, Roshan M, Murray, Heather L, Jenner, Richard G, *et al.* 2005. Core transcriptional regulatory circuitry in human embryonic stem cells. *Cell*, **122**(6), 947–956. (Cited on page 24.)

Brierley, David J, & Martin, Sarah A. 2013. Oxidative stress and the DNA mismatch repair pathway. *Antioxidants & redox signaling*, **18**(18), 2420–2428. (Cited on page 15.)

Brown, A. L., Lee, C. H., Schwarz, J. K., Mitiku, N., Piwnica-Worms, H., & Chung, J. H. 1999. A human Cds1-related kinase that functions downstream of ATM protein in the cellular response to DNA damage. *Proc Natl Acad Sci U S A*, **96**(7), 3745–3750. (Cited on page 100.)

Bruhn, Christopher, Zhou, Zhong-Wei, Ai, Haiyan, & Wang, Zhao-Qi. 2014. The Essential Function of the MRN Complex in the Resolution of Endogenous Replication Intermediates. *Cell reports*, **6**(1), 182–195. (Cited on page 9.)

Brüning, Ansgar, & Kast, Richard E. 2014. Oxidizing to death: Disulfiram for cancer cell killing. *Cell cycle (Georgetown, Tex.)*, **13**(10), 1. (Cited on page 164.)

Buckley, Shannon M, Aranda-Orgilles, Beatriz, Strikoudis, Alexandros, Apostolou, Effie, Loizou, Evangelia, Moran-Crusio, Kelly, Farnsworth, Charles L, Koller, Antonius A, Dasgupta, Ramanuj, Silva, Jeffrey C, *et al.* 2012. Regulation of pluripotency and cellular reprogramming by the ubiquitin-proteasome system. *Cell stem cell*, **11**(6), 783–798. (Cited on page 176.)

Burdon, Roy H. 1995. Superoxide and hydrogen peroxide in relation to mammalian cell proliferation. *Free Radical Biology and Medicine*, **18**(4), 775–794. (Cited on page 163.)

Cairns, Rob A., Harris, Isaac S., & Mak, Tak W. 2011. Regulation of cancer cell metabolism. *Nat Rev Cancer*, **11**(2), 85–95. (Cited on page 177.)

Campisi, Judith, & di Fagagna, Fabrizio d'Adda. 2007. Cellular senescence: when bad things happen to good cells. *Nature reviews Molecular cell biology*, **8**(9), 729–740. (Cited on page 12.)

Carlomagno, F., Chang-Claude, J., Dunning, A. M., & Ponder, B. A. 1999. Determination of the frequency of the common 657Del5 Nijmegen breakage syndrome mutation in the German population: no association with risk of breast cancer. *Genes Chromosomes Cancer*, **25**(4), 393–395. (Cited on pages 4 and 53.)

Carney, J. P., Maser, R. S., Olivares, H., Davis, E. M., Le Beau, M., Yates, 3rd, JR, Hays, L., Morgan, W. F., & Petrini, J. H. 1998. The hMre11/hRad50 protein complex and Nijmegen breakage syndrome: linkage of double-strand break repair to the cellular DNA damage response. *Cell*, **93**(3), 477–486. (Cited on page 6.)

Carreau, Aude, Hafny-Rahbi, Bouchra El, Matejuk, Agata, Grillon, Catherine, & Kieda, Claudine. 2011. Why is the partial oxygen pressure of human tissues a crucial parameter? Small molecules and hypoxia. *Journal of cellular and molecular medicine*, **15**(6), 1239–1253. (Cited on page 159.)

Cerosaletti, K. M., Lange, E., Stringham, H. M., Weemaes, C. M., Smeets, D., Sölder, B., Belohradsky, B. H., Taylor, A. M., Karnes, P., Elliott, A., Komatsu, K., Gatti, R. A., Boehnke, M., & Concannon, P. 1998. Fine localization of the Nijmegen breakage syndrome gene to 8q21: evidence for a common founder haplotype. *Am J Hum Genet*, **63**(1), 125–134. (Cited on page 4.)

Chapman, J Ross, & Jackson, Stephen P. 2008. Phospho-dependent interactions between NBS1 and MDC1 mediate chromatin retention of the MRN complex at sites of DNA damage. *EMBO Rep*, **9**(8), 795–801. (Cited on pages 8 and 175.)

Chapman, J Ross, Taylor, Martin RG, & Boulton, Simon J. 2012. Playing the end game: DNA double-strand break repair pathway choice. *Molecular cell*, **47**(4), 497–510. (Cited on page 9.)

Chaturvedi, P., Eng, W. K., Zhu, Y., Mattern, M. R., Mishra, R., Hurle, M. R., Zhang, X., Annan, R. S., Lu, Q., Faucette, L. F., Scott, G. F., Li, X., Carr, S. A., Johnson, R. K., Winkler, J. D., & Zhou, B. B. 1999. Mammalian Chk2 is a downstream effector of the ATM-dependent DNA damage checkpoint pathway. *Oncogene*, **18**(28), 4047–4054. (Cited on page 100.)

Chehab, N. H., Malikzay, A., Appel, M., & Halazonetis, T. D. 2000. Chk2/hCds1 functions as a DNA damage checkpoint in G(1) by stabilizing p53. *Genes Dev*, **14**(3), 278–288. (Cited on page 100.)

Chen, Longchuan, Nievera, Christian J, Lee, Alan Yueh-Luen, & Wu, Xiaohua. 2008. Cell cycle-dependent complex formation of BRCA1· CtIP· MRN is important for DNA double-strand break repair. *Journal of Biological Chemistry*, **283**(12), 7713–7720. (Cited on page 102.)

Chrzanowska, Krystyna H., Szarras-Czapnik, Maria, Gajdulewicz, Maria, Kalina, Maria A., Gajtko-Metera, Malgorzata, Walewska-Wolf, Malgorzata, Szufladowicz-Wozniak, Jolanta, Rysiewski, Henryk, Gregorek, Hanna, Cukrowska, Bozena, Syczewska, Malgorzata, Piekutowska-Abramczuk, Dorota, Janas, Roman, & Krajewska-Walasek, Malgorzata. 2010. High prevalence of primary ovarian insufficiency in girls and young women with Nijmegen breakage syndrome: evidence from a longitudinal study. *J Clin Endocrinol Metab*, **95**(7), 3133–3140. (Cited on pages 108 and 118.)

Chrzanowska, Krystyna H., Gregorek, Hanna, Dembowska-Baginska, Bozenna, Kalina, Maria A., & Digweed, Martin. 2012. Nijmegen breakage syndrome (NBS). *Orphanet J Rare Dis*, **7**, 13. (Cited on pages 85, 152, 160, 161, 165, and 174.)

Chu, Percy WY, Beart, Philip M, & Jones, Nicole M. 2010. Preconditioning protects against oxidative injury involving hypoxia-inducible factor-1 and vascular endothelial growth factor in cultured astrocytes. *European journal of pharmacology*, **633**(1), 24–32. (Cited on page 93.)

Cilli, Domenica, Mirasole, Cristiana, Pennisi, Rosa, Pallotta, Valeria, D'Alessandro, Angelo, Antoccia, Antonio, Zolla, Lello, Ascenzi, Paolo, & di Masi, Alessandra. 2014. Identification of the Interactors of Human Nibrin (NBN) and of Its 26 kDa and 70 kDa Fragments Arising from the NBN 657del5 Founder Mutation. *PLoS One*, **9**(12), e114651. (Cited on pages 5, 6, and 183.)

Clevers, Hans, Loh, Kyle M., & Nusse, Roel. 2014. Stem cell signaling. An integral program for tissue renewal and regeneration: Wnt signaling and stem cell control. *Science*, **346**(6205), 1248012. (Cited on page 159.)

Cockburn, Katie, Rossant, Janet, *et al.* 2010. Making the blastocyst: lessons from the mouse. *The Journal of clinical investigation*, **120**(4), 995–1003. (Cited on page 23.)

Coller, Hilary A. 2007. What's taking so long? S-phase entry from quiescence versus proliferation. *Nature Reviews Molecular Cell Biology*, **8**(8), 667–670. (Cited on page 12.)

Constantinou, Angelos, Chen, Xiao-Bo, McGowan, Clare H, & West, Stephen C. 2002. Holliday junction resolution in human cells: two junction endonucleases with distinct substrate specificities. *The EMBO journal*, **21**(20), 5577–5585. (Cited on page 17.)

Corneo, Barbara, Wendland, Rebecca L, Deriano, Ludovic, Cui, Xiaoping, Klein, Isaac A, Wong, Serre-Yu, Arnal, Suzzette, Holub, Abigail J, Weller, Geoffrey R, Pancake, Bette A, *et al.* 2007. Rag mutations reveal robust alternative end joining. *Nature*, **449**(7161), 483–486. (Cited on page 19.)

Costes, Audrey, & Lambert, Sarah A E. 2012. Homologous recombination as a replication fork escort: fork-protection and recovery. *Biomolecules*, **3**(1), 39–71. (Cited on page 7.)

Cox, Michael M, Goodman, Myron F, Kreuzer, Kenneth N, Sherratt, David J, Sandler, Steven J, & Marians, Kenneth J. 2000. The importance of repairing stalled replication forks. *Nature*, **404**(6773), 37–41. (Cited on page 22.)

Cvek, Boris, & Dvorak, Zdenek. 2008. The value of proteasome inhibition in cancer: Can the old drug, disulfiram, have a bright new future as a novel proteasome inhibitor? *Drug discovery today*, **13**(15), 716–722. (Cited on page 164.)

Czornak, Kamila, Chughtai, Sanaullah, & Chrzanowska, Krystyna H. 2008. Mystery of DNA repair: the role of the MRN complex and ATM kinase in DNA damage repair. *J Appl Genet*, **49**(4), 383–396. (Cited on pages 9 and 96.)

Da Wei Huang, Brad T Sherman, & Lempicki, Richard A. 2008. Systematic and integrative analysis of large gene lists using DAVID bioinformatics resources. *Nature protocols*, **4**(1), 44–57. (Cited on pages 45, 105, and 172.)

Das, Kumuda C, & Dashnamoorthy, Ravi. 2004. Hyperoxia activates the ATR-Chk1 pathway and phosphorylates p53 at multiple sites. *American Journal of Physiology-Lung Cellular and Molecular Physiology*, **286**(1), L87–L97. (Cited on page 168.)

Davis, Terence, Tivey, Hannah S E., Brook, Amy J C., & Kipling, David. 2014. Nijmegen breakage syndrome fibroblasts expressing the C-terminal truncated NBN(p70) protein undergo p38/MK2-dependent premature senescence. *Biogerontology*, **1**(Sep), 1. (Cited on page 29.)

Della-Maria, Julie, Zhou, Yi, Tsai, Miaw-Sheue, Kuhnlein, Jeff, Carney, James P, Paull, Tanya T, & Tomkinson, Alan E. 2011. Human Mre11/human Rad50/Nbs1 and DNA Ligase IIIα/XRCC1 protein complexes act together in an alternative nonhomologous end joining pathway. *Journal of Biological Chemistry*, **286**(39), 33845–33853. (Cited on page 19.)

Demuth, Ilja, Frappart, Pierre-Olivier, Hildebrand, Gabriele, Melchers, Anna, Lobitz, Stephan, Stöckl, Lars, Varon, Raymonda, Herceg, Zdenko, Sperling, Karl, Wang, Zhao-Qi, & Digweed, Martin. 2004. An inducible null mutant murine model of Nijmegen breakage syndrome proves the essential function of NBS1 in chromosomal stability and cell viability. *Hum Mol Genet*, **13**(20), 2385–2397. (Cited on page 4.)

Deng, C., Zhang, P., Harper, J. W., Elledge, S. J., & Leder, P. 1995. Mice lacking p21CIP1/WAF1 undergo normal development, but are defective in G1 checkpoint control. *Cell*, **82**(4), 675–684. (Cited on page 100.)

Dennis Jr, Glynn, Sherman, Brad T, Hosack, Douglas A, Yang, Jun, Gao, Wei, Lane, H Clifford, Lempicki, Richard A, *et al.* 2003. DAVID: database for annotation, visualization, and integrated discovery. *Genome biol*, **4**(5), P3. (Cited on page 45.)

Deriano, Ludovic, Stracker, Travis H, Baker, Annalee, Petrini, John HJ, & Roth, David B. 2009. Roles for NBS1 in alternative nonhomologous end-joining of V (D) J recombination intermediates. *Molecular cell*, **34**(1), 13–25. (Cited on page 9.)

Desai-Mehta, A., Cerosaletti, K. M., & Concannon, P. 2001. Distinct functional domains of nibrin mediate Mre11 binding, focus formation, and nuclear localization. *Mol Cell Biol*, **21**(6), 2184–2191. (Cited on page 6.)

Dianov, Grigory L, & Hübscher, Ulrich. 2013. Mammalian base excision repair: the forgotten archangel. *Nucleic acids research*, **41**(6), 3483–3490. (Cited on page 15.)

Dickinson, Bryan C, & Chang, Christopher J. 2011. Chemistry and biology of reactive oxygen species in signaling or stress responses. *Nature chemical biology*, **7**(8), 504–511. (Cited on page 22.)

Diebold, Sandra S., Kaisho, Tsuneyasu, Hemmi, Hiroaki, Akira, Shizuo, & Reis e Sousa, Caetano. 2004. Innate antiviral responses by means of TLR7-mediated recognition of single-stranded RNA. *Science*, **303**(5663), 1529–1531. (Cited on page 156.)

Difilippantonio, Simone, Celeste, Arkady, Fernandez-Capetillo, Oscar, Chen, Hua-Tang, Reina San Martin, Bernardo, Van Laethem, Francois, Yang, Yong-Ping, Petukhova, Galina V., Eckhaus, Michael, Feigenbaum, Lionel, Manova, Katia, Kruhlak, Michael, Camerini-Otero, R Daniel, Sharan, Shyam, Nussenzweig, Michel, & Nussenzweig, André. 2005. Role of Nbs1 in the activation of the Atm kinase revealed in humanized mouse models. *Nat Cell Biol*, **7**(7), 675–685. (Cited on pages 4, 161, 165, and 174.)

Dinkelmann, Maria, Spehalski, Elizabeth, Stoneham, Trina, Buis, Jeffrey, Wu, Yipin, Sekiguchi, JoAnn M, & Ferguson, David O. 2009. Multiple functions of MRN in end-joining pathways during isotype class switching. *Nature structural & molecular biology*, **16**(8), 808–813. (Cited on page 9.)

Do, Jeong Tae, & Schöler, Hans R. 2009. Regulatory circuits underlying pluripotency and reprogramming. *Trends in pharmacological sciences*, **30**(6), 296–302. (Cited on page 25.)

Drews, Katharina, Jozefczuk, Justyna, Prigione, Alessandro, & Adjaye, James. 2012. Human induced pluripotent stem cells–from mechanisms to clinical applications. *J Mol Med (Berl)*, **90**(7), 735–745. (Cited on pages 155 and 156.)

Du, Zhong-Wei, & Zhang, Su-Chun. 2010. Lentiviral vector-mediated transgenesis in human embryonic stem cells. *Pages 127–134 of: Lentivirus Gene Engineering Protocols*. Springer. (Cited on page 34.)

Ellenberger, Tom, & Tomkinson, Alan E. 2008. Eukaryotic DNA ligases: structural and functional insights. *Annual review of biochemistry*, **77**, 313. (Cited on page 19.)

FACSCalibur, TM. 1996. System Users Guide. *BD Bioscences, August*, **1**, 1. (Cited on page 40.)

Falck, J., Mailand, N., Syljuåsen, R. G., Bartek, J., & Lukas, J. 2001. The ATM-Chk2-Cdc25A checkpoint pathway guards against radioresistant DNA synthesis. *Nature*, **410**(6830), 842–847. (Cited on page 100.)

Falck, Jacob, Petrini, John HJ, Williams, Bret R, Lukas, Jiri, & Bartek, Jiri. 2002. The DNA damage-dependent intra–S phase checkpoint is regulated by parallel pathways. *Nature genetics*, **30**(3), 290–294. (Cited on page 167.)

Falck, Jacob, Coates, Julia, & Jackson, Stephen P. 2005. Conserved modes of recruitment of ATM, ATR and DNA-PKcs to sites of DNA damage. *Nature*, **434**(7033), 605–611. (Cited on page 6.)

Finkel, Toren, & Holbrook, Nikki J. 2000. Oxidants, oxidative stress and the biology of ageing. *Nature*, **408**(6809), 239–247. (Cited on pages 20, 21, 22, and 23.)

Firoved, Aaron M, Wood, Simon R, Ornatowski, Wojciech, Deretic, Vojo, & Timmins, Graham S. 2004. Microarray analysis and functional characterization of the nitrosative stress response in nonmucoid and mucoid Pseudomonas aeruginosa. *Journal of bacteriology*, **186**(12), 4046–4050. (Cited on page 171.)

Folmes, Clifford DL, Nelson, Timothy J, Martinez-Fernandez, Almudena, Arrell, D Kent, Lindor, Jelena Zlatkovic, Dzeja, Petras P, Ikeda, Yasuhiro, Perez-Terzic, Carmen, & Terzic, Andre. 2011. Somatic oxidative bioenergetics transitions into pluripotency-dependent glycolysis to facilitate nuclear reprogramming. *Cell metabolism*, **14**(2), 264–271. (Cited on page 26.)

Frappart, Pierre-Olivier, Tong, Wei-Min, Demuth, Ilja, Radovanovic, Ivan, Herceg, Zdenko, Aguzzi, Adriano, Digweed, Martin, & Wang, Zhao-Qi. 2005. An essential function for NBS1 in the prevention of ataxia and cerebellar defects. *Nat Med*, **11**(5), 538–544. (Cited on page 161.)

Freiberg, Rachel A, Krieg, Adam J, Giaccia, Amato J, & Hammond, Ester M. 2006. Review Checking in on Hypoxia/Reoxygenation. *Cell Cycle*, **5**(12), 1304–1307. (Cited on page 168.)

Fusaki, Noemi, Ban, Hiroshi, Nishiyama, Akiyo, Saeki, Koichi, & Hasegawa, Mamoru. 2009. Efficient induction of transgene-free human pluripotent stem cells using a vector based on Sendai virus, an RNA virus that does not integrate into

the host genome. *Proc Jpn Acad Ser B Phys Biol Sci*, **85**(8), 348–362. (Cited on page 154.)

Fuster, José J, Fernández, Patricia, González-Navarro, Herminia, Silvestre, Carlos, Nabah, Yafa Naim Abu, & Andrés, Vicente. 2010. Control of cell proliferation in atherosclerosis: insights from animal models and human studies. *Cardiovascular research*, **86**(2), 254–264. (Cited on page 11.)

Gandhi, Nitin Motilal, Gopalaswamy, Usulumarty Venu, & Nair, Cherupally rishnan K. 2003. Radiation protection by disulfiram: protection of membrane and DNA in vitro and in vivo against gamma-radiation. *J Radiat Res*, **44**(3), 255–259. (Cited on page 91.)

Gatz, Susanne A, & Wiesmüller, Lisa. 2008. Take a break: resveratrol in action on DNA. *Carcinogenesis*, **29**(2), 321–332. (Cited on page 163.)

Giampieri, Francesca, Alvarez-Suarez, José M, Mazzoni, Luca, Forbes-Hernandez, Tamara Y, Gasparrini, Massimiliano, Gonzàlez-Paramàs, Ana M, Santos-Buelga, Celestino, Quiles, José L, Bompadre, Stefano, Mezzetti, Bruno, *et al.* 2014. Polyphenol-rich strawberry extract protects human dermal fibroblasts against hydrogen peroxide oxidative damage and Improves mitochondrial functionality. *Molecules*, **19**(6), 7798–7816. (Cited on page 164.)

Glimm, Hanno, Oh, IL-Hoan, & Eaves, Connie J. 2000. Human hematopoietic stem cells stimulated to proliferate in vitro lose engraftment potential during their S/G2/M transit and do not reenter Go. *Blood*, **96**(13), 4185–4193. (Cited on page 26.)

Gordan, John D, Bertout, Jessica A, Hu, Cheng-Jun, Diehl, J Alan, & Simon, M Celeste. 2007. HIF-2α promotes hypoxic cell proliferation by enhancing c-myc transcriptional activity. *Cancer cell*, **11**(4), 335–347. (Cited on page 168.)

Greaves, Mel F, & Wiemels, Joe. 2003. Origins of chromosome translocations in childhood leukaemia. *Nature Reviews Cancer*, **3**(9), 639–649. (Cited on page 19.)

Greber, Boris, Lehrach, Hans, & Adjaye, James. 2007. Silencing of core transcription factors in human EC cells highlights the importance of autocrine FGF signaling for self-renewal. *BMC Dev Biol*, **7**, 46. (Cited on page 25.)

Gu, Bai-Wei, Fan, Jian-Meng, Bessler, Monica, & Mason, Philip J. 2011. Accelerated hematopoietic stem cell aging in a mouse model of dyskeratosis congenita responds to antioxidant treatment. *Aging cell*, **10**(2), 338–348. (Cited on page 164.)

Guzy, Robert D, & Schumacker, Paul T. 2006. Oxygen sensing by mitochondria at complex III: the paradox of increased reactive oxygen species during hypoxia. *Experimental Physiology*, **91**(5), 807–819. (Cited on page 22.)

Hackenbeck, Thomas, Knaup, Karl Xaver, Schietke, Ruth, Schodel, J, Willam, Carsten, Wu, Xiaoqing, Warnecke, Christina, Eckardt, Kai-Uwe, & Wiesener, Michael Sean. 2009. HIF-1 or HIF-2 induction is sufficient to achieve cell cycle arrest in NIH3T3 mouse fibroblasts independent from hypoxia. *Cell Cycle*, **8**(9), 1386–1395. (Cited on page 168.)

Halliwell, Barry. 2005. *Free radicals and other reactive species in disease*. Wiley Online Library. (Cited on pages 21 and 22.)

Hardeland, Rüdiger, Coto-Montes, Ana, & Poeggeler, Burkhard. 2003. Circadian rhythms, oxidative stress, and antioxidative defense mechanisms. *Chronobiol Int*, **20**(6), 921–962. (Cited on page 177.)

Harman, Denham. 1981. The aging process. *Proceedings of the National Academy of Sciences*, **78**(11), 7124–7128. (Cited on page 163.)

Hasegawa, Kouichi, Zhang, Peilin, Wei, Zong, Pomeroy, Jordan E., Lu, Wange, & Pera, Martin F. 2010. Comparison of reprogramming efficiency between transduction of reprogramming factors, cell-cell fusion, and cytoplast fusion. *Stem Cells*, **28**(8), 1338–1348. (Cited on pages 60 and 157.)

Havens, Courtney G, Ho, Alan, Yoshioka, Naohisa, & Dowdy, Steven F. 2006. Regulation of late G1/S phase transition and APCCdh1 by reactive oxygen species. *Molecular and cellular biology*, **26**(12), 4701–4711. (Cited on page 163.)

Hayashi, Naoyuki, Kobayashi, Masahiko, Shamma, Awad, Morimura, Yoko, Takahashi, Chiaki, & Yamamoto, Ken-ichi. 2013. Regulatory interaction between NBS1 and DNMT1 responding to DNA damage. *J Biochem*, **154**(5), 429–435. (Cited on pages 6 and 175.)

HAYFLICK, L. 1965. THE LIMITED IN VITRO LIFETIME OF HUMAN DIPLOID CELL STRAINS. *Exp Cell Res*, **37**(Mar), 614–636. (Cited on pages 53 and 151.)

Hefferin, Melissa L, & Tomkinson, Alan E. 2005. Mechanism of DNA double-strand break repair by non-homologous end joining. *DNA repair*, **4**(6), 639–648. (Cited on page 19.)

Helleday, Thomas, Lo, Justin, van Gent, Dik C, & Engelward, Bevin P. 2007. DNA double-strand break repair: from mechanistic understanding to cancer treatment. *DNA repair*, **6**(7), 923–935. (Cited on page 18.)

Helmink, Beth A, Bredemeyer, Andrea L, Lee, Baeck-Seung, Huang, Ching-Yu, Sharma, Girdhar G, Walker, Laura M, Bednarski, Jeffrey J, Lee, Wan-Ling, Pandita, Tej K, Bassing, Craig H, *et al.* 2009. MRN complex function in the repair of chromosomal Rag-mediated DNA double-strand breaks. *The Journal of experimental medicine*, **206**(3), 669–679. (Cited on page 9.)

Hirao, A., Kong, Y. Y., Matsuoka, S., Wakeham, A., Ruland, J., Yoshida, H., Liu, D., Elledge, S. J., & Mak, T. W. 2000. DNA damage-induced activation of p53 by the checkpoint kinase Chk2. *Science*, **287**(5459), 1824–1827. (Cited on page 100.)

Höhn, Annika, König, Jeannette, & Grune, Tilman. 2013. Protein oxidation in aging and the removal of oxidized proteins. *Journal of proteomics*, **92**, 132–159. (Cited on page 22.)

HOLTFRETER, J. 1947. Neural induction in explants which have passed through a sublethal cytolysis. *J Exp Zool*, **106**(2), 197–222. (Cited on page 157.)

Hopfner, K. P., Karcher, A., Shin, D. S., Craig, L., Arthur, L. M., Carney, J. P., & Tainer, J. A. 2000. Structural biology of Rad50 ATPase: ATP-driven conformational control in DNA double-strand break repair and the ABC-ATPase superfamily. *Cell*, **101**(7), 789–800. (Cited on page 7.)

Hopfner, Karl-Peter, Craig, Lisa, Moncalian, Gabriel, Zinkel, Robert A., Usui, Takehiko, Owen, Barbara A L., Karcher, Annette, Henderson, Brendan, Bodmer, Jean-Luc, McMurray, Cynthia T., Carney, James P., Petrini, John H J., & Tainer, John A. 2002. The Rad50 zinc-hook is a structure joining Mre11 complexes in DNA recombination and repair. *Nature*, **418**(6897), 562–566. (Cited on page 7.)

Howlett, Niall G, Scuric, Zorica, Dï¿œAndrea, Alan D, & Schiestl, Robert H. 2006. Impaired DNA double strand break repair in cells from Nijmegen breakage syndrome patients. *DNA repair*, **5**(2), 251–257. (Cited on page 161.)

Huang, Da Wei, Sherman, Brad T, & Lempicki, Richard A. 2009a. Bioinformatics enrichment tools: paths toward the comprehensive functional analysis of large gene lists. *Nucleic acids research*, **37**(1), 1–13. (Cited on page 172.)

Huang, Jun, Gong, Zihua, Ghosal, Gargi, & Chen, Junjie. 2009b. SOSS complexes participate in the maintenance of genomic stability. *Mol Cell*, **35**(3), 384–393. (Cited on page 6.)

Huangfu, Danwei, Maehr, René, Guo, Wenjun, Eijkelenboom, Astrid, Snitow, Melinda, Chen, Alice E., & Melton, Douglas A. 2008. Induction of pluripotent stem cells by defined factors is greatly improved by small-molecule compounds. *Nat Biotechnol*, **26**(7), 795–797. (Cited on page 157.)

Hubbi, Maimon E, Luo, Weibo, Baek, Jin H, & Semenza, Gregg L. 2011. MCM proteins are negative regulators of hypoxia-inducible factor 1. *Molecular cell*, **42**(5), 700–712. (Cited on page 168.)

Ichida, Justin K., Blanchard, Joel, Lam, Kelvin, Son, Esther Y., Chung, Julia E., Egli, Dieter, Loh, Kyle M., Carter, Ava C., Di Giorgio, Francesco P., Koszka, Kathryn, Huangfu, Danwei, Akutsu, Hidenori, Liu, David R., Rubin, Lee L., & Eggan, Kevin. 2009. A small-molecule inhibitor of tgf-Beta signaling replaces sox2 in reprogramming by inducing nanog. *Cell Stem Cell*, **5**(5), 491–503. (Cited on page 157.)

Iijima, Kenta, Ohara, Maki, Seki, Ryota, & Tauchi, Hiroshi. 2008. Dancing on damaged chromatin: functions of ATM and the RAD50/MRE11/NBS1 complex in cellular responses to DNA damage. *J Radiat Res*, **49**(5), 451–464. (Cited on page 102.)

Iliakis, George. 2009. Backup pathways of NHEJ in cells of higher eukaryotes: cell cycle dependence. *Radiotherapy and Oncology*, **92**(3), 310–315. (Cited on page 19.)

International Nijmegen Breakage Syndrome Study Group, The. 2000. Nijmegen breakage syndrome. *Arch Dis Child*, **82**(5), 400–406. (Cited on page 4.)

Ip, Stephen CY, Rass, Ulrich, Blanco, Miguel G, Flynn, Helen R, Skehel, J Mark, & West, Stephen C. 2008. Identification of Holliday junction resolvases from humans and yeast. *Nature*, **456**(7220), 357–361. (Cited on page 17.)

Ivanov, Evgeny L, Sugawara, Neal, Fishman-Lobell, Jacqueline, & Haber, James E. 1996. Genetic requirements for the single-strand annealing pathway of double-strand break repair in Saccharomyces cerevisiae. *Genetics*, **142**(3), 693–704. (Cited on page 17.)

Jia, Fangjun, Wilson, Kitchener D., Sun, Ning, Gupta, Deepak M., Huang, Mei, Li, Zongjin, Panetta, Nicholas J., Chen, Zhi Ying, Robbins, Robert C., Kay, Mark A., Longaker, Michael T., & Wu, Joseph C. 2010. A nonviral minicircle vector for deriving human iPS cells. *Nat Methods*, **7**(3), 197–199. (Cited on page 155.)

Jozefczuk, Justyna. 2009. Differentiation of human Embryonic Stem Cells into hepatocytes as a tool to analyse dynamic regulatory events during hepatogenesis in vitro. *Inaugural Dissertation*, **1**, 1. (Cited on page 35.)

Jozefczuk, Justyna, Kashofer, Karl, Ummanni, Ramesh, Henjes, Frauke, Rehman, Samrina, Geenen, Suzanne, Wruck, Wasco, Regenbrecht, Christian, Daskalaki, Andriani, Wierling, Christoph, Turano, Paola, Bertini, Ivano, Korf, Ulrike, Zatloukal, Kurt, Westerhoff, Hans V., Lehrach, Hans, & Adjaye, James. 2012. A Systems Biology Approach to Deciphering the Etiology of Steatosis Employing Patient-Derived Dermal Fibroblasts and iPS Cells. *Front Physiol*, **3**, 339. (Cited on page 35.)

Kaina, Bernd, Ochs, Kirsten, Grösch, Sabine, Frizz, Gerhard, Lips, Jochen, Tomicic, Maja, Dunkern, Torsten, & Christmann, Markus. 2001. BER, MGMT, and MMR in defense against alkylation-induced genotoxicity and apoptosis. *Progress in nucleic acid research and molecular biology*, **68**, 41–54. (Cited on page 15.)

Kane, Nicole M., Nowrouzi, Ali, Mukherjee, Sayandip, Blundell, Michael P., Greig, Jenny A., Lee, Wai Kwong, Houslay, Miles D., Milligan, Graeme, Mountford, Joanne C., von Kalle, Christof, Schmidt, Manfred, Thrasher, Adrian J., & Baker, Andrew H. 2010. Lentivirus-mediated reprogramming of somatic cells in the absence of transgenic transcription factors. *Mol Ther*, **18**(12), 2139–2145. (Cited on page 154.)

Kang, Jian, Bronson, Roderick T., & Xu, Yang. 2002. Targeted disruption of NBS1 reveals its roles in mouse development and DNA repair. *EMBO J*, **21**(6), 1447–1455. (Cited on page 118.)

Kanu, Nnennaya, & Behrens, Axel. 2007. ATMIN defines an NBS1-independent pathway of ATM signalling. *The EMBO journal*, **26**(12), 2933–2941. (Cited on page 168.)

Kato, Tatsuya, Sato, Nagato, Hayama, Satoshi, Yamabuki, Takumi, Ito, Tomoo, Miyamoto, Masaki, Kondo, Satoshi, Nakamura, Yusuke, & Daigo, Yataro. 2007. Activation of Holliday junction recognizing protein involved in the chromosomal stability and immortality of cancer cells. *Cancer Res*, **67**(18), 8544–8553. (Cited on page 6.)

Kawai, Taro, & Akira, Shizuo. 2007. Antiviral signaling through pattern recognition receptors. *J Biochem*, **141**(2), 137–145. (Cited on page 156.)

Kawamura, Teruhisa, Suzuki, Jotaro, Wang, Yunyuan V, Menendez, Sergio, Morera, Laura Batlle, Raya, Angel, Wahl, Geoffrey M, & Belmonte, Juan Carlos Izpisúa. 2009. Linking the p53 tumour suppressor pathway to somatic cell reprogramming. *Nature*, **460**(7259), 1140–1144. (Cited on page 25.)

Khalil, Hilal S, Tummala, Hemanth, Chakarov, Stoyan, Zhelev, Nikolai, & Lane, David P. 2012. Targeting ATM pathway for therapeutic intervention in cancer. *Biodiscovery*, **1**, 1. (Cited on pages 8, 10, 14, and 15.)

Kim, Jung-whan, Tchernyshyov, Irina, Semenza, Gregg L, & Dang, Chi V. 2006. HIF-1-mediated expression of pyruvate dehydrogenase kinase: a metabolic switch required for cellular adaptation to hypoxia. *Cell metabolism*, **3**(3), 177–185. (Cited on page 22.)

Kobayashi, Junya, Tauchi, Hiroshi, Sakamoto, Shuichi, Nakamura, Asako, Morishima, Ken-ichi, Matsuura, Shinya, Kobayashi, Toshiko, Tamai, Katsuyuki, Tanimoto, Keiji, & Komatsu, Kenshi. 2002. NBS1 localizes to gamma-H2AX foci through interaction with the FHA/BRCT domain. *Curr Biol*, **12**(21), 1846–1851. (Cited on pages 6, 8, and 175.)

Kobayashi, Junya, Okui, Michiyo, Asaithamby, Aroumougame, Burma, Sandeep, Chen, Benjamin P C., Tanimoto, Keiji, Matsuura, Shinya, Komatsu, Kenshi, & Chen, David J. 2010. WRN participates in translesion synthesis pathway through interaction with NBS1. *Mech Ageing Dev*, **131**(6), 436–444. (Cited on pages 6 and 175.)

Konigsberg, M, Pérez, VI, Ríos, C, Liu, Y, Lee, S, Shi, Y, & Van Remmen, H. 2013. Effect of oxygen tension on bioenergetics and proteostasis in young and old myoblast precursor cells. *Redox biology*, **1**(1), 475–482. (Cited on page 159.)

Koshiji, Minori, Kageyama, Yukio, Pete, Erin A, Horikawa, Izumi, Barrett, J Carl, & Huang, L Eric. 2004. HIF-1α induces cell cycle arrest by functionally counteracting Myc. *The EMBO journal*, **23**(9), 1949–1956. (Cited on page 168.)

Kousholt, Arne Nedergaard, Fugger, Kasper, Hoffmann, Saskia, Larsen, Brian D, Menzel, Tobias, Sartori, Alessandro A, & Sørensen, Claus Storgaard. 2012. CtIP-dependent DNA resection is required for DNA damage checkpoint maintenance but not initiation. *The Journal of cell biology*, **197**(7), 869–876. (Cited on page 17.)

Krüger, Lars, Demuth, Ilja, Neitzel, Heidemarie, Varon, Raymonda, Sperling, Karl, Chrzanowska, Krystyna H., Seemanova, Eva, & Digweed, Martin. 2007. Cancer incidence in Nijmegen breakage syndrome is modulated by the amount of a variant NBS protein. *Carcinogenesis*, **28**(1), 107–111. (Cited on pages 4 and 176.)

Kruse, Jan-Philipp, & Gu, Wei. 2008. SnapShot: p53 posttranslational modifications. *Cell*, **133**(5), 930–930. (Cited on page 168.)

Kuhn, Kenneth, Baker, Shawn C, Chudin, Eugene, Lieu, Minh-Ha, Oeser, Steffen, Bennett, Holly, Rigault, Philippe, Barker, David, McDaniel, Timothy K, & Chee, Mark S. 2004. A novel, high-performance random array platform for quantitative gene expression profiling. *Genome research*, **14**(11), 2347–2356. (Cited on page 44.)

Lammens, Katja, Bemeleit, Derk J., Möckel, Carolin, Clausing, Emanuel, Schele, Alexandra, Hartung, Sophia, Schiller, Christian B., Lucas, Maria, Angermüller, Christof, Söding, Johannes, Strässer, Katja, & Hopfner, Karl-Peter. 2011. The Mre11:Rad50 structure shows an ATP-dependent molecular clamp in DNA double-strand break repair. *Cell*, **145**(1), 54–66. (Cited on page 7.)

Larsen, Dorthe H., Hari, Flurina, Clapperton, Julie A., Gwerder, Myriam, Gutsche, Katrin, Altmeyer, Matthias, Jungmichel, Stephanie, Toledo, Luis I., Fink, Daniel, Rask, Maj-Britt, Grøfte, Merete, Lukas, Claudia, Nielsen, Michael L., Smerdon, Stephen J., Lukas, Jiri, & Stucki, Manuel. 2014. The NBS1-Treacle complex controls ribosomal RNA transcription in response to DNA damage. *Nat Cell Biol*, **16**(8), 792–803. (Cited on page 6.)

Lawson, Terence, & Stohs, Sidney. 1985. Changes in endogenous DNA damage in aging mice in response to butylated hydroxyanisole and oltipraz. *Mechanisms of ageing and development*, **30**(2), 179–185. (Cited on page 164.)

Lee, Andrew S, Tang, Chad, Rao, Mahendra S, Weissman, Irving L, & Wu, Joseph C. 2013. Tumorigenicity as a clinical hurdle for pluripotent stem cell therapies. *Nature medicine*, **19**(8), 998–1004. (Cited on page 26.)

Lee, Ji-Hoon, & Paull, Tanya T. 2005. ATM activation by DNA double-strand breaks through the Mre11-Rad50-Nbs1 complex. *Science*, **308**(5721), 551–554. (Cited on page 7.)

Lee, Jieun, Sayed, Nazish, Hunter, Arwen, Au, Kin Fai, Wong, Wing H., Mocarski, Edward S., Pera, Renee Reijo, Yakubov, Eduard, & Cooke, John P. 2012. Activation of innate immunity is required for efficient nuclear reprogramming. *Cell*, **151**(3), 547–558. (Cited on pages 48 and 156.)

Lee, Joo Hyeon, Xu, Bo, Lee, Chang-Hun, Ahn, Jun-Young, Song, Min Sup, Lee, Ho, Canman, Christine E, Lee, Jong-Soo, Kastan, Michael B, & Lim, Dae-Sik. 2003. Distinct Functions of Nijmegen Breakage Syndrome in Ataxia Telangiectasia Mutated-Dependent Responses to DNA Damage. *Molecular cancer research*, **1**(9), 674–681. (Cited on page 8.)

Lee, Joon, & Dunphy, William G. 2013. The Mre11-Rad50-Nbs1 (MRN) complex has a specific role in the activation of Chk1 in response to stalled replication forks. *Molecular biology of the cell*, **24**(9), 1343–1353. (Cited on page 9.)

Lee-Theilen, Mieun, Matthews, Allysia J, Kelly, Dierdre, Zheng, Simin, & Chaudhuri, Jayanta. 2011. CtIP promotes microhomology-mediated alternative end joining during class-switch recombination. *Nature structural & molecular biology*, **18**(1), 75–79. (Cited on page 19.)

Leslie, Mitch. 2013. How to live without BRCA1. *The Journal of cell biology*, **200**(2), 127–127. (Cited on page 17.)

Li, Bin, Takeda, Kazuhisa, Yokoyama, Satoru, & Shibahara, Shigeki. 2008. A prolyl-hydroxylase inhibitor, ethyl-3, 4-dihydroxybenzoate, induces haem oxygenase-1 expression in human cells through a mechanism independent of hypoxia-inducible factor-1α. *Journal of biochemistry*, **144**(5), 643–654. (Cited on page 164.)

Li, Ronghui, Liang, Jialiang, Ni, Su, Zhou, Ting, Qing, Xiaobing, Li, Huapeng, He, Wenzhi, Chen, Jiekai, Li, Feng, Zhuang, Qiang, *et al.* 2010. A mesenchymal-to-epithelial transition initiates and is required for the nuclear reprogramming of mouse fibroblasts. *Cell stem cell*, **7**(1), 51–63. (Cited on page 25.)

Li, Tao-Sheng, & Marbán, Eduardo. 2010. Physiological levels of reactive oxygen species are required to maintain genomic stability in stem cells. *Stem Cells*, **28**(7), 1178–1185. (Cited on pages 22 and 23.)

Li, Wenlin, Wei, Wei, Zhu, Saiyong, Zhu, Jinliang, Shi, Yan, Lin, Tongxiang, Hao, Ergeng, Hayek, Alberto, Deng, Hongkui, & Ding, Sheng. 2009. Generation of rat and human induced pluripotent stem cells by combining genetic reprogramming and chemical inhibitors. *Cell Stem Cell*, **4**(1), 16–19. (Cited on page 156.)

Li, Xuan, & Heyer, Wolf-Dietrich. 2009. RAD54 controls access to the invading 3 -OH end after RAD51-mediated DNA strand invasion in homologous recombination in Saccharomyces cerevisiae. *Nucleic acids research*, **37**(2), 638–646. (Cited on page 17.)

Liao, Baojian, Bao, Xichen, Liu, Longqi, Feng, Shipeng, Zovoilis, Athanasios, Liu, Wenbo, Xue, Yanting, Cai, Jie, Guo, Xiangpeng, Qin, Baoming, *et al.* 2011. MicroRNA cluster 302–367 enhances somatic cell reprogramming by accelerating a mesenchymal-to-epithelial transition. *Journal of Biological Chemistry*, **286**(19), 17359–17364. (Cited on page 25.)

Lieber, Michael R. 2010. The mechanism of double-strand DNA break repair by the nonhomologous DNA end joining pathway. *Annual review of biochemistry*, **79**, 181. (Cited on page 18.)

Lim, Dae-Sik, Kim, Seong-Tae, Xu, Bo, Maser, Richard S, Lin, Junyu, Petrini, John HJ, & Kastan, Michael B. 2000. ATM phosphorylates p95/nbs1 in an S-phase checkpoint pathway. *Nature*, **404**(6778), 613–617. (Cited on page 8.)

Lima, Cristovao F, Pereira-Wilson, Cristina, & Rattan, Suresh IS. 2011. Curcumin induces heme oxygenase-1 in normal human skin fibroblasts through redox signaling: Relevance for anti-aging intervention. *Molecular nutrition & food research*, **55**(3), 430–442. (Cited on page 164.)

Lin, Jianqing, Haffner, Michael C., Zhang, Yonggang, Lee, Byron H., Brennen, W Nathaniel, Britton, Justin, Kachhap, Sushant K., Shim, Joong Sup, Liu, Jun O., Nelson, William G., Yegnasubramanian, Srinivasan, & Carducci, Michael A. 2011. Disulfiram is a DNA demethylating agent and inhibits prostate cancer cell growth. *Prostate*, **71**(4), 333–343. (Cited on page 91.)

Lin, Shi-Lung, Chang, Donald C., Chang-Lin, Samantha, Lin, Chun-Hung, Wu, David T S., Chen, David T., & Ying, Shao-Yao. 2008. Mir-302 reprograms human skin cancer cells into a pluripotent ES-cell-like state. *RNA*, **14**(10), 2115–2124. (Cited on pages 155 and 156.)

Lin, Tongxiang, Ambasudhan, Rajesh, Yuan, Xu, Li, Wenlin, Hilcove, Simon, Abujarour, Ramzey, Lin, Xiangyi, Hahm, Heung Sik, Hao, Ergeng, Hayek, Alberto, & Ding, Sheng. 2009. A chemical platform for improved induction of human iPSCs. *Nat Methods*, **6**(11), 805–808. (Cited on pages 155 and 156.)

Liochev, Stefan I, & Fridovich, Irwin. 1999. Superoxide and iron: partners in crime. *IUBMB life*, **48**(2), 157–161. (Cited on page 21.)

Liu, Jinmiao, Liu, Mengyuan, Ye, Xiaoying, Liu, Kai, Huang, Junjiu, Wang, Lingling, Ji, Guangzhen, Liu, Na, Tang, Xiangdong, Baltz, Jay M, *et al.* 2012. Delay in oocyte aging in mice by the antioxidant N-acetyl-L-cysteine (NAC). *Human reproduction*, **27**(5), 1411–1420. (Cited on page 164.)

Liu, Q., Guntuku, S., Cui, X. S., Matsuoka, S., Cortez, D., Tamai, K., Luo, G., Carattini-Rivera, S., DeMayo, F., Bradley, A., Donehower, L. A., & Elledge, S. J. 2000. Chk1 is an essential kinase that is regulated by Atr and required for the G(2)/M DNA damage checkpoint. *Genes Dev*, **14**(12), 1448–1459. (Cited on page 99.)

Livak, Kenneth J, & Schmittgen, Thomas D. 2001. Analysis of Relative Gene Expression Data Using Real-Time Quantitative PCR and the 2< sup>- ΔΔCT</sup> Method. *methods*, **25**(4), 402–408. (Cited on page 39.)

Lloyd, Janette, Chapman, J Ross, Clapperton, Julie A., Haire, Lesley F., Hartsuiker, Edgar, Li, Jiejin, Carr, Antony M., Jackson, Stephen P., & Smerdon, Stephen J. 2009. A supramodular FHA/BRCT-repeat architecture mediates Nbs1 adaptor function in response to DNA damage. *Cell*, **139**(1), 100–111. (Cited on pages 29 and 175.)

Lluis, Frederic, & Cosma, Maria Pia. 2013. Resetting epigenetic signatures to induce somatic cell reprogramming. *Cell Mol Life Sci*, **70**(8), 1413–1424. (Cited on page 176.)

Lord, Christopher J, & Ashworth, Alan. 2012. The DNA damage response and cancer therapy. *Nature*, **481**(7381), 287–294. (Cited on page 14.)

Mah, Nancy, Wang, Ying, Liao, Mei-Chih, Prigione, Alessandro, Jozefczuk, Justyna, Lichtner, Björn, Wolfrum, Katharina, Haltmeier, Manuela, Flöttmann, Max, Schaefer, Martin, Hahn, Alexander, Mrowka, Ralf, Klipp, Edda, Andrade-Navarro, Miguel A., & Adjaye, James. 2011. Molecular insights into reprogramming-initiation events mediated by the OSKM gene regulatory network. *PLoS One*, **6**(8), e24351. (Cited on pages 25 and 156.)

Mao, Gen-xiang, Wang, Yan, Qiu, Qiang, Deng, Hong-bin, Yuan, Long-guo, Li, Rui-guo, Song, Dan-qing, Li, Yi-yang Yvonne, Li, Dian-dong, & Wang, Zhen. 2010. Salidroside protects human fibroblast cells from premature senescence induced by H< sub> 2</sub> O< sub> 2</sub> partly through modulating oxidative status. *Mechanisms of ageing and development*, **131**(11), 723–731. (Cited on page 164.)

Maraschio, P., Danesino, C., Antoccia, A., Ricordy, R., Tanzarella, C., Varon, R., Reis, A., Besana, D., Guala, A., & Tiepolo, L. 2001. A novel mutation and novel features in Nijmegen breakage syndrome. *J Med Genet*, **38**(2), 113–117. (Cited on page 4.)

Marión, Rosa M., Strati, Katerina, Li, Han, Murga, Matilde, Blanco, Raquel, Ortega, Sagrario, Fernandez-Capetillo, Oscar, Serrano, Manuel, & Blasco, Maria A. 2009. A p53-mediated DNA damage response limits reprogramming to ensure iPS cell genomic integrity. *Nature*, **460**(7259), 1149–1153. (Cited on pages 25 and 151.)

Martin, K., Trouche, D., Hagemeier, C., Sørensen, T. S., La Thangue, N. B., & Kouzarides, T. 1995. Stimulation of E2F1/DP1 transcriptional activity by MDM2 oncoprotein. *Nature*, **375**(6533), 691–694. (Cited on page 175.)

Martin, KR, & Barrett, JC. 2002. Reactive oxygen species as double-edged swords in cellular processes: low-dose cell signaling versus high-dose toxicity. *Human & experimental toxicology*, **21**(2), 71–75. (Cited on page 22.)

Maser, R. S., Zinkel, R., & Petrini, J. H. 2001a. An alternative mode of translation permits production of a variant NBS1 protein from the common Nijmegen breakage syndrome allele. *Nat Genet*, **27**(4), 417–421. (Cited on pages 5, 57, 152, 181, and 183.)

Maser, R. S., Mirzoeva, O. K., Wells, J., Olivares, H., Williams, B. R., Zinkel, R. A., Farnham, P. J., & Petrini, J. H. 2001b. Mre11 complex and DNA replication: linkage to E2F and sites of DNA synthesis. *Mol Cell Biol*, **21**(17), 6006–6016. (Cited on pages 152 and 175.)

Mason, Chris, & Dunnill, Peter. 2008. A brief definition of regenerative medicine. *1*, **1**, 1. (Cited on page 26.)

Matsuoka, S., Huang, M., & Elledge, S. J. 1998. Linkage of ATM to cell cycle regulation by the Chk2 protein kinase. *Science*, **282**(5395), 1893–1897. (Cited on page 100.)

Matsuura, S., Tauchi, H., Nakamura, A., Kondo, N., Sakamoto, S., Endo, S., Smeets, D., Solder, B., Belohradsky, B. H., Der Kaloustian, V. M., Oshimura, M., Isomura, M., Nakamura, Y., & Komatsu, K. 1998. Positional cloning of the gene for Nijmegen breakage syndrome. *Nat Genet*, **19**(2), 179–181. (Cited on page 5.)

Maury, Julien Jean Pierre, Choo, Andre Boon-Hwa, & Chan, Ken Kwok-Keung. 2011. Technical advances to genetically engineering human embryonic stem cells. *Integrative Biology*, **3**(7), 717–723. (Cited on page 27.)

McCarthy, C. 1996. Chromas: version 2.0. *Technelysium PTY, Australia*, **1**, 1. (Cited on page 39.)

McFarland, G. A., & Holliday, R. 1994. Retardation of the senescence of cultured human diploid fibroblasts by carnosine. *Exp Cell Res*, **212**(2), 167–175. (Cited on page 53.)

McVey, Mitch, & Lee, Sang Eun. 2008. MMEJ repair of double-strand breaks (directors cut): deleted sequences and alternative endings. *Trends in Genetics*, **24**(11), 529–538. (Cited on pages 19 and 161.)

Meek, Katheryn, Gupta, Shikha, Ramsden, Dale A, & Lees-Miller, Susan P. 2004. The DNA-dependent protein kinase: the director at the end. *Immunological reviews*, **200**(1), 132–141. (Cited on page 18.)

Melander, Fredrik, Bekker-Jensen, Simon, Falck, Jacob, Bartek, Jiri, Mailand, Niels, & Lukas, Jiri. 2008. Phosphorylation of SDT repeats in the MDC1 N terminus triggers retention of NBS1 at the DNA damage-modified chromatin. *J Cell Biol*, **181**(2), 213–226. (Cited on page 175.)

Metzger, L, & Iliakis, G. 1991. Kinetics of DNA double-strand break repair throughout the cell cycle as assayed by pulsed field gel electrophoresis in CHO cells. *International journal of radiation biology*, **59**(6), 1325–1339. (Cited on page 18.)

Mimeault, M, Hauke, R, & Batra, SK. 2007. Stem cells: a revolution in therapeuticsï¿œrecent advances in stem cell biology and their therapeutic applications in regenerative medicine and cancer therapies. *Clinical Pharmacology & Therapeutics*, **82**(3), 252–264. (Cited on page 26.)

Miyoshi, Norikatsu, Ishii, Hideshi, Nagano, Hiroaki, Haraguchi, Naotsugu, Dewi, Dyah Laksmi, Kano, Yoshihiro, Nishikawa, Shinpei, Tanemura, Masahiro, Mimori, Koshi, Tanaka, Fumiaki, Saito, Toshiyuki, Nishimura, Junichi, Takemasa, Ichiro, Mizushima, Tsunekazu, Ikeda, Masataka, Yamamoto, Hirofumi, Sekimoto, Mitsugu, Doki, Yuichiro, & Mori, Masaki. 2011. Reprogramming of mouse and human cells to pluripotency using mature microRNAs. *Cell Stem Cell*, **8**(6), 633–638. (Cited on pages 155 and 156.)

Mladenov, Emil, & Iliakis, George. 2011. Induction and repair of DNA double strand breaks: the increasing spectrum of non-homologous end joining pathways. *Mutation Research/Fundamental and Molecular Mechanisms of Mutagenesis*, **711**(1), 61–72. (Cited on page 19.)

Mladenov, Emil, Magin, Simon, Soni, Aashish, & Iliakis, George. 2013. DNA double-strand break repair as determinant of cellular radiosensitivity to killing and target in radiation therapy. *Frontiers in oncology*, **3**, 1. (Cited on pages 18 and 19.)

Mohammad, Duaa H., & Yaffe, Michael B. 2009. 14-3-3 proteins, FHA domains and BRCT domains in the DNA damage response. *DNA Repair (Amst)*, **8**(9), 1009–1017. (Cited on pages 29, 175, and 183.)

Moss, D. W. 1982. Alkaline phosphatase isoenzymes. *Clin Chem*, **28**(10), 2007–2016. (Cited on page 158.)

Mukherjee, Bipasha, Kessinger, Chase, Kobayashi, Junya, Chen, Benjamin PC, Chen, David J, Chatterjee, Aloke, & Burma, Sandeep. 2006. DNA-PK phosphorylates histone H2AX during apoptotic DNA fragmentation in mammalian cells. *DNA repair*, **5**(5), 575–590. (Cited on page 169.)

Müller, Franz-Josef, Schuldt, Bernhard M, Williams, Roy, Mason, Dylan, Altun, Gulsah, Papapetrou, Eirini P, Danner, Sandra, Goldmann, Johanna E, Herbst, Arne, Schmidt, Nils O, *et al.* 2011. A bioinformatic assay for pluripotency in human cells. *Nature methods*, **8**(4), 315–317. (Cited on page 131.)

Müller, Gerd, Tarasov, Kirill V., Gundry, Rebekah L., & Boheler, Kenneth R. 2012a. Human ESC/iPSC-based "Omics" and Bioinformatics for Translational Research. *Drug Discov Today Dis Models*, **9**(4), e161–e170. (Cited on page 158.)

Müller, Lars U W., Schlaeger, Thorsten M., DeVine, Alexander L., & Williams, David A. 2012b. Induced pluripotent stem cells as a tool for gaining new insights into Fanconi anemia. *Cell Cycle*, **11**(16), 2985–2990. (Cited on page 153.)

Müller, Lars U W., Milsom, Michael D., Harris, Chad E., Vyas, Rutesh, Brumme, Kristina M., Parmar, Kalindi, Moreau, Lisa A., Schambach, Axel, Park, In-Hyun, London, Wendy B., Strait, Kelly, Schlaeger, Thorsten, Devine, Alexander L., Grassman, Elke, D'Andrea, Alan, Daley, George Q., & Williams, David A. 2012c. Overcoming reprogramming resistance of Fanconi anemia cells. *Blood*, **119**(23), 5449–5457. (Cited on pages 80, 153, and 181.)

Nagendra, SN, Taranath Shetty, K, Subhash, MN, & Guru, SC. 1991. Role of glutathione reductase system in disulfiram conversion to diethyldithiocarbamate. *Life sciences*, **49**(1), 23–28. (Cited on page 164.)

Naka, Kazuhito, Ikeda, Kyoji, & Motoyama, Noboru. 2002. Recruitment of NBS1 into PML oncogenic domains via interaction with SP100 protein. *Biochem Biophys Res Commun*, **299**(5), 863–871. (Cited on page 6.)

Nakahara, Makoto, Sonoda, Eiichiro, Nojima, Kuniharu, Sale, Julian E., Takenaka, Katsuya, Kikuchi, Koji, Taniguchi, Yoshihito, Nakamura, Kyoko, Sumitomo, Yoshiki, Bree, Ronan T., Lowndes, Noel F., & Takeda, Shunichi. 2009. Genetic evidence for single-strand lesions initiating Nbs1-dependent homologous recombination in diversification of Ig v in chicken B lymphocytes. *PLoS Genet*, **5**(1), e1000356. (Cited on page 152.)

Nemavarkar, Purva, Chourasia, Bishnavath K, & Pasupathy, Karpagam. 2004. Evaluation of Radioprotective Action of Compounds Using Saccharomyces cerevisiae. *Journal of environmental pathology, toxicology and oncology*, **23**(2), 1. (Cited on page 164.)

Nishino, Koichiro, Toyoda, Masashi, Yamazaki-Inoue, Mayu, Fukawatase, Yoshihiro, Chikazawa, Emi, Sakaguchi, Hironari, Akutsu, Hidenori, & Umezawa, Akihiro. 2011. DNA methylation dynamics in human induced pluripotent stem cells over time. *PLoS Genet*, **7**(5), e1002085. (Cited on page 158.)

Obokata, Haruko, Wakayama, Teruhiko, Sasai, Yoshiki, Kojima, Koji, Vacanti, Martin P., Niwa, Hitoshi, Yamato, Masayuki, & Vacanti, Charles A. 2014a. Retraction: Stimulus-triggered fate conversion of somatic cells into pluripotency. *Nature*, **511**(7507), 112. (Cited on page 157.)

Obokata, Haruko, Wakayama, Teruhiko, Sasai, Yoshiki, Kojima, Koji, Vacanti, Martin P., Niwa, Hitoshi, Yamato, Masayuki, & Vacanti, Charles A. 2014b. Stimulus-triggered fate conversion of somatic cells into pluripotency. *Nature*, **505**(7485), 641–647. (Cited on page 157.)

Ohara, Maki, Funyu, Yumi, Ebara, Shunsuke, Sakamoto, Yuki, Seki, Ryota, Iijima, Kenta, Ohishi, Akiko, Kobayashi, Junya, Komatsu, Kenshi, Tachibana, Akira, *et al.* 2014. Mutations in the FHA-domain of ectopically expressed NBS1 lead to radiosensitization and to no increase in somatic mutation rates via a partial suppression of homologous recombination. *Journal of radiation research*, **1**, rru011. (Cited on page 160.)

Okita, Keisuke, Nakagawa, Masato, Hyenjong, Hong, Ichisaka, Tomoko, & Yamanaka, Shinya. 2008. Generation of mouse induced pluripotent stem cells without viral vectors. *Science*, **322**(5903), 949–953. (Cited on page 155.)

Oliveros, Juan C. 2007. VENNY. An interactive tool for comparing lists with Venn Diagrams. *1*, **1**, 1. (Cited on page 45.)

Olson, Erin, Nievera, Christian J., Lee, Alan Yueh-Luen, Chen, Longchuan, & Wu, Xiaohua. 2007. The Mre11-Rad50-Nbs1 complex acts both upstream and downstream of ataxia telangiectasia mutated and Rad3-related protein (ATR) to regulate the S-phase checkpoint following UV treatment. *J Biol Chem*, **282**(31), 22939–22952. (Cited on page 6.)

Onn, Itay, Heidinger-Pauli, Jill M, Guacci, Vincent, Ünal, Elçin, & Koshland, Douglas E. 2008. Sister chromatid cohesion: a simple concept with a complex reality. *Annual review of cell and developmental biology*, **24**, 105–129. (Cited on page 16.)

Ozbek, Emin. 2012. Induction of oxidative stress in kidney. *International journal of nephrology*, **2012**, 1. (Cited on page 20.)

Pan, Chuanying, Lu, Baisong, Chen, Hong, & Bishop, Colin E. 2010. Reprogramming human fibroblasts using HIV-1 TAT recombinant proteins OCT4, SOX2, KLF4 and c-MYC. *Molecular biology reports*, **37**(4), 2117–2124. (Cited on page 48.)

Panier, Stephanie, & Boulton, Simon J. 2013. Double-strand break repair: 53BP1 comes into focus. *Nature Reviews Molecular Cell Biology*, **1**, 1. (Cited on pages 19 and 20.)

Papapetrou, Eirini P., Tomishima, Mark J., Chambers, Stuart M., Mica, Yvonne, Reed, Evan, Menon, Jayanthi, Tabar, Viviane, Mo, Qianxing, Studer, Lorenz, & Sadelain, Michel. 2009. Stoichiometric and temporal requirements of Oct4, Sox2, Klf4, and c-Myc expression for efficient human iPSC induction and differentiation. *Proc Natl Acad Sci U S A*, **106**(31), 12759–12764. (Cited on page 156.)

Pâques, Frédéric, & Haber, James E. 1999. Multiple pathways of recombination induced by double-strand breaks in Saccharomyces cerevisiae. *Microbiology and molecular biology reviews*, **63**(2), 349–404. (Cited on page 17.)

Paranjpe, Ameya, & Srivenugopal, Kalkunte S. 2013. Degradation of NF-κB, p53 and other regulatory redox-sensitive proteins by thiol-conjugating and-nitrosylating drugs in human tumor cells. *Carcinogenesis*, **1**, bgt032. (Cited on page 164.)

Paranjpe, Ameya, Zhang, Ruiwen, Ali-Osman, Francis, Bobustuc, George C, & Srivenugopal, Kalkunte S. 2014. Disulfiram is a direct and potent inhibitor of human O6-methylguanine-DNA methyltransferase (MGMT) in brain tumor cells and mouse brain and markedly increases the alkylating DNA damage. *Carcinogenesis*, **35**(3), 692–702. (Cited on page 164.)

Pardue, Mary-Lou, Wizemann, Theresa M, *et al.* 2001. *Exploring the Biological Contributions to Human Health: Does Sex Matter?* National Academies Press. (Cited on page 174.)

Park, Hye-joon, Kim, Min-sung, Cho, Kumsun, Yun, Jang-hyuk, Choi, Yong-joon, & Cho, Chung-hyun. 2013. Disulfiram deregulates HIF-α subunits and blunts tumor adaptation to hypoxia in hepatoma cells. *Acta Pharmacologica Sinica*, **34**(9), 1208–1216. (Cited on page 164.)

Park, In-Hyun, Zhao, Rui, West, Jason A., Yabuuchi, Akiko, Huo, Hongguang, Ince, Tan A., Lerou, Paul H., Lensch, M William, & Daley, George Q. 2008. Reprogramming of human somatic cells to pluripotency with defined factors. *Nature*, **451**(7175), 141–146. (Cited on page 38.)

Pascucci, Barbara, Lemma, Tiziana, Iorio, Egidio, Giovannini, Sara, Vaz, Bruno, Iavarone, Ivano, Calcagnile, Angelo, Narciso, Laura, Degan, Paolo, Podo, Franca, *et al.* 2012. An altered redox balance mediates the hypersensitivity of Cockayne syndrome primary fibroblasts to oxidative stress. *Aging cell*, **11**(3), 520–529. (Cited on page 164.)

Pasque, Vincent, Jullien, Jerome, Miyamoto, Kei, Halley-Stott, Richard P., & Gurdon, J. B. 2011. Epigenetic factors influencing resistance to nuclear reprogramming. *Trends Genet*, **27**(12), 516–525. (Cited on page 176.)

Paull, T. T., & Gellert, M. 1999. Nbs1 potentiates ATP-driven DNA unwinding and endonuclease cleavage by the Mre11/Rad50 complex. *Genes Dev*, **13**(10), 1276–1288. (Cited on page 7.)

Pichierri, Pietro, & Franchitto, Annapaola. 2004. Werner syndrome protein, the MRE11 complex and ATR: menage-à-trois in guarding genome stability during DNA replication? *Bioessays*, **26**(3), 306–313. (Cited on page 9.)

Potter, Alan J., Gollahon, Katherine A., Palanca, Ben J A., Harbert, Mary J., Choi, Young M., Moskovitz, Alexander H., Potter, John D., & Rabinovitch, Peter S. 2002. Flow cytometric analysis of the cell cycle phase specificity of DNA damage induced by radiation, hydrogen peroxide and doxorubicin. *Carcinogenesis*, **23**(3), 389–401. (Cited on page 162.)

Prigione, Alessandro, & Adjaye, James. 2010. Modulation of mitochondrial biogenesis and bioenergetic metabolism upon in vitro and in vivo differentiation of human ES and iPS cells. *Int J Dev Biol*, **54**(11-12), 1729–1741. (Cited on pages 164 and 166.)

Prigione, Alessandro, Fauler, Beatrix, Lurz, Rudi, Lehrach, Hans, & Adjaye, James. 2010. The senescence-related mitochondrial/oxidative stress pathway is repressed in human induced pluripotent stem cells. *Stem Cells*, **28**(4), 721–733. (Cited on page 25.)

Prigione, Alessandro, Hossini, Amir M., Lichtner, Björn, Serin, Akdes, Fauler, Beatrix, Megges, Matthias, Lurz, Rudi, Lehrach, Hans, Makrantonaki, Eugenia, Zouboulis, Christos C., & Adjaye, James. 2011. Mitochondrial-associated cell death mechanisms are reset to an embryonic-like state in aged donor-derived iPS cells harboring chromosomal aberrations. *PLoS One*, **6**(11), e27352. (Cited on pages 25 and 74.)

Prigione, Alessandro, Rohwer, Nadine, Hoffmann, Sheila, Mlody, Barbara, Drews, Katharina, Bukowiecki, Raul, Blümlein, Katharina, Wanker, Erich E, Ralser, Markus, Cramer, Thorsten, *et al.* 2014. HIF1α Modulates Cell Fate Reprogramming Through Early Glycolytic Shift and Upregulation of PDK1–3 and PKM2. *Stem Cells*, **32**(2), 364–376. (Cited on pages 25, 164, 166, and 177.)

Qin, Jane Yuxia, Zhang, Li, Clift, Kayla L., Hulur, Imge, Xiang, Andy Peng, Ren, Bing-Zhong, & Lahn, Bruce T. 2010. Systematic comparison of constitutive promoters and the doxycycline-inducible promoter. *PLoS One*, **5**(5), e10611. (Cited on page 80.)

Rais, Yoach, Zviran, Asaf, Geula, Shay, Gafni, Ohad, Chomsky, Elad, Viukov, Sergey, Mansour, Abed AlFatah, Caspi, Inbal, Krupalnik, Vladislav, Zerbib, Mirie, Maza, Itay, Mor, Nofar, Baran, Dror, Weinberger, Leehee, Jaitin, Diego A., Lara-Astiaso, David, Blecher-Gonen, Ronnie, Shipony, Zohar, Mukamel, Zohar, Hagai, Tzachi, Gilad, Shlomit, Amann-Zalcenstein, Daniela, Tanay, Amos, Amit, Ido, Novershtern, Noa, & Hanna, Jacob H. 2013. Deterministic direct reprogramming of somatic cells to pluripotency. *Nature*, **502**(7469), 65–70. (Cited on pages 154 and 157.)

Ray, Paul D, Huang, Bo-Wen, & Tsuji, Yoshiaki. 2012. Reactive oxygen species (ROS) homeostasis and redox regulation in cellular signaling. *Cellular signalling*, **24**(5), 981–990. (Cited on page 22.)

Raya, Ángel, Rodríguez-Pizà, Ignasi, Navarro, Susana, Richaud-Patin, Yvonne, Guenechea, Guillermo, Sánchez-Danés, Adriana, Consiglio, Antonella, Bueren, Juan, & Belmonte, Juan Carlos Izpisúa. 2010. A protocol describing the genetic correction of somatic human cells and subsequent generation of iPS cells. *nature protocols*, **5**(4), 647–660. (Cited on page 181.)

Reinhardt, H Christian, & Yaffe, Michael B. 2009. Kinases that control the cell cycle in response to DNA damage: Chk1, Chk2, and MK2. *Curr Opin Cell Biol*, **21**(2), 245–255. (Cited on page 96.)

Reiter, Russel J. 1997. Aging and oxygen toxicity: relation to changes in melatonin. *Age*, **20**(4), 201–213. (Cited on page 164.)

Reitsema, Tarren, Klokov, Dmitry, Banáth, Judit P, & Olive, Peggy L. 2005. DNA-PK is responsible for enhanced phosphorylation of histone H2AX under hypertonic conditions. *DNA repair*, **4**(10), 1172–1181. (Cited on page 169.)

Ren, Bing, Cam, Hieu, Takahashi, Yasuhiko, Volkert, Thomas, Terragni, Jolyon, Young, Richard A., & Dynlacht, Brian David. 2002. E2F integrates cell cycle progression with DNA repair, replication, and G(2)/M checkpoints. *Genes Dev*, **16**(2), 245–256. (Cited on page 6.)

Resnick, Igor B., Kondratenko, Irina, Togoev, Oleg, Vasserman, Natalia, Shagina, Irena, Evgrafov, Oleg, Tverskaya, Svetlana, Cerosaletti, Karen M., Gatti, Richard A., & Concannon, Patrick. 2002. Nijmegen breakage syndrome: clinical characteristics and mutation analysis in eight unrelated Russian families. *J Pediatr*, **140**(3), 355–361. (Cited on page 4.)

Reynolds, Pamela, Anderson, Jennifer A, Harper, Jane V, Hill, Mark A, Botchway, Stanley W, Parker, Anthony W, & Oï¿œNeill, Peter. 2012. The dynamics of Ku70/80 and DNA-PKcs at DSBs induced by ionizing radiation is dependent on the complexity of damage. *Nucleic acids research*, **1**, gks879. (Cited on pages 15, 99, and 166.)

Riccardi, V. M. 1977. Trisomy 8: an international study of 70 patients. *Birth Defects Orig Artic Ser*, **13**(3C), 171–184. (Cited on page 77.)

Richter, C., Park, J. W., & Ames, B. N. 1988. Normal oxidative damage to mitochondrial and nuclear DNA is extensive. *Proc Natl Acad Sci U S A*, **85**(17), 6465–6467. (Cited on page 23.)

Rivera, S, Synenki, L, Zirk, A, Eisenbart, J, Feghali-Black, C, Mutlu, GM, Budinger, GS, Chandel, NS, & Jain, M. 2013. Mitochondrial Reactive Oxygen Species Regulate Tgf-Beta Signaling. *Am J Respir Crit Care Med*, **187**, A3998. (Cited on page 22.)

Rocha, Clarissa Ribeiro Reily, Lerner, Leticia Koch, Okamoto, Oswaldo Keith, Marchetto, Maria Carolina, & Menck, Carlos Frederico Martins. 2013. The role of DNA repair in the pluripotency and differentiation of human stem cells. *Mutat Res*, **752**(1), 25–35. (Cited on page 60.)

Rosenberg, Noah A, Pritchard, Jonathan K, Weber, James L, Cann, Howard M, Kidd, Kenneth K, Zhivotovsky, Lev A, & Feldman, Marcus W. 2002. Genetic structure of human populations. *Science*, **298**(5602), 2381–2385. (Cited on page 105.)

Rothkamm, Kai, Krüger, Ines, Thompson, Larry H, & Löbrich, Markus. 2003. Pathways of DNA double-strand break repair during the mammalian cell cycle. *Molecular and cellular biology*, **23**(16), 5706–5715. (Cited on page 18.)

Ryba, Tyrone, Battaglia, Dana, Pope, Benjamin D., Hiratani, Ichiro, & Gilbert, David M. 2011. Genome-scale analysis of replication timing: from bench to bioinformatics. *Nat Protoc*, **6**(6), 870–895. (Cited on page 85.)

Saeed, AI, Sharov, Vasily, White, Joe, Li, Jerry, Liang, Wei, Bhagabati, Nirmal, Braisted, J, Klapa, M, Currier, T, Thiagarajan, M, *et al.* 2003. TM4: a free, open-source system for microarray data management and analysis. *Biotechniques*, **34**(2), 374. (Cited on page 45.)

Saeed, Alexander I., Bhagabati, Nirmal K., Braisted, John C., Liang, Wei, Sharov, Vasily, Howe, Eleanor A., Li, Jianwei, Thiagarajan, Mathangi, White, Joseph A., & Quackenbush, John. 2006. TM4 microarray software suite. *Methods Enzymol*, **411**, 134–193. (Cited on page 45.)

Sakurai, Yasuteru, Komatsu, Kenshi, Agematsu, Kazunaga, & Matsuoka, Masao. 2009. DNA double strand break repair enzymes function at multiple steps in retroviral infection. *Retrovirology*, **6**, 114. (Cited on page 155.)

Saleh-Gohari, Nasrollah, & Helleday, Thomas. 2004. Conservative homologous recombination preferentially repairs DNA double-strand breaks in the S phase of the cell cycle in human cells. *Nucleic acids research*, **32**(12), 3683–3688. (Cited on page 163.)

Salewsky, Bastian, Wessendorf, Petra, Hirsch, Daniel, Krenzlin, Harald, & Digweed, Martin. 2013. Nijmegen breakage syndrome: the clearance pathway for mutant nibrin protein is allele specific. *Gene*, **519**(2), 217–221. (Cited on page 176.)

Samavarchi-Tehrani, Payman, Golipour, Azadeh, David, Laurent, Sung, Hoon-ki, Beyer, Tobias A, Datti, Alessandro, Woltjen, Knut, Nagy, Andras, & Wrana, Jeffrey L. 2010. Functional genomics reveals a BMP-driven mesenchymal-to-epithelial transition in the initiation of somatic cell reprogramming. *Cell stem cell*, **7**(1), 64–77. (Cited on page 25.)

San Filippo, Joseph, Sung, Patrick, & Klein, Hannah. 2008. Mechanism of eukaryotic homologous recombination. *Annu. Rev. Biochem.*, **77**, 229–257. (Cited on page 16.)

Sanchez, Y., Wong, C., Thoma, R. S., Richman, R., Wu, Z., Piwnica-Worms, H., & Elledge, S. J. 1997. Conservation of the Chk1 checkpoint pathway in mammals: linkage of DNA damage to Cdk regulation through Cdc25. *Science*, **277**(5331), 1497–1501. (Cited on page 99.)

Sartori, Alessandro A, Lukas, Claudia, Coates, Julia, Mistrik, Martin, Fu, Shuang, Bartek, Jiri, Baer, Richard, Lukas, Jiri, & Jackson, Stephen P. 2007. Human CtIP promotes DNA end resection. *Nature*, **450**(7169), 509–514. (Cited on page 17.)

Sasaki, T, Majamaa, KARI, & Uitto, J. 1987. Reduction of collagen production in keloid fibroblast cultures by ethyl-3, 4-dihydroxybenzoate. Inhibition of prolyl hydroxylase activity as a mechanism of action. *Journal of Biological Chemistry*, **262**(19), 9397–9403. (Cited on page 164.)

Sauer, Heinrich, Wartenberg, Maria, & Hescheler, Juergen. 2001. Reactive oxygen species as intracellular messengers during cell growth and differentiation. *Cellular Physiology and Biochemistry*, **11**(4), 173–186. (Cited on page 163.)

Saugar, Irene, Ortiz-Bazán, María Ángeles, & Tercero, José Antonio. 2014. Tolerating DNA damage during eukaryotic chromosome replication. *Experimental cell research*, **329**(1), 170–177. (Cited on page 12.)

Schärer, Orlando D. 2013. Nucleotide excision repair in eukaryotes. *Cold Spring Harbor perspectives in biology*, **5**(10), a012609. (Cited on page 15.)

Schmid, Tobias, Zhou, Jie, Kohl, Roman, & Brune, Bernhard. 2004. p300 relieves p53-evoked transcriptional repression of hypoxia-inducible factor-1 (HIF-1). *Biochem. J*, **380**, 289–295. (Cited on page 168.)

Schröter, Friederike, & Adjaye, James. 2014. The proteasome complex and the maintenance of pluripotency: sustain the fate by mopping up? *Stem Cell Research & Therapy*, **5**(1), 24. (Cited on page 176.)

Schulz, Tim J, Zarse, Kim, Voigt, Anja, Urban, Nadine, Birringer, Marc, & Ristow, Michael. 2007. Glucose Restriction Extends Caenorhabditis elegans Life Span by Inducing Mitochondrial Respiration and Increasing Oxidative Stress. *Cell metabolism*, **6**(4), 280–293. (Cited on page 163.)

Schwartz, Steven D, Hubschman, Jean-Pierre, Heilwell, Gad, Franco-Cardenas, Valentina, Pan, Carolyn K, Ostrick, Rosaleen M, Mickunas, Edmund, Gay, Roger, Klimanskaya, Irina, & Lanza, Robert. 2012. Embryonic stem cell trials for macular degeneration: a preliminary report. *The Lancet*, **379**(9817), 713–720. (Cited on page 26.)

Seeman, Pavel, Gebertová, Kateřina, Paděrová, Kateřina, Sperling, Karl, & Seemanová, E., Eva. 2004. Nijmegen breakage syndrome in 13primary microcephaly. *Pediatric Neurology*, **30**(3), 195–200. (Cited on page 3.)

Seemanová, E., Sperling, K., Neitzel, H., Varon, R., Hadac, J., Butova, O., Schröck, E., Seeman, P., & Digweed, M. 2006. Nijmegen breakage syndrome (NBS) with neurological abnormalities and without chromosomal instability. *J Med Genet*, **43**(3), 218–224. (Cited on page 4.)

Semenza, Gregg L. 2009. Regulation of oxygen homeostasis by hypoxia-inducible factor 1. *Physiology*, **24**(2), 97–106. (Cited on page 22.)

Shah, Kalpit, McCormack, Charles E, & Bradbury, Neil A. 2014. Do you know the sex of your cells? *American Journal of Physiology-Cell Physiology*, **306**(1), C3–C18. (Cited on pages 108 and 174.)

Shahar, OD, Ram, EVS Raghu, Shimshoni, E, Hareli, S, Meshorer, E, & Goldberg, M. 2011. Live imaging of induced and controlled DNA double-strand break formation reveals extremely low repair by homologous recombination in human cells. *Oncogene*, **31**(30), 3495–3504. (Cited on page 167.)

Shaheen, Montaser, Allen, Christopher, Nickoloff, Jac A, & Hromas, Robert. 2011. Synthetic lethality: exploiting the addiction of cancer to DNA repair. *Blood*, **117**(23), 6074–6082. (Cited on page 16.)

Shi, Yan, Desponts, Caroline, Do, Jeong Tae, Hahm, Heung Sik, Schöler, Hans R., & Ding, Sheng. 2008. Induction of pluripotent stem cells from mouse embryonic fibroblasts by Oct4 and Klf4 with small-molecule compounds. *Cell Stem Cell*, **3**(5), 568–574. (Cited on page 157.)

Shieh, S. Y., Ahn, J., Tamai, K., Taya, Y., & Prives, C. 2000. The human homologs of checkpoint kinases Chk1 and Cds1 (Chk2) phosphorylate p53 at multiple DNA damage-inducible sites. *Genes Dev*, **14**(3), 289–300. (Cited on page 100.)

Shieh, Sheau-Yann, Ikeda, Masako, Taya, Yoichi, & Prives, Carol. 1997. DNA damage-induced phosphorylation of p53 alleviates inhibition by MDM2. *Cell*, **91**(3), 325–334. (Cited on pages 100 and 168.)

Shrivastav, Meena, De Haro, Leyma P, & Nickoloff, Jac A. 2007. Regulation of DNA double-strand break repair pathway choice. *Cell research*, **18**(1), 134–147. (Cited on pages 9 and 15.)

Silva, João P, Gomes, Andreia C, Proença, Fernanda, & Coutinho, Olga P. 2009. Novel nitrogen compounds enhance protection and repair of oxidative DNA damage in a neuronal cell model: Comparison with quercetin. *Chemico-biological interactions*, **181**(3), 328–337. (Cited on page 164.)

Simonato, L., Baris, R., Saracci, R., Skidmore, J., & Winkelmann, R. 1989. Relation of environmental exposure to erionite fibres to risk of respiratory cancer. *IARC Sci Publ*, **1**(90), 398–405. (Cited on page 6.)

Simsek, Deniz, Brunet, Erika, Wong, Sunnie Yan-Wai, Katyal, Sachin, Gao, Yankun, McKinnon, Peter J, Lou, Jacqueline, Zhang, Lei, Li, James, Rebar, Edward J, *et al.* 2011. DNA ligase III promotes alternative nonhomologous end-joining during chromosomal translocation formation. *PLoS genetics*, **7**(6), e1002080. (Cited on page 19.)

Sohal, Rajindar S, & Weindruch, Richard. 1996. Oxidative stress, caloric restriction, and aging. *Science*, **273**(5271), 59–63. (Cited on page 163.)

Spycher, Christoph, Miller, Edward S., Townsend, Kelly, Pavic, Lucijana, Morrice, Nicholas A., Janscak, Pavel, Stewart, Grant S., & Stucki, Manuel. 2008. Constitutive phosphorylation of MDC1 physically links the MRE11-RAD50-NBS1 complex to damaged chromatin. *J Cell Biol*, **181**(2), 227–240. (Cited on page 175.)

Stadtman, Earl R. 1992. Protein oxidation and aging. *Science*, **257**(5074), 1220–1224. (Cited on page 22.)

Stanley, J. F., Pye, D., & MacGregor, A. 1975. Comparison of doubling numbers attained by cultured animal cells with life span of species. *Nature*, **255**(5504), 158–159. (Cited on page 53.)

Sterneckert, Jared L, Reinhardt, Peter, & Schöler, Hans R. 2014. Investigating human disease using stem cell models. *Nature Reviews Genetics*, **15**(9), 625–639. (Cited on pages 27 and 28.)

Stevens, R, Stevens, L, & Price, NC. 1983. The stabilities of various thiol compounds used in protein purifications. *Biochemical Education*, **11**(2), 70–70. (Cited on page 90.)

Stopper, H, Schmitt, E, & Kobras, K. 2005. Genotoxicity of phytoestrogens. *Mutation Research/Fundamental and Molecular Mechanisms of Mutagenesis*, **574**(1), 139–155. (Cited on page 163.)

Suhr, Steven T, Chang, Eun Ah, Tjong, Jonathan, Alcasid, Nathan, Perkins, Guy A, Goissis, Marcelo D, Ellisman, Mark H, Perez, Gloria I, & Cibelli, Jose B. 2010. Mitochondrial rejuvenation after induced pluripotency. *PLoS One*, **5**(11), e14095. (Cited on page 25.)

Szablowska-Gadomska, Ilona, Zayat, Valery, & Buzanska, Leonora. 2011. Influence of low oxygen tensions on expression of pluripotency genes in stem cells. *Acta neurobiologiae experimentalis*, **71**(1), 86–93. (Cited on page 159.)

Takahashi, Kazutoshi, & Yamanaka, Shinya. 2006. Induction of pluripotent stem cells from mouse embryonic and adult fibroblast cultures by defined factors. *Cell*, **126**(4), 663–676. (Cited on pages 25 and 154.)

Takahashi, Kazutoshi, Tanabe, Koji, Ohnuki, Mari, Narita, Megumi, Ichisaka, Tomoko, Tomoda, Kiichiro, & Yamanaka, Shinya. 2007. Induction of pluripotent stem cells from adult human fibroblasts by defined factors. *Cell*, **131**(5), 861–872. (Cited on pages 25, 27, 69, and 154.)

Tategu, Moe, Arauchi, Takako, Tanaka, Rena, Nakagawa, Hiroki, & Yoshida, Kenichi. 2007. Systems biology-based identification of crosstalk between E2F transcription factors and the Fanconi anemia pathway. *Gene Regul Syst Bio*, **1**, 1–8. (Cited on page 175.)

Tauchi, Hiroshi, Kobayashi, Junya, Morishima, Ken-ichi, van Gent, Dik C, Shiraishi, Takahiro, Verkaik, Nicole S, Ito, Emi, Nakamura, Asako, Sonoda, Eiichiro, Takata, Minoru, *et al.* 2002. Nbs1 is essential for DNA repair by homologous recombination in higher vertebrate cells. *Nature*, **420**(6911), 93–98. (Cited on page 182.)

Tavernier, Geertrui, Mlody, Barbara, Demeester, Jo, Adjaye, James, & De Smedt, Stefaan C. 2013. Current methods for inducing pluripotency in somatic cells. *Adv Mater*, **25**(20), 2765–2771. (Cited on pages 26, 154, and 157.)

Tello, Daniel, Balsa, Eduardo, Acosta-Iborra, Bárbara, Fuertes-Yebra, Esther, Elorza, Ainara, Ordóñez, Ángel, Corral-Escariz, María, Soro, Inés, López-Bernardo, Elia, Perales-Clemente, Ester, *et al.* 2011. Induction of the mitochondrial NDUFA4L2 protein by HIF-1α decreases oxygen consumption by inhibiting Complex I activity. *Cell metabolism*, **14**(6), 768–779. (Cited on page 159.)

Thomson, J. A., Itskovitz-Eldor, J., Shapiro, S. S., Waknitz, M. A., Swiergiel, J. J., Marshall, V. S., & Jones, J. M. 1998. Embryonic stem cell lines derived from human blastocysts. *Science*, **282**(5391), 1145–1147. (Cited on pages 24, 25, 27, 34, and 159.)

Tibbetts, Randal S, Brumbaugh, Kathryn M, Williams, Josie M, Sarkaria, Jann N, Cliby, William A, Shieh, Sheau-Yann, Taya, Yoichi, Prives, Carol, & Abraham, Robert T. 1999. A role for ATR in the DNA damage-induced phosphorylation of p53. *Genes & development*, **13**(2), 152–157. (Cited on page 168.)

Tseng, Shun-Fu, Chang, Chun-Yu, Wu, Kou-Juey, & Teng, Shu-Chun. 2005. Importin KPNA2 is required for proper nuclear localization and multiple functions of NBS1. *J Biol Chem*, **280**(47), 39594–39600. (Cited on page 6.)

Turrens, Julio F. 2003. Mitochondrial formation of reactive oxygen species. *The Journal of physiology*, **552**(2), 335–344. (Cited on page 21.)

Varon, R., Vissinga, C., Platzer, M., Cerosaletti, K. M., Chrzanowska, K. H., Saar, K., Beckmann, G., Seemanová, E., Cooper, P. R., Nowak, N. J., Stumm, M., Weemaes, C. M., Gatti, R. A., Wilson, R. K., Digweed, M., Rosenthal, A., Sperling, K., Concannon, P., & Reis, A. 1998. Nibrin, a novel DNA double-strand break repair protein, is mutated in Nijmegen breakage syndrome. *Cell*, **93**(3), 467–476. (Cited on page 4.)

Varon, R., Seemanova, E., Chrzanowska, K., Hnateyko, O., Piekutowska-Abramczuk, D., Krajewska-Walasek, M., Sykut-Cegielska, J., Sperling, K., & Reis, A. 2000. Clinical ascertainment of Nijmegen breakage syndrome (NBS) and prevalence of the major mutation, 657del5, in three Slav populations. *Eur J Hum Genet*, **8**(11), 900–902. (Cited on pages 4 and 53.)

Varon, Raymonda, Dutrannoy, Véronique, Weikert, Georg, Tanzarella, Caterina, Antoccia, Antonio, Stöckl, Lars, Spadoni, Emanuela, Krüger, Lars-Arne, di Masi, Alessandra, Sperling, Karl, Digweed, Martin, & Maraschio, Paola. 2006. Mild Nijmegen breakage syndrome phenotype due to alternative splicing. *Hum Mol Genet*, **15**(5), 679–689. (Cited on page 4.)

Vessoni, AT, Filippi-Chiela, EC, Menck, C FM, & Lenz, G. 2013. Autophagy and genomic integrity. *Cell Death & Differentiation*, **20**(11), 1444–1454. (Cited on page 176.)

Vidal, Anxo, & Koff, Andrew. 2000. Cell-cycle inhibitors: three families united by a common cause. *Gene*, **247**(1), 1–15. (Cited on page 11.)

Vilenchik, Michael M., & Knudson, Alfred G. 2003. Endogenous DNA double-strand breaks: production, fidelity of repair, and induction of cancer. *Proc Natl Acad Sci U S A*, **100**(22), 12871–12876. (Cited on pages 14 and 161.)

Vousden, Karen H., & Prives, Carol. 2009. Blinded by the Light: The Growing Complexity of p53. *Cell*, **137**(3), 413–431. (Cited on page 100.)

Wagner, Wolfgang, Horn, Patrick, Castoldi, Mirco, Diehlmann, Anke, Bork, Simone, Saffrich, Rainer, Benes, Vladimir, Blake, Jonathon, Pfister, Stefan, Eckstein, Volker, *et al.* 2008. Replicative senescence of mesenchymal stem cells: a continuous and organized process. *PloS one*, **3**(5), e2213. (Cited on page 26.)

Wang, Huichen, Rosidi, Bustanur, Perrault, Ronel, Wang, Minli, Zhang, Lihua, Windhofer, Frank, & Iliakis, George. 2005. DNA ligase III as a candidate component of backup pathways of nonhomologous end joining. *Cancer research*, **65**(10), 4020–4030. (Cited on page 19.)

Wang, Jian-Qiu, Chen, Jian-Hong, Chen, Yen-Chung, Chen, Mei-Yu, Hsieh, Chia-Ying, Teng, Shu-Chun, & Wu, Kou-Juey. 2013. Interaction between NBS1 and the mTOR/Rictor/SIN1 complex through specific domains. *PLoS One*, **8**(6), e65586. (Cited on page 6.)

Wang, Jin, Clauson, Cheryl L, Robbins, Paul D, Niedernhofer, Laura J, & Wang, Yinsheng. 2012. The oxidative DNA lesions 8, 5 -cyclopurines accumulate with aging in a tissue-specific manner. *Aging cell*, **11**(4), 714–716. (Cited on page 162.)

Wang, Minli, Wu, Weizhong, Wu, Wenqi, Rosidi, Bustanur, Zhang, Lihua, Wang, Huichen, & Iliakis, George. 2006. PARP-1 and Ku compete for repair of DNA double strand breaks by distinct NHEJ pathways. *Nucleic acids research*, **34**(21), 6170–6182. (Cited on page 19.)

Wang, Y., Cortez, D., Yazdi, P., Neff, N., Elledge, S. J., & Qin, J. 2000. BASC, a super complex of BRCA1-associated proteins involved in the recognition and repair of aberrant DNA structures. *Genes Dev*, **14**(8), 927–939. (Cited on page 6.)

Wang, Ying, Mah, Nancy, Prigione, Alessandro, Wolfrum, Katharina, Andrade-Navarro, Miguel A., & Adjaye, James. 2010. A transcriptional roadmap to the induction of pluripotency in somatic cells. *Stem Cell Rev*, **6**(2), 282–296. (Cited on page 171.)

Ward, Irene M, Minn, Kay, & Chen, Junjie. 2004. UV-induced ataxia-telangiectasia-mutated and Rad3-related (ATR) activation requires replication stress. *Journal of Biological Chemistry*, **279**(11), 9677–9680. (Cited on page 169.)

Warren, Luigi, Manos, Philip D., Ahfeldt, Tim, Loh, Yuin-Han, Li, Hu, Lau, Frank, Ebina, Wataru, Mandal, Pankaj K., Smith, Zachary D., Meissner, Alexander, Daley, George Q., Brack, Andrew S., Collins, James J., Cowan, Chad, Schlaeger, Thorsten M., & Rossi, Derrick J. 2010. Highly efficient reprogramming to pluripotency and directed differentiation of human cells with synthetic modified mRNA. *Cell Stem Cell*, **7**(5), 618–630. (Cited on pages 155 and 156.)

Waters, David J, Shen, Shuren, Cooley, Dawn M, Bostwick, David G, Qian, Junqi, Combs, Gerald F, Glickman, Lawrence T, Oteham, Carol, Schlittler, Deborah, & Morris, J Steven. 2003. Effects of dietary selenium supplementation on DNA damage and apoptosis in canine prostate. *Journal of the National Cancer Institute*, **95**(3), 237–241. (Cited on page 164.)

Weemaes, C. M., Hustinx, T. W., Scheres, J. M., van Munster, P. J., Bakkeren, J. A., & Taalman, R. D. 1981. A new chromosomal instability disorder: the Nijmegen breakage syndrome. *Acta Paediatr Scand*, **70**(4), 557–564. (Cited on pages 3 and 29.)

Wei, Caimiao, Li, Jiangning, & Bumgarner, Roger E. 2004. Sample size for detecting differentially expressed genes in microarray experiments. *BMC genomics*, **5**(1), 87. (Cited on page 171.)

West, A Phillip, Brodsky, Igor E, Rahner, Christoph, Woo, Dong Kyun, Erdjument-Bromage, Hediye, Tempst, Paul, Walsh, Matthew C, Choi, Yongwon, Shadel, Gerald S, & Ghosh, Sankar. 2011. TLR signalling augments macrophage bactericidal activity through mitochondrial ROS. *Nature*, **472**(7344), 476–480. (Cited on page 163.)

West, Stephen C. 2003. Molecular views of recombination proteins and their control. *Nature reviews Molecular cell biology*, **4**(6), 435–445. (Cited on page 17.)

Wilda, M., Demuth, I., Concannon, P., Sperling, K., & Hameister, H. 2000. Expression pattern of the Nijmegen breakage syndrome gene, Nbs1, during murine development. *Hum Mol Genet*, **9**(12), 1739–1744. (Cited on page 4.)

Williams, Gareth J., Lees-Miller, Susan P., & Tainer, John A. 2010. Mre11-Rad50-Nbs1 conformations and the control of sensing, signaling, and effector responses at DNA double-strand breaks. *DNA Repair (Amst)*, **9**(12), 1299–1306. (Cited on pages 7, 8, and 9.)

Williams, R Scott, Moncalian, Gabriel, Williams, Jessica S., Yamada, Yoshiki, Limbo, Oliver, Shin, David S., Groocock, Lynda M., Cahill, Dana, Hitomi, Chiharu, Guenther, Grant, Moiani, Davide, Carney, James P., Russell, Paul, & Tainer, John A. 2008. Mre11 dimers coordinate DNA end bridging and nuclease processing in double-strand-break repair. *Cell*, **135**(1), 97–109. (Cited on page 7.)

Williams, R Scott, Dodson, Gerald E, Limbo, Oliver, Yamada, Yoshiki, Williams, Jessica S, Guenther, Grant, Classen, Scott, Glover, JN, Iwasaki, Hiroshi, Russell, Paul, *et al.* 2009. Nbs1 flexibly tethers Ctp1 and Mre11-Rad50 to coordinate DNA double-strand break processing and repair. *Cell*, **139**(1), 87–99. (Cited on pages 6, 8, and 175.)

Willis, Jeremy, DeStephanis, Darla, Patel, Yogin, Gowda, Vrushab, & Yan, Shan. 2012. Study of the DNA damage checkpoint using Xenopus egg extracts. *Journal of visualized experiments: JoVE*, **1**(69), 1. (Cited on page 168.)

Wolfrum, Katharina, Wang, Ying, Prigione, Alessandro, Sperling, Karl, Lehrach, Hans, & Adjaye, James. 2010. The LARGE principle of cellular reprogramming: lost, acquired and retained gene expression in foreskin and amniotic fluid-derived human iPS cells. *PLoS One*, **5**(10), e13703. (Cited on page 171.)

Wood, Zachary A, Schröder, Ewald, Robin Harris, J, & Poole, Leslie B. 2003. Structure, mechanism and regulation of peroxiredoxins. *Trends in biochemical sciences*, **28**(1), 32–40. (Cited on page 22.)

Woodbine, Lisa, Brunton, H, Goodarzi, AA, Shibata, A, & Jeggo, PA. 2011. Endogenously induced DNA double strand breaks arise in heterochromatic DNA regions and require ataxia telangiectasia mutated and Artemis for their repair. *Nucleic acids research*, **39**(16), 6986–6997. (Cited on pages 22 and 163.)

Wu, Leonard, & Hickson, Ian D. 2003. The Bloom's syndrome helicase suppresses crossing over during homologous recombination. *Nature*, **426**(6968), 870–874. (Cited on page 17.)

Wu, Liming, Luo, Kuntian, Lou, Zhenkun, & Chen, Junjie. 2008a. MDC1 regulates intra-S-phase checkpoint by targeting NBS1 to DNA double-strand breaks. *Proc Natl Acad Sci U S A*, **105**(32), 11200–11205. (Cited on page 175.)

Wu, Wenqi, Wang, Minli, Wu, Weizhong, Singh, Satyendra K., Mussfeldt, Tamara, & Iliakis, George. 2008b. Repair of radiation induced DNA double strand breaks by backup NHEJ is enhanced in G2. *DNA Repair (Amst)*, **7**(2), 329–338. (Cited on page 114.)

Xia, Xiaofeng, Zhang, Yingsha, Zieth, Caroline R., & Zhang, Su-Chun. 2007. Transgenes delivered by lentiviral vector are suppressed in human embryonic stem cells in a promoter-dependent manner. *Stem Cells Dev*, **16**(1), 167–176. (Cited on page 80.)

Xu, C., Inokuma, M. S., Denham, J., Golds, K., Kundu, P., Gold, J. D., & Carpenter, M. K. 2001. Feeder-free growth of undifferentiated human embryonic stem cells. *Nat Biotechnol*, **19**(10), 971–974. (Cited on page 34.)

Xu, Xingzhi, Tsvetkov, Lyuben M., & Stern, David F. 2002. Chk2 activation and phosphorylation-dependent oligomerization. *Mol Cell Biol*, **22**(12), 4419–4432. (Cited on page 100.)

Yanagihara, Hiromi, Kobayashi, Junya, Tateishi, Satoshi, Kato, Akihiro, Matsuura, Shinya, Tauchi, Hiroshi, Yamada, Kouichi, Takezawa, Jun, Sugasawa, Kaoru, Masutani, Chikahide, Hanaoka, Fumio, Weemaes, Corry M., Mori, Toshio, Zou, Lee, & Komatsu, Kenshi. 2011. NBS1 recruits RAD18 via a RAD6-like domain and regulates Pol η-dependent translesion DNA synthesis. *Mol Cell*, **43**(5), 788–797. (Cited on pages 152 and 153.)

Ying, Qi-Long, Wray, Jason, Nichols, Jennifer, Batlle-Morera, Laura, Doble, Bradley, Woodgett, James, Cohen, Philip, & Smith, Austin. 2008. The ground state of embryonic stem cell self-renewal. *Nature*, **453**(7194), 519–523. (Cited on page 157.)

Yu, Junying, Hu, Kejin, Smuga-Otto, Kim, Tian, Shulan, Stewart, Ron, Slukvin, Igor I., & Thomson, James A. 2009. Human induced pluripotent stem cells free of vector and transgene sequences. *Science*, **324**(5928), 797–801. (Cited on pages 47, 64, and 155.)

Yu, Junying, Chau, Kevin Fongching, Vodyanik, Maxim A., Jiang, Jinlan, & Jiang, Yong. 2011. Efficient feeder-free episomal reprogramming with small molecules. *PLoS One*, **6**(3), e17557. (Cited on pages 47, 48, 64, 155, and 156.)

Yuan, Jingsong, & Chen, Junjie. 2009. N terminus of CtIP is critical for homologous recombination-mediated double-strand break repair. *J Biol Chem*, **284**(46), 31746–31752. (Cited on page 6.)

Yuan, Zhigang, Zhang, Xiaohong, Sengupta, Nilanjan, Lane, William S., & Seto, Edward. 2007. SIRT1 regulates the function of the Nijmegen breakage syndrome protein. *Mol Cell*, **27**(1), 149–162. (Cited on pages 5 and 6.)

Zha, Shan, Boboila, Cristian, & Alt, Frederick W. 2009. Mre11: roles in DNA repair beyond homologous recombination. *Nature structural & molecular biology*, **16**(8), 798–800. (Cited on page 19.)

Zhang, Junran, Willers, Henning, Feng, Zhihui, Ghosh, Jagadish C, Kim, Sang, Weaver, David T, Chung, Jay H, Powell, Simon N, & Xia, Fen. 2004. Chk2 phosphorylation of BRCA1 regulates DNA double-strand break repair. *Molecular and cellular biology*, **24**(2), 708–718. (Cited on page 102.)

Zhang, P, & Omaye, ST. 2001. Antioxidant and prooxidant roles for β-carotene, α-tocopherol and ascorbic acid in human lung cells. *Toxicology in vitro*, **15**(1), 13–24. (Cited on page 164.)

Zhang, Ying, Zhou, Junqing, & Lim, Chang Uk. 2006. The role of NBS1 in DNA double strand break repair, telomere stability, and cell cycle checkpoint control. *Cell Res*, **16**(1), 45–54. (Cited on page 9.)

Zhao, H., & Piwnica-Worms, H. 2001. ATR-mediated checkpoint pathways regulate phosphorylation and activation of human Chk1. *Mol Cell Biol*, **21**(13), 4129–4139. (Cited on page 99.)

Zhao, Hong, Tanaka, Toshiki, Mitlitski, Vadim, Heeter, Julie, Balazs, Endre A, & Darzynkiewicz, Zbigniew. 2008. Protective effect of hyaluronate on oxidative DNA damage in WI-38 and A549 cells. *International journal of oncology*, **32**(6), 1159. (Cited on page 164.)

Zhong, Q., Chen, C. F., Li, S., Chen, Y., Wang, C. C., Xiao, J., Chen, P. L., Sharp, Z. D., & Lee, W. H. 1999. Association of BRCA1 with the hRad50-hMre11-p95 complex and the DNA damage response. *Science*, **285**(5428), 747–750. (Cited on page 6.)

Zhou, Hongyan, Wu, Shili, Joo, Jin Young, Zhu, Saiyong, Han, Dong Wook, Lin, Tongxiang, Trauger, Sunia, Bien, Geoffery, Yao, Susan, Zhu, Yong, Siuzdak, Gary, Schöler, Hans R., Duan, Lingxun, & Ding, Sheng. 2009. Generation of induced pluripotent stem cells using recombinant proteins. *Cell Stem Cell*, **4**(5), 381–384. (Cited on page 48.)

Zhu, J., Petersen, S., Tessarollo, L., & Nussenzweig, A. 2001. Targeted disruption of the Nijmegen breakage syndrome gene NBS1 leads to early embryonic lethality in mice. *Curr Biol*, **11**(2), 105–109. (Cited on pages 56 and 152.)

Zhu, X. D., Küster, B., Mann, M., Petrini, J. H., & de Lange, T. 2000. Cell-cycle-regulated association of RAD50/MRE11/NBS1 with TRF2 and human telomeres. *Nat Genet*, **25**(3), 347–352. (Cited on page 6.)

Der Lebenslauf ist in der Online-Version aus Gründen des Datenschutzes nicht enthalten.

The curriculum is not included in the online version for reasons of data protection.

PUBLICATIONS

HIF1alpha modulates cell fate reprogramming through early glycolytic shift and upregulation of PDK1-3 and PKM2.
Prigione A, Rohwer N, Hoffmann S, **Mlody B**, Drews K, Bukowiecki R, Blümlein K, Wanker EE, Ralser M, Cramer T, Adjaye J.
Stem Cells. 2014 Feb;32(2):364-76. doi: 10.1002/stem.1552.

Current methods for inducing pluripotency in somatic cells.
Tavernier G, **Mlody B**, Demeester J, Adjaye J, De Smedt SC.
Adv Mater. 2013 May 28;25(20):2765-71. doi: 10.1002/adma.201204874.

Comparative molecular portraits of human unfertilized oocytes and primordial germ cells at 10 weeks of gestation.
Diedrichs F, **Mlody B**, Matz P, Fuchs H, Chavez L, Drews K, Adjaye J.
Int J Dev Biol. 2012;56(10-12):789-97. doi: 10.1387/ijdb.120230ja.

Identification of biomarkers of human skin ageing in both genders. Wnt signalling - a label of skin ageing?
Makrantonaki E, Brink TC, Zampeli V, Elewa RM, **Mlody B**, Hossini AM, Hermes B, Krause U, Knolle J, Abdallah M, Adjaye J, Zouboulis CC.
PLoS One. 2012;7(11):e50393. doi: 10.1371/journal.pone.0050393.

Coexpression of Argonaute-2 enhances RNA interference toward perfect match binding sites.
Diederichs S, Jung S, Rothenberg SM, Smolen GA, **Mlody BG**, Haber DA.
Proc Natl Acad Sci U S A. 2008 Jul 8;105(27):9284-9. doi: 10.1073/pnas.0800803105.

In vivo analyses of UV-irradiation-induced p53 promoter binding using a novel quantitative real-time PCR assay.
Potratz JC, **Mlody B**, Berdel WE, Serve H, Müller-Tidow C.
Int J Oncol. 2005 Feb;26(2):493-8.

The serine-threonine kinase MNK1 is post-translationally stabilized by PML-RARalpha and regulates differentiation of hematopoietic cells.
Worch J, Tickenbrock L, Schwäble J, Steffen B, Cauvet T, **Mlody B**, Buerger H, Koeffler HP, Berdel WE, Serve H, Müller-Tidow C.
Oncogene. 2004 Dec 9;23(57):9162-72.

A

SUPPLEMENTARY MATERIALS

A.1 LIST OF CHEMICALS

Name	**Supplier; Order #**
2´,7´-Dichlorofluorescin diacetate (DCF-DA)	SigmaAldrich; D6883-50MG
3-(4,5-dimethylthiazol-2-yl) -2,5-diphenyltetrazolium bromide (MTT)	Invitrogen; M-6494
6-Aminohexanoic acid	Carl Roth; # 3113.3
Acetic Acid, 96 %	Merck
Acrylamid, 40 % (Rotiphorese R Gel 40)	CarlRoth
Agarose Standard	Roth; 3810.2
Albumin, from bovine serum (BSA)	Sigma; A3059
Ammoniumperoxodisulfate (APS)	CarlRoth
Boric acid	Merck
Bromphenol Blue	AppliChemGmbH
Dimethyl sulfoxide (DMSO)	Sigma
Dimethylformamide	Sigma
Doxycycline hyclate $\geq$98% (TLC)	D9891-1G; Sigma
Ethanol $\geq$99,8 %	Roth; 5054.2
Ethidium bromide	Sigma; E1510
Ethylenediaminetetraacetic acid (EDTA)	Merck
Gelatine from bovine skin, Type B	Sigma
Glycerol	Merck
Glycine	Merck
Hydrochloric acid (HCl), 37 %	Merck
Hydrogen peroxide (H_2O_2), 30 %	Merck; 1.07209
Hygromycin B from Streptomyces hygroscopicus	H3274-50MG; SIGMA
Isopropanol	CarlRoth
Lumi-Film Chemiluminescent Detection Film	Roche; 11 666 657 001
Methanol	Merck
Milk powder, low protein	Gedimex
Mitomycin C	Roche
NP-40	USB
Oligo(dT)	Eurofins MWG Operon

Name	**Supplier; Order #**
Paraformaldhyde, 16 %, EM grade	Electron Microscopy Sciences; #15710
Polybrene®	Sigma; 107689
Ponceau S	Sigma; P3504
Propidium iodide	SigmaAldrich; 81845-25MG
Proteinase K	Sigma
Sodium chloride (NaCl)	Fluka
Sodium deoxycholate >97 %	Sigma
Sodium dodecyl sulphate (SDS)	BioRad
Sodium hydroxide (NaOH) pellets	Merck
TEMED	CarlRoth
TRIS (Tris-hydroxymethyl-aminomethan)	Merck
Triton-X-100	Sigma; T9284
Tween-20	Sigma; P1379
Water, LiChrosolv	Merck; 1.15333
β-Mercaptoethanol	Sigma; M6250

A.2 LABORATORY DEVICES

ABI Prism 7700 (Applied Biosystems)
Agarose gel electrophoresis equipment (Amersham)
C60 O_2/CO_2 Incubator (Labortect; SN:117)
Camera for microscopy model AxioCam ICc3
Clean bench type HeraSafe (Hereaus Instruments)
Centrifuge 5415D (Eppendorf)
Curix 60 film developing machine (AGFA, Cologne, Germany)
Digital Camera, model Power shot (Canon, A650IS).
FACSCalibur (Becton Dickinson)
Filter (Corning, 0.22µM, PAS)
Freezing Container (Nalgene)
HERAguard R Clean Bench (Heraeus, Thermo Fischer Scientific Inc.)
Hypercassette™ (Amersham)
INNOVA CO-170 Incubator (New Brunswick Scientific)
Incubator type Hereaus 6.000 (Hereaus Instruments)
Inverted microscope model CK2 (Olympus)
Leica MZ 95 Stereo Microscope (Leica)
Mobile pipettor PIPETBOY acu
Neubauer Counting Chamber (Roth)
Nucleofector® II Device (Amaxa)
Objective 10xCplanF 10x/0.25 pHC (Olympus)
Objective 4xUplanF 4x/0.13 pHL (Olympus)
Omega FLUOstar Microplate Reader (BMG LABTECH)
Semi-Dry Blotter; Trans-Blot SD (BioRad)
Spectrophotometer type NanoDrop ® ND-1.000
Thermo Block type DRI Block DB2A (Techne)
Thermocycler PTC100 (MJ Research Inc)
Thermomixer (Eppendorf)
Ultraspec 3100 pro (GE Healthcare, Munich, Germany)
Water bath (Heratable)
Zeiss, LSM 510 Meta confocal microscope

A.3 COMPOSITION OF BUFFERS, MEDIUMS AND SOLUTIONS

All buffers and solutions were prepared with double-distilled water. The pH was adjusted using NaOH or HCl unless otherwise specified.

Name	Style/Supplier/ Order #	Composition
Phosphate Buffered Saline (PBS)	Tablets; Calbiochem	0.137 M NaCl; 4.3 mM Na2HPO4 pH7.4; 2.7 mM KCl; 1.4 mM Na2HPO4
Dulbecco's Phosphate Buffered Saline (D-PBS)	1X; GIBCO	0.137 M NaCl; 4.3 mM Na2HPO4 pH7.4; 2.7 mM KCl; 1.4 mM Na2HPO4
hESC medium	1x	KO-DMEM; 20 % SR; 1 % Glutamine; 1 % Amino acids; 1 % P/S; 0.1 mM β-Mercaptoethanol
Conditioned Medium (CM)	1x	see section 2.1.16.8
Freezing Medium for mammalian cells	1x	10 % DMSO; 50 % FBS; 40 % DMEM
Freezing Medium for hESCs/iPSCs	1x	10 % DMSO; 50 % SR; 40 % KO-DMEM
SDS Running buffer	1X	25 mM Tris-Base; 195 mM Glycine; 0.1 % SDS
Separating gel buffer	1x	1.5 M Tris-Cl pH 8.8
stacking gel buffer	1x	0.5 M Tris-Cl pH 6.8
Semi-dry blotting buffer 1	1x	0.3 M Tris-Base; 20 % (v/v) Methanol
Semi-dry blotting buffer 2	1x	25 mM Tris-Base; 20 % (v/v) Methanol
Semi-dry blotting buffer 3	1x	40 mM 6-Aminohexanoic acid; 0.01 % SDS; 20 % (v/v) Methanol
Ponceau staining	1x	0.1 % Ponceau S; 5 % acetic acid
Milk-Blocking solution (for WB)	1x	5 % milk; 0,05 % Tween-20 in PBS
BSA-Blocking solution (for WB)	1x	5 % BSA; 0.05 % Tween-20 in PBS
PBS-T Washing buffer	1x	0.05 % Tween-20 in PBS
RIPA Lysis buffer	1x	50 mM Tris; 150 mM NaCl; 0.1 % SDS; 0.5 % Sodium-Deoxycholate; 1 % NP-40

Name	Style/Supplier/ Order #	Composition
Immunoblocking buffer	1x	10 % FBS; 0.05 % Tween-20 in PBS
DNA loading dye	6X	30 % Glycerol; 60 mM EDTA; 0,1 % bromphenol blue
SB- Agarose Gel running buffer	20X	10 mM NaOH; 5 % boric acid
SDS protein loading buffer	5X	250 mM Tris-Cl pH 6.8; 10 % SDS; 50 % glycerol; 5 % β-Mercaptoethanol; 62.5 mM EDTA; 0.1 % bromphenol-blue
Phosphatase Inhibitors, PhosSTOP	Tablets; Roche; 04 906 845 001	One tablet was dissolved in 1 ml water or RIPA buffer to gain 10X stock solution
Protease inhibitors, Complete Mini	Tablets; EDTA-free; Roche	One tablet was dissolved in 2 ml water or RIPA buffer to gain 25X stock solution
DAPI working solution	1x	100 ng/ml in PBS
DAPI stock solution	Molecular Probes	10 mg of DAPI in 2 ml of Dimethylformamide (DMF)
DCF-DA stock solution	1x	10 mM in DMSO
LB-Medium	1x	10 g tryptone, 5 g yeast extract and 10 g NaCl are dissolved in destilled water before autoclaving.
TBE-buffer	10x	108 g TrisBase, 55 g Boric acid and 7.45 g EDTA were dissolved in destilled water to a final volume of 1 litre
Acrylamid-gel (Fingerprinting)	10 %	4.63 ml H_2O; 1 ml 10x TBE buffer; 0.94 ml 85% glycerol; 3.33 ml 30% acrylamide; 0.1 ml 10% APS; 5 µl TEMED
SOB medium	1x	2 % tryptone; 0.5 % Yeast extract; 10 mM NaCl; 2.5 mM KCl; 10 mM $MgCl_2$; ddH_2O to 1 L
SOC medium	1x	SOB + 20 mM glucose

A.4 ANTIBODIES

Name	Source	Company (Order #)
β-Actin (AC-74) antibody	mouse	Sigma (A5316)
GAPDH antibody	mouse	Ambion (AM4300)
OCT-3/4 (C-10) antibody	mouse	Santa Cruz (sc-5279)
SOX-2 (Y-17) antibody	goat	Santa Cruz (sc-17320)
KLF4 (GKLF; H180) antibody	rabbit	Santa Cruz (sc-20691)
C-MYC (N-262) antibody	rabbit	Santa Cruz (sc-764)
NANOG antibody	mouse	R&D Systems (AF1997)
SSEA4 antibody	mouse	Millipore (MAB4304)
TRA1-60 antibody	mouse	SantaCruz (sc-21705)
TRA1-81 antibody	mouse	SantaCruz (sc-21706)
SOX17 antibody	goat	R&D Systems (AF1924)
Smooth nuscle actin (SMA)	mouse	DakoCytomation (M0851)
Nestin (NES) antibody	mouse	Millipore (MAB5326)
Class III beta-tubulin (TUJ1) antibody	mouse	Sigma-Aldrich (T8660)
NBS1 antibody	rabbit	Novus Biolog. (NB100-143)
Brachiury (Large T) antibody	goat	R&D (AF2085)
HNF-3ß (=FOXA2) antibody	goat	R&D (AF2400)
Myc-Tag (9B11) Monoclonal Antibody	mouse	NEB (2276 S)
Anti-phospho-Histone H2A.X (Ser139), clone JBW301, FITC conjugate	mouse	Millipore, 16-202A
phospho-CHEK1 antibody	rabbit	Cell Signaling (#9947; 2348)
phospho-CHEK2 antibody	rabbit	Cell Signaling (#9947; 2661)
phospho-P53 (Ser15) antibody	mouse	Cell Signaling (#9947; 9286)
phospho-BRCA1 (Ser1524) antibody	rabbit	Cell Signaling (#9947; 9009)
phospho-ATM (Ser1981) antibody	rabbit	Cell Signaling (#9947; 5883)
phospho-ATR (Ser428) antibody	rabbit	Cell Signaling (#9947; 2853)
phospho-Histone H2A.X (Ser139) antibody	rabbit	Cell Signaling (#9947; 9718)
Anti-rabbit IgG-HRP	goat	Santa Cruz (sc-2030)
ECL™ Anti-mouse IgG, Horseradish Peroxidase linked F(ab') 2 fragment	sheep	GE healthcare (NA9310V)
Anti-Rabbit IgG Peroxidase Conjugate	goat	Calbiochem (#DC03L)
Anti-mouse AlexaFluor® 594	goat	Life Technologies (A11005)
Anti-goat AlexaFluor® 594	chicken	Life Technologies (A21468)
Anti-rabbit AlexaFluor® 488	donkey	Life Technologies (A21206)
Alexa Fluor® 488 Goat Anti-Mouse IgG (H+L)	goat	Life Technologies (A-11001)
Alexa Fluor® 594 Chicken Anti-Goat IgG (H+L)	chicken	Life Technologies (A-21468)

A.5 ANTIOXIDANTS & SMALL MOLECULES

Name	Company; Order #
3-Hydroxytyrosol	Sigma; H4291-25mg
Bleomycin Sulfate	Merck; 203401-10MG
Ethyl 3,4-dihydroxybenzoate (EDHB)	Sigma, #E24859
Gallic Acid	SIGMA; G7384-100G
GSK3-β inhibitor (CHIR99021)	Cay13122-5; BIOMOL
Hydrogen peroxide (H_2O_2), 30 %	Merck; 1.07209
L-Ascorbic acid (Vitamin C)	Sigma; A4403
L-Glutathione, reduced	Sigma, G6013-25G
MEK inhibitor (PD0325901)	Miltenyi Biotec; 130-103-923
Nω-Nitro-L-Arginine methyl ester hydrochloride (L-NAME)	Sigma; N5751
Tetraethylthiuram disulfide (Disulfiram)	SIGMA; 86720-50G
TGF-beta/Activin/Nodal receptor inhibitor (A-83-01)	Miltenyi Biotec; 130-095-565
Vitamin B5 (D-Pantothenic acid)	Sigma; P5155

A.6 REAGENTS FOR CELL CULTURE, WESTERN BLOT, PCR AND FACS

Name	Company; Order #
Dulbecco's Modified Eagle Medium (DMEM)	1x; Gibco; 41966
Knockout-DMEM	1x; Gibco; 10829
Eagle's Minimum Essential Medium (EMEM)	LONZA, BE12-125F
Essential 8™ Medium; Gibco	Life Technologies; A1517001
mTeSR™1	Stemcell; 05850
Fetal Bovine Serum (FBS)	Biochrome; S0115
Tet System Approved FBS, USDA-Approved	Clontech; 631106
Knockout Serum Replacement (SR)	Gibco; 10828
Penicillin/Steptomycin (P/S), Stock Solution for Cell Culture	100X; Lonza
L-Glutamine, Stock Solution for Cell Culture	100X; Lonza
2-Mercaptoethanol,	500X; 50 mM; Gibco; 31350-010
0.05% Trypsin/EDTA	Invitrogen; 25300-054
Matrigel®	Becton Dickinson

Name	Company; Order #
Opti-MEM	Gibco, 51985
FGF-2 (basic fibroblast growth factor 2)	PeproTech; 100-18B
Stemgent® Recombinant Human Protein Set: OSKM-11R	Miltenyi Biotec; 130-096-119,
ECL Plus Western Blotting Detection Reagents	GE Healthcare, Amersham
Amersham™ ECL™ Prime Western Blotting Detection Reagent	GE Healthcare, RPN2232
Restore Western Blot Stripping Buffer	Thermo Scientific; 21059
PageRuler™ Prestained Protein Ladder	Fermentas, SM0671
Hyper Ladder V	Bioline; BIO-33031
GeneRuler 1 kb DNA Ladder	Thermo Scientific; # SM0311
SYBR Green PCR Master Mix	Applied Biosystems 4364344
MMLV (Moloney Murine Leukemia Virus) reverse transcriptase	200 U/µl; USB
Reaction buffer (for MMLV reverse transcriptase)	5x; Promega
DNase/RNase free distilled water	Gibco
Random Primers	3 µg/µl; Invitrogen
dNTPs	25 mM; Invitrogen
Dako Fluorescent Mounting Medium	Dako; S3023
BD FACSFlow Sheath Fluid	BD biosciences; 342003

A.7 ENZYMES

Name	Company; Order #
Alkaline Phosphatase, Calf Intestinal (CIP)	NEB; M0290S
BamH1	Roboklon; E2050
DNase I	USB
EcoRI	Roboklon; E2150
EcoRV	Roboklon; E2160
HindIII	NEB; R0104S
MMLV (Moloney Murine Leukemia Virus) reverse transcriptase (200 U/µl)	USB
Proteinase K	Sigma; P2308
RNase A (7000 units/ml)	Qiagen; 19101
T4 Ligase	NEB; M0202S
Taq-Polymerase	in-house production
XbaI	NEB; R0145S
XhoI	NEB; R0146S

A.8 MOLECULAR BIOLOGY KITS

Name	Company; Order #
Alkaline Phosphatase Staining Kit	Stemgent™; #00-0009
BCA Protein Assay Kit	ThermoScientific; #23227
Cell Line Nucleofector® Kit R (25 RCT)	LONZA; VCA-1001
Human/Mouse/Rat Activin A Quantikine ELISA Kit	R&D Systems; DAC00B
Invisorb® Spin Plasmid Mini Two	Invitek; 1010140300
NucleoBond® Xtra Maxi EF	Macherey-Nagel; 740424.10
QIAamp DNA Mini Kit	Qiagen; 51304
QiaQuick Gel Extraction Kit	Qiagen; 28704
RNase-free DNase set	Qiagen; 79254
RNeasy® Mini Kit	Qiagen; 74106

A.9 SYNTHETIC OLIGONUCLEOTIDES

Synthetic oligonucleotides were purchased from Eurofins MWG Operon if not mentioned otherwise. The oligonucleotides, received as lysophilic powder, were dissolved in ultrapure water to produce a stock concentration of 100 mM.

Table 21: **Synthetic Oligonucleotides**

Name	Forward sequence (5′-3′)	Reverse sequence (5′-3′)	Application
NFKB1	CTGAGTCCTGCTCCTTCCAA	CTTCGGTGTAGCCCATTTGT	real-time PCR
CDKN1B	GCCCTCCCCAGTCTCTCTTA	TCAAAACTCCCAAGCACCTC	real-time PCR
GSK3B	CTTTTCTCCCCTGTGTGGAA	AACGGCATAACCCTTGTGAA	real-time PCR
CHEK1	CAAGAAAGGGGCAAAAAGG	TGTATGAGGGGCTGGTATCC	real-time PCR
CHEK2	TTCAGCAAGAGAGGCAGACC	GCGTTTATTCCCCACCACTT	real-time PCR
RB1	TGGGTGATTCCTAAGCCACT	ATGCTACAAAAGAAGGCAAAGT	real-time PCR
TP53I3	CTGATGGGAGGAGGTGACAT	CGTGGAGAAGTGAGGCAGA	real-time PCR
CREB1	TCTCCACACCTTCACCAACA	GGAACTCAGAACCCAACAACA	real-time PCR
SESN1	CTCTCCAAATCCTGTTGCTTT	AGCCATCTATTCATTCCTCCA	real-time PCR
FANCE	GTGGAGATGACCCCTGAGAA	CAGTGATGTTAGCCTGATACTTGG	real-time PCR
RPA2	TGACACAGATGACACCAGCA	AAGGCTACCAGGCTCTTTTTG	real-time PCR
STRA13	CACCTGCACTTCAAGGATGA	CGGAAGCACCTTCTCCAG	real-time PCR
FANCG	GTCGTGGACTGGAATGGGTA	GCAGGTGAAAGTAAGTGTCTCG	real-time PCR
UBE2T	GCTGGAAGGATTTGTCTGGA	GTCATCAGGGTTGGGTTCTG	real-time PCR
RPA3	TTGTGGAAGTGGTTGGAAGA	AAAGGATAAAACTGAGGGAAGTCA	real-time PCR
FANCD2	CAGGAGAGCACAGCAGATGA	TGCTCCTTTTCTCCAGCACT	real-time PCR
NBS Ex6	CAGATAGTCACTCCGTTTACAA	ATGAATAGGCCAGTTATCACAG	Sequencing PCR
NBS 657del5	AATGTTGATCTGTCAGGACG	TATAAATGTTTTCCCTTTGAAGA	PCR
D7S796	TTTTGGTATTGGCCATCCTA	GAAAGGAACAGAGAGACAGGG	Fingerprinting PCR
D10S1214	ATTGCCCCAAAACTTTTTTG	TTGAAGACCAGTCTGGGAAG	Fingerprinting PCR
D17S1290	GCAACAGAGCAAGACTGTC	GGAAACAGTTAAATGGCCAA	Fingerprinting PCR
D21S2055	AACAGAACCAATAGGCTATCTATC	TACAGTAAATCACTTGGTAGGAGA	Fingerprinting PCR

A.10 PLASMIDS

Name	Company; Order #	Notes
pMXs-hOCT3/4	Addgene; plasmid 17217	The pMXs vectors containing OCT4, SOX2, KLF4 and c-Myc transgenes were created by Dr. Toshio Kitamura of the University of Tokyo, the Institute of Medical Science.
pMXs-hSOX2	Addgene; plasmid 17218	
pMXs-hKLF4	Addgene; plasmid 17219	
pMXs-hC-MYC	Addgene; plasmid 17220	
pLIB-GFP		pLIB kindly provided by Marius Wernig; GFP was cloned by Alessandro Prigione.
pEF1α-TET3G	Clontech; 631342	Tet-On® 3G Bidirectional Inducible Expression System
pTRE3G-BI-ZsGreen1	Clontech; 631343	
NBN (NM_002485) Human cDNA ORF Clone	www.origene.com; RC214682	
pEP4EO2SEN2K	Addgene; plasmid 20925	Plasmids were generated by Junying Yu et al. (2011) "Efficient Feeder-Free Episomal Reprogramming with Small Molecules;" PLOS one
pEP4EO2SET2K	Addgene; plasmid 20927	
pCEP4-M2L	Addgene; plasmid 20926	

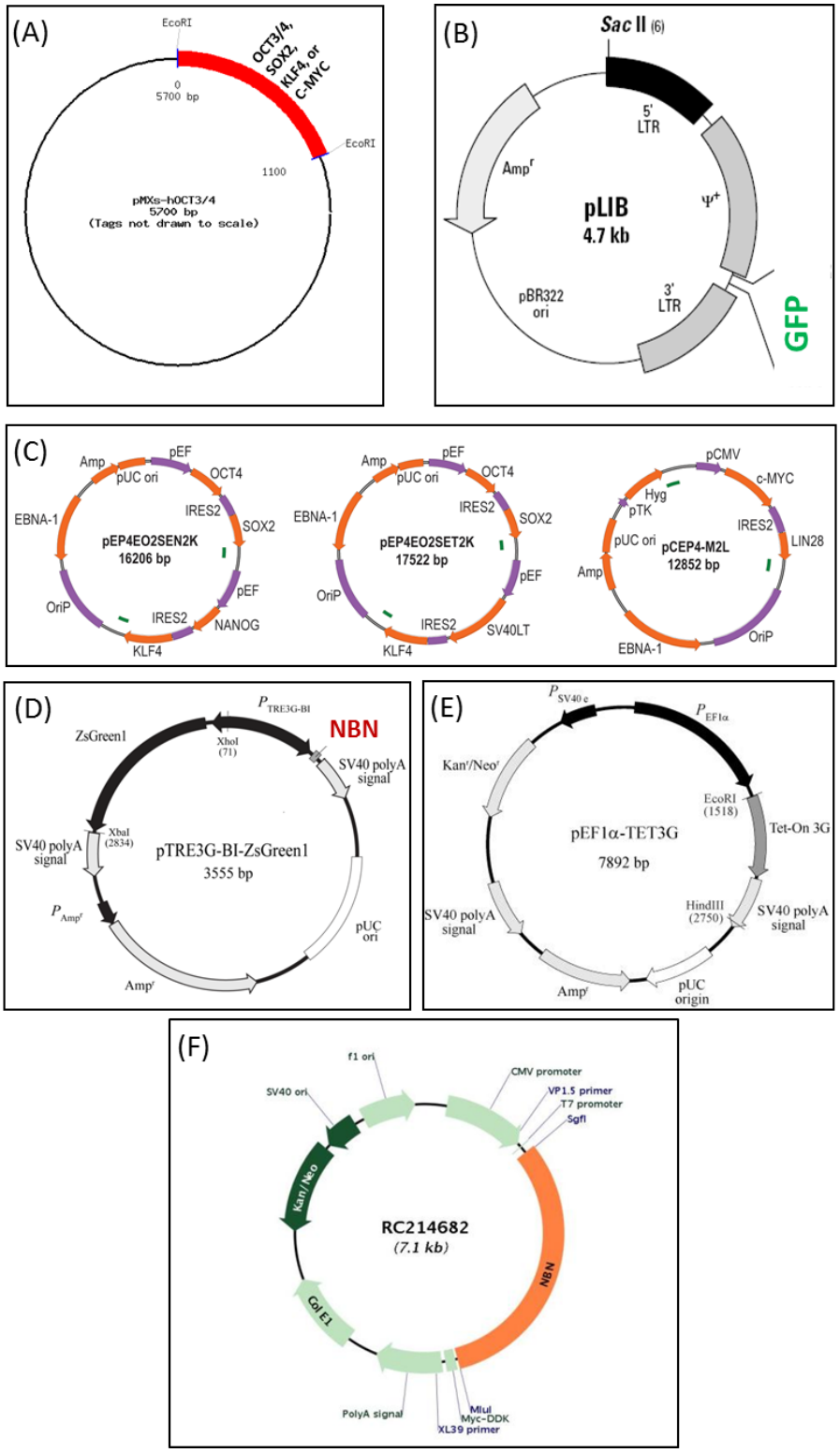

Figure 56: **Plasmid Maps**
(A) Retroviral vectors used for viral reprogramming, containing either human OCT4, SOX2, KLF4 or C-MYC. (B) Retroviral vector containing GFP was used to determine virus titer. (C) Set of episomal vectors used for episomal reprogramming. (D-E) Doxycycline inducible expression system for ectopic expression of wild-type NBN in NBS cells. (F) Human NBN cDNA ORF Clone which was used to clone wild-type NBN into pTRE3G-BI-ZsGreen1.

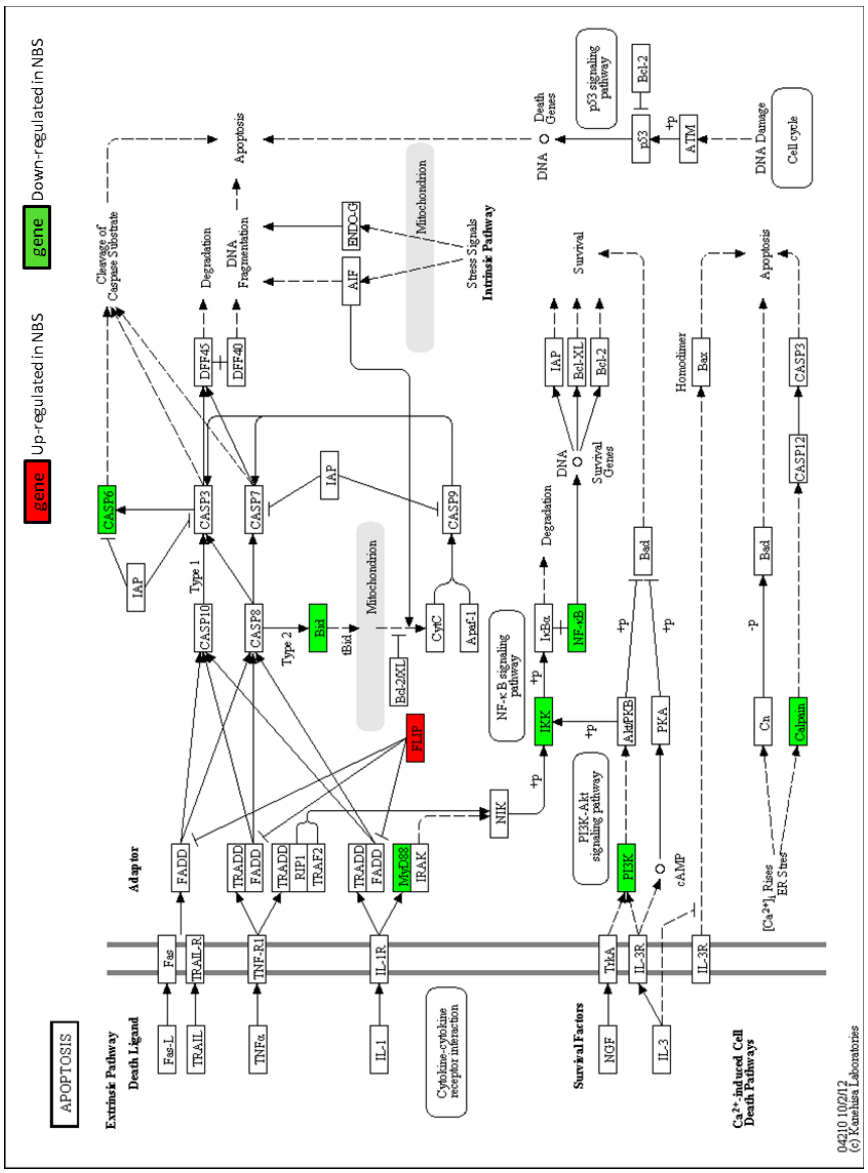

Figure 57: **Regulated genes of apoptosis pathway in NBS iPSCs**
The DAVID output shows regulated genes in apoptosis signaling using KEGG pathways. Regulated genes are selected by diff. p-value $\leq$ 0,05 and $\geq$ 1,5fold ratio. Expression levels of NBS iPSCs relative to normal hESCs are indicated by green and red boxes for decreased and increased expression respectively.

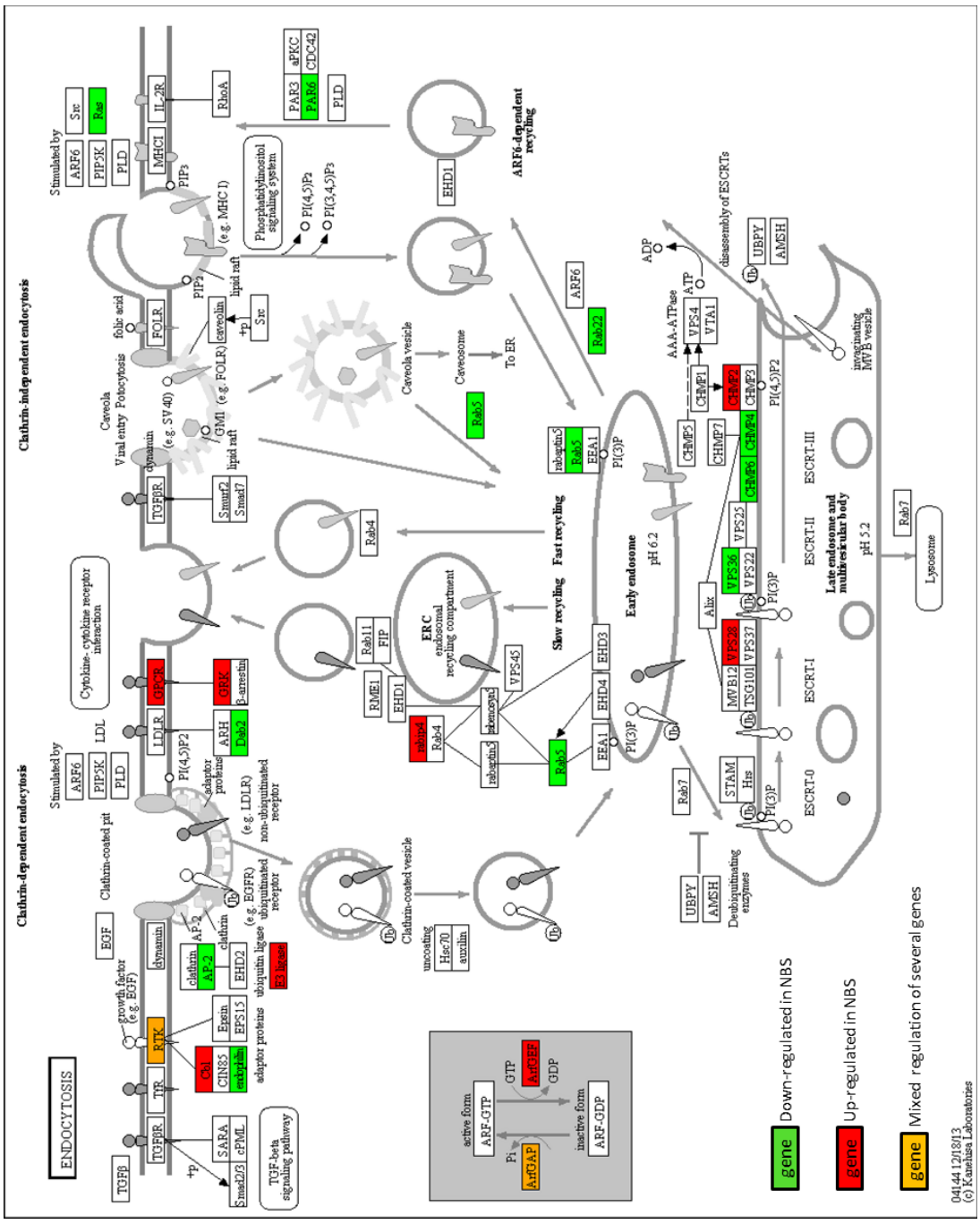

Figure 58: **Regulated genes of endocytosis pathway in NBS iPSCs**
The DAVID output shows regulated genes in endocytosis signaling using KEGG pathways. Regulated genes are selected by diff. p-value $\leq$ 0,05 and $\geq$ 1,5fold ratio. Expression levels of NBS iPSCs relative to normal hESCs are indicated by green and red boxes for decreased and increased expression respectively. Some boxes represent several genes, so in some cases up-regulated and down-regulated are found together in the same box, which is indicated with orange color.

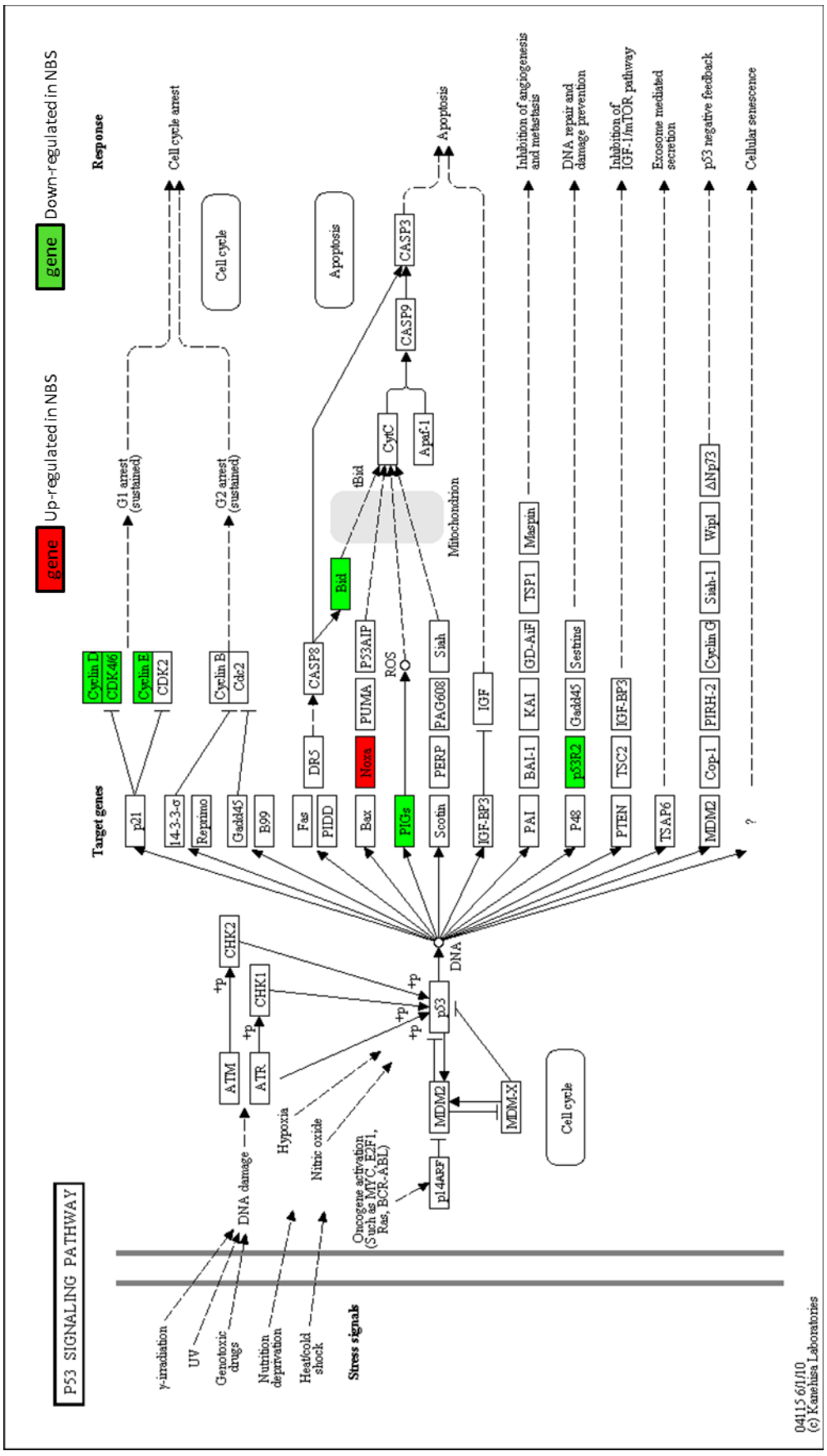

Figure 59: **Regulated genes of the TP53 pathway in NBS iPSCs**
The DAVID output shows regulated genes in TP53 signaling using KEGG pathways. Regulated genes are selected by diff. p-value $\leq$ 0,05 and $\geq$ 1,5fold ratio. Expression levels of NBS iPSCs relative to normal hESCs are indicated by green and red boxes for decreased and increased expression respectively.

SELBSTÄNDIGKEITSERKLÄRUNG

Hiermit erkläre ich, dass ich die vorliegende Arbeit selbständig und unter Verwendung keiner anderen als der von mir angegebenen Quellen und Hilfsmittel verfasst habe. Ferner erkläre ich, dass ich bisher weder an der Freien Universität Berlin noch anderweitig versucht habe, eine Dissertation einzureichen oder mich einer Doktorprüfung zu unterziehen.

Berlin,

Barbara Mlody